Responses of microbial communities to atmospheric nitrogen deposition within different soil horizons in High Arctic tundra

Aimeric Blaud

Department of Animal and Plant Sciences

The University of Sheffield

Thesis presented for the degree of Doctor of Philosophy

August 2012

Abstract

Arctic environments are subject to acute nitrogen deposition events, in which 40% or more of annual atmospheric N input can be deposited as acidic rainfall in less than one week. The overall aim of this research was to investigate the impact of acute N deposition events upon soil microbial communities in High Arctic tundra. A plot scale field experiment, established on the High Arctic tundra (Ny-Ålesund, Svalbard), and a microcosm experiment, were used to simulate acute N deposition over the summer by the application of NH_4NO_3 solution at ~pH 4, at rates of 0.4, 4 and 12 kg N ha^{-1} yr^{-1}. Changes in soil characteristics were measured on soil samples from the organic and mineral horizons. Variation in the structure and abundance of bacterial, archaeal, and fungal communities and in the presence and abundance of N-cycling functional guilds were investigated using molecular (DNA)-based approaches such as Terminal Restriction Fragment Polymorphism (T-RFLP) and quantitative-PCR.

T-RFLP analysis revealed significant ($P < 0.001$) differences in the structure of bacterial and archaeal communities between the organic and mineral horizons within field plots, whilst the fungal community structure showed high variability between soil horizons. Both bacterial and fungal abundance were higher within the mineral horizon in 2009 at the end of the summer, but similar between soil horizons in 2010 earlier in the summer. In contrast, archaeal abundance was always higher in the mineral than in the organic horizon, despite sharp decreases in C, N and water content from organic to mineral horizons. Significant changes ($P < 0.05$) in both bacterial and fungal community structure in the 12 kg N ha^{-1} yr^{-1} plots were found in the mineral horizon only after one and seven days post treatment, respectively, with no subsequent changes thereafter. Bacterial community structure within the mineral horizon also varied with lower N addition rate (4 kg N ha^{-1} yr^{-1}) one day post N application. The microcosm experiment showed that addition of water had a stronger effect on bacterial and archaeal community structure and bacterial abundance within both soil horizons than N addition. Overall, this study showed that microbial community in High Arctic tundra can be rapidly affected by acute N deposition event.

Table of contents

Acknowledgments

This PhD was funded by a European Union Marie Curie Initial Stage Training Network award NSINK (FP7 215503). I would like to thank my supervisors: Prof Mark Osborn and Dr Gareth Phoenix for choosing me, and to trust a French man to come over from the south of France to the Steel City to work on the microbial community in the Arctic. Thanks to both of you for giving me the opportunity to work on such interesting project and to spend a few months in the Arctic. In particular, I would like to thank Gareth Phoenix for his help in 2009 for the fieldwork, particularly with helping me to set up the plots experiment, for his advice throughout my PhD and his valuable feedback on my thesis; and Mark Osborn for his intensive support with all the molecular work, his crucial corrections on my (long…) thesis and articles from and outside my thesis, as well as for the rewarding discussions that we had about science, and also about non-scientific subjects. I would like to particularly thank both of them for the freedom they gave me to fully drive and own my PhD.

I would like to thank the Natural Environment Research Council (NERC) for access to and use of their Arctic Research station in Ny-Ålesund. I would particularly like to thank Mr Nick Cox, manager of the NERC Arctic research station, for his help and support throughout the fieldwork, for his contagious good mood and for his ability to tell stories about his polar adventures. Throughout the fieldwork period, several people helped me with the painful work of transporting water and material to the plots, as well as processing material for experiment: Aga Nowak-Zwierz (PhD of NSINK project) for her help during the fieldwork in 2009; Dr Filip Oulehle (Postdoc of NSINK project), Dr Christopher Evans (NSINK member) and Sonal Choudhary (PhD of NSINK project) for their support and the work carried out together throughout the fieldwork in 2010. Special thanks to Sonal Choudhary for being my fieldwork mate in 2010, and for surviving doing fieldwork with me (I know it was not always easy), and for her work in Sheffield with the C, N, ^{15}N and inorganic N analysis, and most importantly for being my friend.

The support, help and friendship throughout my PhD from my laboratory mates: Jesse Harrison, Kat Fish and others from C51 lab, has been important to keep me happy,

by keeping a good atmosphere within and outside of the lab. Special thanks to you Jesse for supporting the constant complaints and swearing from a French man, and for being my friend. I would like to thank Maggi Killon (C51 lab technician) for her help and support with the laboratory work. I would like to thank the NSINKers (i.e. other PhD, Postdoc and other members of NSINK) for the good times shared during the different NSINK meeting over Europe. Finally I cannot conclude this paragraph without acknowledging my friends in Sheffield and in France: Mamadou Cissoko for being my mate in Sheffield, for sharing together all the difficulties of the PhD and for the Friday nights in pub (and I do not forget all my friends in Sheffield); all my friends in France (and other countries) Léa, Violette, Olivier, Romain, Vincent etc.

I could not write this acknowledgment without thank my girlfriend, Susan Johnston, for the support she gave me throughout my PhD, by being (physically or electronically) beside me all the time, cooking delicious meal such as Haggis (Vive l'Ecosse), Toad in The Hole, Syrup sponge cake (etc.), and all the good time shared together in Sheffield and other places in the world. Without you, I would not be able to speak English properly, to know and understand better British culture... You also help me a lot throughout my PhD, by being my R master, my English teacher, my adviser and my number one supporter. Merci beaucoup ma Susie !

Je voudrais terminer, par remercier mes parents (Martine et Max), mon frère (Vincent) et toute ma famille pour leur soutien direct et indirect tout au long de mes études et de ma thèse. Sans l'appuie, le soutien, la confiance, la liberté de choix donner par mes parents, je n'aurais pas peux réaliser mes études, ma thèse, changer de pays etc. Merci pour tout !

List of abbreviations

α: alpha

β: beta

δ: delta

γ: gamma

ρ: Spearman coefficient

μ: micro (10^{-6})

χ^2: chi-square (Kruskal-Wallis test)

%: percent

$^{-1}$: per

2D: two dimensions

3D: three dimensions

0.4N 6: addition of 0.4 kg N ha^{-1} yr^{-1} at ~pH 6 for the 2009 plot experiment

0.4N 4: addition of 0.4 kg N ha^{-1} yr^{-1} at ~pH 4 for the 2009 plot experiment

4N: addition of 4 kg N ha^{-1} yr^{-1} at ~pH 4 for the 2010 plot and microcosm experiment

4N 4: addition of 4 kg N ha^{-1} yr^{-1} at ~pH 4 for the 2009 plot experiment

12N: addition of 12 kg N ha^{-1} yr^{-1} at ~pH 4 for the 2010 plot and microcosm experiment

A: mineral soil horizon

alt: altitude

Anammox: anaerobic ammonium oxidation

ANOSIM: analysis of similarity

ANOVA: analysis of variance

ARISA: automated ribosomal intergenic spacer analysis

BLASTn: basic local alignment search tool for nucleotide

BSA: bovine serum albumin

bp: base pair

C: carbon

C: control plot or microcosm (no treatment)

ºC: degree Celsius

CFB bacteria: Cytophaga-Flavobacteria-Bacteroides bacteria

CH_4: methane

cm: centimetre

CO_2: carbon dioxide

C_t: cycle threshold

C+W: control water plot or microcosm (addition of water)

Da: Dalton

Day-6 (or D-6): two days before treatment application

Day-3 (or D-3): after the second treatment application

Day-2 (or D-2): before the first treatment application

Day-1 (or D-1): before the second treatment application

Day0 (or D0): beginning of the microcosm experiment

Day+1 (or D+1, D1): one day post treatment application

Day+4 (or D+4): four days post treatment application

Day+7 (or D+7, D7): seven days post treatment application

Day+14: fourteen days post treatment application

Day+21 (or D+21): twenty one days post treatment application

Day+35 (or D+35): thirty five days post treatment application

df: degree of freedom

DGGE: denaturant gradient gel electrophoresis

DNA: deoxyribonucleic acid

DNRA: dissimilatory nitrate reduction to ammonium

dNTP: deoxyribonucleoside triphosphate

dT: first derivative of temperature

d(RFU): first derivative of RFU

E: amplification efficiency

EDTA: ethylenediaminetetraacetic acid

et al.,: and others

F: F value (ANOVA)

GenBank: genetic sequence database

GNS bacteria: green non-sulphur bacteria

g: gramme

h: hour

H': Shannon diversity index

HNO_3: nitric acid

ITS: internal transcribed spacer

K: potassium

KCl: potassium chloride

k: kilo (10^3)

KH_2PO_4: monopotassium phosphate

l: litre

LB: Luria-Bertina

ln: natural logarithm

LSU: large sub-unit

m: metre

m (as a prefix): milli (10^{-3})

M: molar

mm: millimetre

$MgSO_4.7H_2O$: magnesium sulphate heptahydrate

min: minute

mol: mole

MW: molecular weight

N: nitrogen

n: number of replicates

n (as a prefix): nano (10^{-9})

N_2: dinitrogen

N_2H_4: hydrazine

N_2O: nitrous oxide

$NaNO_3$: sodium nitrate

NCBI: National Centre for Biotechnology Information

NH_2OH: hydroxylamine

NH_3: ammonia

NH_4^+: ammonium

NH_4Cl: ammonium chloride

NO: nitrogen oxide (nitrogen monoxide)

NO_2: nitrogen dioxide

NO_2^-: nitrite

NO_3^-: nitrate

NO_x: sum of NO and NO_2

NPK: nitrogen, phosphate and potassium fertiliser

Nr: reactive nitrogen

nMDS: non-metric multi-dimensional scaling

NTC: no template control

O: organic soil horizon

O_2: dioxygene

OM: organic matter

P: phosphate

P: *P*-value (statistical significance)

PCA: principal component analysis

PCR: polymerase chain reaction

pH~4: addition of ~pH 4 solution for the 2009 plot experiment

PLFA: phospholipids fatty acids

P_2O_5: phosphorus peroxide

R: T-RF richness

r^2: linear regression coefficient

RDP: ribosomal database project

RFU: relative fluorescence

rpm: rotation per minute

rRNA: ribosomal ribonucleic acid

WRB world reference base for soil resources

s: second

6-FAM: six-carboxyfluorescein

SIP: stable-isotope probing

SIR: substrate-induced respiration

SOC (media): super optimal broth with catabolite repression

SOM: soil organic matter

SSU: small sub-unit

T_a: annealing temperature

TAE: tris acetate ethylenediaminetetraacetic acid

TD: touch down polymerase chain reaction

T_m: melting temperature

T-RFLP: terminal restriction fragment length polymorphism

T-RF: terminal restriction fragment

U: unit

UK: United Kingdom

USA: United States of America

UV: ultra-violet

V: Volt

w/v: weight / volume percentage solution

X-Gal: 5-bromo-4-chloro-3-indolyl-β-D-galactoside

y: intercept

yr: year

List of figures

List of tables

Chapter 1: Introduction

View of Ny-Ålesund and its airport from Schetelig mountain (694 m alt.) the 1st of August 2010.

1.1 Arctic ecosystems

1.1.1 Arctic region

The Arctic region is defined as the area centred on the North Pole and it includes terrestrial, freshwater and marine environments across northern Asia, northern Europe and northern North America. It is characterised by cold temperatures, as low as -40 ºC in winter (sometimes lower in Siberia) rising to 15 ºC (and higher in continental Asia) in summer across the southern Arctic regions (Jones *et al.*, 2009). Annual precipitation is low in the Arctic, with less than 500 mm for most of the Arctic with precipitation occurring mostly in the form of snow. The annual solar radiation received in the Arctic represents a third to a half of the radiation received in temperate and equatorial zone (AMAP, 1998), although during the summer period there is 24 h sunlight. Winter is long in the Arctic (9-11 months), whilst the summer, i.e. the growing season, varies from 1-3 months with latitude.

The boundary of the Arctic region is often defined by the Arctic Circle (66º32'N), but the boundary can be drawn far below this, when based on climate (e.g. temperature), or marine (e.g. water characteristics) or terrestrial (e.g. vegetation) environments (AMAP, 1998). When based on temperature, the Arctic region boundary is often delimited by the 10 ºC July isotherm, which corresponds to the region having an average temperature for July (the warmest month) of below 10 ºC. However, the Arctic exhibits large variation in temperature, precipitation and soil characteristics. This current study focuses on the Arctic terrestrial environment, hence the Arctic region will be defined and delimited based on the terrestrial environment and on ecological regions relevant to this study.

Arctic terrestrial ecosystems can be divided into three different biogeographical zones: High Arctic, Low Arctic and subarctic (AMAP, 1998). The criteria used to define these zones can be based on climate, vegetation and fauna. The High Arctic (the focus for this thesis) is the northern part of the Arctic region including Greenland, Nunavut Canadian islands (i.e. Baffin Island, Parry Islands, Queen Elizabeth Islands and Ellsmere Islands), Russian islands (i.e. Franz Josef Land, New Siberia Islands and part of Novaya

Zemlya), Severnaya Zemlya and Svalbard (Figure 1.1). The duration of the growing season varies between 1-2.5 months, with mean July temperatures varying between 4-8 ºC while the average annual temperature is in general < -15 ºC (Figure 1.2). Most of the High Arctic receives annual precipitation of < 250 mm or between 250 and 500 mm. Only the Greenland ice cap receives precipitation of > 1000 mm (Figure 1.2). Plant cover in the High Arctic is dominated by bryophytes and lichens which can represent 50% to 80% of the total plant cover, while vascular plants represent 0% to 20% typically (AMAP, 1998). The plant cover in the High Arctic is discontinuous and alternates between polar desert and polar semi-desert (with low plant coverage) and tundra of more continuous cover.

The Low Arctic extends mainly from the Arctic continental coastline to the treeline (Figure 1.1) and is characterised by a growing season of 3-4 months with mean July temperatures varying from 4-11 ºC (AMAP, 1998) and an annual temperature varying between -15 ºC to -10 ºC (Figure 1.2). Annual precipitation in the Low Arctic is similar to that of the High Arctic, i.e. < 500 mm and often < 250 mm (Figure 1.2). Plant cover increases in comparison to the High Arctic and reaches 80-100%, resulting in an increase of tundra area and a decrease of polar desert and semi-desert area (AMAP, 1998). The subarctic boundaries start from the treeline to the limit of the boreal forest (Figure 1.1). The growing season in the subarctic zone varies from 3.5 months to a year. The subarctic has large fluctuations in temperature, with an annual temperature ranging from 5 ºC down to -20 ºC and even below in Siberia (Figure 1.2), where the average temperature in January is -50 ºC (Jones *et al.*, 2009). Annual precipitations also show large variations in the subarctic with annual precipitation varying between < 250 mm, up to 750 mm (Figure 1.2). Plant cover is continuous in the subarctic and represents the transition zone between arctic tundra and boreal forest.

The differentiation between High Arctic, Low Arctic and subarctic are widely used in the literature. Although the limits of the different zones vary in relation to the data used to define them, these zones refer to similar biogeographical characteristics regardless of their limits. Thus, throughout the thesis, references will be made to these different zones in the Arctic region.

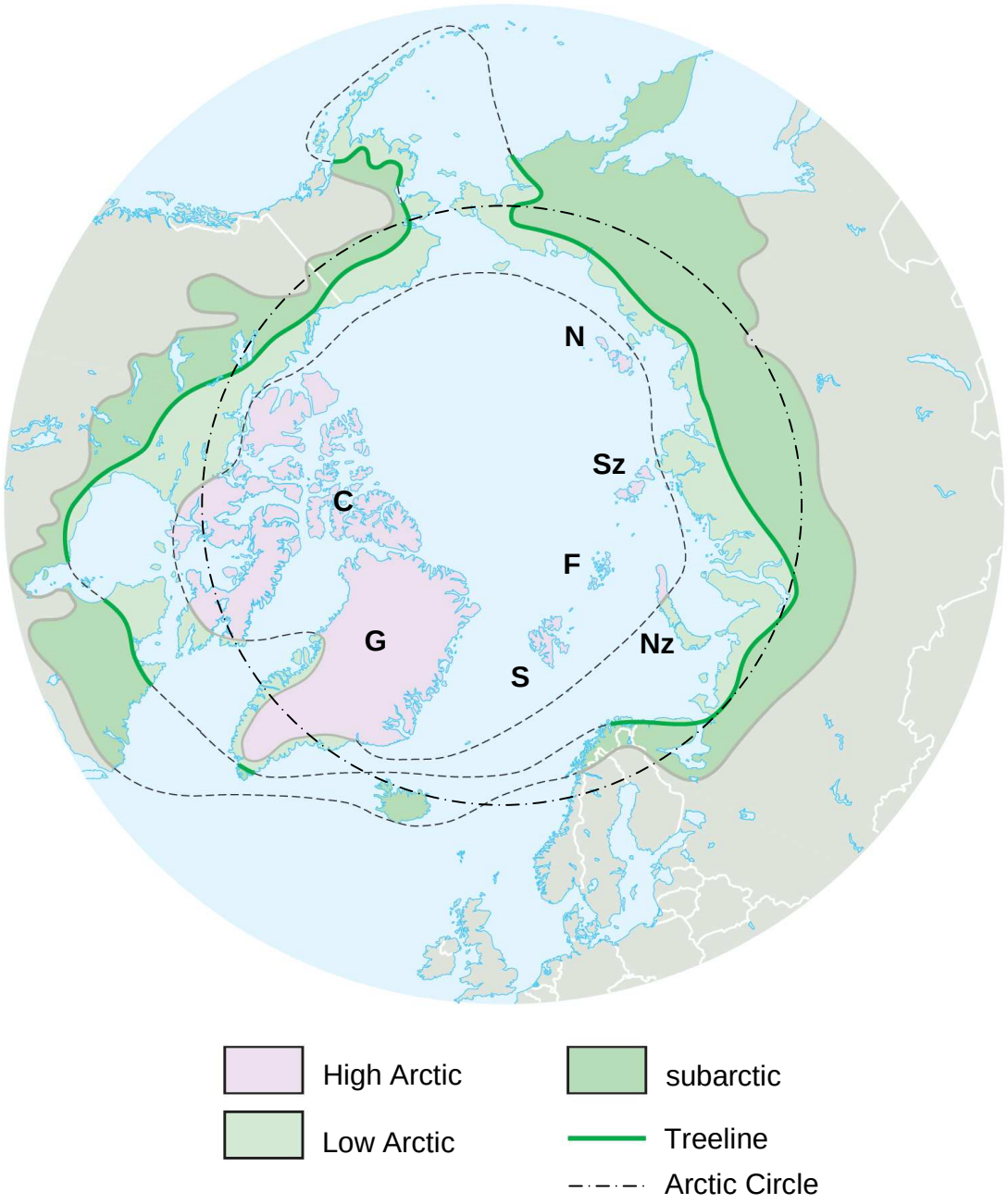

Figure 1.1: Map of the different Arctic ecological regions (i.e. High Arctic, Low Arctic and subarctic) based on vegetation (adapted from AMAP, 1998). The treeline corresponds to the northern boundary of tree occurrence. Letters correspond to the different High Arctic lands: C: Canada, F: Franz Josef Land (Russia), G: Greenland, N: New Siberia Islands (Russia), Nz: Novaya Zemlya (Russia), S: Svalbard (Norway), Sz: Severnaya Zemlya (Russia).

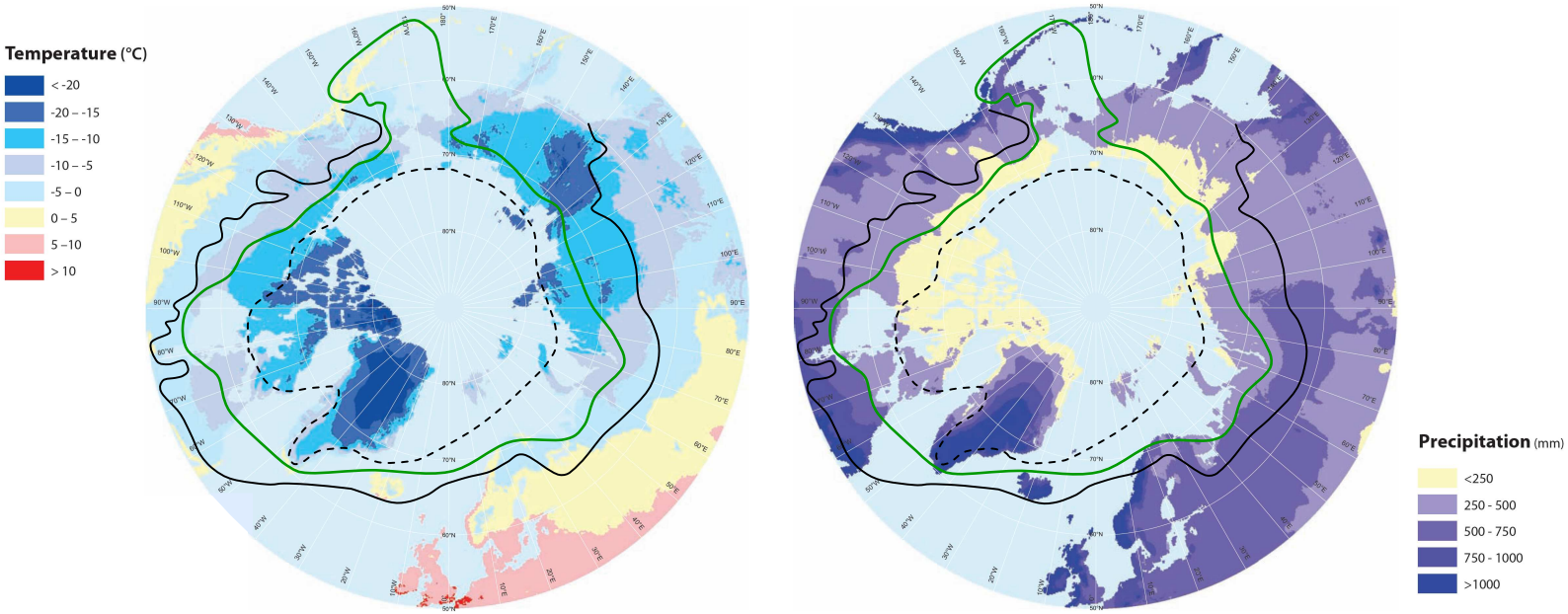

Figure 1.2: Maps of mean annual air temperature (ºC) and mean annual precipitation (including liquid and solid precipitations; mm) in the Arctic region and in the: High Arctic, Low Arctic and subarctic zones (map adapted from Jones *et al.*, 2009). Dashed line indicates the outer border of the High Arctic. Green line indicates outer border of the Low Arctic and the treeline (i.e. the northern boundary of tree occurrence). Black line indicates the outer border of subarctic.

1.1.2 Arctic tundra ecosystems

The Arctic tundra is a treeless ecosystem representing ~5 % of the land on earth (Nemergut *et al.*, 2005). Plant cover of arctic tundra ecosystems is typically limited to dwarf/low shrubs, sedges, grasses, lichens and bryophytes. Moving north to south, i.e. from High Arctic to the subarctic, shrubs such as *Betula nana* or *Salix spp.* increase in density and size whilst bryophytes and lichens decrease in density (Nadelhofer & Geiser, 2010). The presence of bare soils also decreases from the High Arctic to the subarctic. High Arctic tundra plant cover consists of high densities of bryophytes and lichens (up to nearly 50% of the cover), then vascular plants (~360 vascular plant species; AMAP, 1998): shrubs (e.g. *Salix polaris*, *Salix arctica*), cushion plants (e.g. *Dryas octopetala*, *Saxifraga oppositifolia*), rosette species (e.g. *Draba spp.*, *Minuartia rubella*) and grasses (e.g. *Luzula arctica*, *Poa alpine*) (AMAP, 1998).

Plant production in arctic regions is low due to low temperatures, and is often considered to be nitrogen (N)-limited (Shaver & Chapin 1980; Shaver *et al.*, 1992; Van Wijk *et al.*, 2004) with plant production in High Arctic polar desert varying between 1 - 10 g m^{-2} yr^{-1}, and between 10 - 50 g m^{-2} yr^{-1} in the polar semi-desert (see AMAP, 1998). Plant communities were also found to be phosphorus (P)-limited in some areas in the High Arctic, with some N and P co-limiting plant communities (Gordon *et al.*, 2001).

1.1.3 Arctic soils

A common characteristic of arctic soils is the presence of permafrost, defined as ground (including soil, rocks, ice and organic material) that remains at or below 0 ºC for at least two consecutive years. The upper part of arctic soils thaw during summer to a depth of between 20 cm and 150 cm and refreezing each winter (Jones *et al.*, 2009). This part of the Arctic soil is named the active layer. The soil active layer is considered to be where soil processes occur, and where biological activity takes place, although recent studies have shown the microbial potential of permafrost and some microbial activity occurring in frozen soil (McMahon *et al.*, 2009; Yergeau *et al.*, 2010). The thickness of

the active layer in summer depends upon temperature, ground material, soil water content and plant cover, and increases in depth from the High Arctic to the subarctic.

The temperature of arctic soils can go down to -38 ºC in winter, up to nearly 10 ºC in summer for the topsoil of the active layer, and is directly related to air temperature (Jones *et al.*, 2009). However, soil temperature is always lower than the air temperature in summer due to the presence of permafrost and insulation from plant cover. The influence of air temperature on the active layer temperature is greater for the upper than the lower parts of the soil. Inversely, the soil temperature in winter is slightly warmer than the air temperature due to the presence of permafrost and also the snow cover which insulates the soil from the air temperature.

The water within arctic soils is influenced by precipitation, soil draining characteristics and permafrost. Precipitation in the Arctic is low and mainly occurs in the form of snow. Arctic soils are either poorly drained, representing 85 - 90% of the Low Arctic and in some wet meadows of High Arctic, or well drained which is common in the High Arctic (AMAP, 1998). The presence of permafrost regulates soil moisture in arctic soils by acting as a barrier to water drainage from precipitation/snowmelt and by being a source of water from its melting. Hence, water from precipitation is mainly retained in soil, especially in the Low Arctic where many wetlands are present (AMAP, 1998). However, a few studies have shown that the annual runoff in High Arctic soil can reach 80 - 90% over two or three weeks during the snowmelt period, resulting in a low water runoff during the growing season (Bliss *et al.*, 1984). In the High Arctic, where precipitation can be extremely low, snowmelt is the main water source for soil, and the reduction of water runoff in High Arctic soils can lead to an extremely low water availability during the growing season (AMAP, 1998).

Different type of soils can be found in arctic regions, which can have organic and mineral layers, cemented horizons or acidic subsoil. The High Arctic is nearly exclusively characterised by Cryosols which are defined by the World Reference Base for Soil Resources (WRB) as soils in cold regions where permafrost is present, and where water occurs mainly in a solid form. Cryosols are formed under cryogenic processes such as freeze-thaw cycles, cryoturbation, frost heave, cryogenic sorting, cracking and ice segregation (Jones *et al.*, 2009). Only a few other soil types can be

found in the High Arctic such as Leptosols, defined by WRB as shallow soil over hard rock with an extremely low soil water content. Leptosols are found mainly in mountainous regions such as the Russian Severnaya Zemlya Islands.

Arctic soils consist of multiple soil horizons, with, in general, at the soil surface an organic horizon which is a dark layer containing partially decomposed plant residue (Jones *et al.*, 2009). The organic horizon, referred by the letter "O", is found in most High Arctic, Low Arctic and subarctic soils when the soil supports some plant cover (see Figure 2.6, chapter 2). The thickness of the O horizon can vary from a few cm in the High Arctic to 40 cm in peat and up to several meters in the subarctic zone (Jones *et al.*, 2009). Beneath the organic horizon, the mineral horizon, which is referred to by the letter "A", is characterised by a clearer colour than the O horizon and contains a mix or organic and mineral material (see Figure 2.6, chapter 2). Further mineral horizons can be found beneath the A horizon, and are referred to by the letters B and C and are characterised by an increase in mineral material and a decrease in organic material. Characteristic to Arctic soils, is the presence of ice lenses and wedges as a soil layer, defined as the "I" horizon (Jones *et al.*, 2009). Throughout the thesis, O and A horizons will be used, referring to the organic and mineral horizons, respectively.

In arctic soils, both the active layer and permafrost are characterised by large amounts of total C and especially of organic C which represent an important C pool on earth (Schuur *et al.*, 2008). Input of organic C is mainly limited to plant sources, which provide a low annual biomass production (see section 1.1.2), leading to a low annual C-input in arctic soils ranging from ~ 1 g C m^{-2} to 12 g C m^{-2} in different High Arctic soils types (Jones *et al.*, 2009). However, organic C accumulates in arctic soils as plant material is only partially decomposed in arctic soils due to the low soil temperatures, low biological activity, and sometimes acidic and/or anoxic conditions. Carbon is accumulated near the surface as plant materials are deposited as litter. However, deeper soil horizons can also store large amounts of C due to cryogenic processes that move plant material and soluble compounds, i.e. organic matter, deep into the soil, and up to the permafrost where a horizon rich in organic matter can be formed. The migration of organic matter into arctic soils can take thousands of years, and enable long-term storage of C (Jones *et al.*, 2009). There is variation in estimates of total C within arctic soils that

vary additionally in relation to the area of arctic soils being considered. Nevertheless, the C pool in arctic soils is generally described as being more than twice the atmospheric C pool (Schuur *et al.*, 2008; Jones *et al.*, 2009). One estimation of the total soil C in the circumpolar region is 1672 petagrams (1 petagrams = 1 billion tons), including peatlands which represent 227 petagrams (Schuur *et al.*, 2008). However, an accurate estimation of the total amount of C present in arctic soils is difficult, but soils affected by permafrost represent an important C pool on earth, containing potentially ~50% of the global organic C (Schuur *et al.*, 2008; Jones *et al.*, 2009). In contrast, nutrients such as N and P are considered to be in low abundance in arctic soils. Hence, nutrient availability is limiting plant production in arctic soils, especially nitrogen (Shaver & Chapin, 1980; Shaver *et al.*, 1992), and also the activity of microbial communities (Nordin *et al.*, 2004; Rinnan *et al.*, 2007).

1.1.4 Vulnerability of arctic tundra ecosystems to environmental changes

Arctic regions are subject to extreme environmental conditions such as extremely cold temperatures and extreme seasonal temperature fluctuation, and considerable snow and ice cover. These environmental conditions directly affect plant productivity, microbial activities, plant, animal and microbial diversity/abundance and animal behaviours (i.e. migration, hibernation). Hence, animal, plant and microbial communities are sensitive to changes under these extreme environmental conditions. Arctic regions are facing and will face several threats due to anthropogenic activities which are likely to directly affect these environmental conditions.

Climate changes are predicted to be stronger at the Polar Regions than across other regions on earth, and especially in the Arctic (ACIA, 2005). At the end of the 21st century, the mean annual surface air temperature in the Arctic is predicted to increase by between 2.8 ºC and 4.6 ºC depending on the model used, and on average, using different models, by 3.7 ºC (ACIA, 2005). The increase of temperature is predicted to be stronger in autumn and winter seasons with increases in temperature ranging from 3 to 5 ºC, while increases in temperature in summer are predicted to be less than 1 ºC (ACIA, 2005). Increases in air temperature are also leading to decrease in snow, glacier and sea

ice cover. Snow cover in the Northern Hemisphere has been decreasing by 5 to 10% since the 1970s (ACIA, 2005). If the air temperature rises by up to 4 ºC by the end of the 21st century, it is predicted that the snow cover will decrease by 13% (ACIA, 2005). Glacier front retreats have been reported since the 1920s in the Arctic, with large variability between arctic lands. Increased melting of the glacier and snow cover releases water and nutrients to arctic soils which are available to plant and microbial communities, and might increase the summer period via early snowmelt. Secondly, increases in air temperature lead to increases in arctic soil temperature, causing the permafrost to melt. Since the 1970s, the temperature of permafrost in arctic regions has increased by several tenths of a degree up to 2 to 3 ºC (ACIA, 2005). Models predict that 10 to 20% of the permafrost might be degraded over the 21st century, and that the southern limit of permafrost will move northward by several hundred kilometres (ACIA, 2005). Melting of the permafrost increases the depth of the active layer, enabling plant roots to go deeper in the soil, releasing frozen organic matter for mineralisation, changing the soil water content (either increased by releasing frozen water or decreased by increasing soil drainage). Increases in the active layer temperature might also have a direct effect on plant and microbial activities. Thirdly, increases in air temperature lead to an increase in precipitation, due to an increase in the capacity of atmospheric circulation to transport moisture from lower to higher latitudes (ACIA, 2005). Models predict an increase in mean annual precipitation in arctic region by 7.5 to 18.1% at the end of the 21st century, with an average between models of 12.3% (ACIA, 2005). Predictions of increases in precipitation vary importantly in the Arctic, with 5 to 10% increases in precipitation in the Atlantic sector, and up to 35% increases in some parts of the High Arctic (ACIA, 2005). Increases in precipitation are predicted to be higher in autumn and winter than in summer, with increased probability of rain in winter, leading to more frequent ice cover on land (ACIA, 2005).

Arctic region also encounter atmospheric pollution events which lead to deposition of compounds and elements, such as N which can represent a source of nutrients for biotic activities in this nutrient poor region. Atmospheric pollution can originate from localised sources of fossil fuel burning (Sander *et al.*, 2006), or be carried

from low latitudes (Kühnel *et al.*, 2011). Atmospheric N deposition will be discussed in detail in section 1.2.2.

1.2 Nitrogen deposition

1.2.1 N deposition at a global scale

The global N cycle is the biogeochemical cycle most altered by human activities on Earth (Fields, 2004; Galloway *et al.*, 2004). N inputs to terrestrial ecosystems have more than doubled with human activities compared to pre-industrial times, with a major increase in the last half century (Vitousek *et al.*, 1997; Galloway *et al.*, 2004) and atmospheric N deposition rates have increased by one order of magnitude in most areas compared to pre-industrial times (Holland *et al.*, 1999). The mains sources of anthropogenic N emissions are the combustion of fossil fuel (e.g. motor vehicles, power stations and industrial production), and the production and use of organic and mineral fertilisers (e.g. animal manure and NPK fertiliser) (Galloway *et al.*, 2003). For example, combustion of fossil fuel by transport in America in 2002 was estimated to represent ~50% of the total NO_x (e.g. NO and NO_2 gas) emissions, while agricultural activities represented the primary source of NH_3 and NH_4^+ (Weathers & Lyinch, 2010).

Atmospheric nitrogen deposition is the downfall of nitrogen from the atmosphere onto ecosystems (Holland *et al.*, 1999). Nitrogen is deposited onto terrestrial systems by different routes: via precipitation (rain and snow), named wet deposition; and via gases and particles, named dry deposition. Clouds and fog can also be a vector of N deposition but are rarely measured, although they can represent an important part of the total N deposition (Weathers & Lyinch, 2010). There is no dominant route of N deposition (i.e. wet, dry or cloud deposition), as each form can dominate total N deposition and is directly influenced by atmospheric conditions (e.g. precipitation, temperature, wind) and landscape. N deposition occurs in the form of reactive nitrogen (Nr) which is defined as any chemical form of nitrogen other than dinitrogen (N_2), such as NH_3, NH_4^+, NO_x N_2O, NO_3^- and other chemical forms (Sutton *et al.*, 2011). With movement of air masses, atmospheric nitrogen can reach ecosystems that are distant from the N sources and from

anthropogenic activities, which are often considered as natural or semi-natural ecosystems.

Rates of atmospheric N deposition vary between a few tenths of 1 kg N ha^{-1} yr^{-1} up to several tens of kg N ha^{-1} yr^{-1} across the globe, and is sometimes even more. For example in the United States, rates of N deposition vary between 0.5 to 17 kg N ha^{-1} yr^{-1}, but can reach locally high rates such as 31 kg N ha^{-1} yr^{-1} at Clingman's Dome, North Carolina, or 71 kg N ha^{-1} yr^{-1}, in the San Bernardino Mountains (Weathers & Lyinch, 2010). The high rates of N deposition can be similar or even higher than N input due to crop fertilisation. In Europe, the use of fertilisation varies greatly from 10 to 200 kg N ha^{-1} yr^{-1} depending on the crop, soil and countries (Stoumann Jensen & Schjoerring, 2011). Historically, N deposition occurred primarily in developed regions of the Northern Hemisphere (i.e. North America, Europe, East Asia; Holland *et al.*, 1999). Nowadays, N deposition affects not only developed countries, but also developing countries (Galloway *et al.*, 1994; Matson *et al.*, 1999; Bleeker *et al.*, 2011) due to increasing fossil fuel combustion in the Southern Hemisphere (mainly in tropical and subtropical regions) linked with the continuous growth of these populations (Galloway *et al.*, 1994). Hence, Galloway *et al.* (1994) estimated that N deposition in developing countries will at least double by 2020 compared to the 1990s. N deposition is also predicted to increase by the middle of 21st century over biodiversity hotspots (where ~50% of the floristic diversity of the word is located), which are mainly located in the South Hemisphere, where N deposition could reach a few tens of kg N ha^{-1} yr^{-1} (Phoenix *et al.*, 2006; Bleeker *et al.*, 2011).

1.2.2 N deposition in the Arctic

1.2.2.1 Chronic N deposition in the Arctic

Despite the remote location of the Arctic, it is susceptible to atmospheric reactive nitrogen (Nr) deposition resulting from polluted air masses which travel from lower latitudes to the Arctic or directly from the Arctic region. The Nr content of the Greenland ice cap has doubled since the industrial revolution (Laj *et al.*, 1992; Fischer *et*

al., 1998). Arctic N deposition is estimated to range from 1 – 5 kg N ha^{-1} yr^{-1} across arctic region but can reach up to 10 kg N ha^{-1} yr^{-1} in Northern Norway, Northern Alaska and in the Taymir Peninsular in Russia (Woodin, 1997). Near Nikiski, in Kenai Peninsula (Alaska), close to the subarctic boundary, a fertiliser factory established in 1968 released NH_3 gas leading to N deposition up to 20 kg N ha^{-1} yr^{-1} in its vicinity (Lilleskov *et al.*, 2001, 2002). At Ny-Ålesund, where the research site of this thesis was established, the total annual N deposition varied from 0.24 to 2.36 kg N ha^{-1} yr^{-1} between 1987 to 2007, with an average of 0.74 kg N ha^{-1} yr^{-1} (Kühnel *et al.*, 2011).

The source of N deposition can be localised, coming from human activities in the Arctic itself. The number of ships in the Arctic is expected to increase, especially if the sea-ice retreat in summer leads to an ice-free Arctic Ocean (Serreze *et al.*, 2007), opening new commercial routes. Hence, maritime transport can represent an important source of Nr via the combustion of fossil fuels (Peters *et al.*, 2011). The number of cruise ships has already increased in some part of the Arctic, such as in Ny-Ålesund: the number of calls from large tourist cruise ship carrying more than 200 passengers (and sometimes several thousand) has tripled between 1996 and 2005 (the average of all ships calling at Ny Ålesund was 120 ships per year between 1996 and 2005; Sander *et al.*, 2006). The combustion of fossil fuel in the Arctic can also come from flights, vehicles, or energy production. For example, at Ny-Ålesund the average number of flights between 1996 and 2005 was 248 flights (including planes and helicopters), and the production of energy required the combustion of 1131 m^3 of diesel at the power station in 2005 (Sander *et al.*, 2006).

1.2.2.2 Episodic acute N deposition in the Arctic

Arctic ecosystems are also in receipt of episodic atmospheric N deposition resulting from polluted air masses that travel rapidly from lower latitudes to the Arctic with mineral dispersal (Hodson *et al.*, 2005; Morin *et al.*, 2008; Hodson *et al.*, 2010; Kühnel *et al.*, 2011). Hodson *et al.*, (2005; 2010) witnessed in 1999, at Ny-Ålesund, an acute episodic N deposition event in which ~40% of the annual atmospheric N input was deposited as acidic rainfall (~pH 4) in less than one week, representing nearly 0.4 kg N

ha^{-1} in the form of NO_3^- (~ 70% of the event) and NH_4^+. A recent study confirmed that annual N deposition in Ny-Ålesund was dominated by acute episodic N deposition events (Kühnel *et al.*, 2011). Between 1987 and 2007, weekly precipitation sampling and N analysis at Ny-Ålesund showed that 10% of the precipitation samples could be defined as "strong" samples (i.e. N content > 0.02 kg N ha^{-1}) and contributed up to 2.25 kg N ha^{-1} yr^{-1} to the total N deposition (Kühnel *et al.*, 2011). In contrast, precipitation samples with N content < 0.02 kg N ha^{-1} represented 90% of the samples but contributed only to an annual N deposition of ~0.17 kg N ha^{-1} yr^{-1} (Kühnel *et al.*, 2011). Occurrence of acute episodic N deposition events is highly variable between years with some years lacking such events, and other years having several. However, these events have occurred more often during the time of the year when the daily mean temperature is below 0 ºC (Kühnel *et al.*, 2011). Nitrogen deposition under the form of NO_3^- ranges between 0.01 and 0.60 kg N ha^{-1} yr^{-1}, while NH_4^+ deposition ranges between 0.04 and 0.98 kg N ha^{-1} yr^{-1} (Kühnel *et al.*, 2011).

Acute episodic N deposition events related to NO_3^- occur mainly when the daily mean temperature is below 0 ºC, while acute N deposition events related to NH_4^+ occur throughout the year with the highest events in summer. Although annual N deposition is relatively low in the Arctic, acute N deposition events represent an important part of the annual N input, and might significantly affect arctic region, considered as nutrient-limited (Henry & Svoboda,1986; Chapin *et al.*, 1995). Moreover, due to climate change, the frequency of cyclonic activity in the North Atlantic is predicted to increase, leading to more acute N deposition events to be carried to Svalbard (Kühnel *et al.*, 2011).

1.3 Nitrogen-cycle

1.3.1 N-cycle

Nitrogen (N) is a fundamental element for life on earth, present in a variety of compounds such as nucleic acids (i.e. DNA), chitin, proteins and chlorophyll, and the N-cycle include a number of processes from transformations of organic and inorganic N, and N-uptake and -immobilisation. Although N is an abundant element on earth, with

about 78% of the atmosphere made of N_2, this form of N is un-reactive and cannot be used directly by plants or animals, which instead require reactive nitrogen (Nr). N_2 can be transformed into Nr by lightning, biomass burning and volcanoes. However, only some microorganisms (i.e. some bacteria and archaea) are able to transform N_2 into Nr via N fixation, through transformation of N_2 into NH_3 using the nitrogenase enzyme (Figure 1.3). The NH_3 produced is available for biological use and is readily converted to NH_4^+ (Howard & Rees, 1996). The NH_4^+ produced can be oxidised to NO_3^- through the aerobic process of nitrification by bacteria, archaea and fungi (Nicol & Schleper, 2006). First, NH_4^+ is oxidised by ammonia-oxidising organisms to NH_2OH (hydroxylamine) using ammonia monooxygenase and to NO_2^- using hydroxylamine oxidoreductase. Secondly, NO_2^- is oxidised by nitrite oxidisers (organisms using nitrite oxidoreductase; Figure 1.3).

The NH_4^+ and NO_3^- produced by N-fixation and nitrification are available for plant assimilation via roots and can be accessed also by mycorrhizal fungi (Figure 1.3). Plants assimilate preferentially NH_4^+ over NO_3^- when both are present in soil (Butterbach-Bahl & Gundersen, 2011). Inorganic N (i.e. NH_4^+ and NO_3^-) are the major nutrients for plants, but studies in the past 2 decades have shown that plants are also able to uptake organic monomers (e.g. amino acids) (Nordin *et al.*, 2004; Butterbach-Bahl & Gundersen, 2011). Microbial communities uptake many organic and inorganic N compounds, and can also immobilise NH_4^+ and NO_3^- in soil. Plants, animals and microorganisms represent the soil organic matter (SOM), and contain large amounts of N in many forms. The SOM is decomposed by microorganisms (i.e. bacteria and fungi) via the depolymerisation of the SOM using extracellular enzymes (Figure 1.3). Hence, the different N compounds of the SOM become bioavailable for either plant or microbial uptake (Butterbach-Bahl & Gundersen, 2011). Bioavailable N forms can be further transformed by microorganisms (i.e. mainly bacteria and some fungi) via the mineralisation into NH_4^+ that can be taken up and assimilated by plants and microorganisms or go through nitrification (Figure 1.3). The production of SOM, and especially of plant litter/roots and its decomposition and mineralisation represent the main driver of the N-cycle turnover in terrestrial ecosystems (Butterbach-Bahl & Gundersen, 2011).

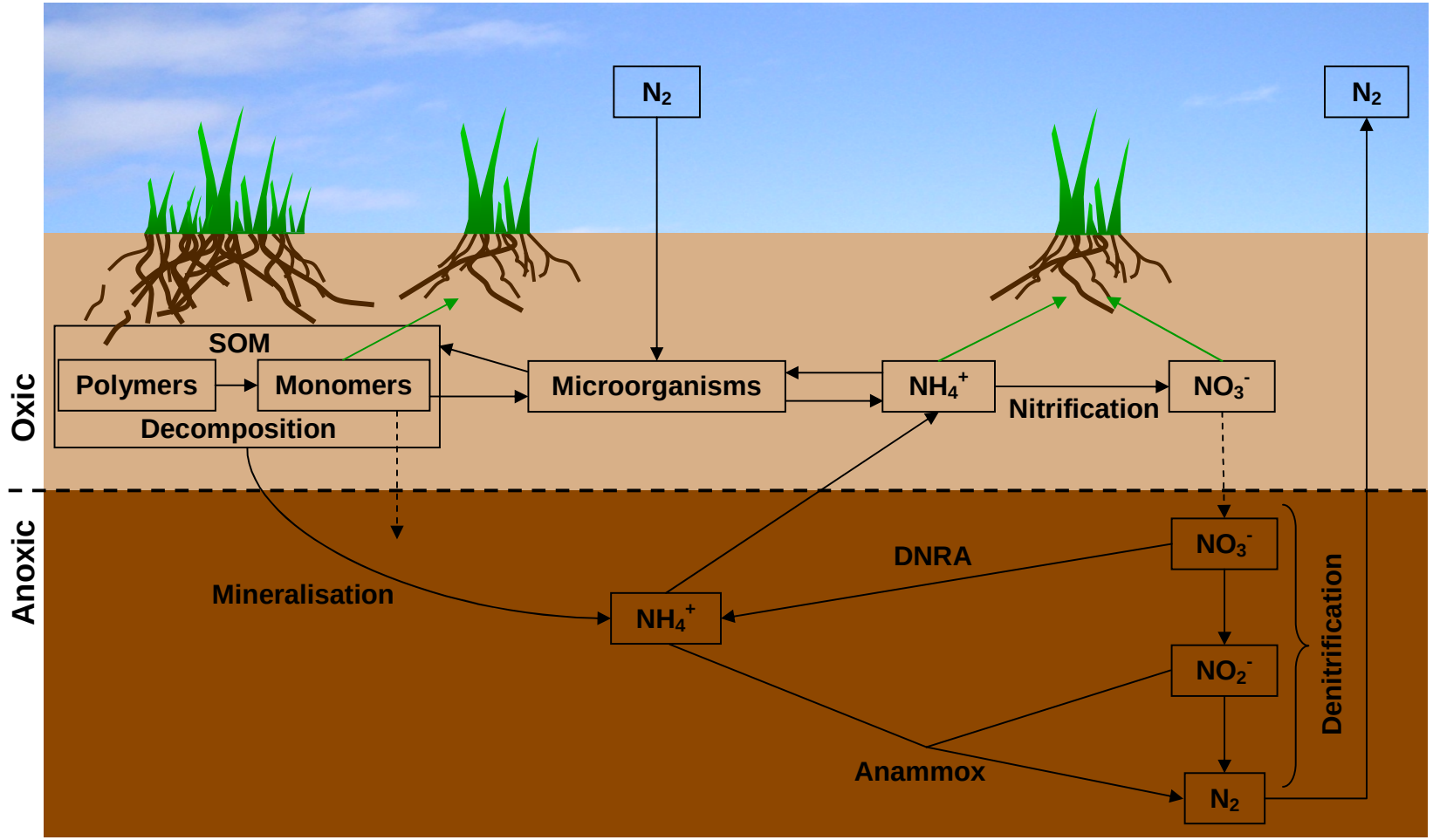

Figure 1.3: Terrestrial N-cycle within the oxic and anoxic part of the soil. The N-cycle processes are: N fixation, decomposition, mineralisation, assimilation, immobilisation, nitrification, denitrification, dissimilatory nitrate reduction to ammonium (DNRA) and the anaerobic ammonium oxidation (anammox) (adapted from Rennenberg *et al.*, 2009). The green arrows indicate plant assimilation. The dash arrows indicate soil leaching of monomers and NO_3^- (which can be further denitrified). SOM: soil organic matter.

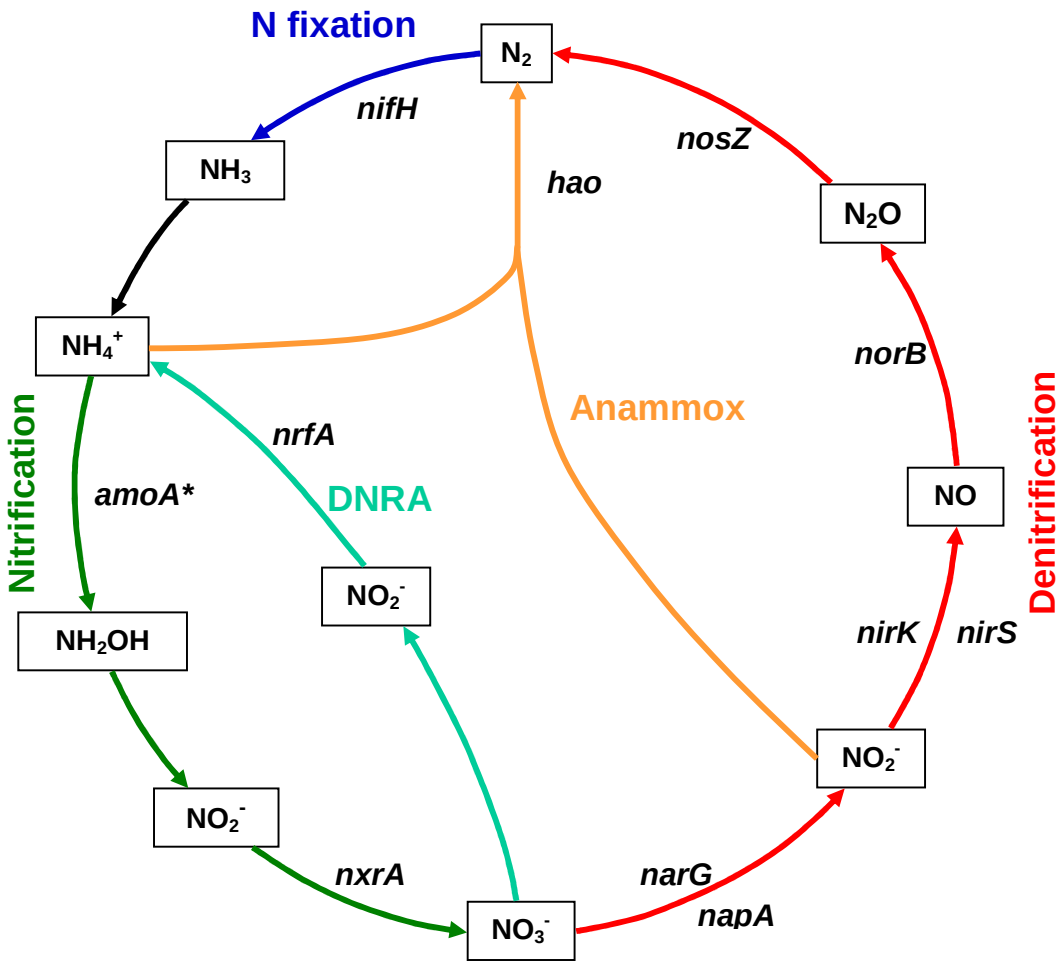

Figure 1.4: The principal microbial processes of the N-cycle and the main bacterial and archaeal N-cycling functional genes used in microbial ecology to study the communities involved in each process. The N-cycle processes are: N fixation, nitrification, denitrification, dissimilatory nitrate reduction to ammonium (DNRA) and the anaerobic ammonium oxidation (anammox) (adapted from Jetten *et al.*, 2008). * *amoA* gene can be investigated for the bacteria and archaea specifically using different primer pairs.

Several N processes are preferentially (i.e. denitrification) or exclusively anaerobic (i.e. DNRA and Anammox; Figure 1.3), occurring either in deeper soil horizons where gas diffusion is reduced, in soil saturated with water, and in some soil microhabitats such as microaggregates (Lensi *et al.*, 1995). The main process is denitrification, which corresponds to a four steps reduction of NO_3^- into N_2 (Figure 1.4) using metalloenzymes: i) NO_3^- is reduced to NO_2^- by nitrate reductase, ii) NO_2^- is reduced to NO by nitrite reductase, iii) NO is reduced to N_2O by nitric oxide reductase, and iv) N_2O is reduced to N_2 by nitrous oxide reductase (Zumft, 1997). Denitrification

can be performed by bacteria and archaea but also some fungi (Philippot, 2002; Ma *et al.*, 2008). NO_3^- can also be reduced into NH_4^+ via NO_2^- by the dissimilatory nitrate reduction to ammonium (DNRA) pathway, catalysed by fermentative bacteria (Mohan *et al.*, 2004). Some bacteria can also transform NO_2^- and NH_4^+ into N_2 by the anaerobic ammonium oxidation (anammox) via N_2H_4 and NH_2OH intermediates (Penton *et al.*, 2006; Francis *et al.*, 2007). Anammox mainly occurs in aquatic ecosystems, although "anammox bacteria" have been found in Siberian permafrost (Penton *et al.*, 2006). Finally, gases produced by denitrification and anammox, such as N_2O or N_2, can be returned into the atmosphere, completing the N-cycle.

1.3.2 Role and genetics of microorganisms in N-cycle processes

Microorganisms dominate the N-cycle in the biosphere and are involved in a variety of reductive or oxidative reactions important in assimilatory pathways (e.g. N fixation, nitrate assimilation) or respiratory processes for energy conservation (e.g. nitrification, denitrification). Different groups of bacteria generally performed N fixation, nitrification and denitrification. Nevertheless, some studies showed that some bacteria are able to catalyse both nitrification and denitrification, while others can catalyse both N fixation and denitrification (Mohan *et al.*, 2004). The microbial N-cycling guild is one the best described soil community of the biogeochemical cycles. Hence, different functional genes encoding for the different enzymatic activities can be used as proxies to enable the investigation of the diversity, structure, abundance and activity of the different microbial communities involved in the different N-cycling processes (Figure 1.4).

N fixation and its conversion to NH_3 is performed by free-living bacteria (e.g. *Azotobacter*) but also archaea (e.g. *Methanocarcinia*) (Zehr *et al.*, 2003; Cabello *et al.*, 2004) or by symbiotic bacteria associated with plants (e.g. *Rhizobium*) (Vitousek *et al.*, 2002), and are grouped under the term of diazotrophs organisms. The physiology of diazotrophs organisms vary widely from chemotrophs, phototrophs, autotrophs and heterotrophs (Burgmann *et al.*, 2004). The nitrogenase enzyme catalyses N fixation and is composed of two subunit proteins encoded by several *nif* genes (Howard & Rees,

1996). In microbial ecology, the highly conserved *nifH* gene encoding for the Fe protein subunit of the nitrogenase reductase is nearly exclusively used to investigate bacterial diazotrophs communities (Figure 1.4).

The oxidation of NH_4^+ into NO_2^- via nitrification, is performed by autotrophic nitrifying bacteria (e.g. *Nitrosomonas*) and archaea (e.g. from the Thraumarchaeota phylum; Zhang *et al.*, 2010), but also by heterotrophic nitrifiers (i.e. bacteria and fungi) (Wrage *et al.*, 2001). The archaeal community was recently shown to be an important player in ammonia-oxidation in soil dominating bacteria (Leininger *et al.*, 2006; Nicol & Schleper, 2006; Nicol *et al.*, 2008). Both bacterial and archaeal ammonia-oxidiser communities seem to be active in different environmental conditions (Gubry-Rangin *et al.*, 2010; Yao *et al.*, 2011). The enzymes from the autotrophic and heterotrophic nitrifiers differ; although substrate, intermediates and products are the same. The microbial communities involved in the oxidation of NH_4^+ into NO_2^- are investigated via the genes encoding for the ammonia monooxygenase enzyme, which is composed of three subunits encoded by *amoA*, *amoB* and *amoC* genes. However, generally in microbial ecology the *amoA* gene, encoding for the first subunit of the enzyme, is investigated for either bacteria or archaea (Nicol & Schleper, 2006) (Figure 1.4). The oxidation of NO_2^- to NO_3^- is performed by bacteria (e.g. *Nitrobacter*) via the enzyme nitrite oxidoreductase encoded by the *nxr* operon. The *nxrA* gene, encoding for the catalytic subunit of the nitrite oxidoreductase in *Nitrobacter* species, can be used to target the nitrite oxidiser community (Poly *et al.*, 2008) (Figure 1.4).

Many taxa of bacteria and archaea are generally involved in the complete process of denitrification, with many of these taxa capable of performing the sequential process entirely (e.g. *Neisseria*, *Pseudomonas*, *Ralstonia*) (Philippot, 2002; Francis *et al.*, 2005). The reduction of NO_3^- to NO_2^- is catalysed by two different nitrate reductase enzymes: one membrane-bound and the other one is periplasmic. The membrane-bound nitrate reductase is composed of three subunits encoded by *narG*, *narH* and *narI* (Philippot, 2005). These genes are organised in an operon, but other genes are required to complete the reductase (Philippot, 2002). The periplasmic nitrate reductase, present only in Gram-negative bacteria, is composed of two subunits encoded by *napA* and *napB* genes, and other genes (e.g. *napC*, *napD*, *napE*) regulate them and are needed to assemble the

enzyme (Zumft, 1997). The reduction of NO_2^- to NO is catalysed by two different metalloenzymes, one copper-reductase and another one cytochrome *cd1*-nitrite reductase which are encoded by *nirK* and *nirS* gene, respectively. Both of these genes are organised in clusters, including several others genes (Philippot, 2002). The reduction of NO to N_2O is catalysed by the nitric oxide reductase which is composed of two subunits encoded by the *norC* and *norB* genes (Zumft, 1997; Philippot, 2002). Both of these genes are generally clustered with other genes. The reduction of N_2O to N_2 is catalysed by the nitrous oxide reductase which is composed of two identical subunits encoded by three transcriptional units: i) *nosZ* gene, ii) *nosR* gene, and iii) *nosDFYL* genes (Philippot, 2002). Fungi are also capable of denitrification, but the process stops at the third step, making N_2O the final product of fungal denitrificaton (Ma *et al.*, 2008). The nitric oxide reductase of the fungi differ from the bacteria, but the limited knowledge of genes involved in this process do not enable targeting of this group (Ma *et al.*, 2008). In microbial ecology, specific functional genes are used to specifically target the microorganisms involved in the different processes of denitrification because they are highly conserved, encoding for subunit of the enzyme: i) *narG* and *napA* are used for the communities reducing NO_3^- to NO_2^- (Flanagan *et al.*, 1999; Gregory *et al.*, 2000) ii) *nirK* and *nirS* gene are used for the communities reducing NO_2^- to NO (Throbäck *et al.*, 2004) iii) *norB* is used for the communities reducing NO to N_2O (Braker & Tiedje, 2003), and iv) the *nosZ* gene is used for the communities reducing N_2O to N_2 (Scala & Kerkhof, 1999) (Figure 1.4).

Little is known about the bacterial community involved in the DNRA process, except that it had been found predominantly in anaerobic environments (e.g. anaerobic sludge and sediments) (Butterbach-Bahl & Gundersen, 2011). However, this process could play an important and valuable role in ecosystems as it provides NH_4^+ for plant and microbial immobilisation, and reduces the amount of NO_3^- available for denitrification (leading to gas emission of N_2O, which is an important greenhouse gas) and leaching. The *nrfA* gene encoding for the calcium-dependant cytochrome *c* nitrite reductase can be used to target this community (Mohan *et al.*, 2004) (Figure 1.4).

Finally, the anammox process performed by bacteria has been mainly investigated in marine ecosystems and in wastewater treatment plants and their role in

terrestrial ecosystems remains unknown (Jetten, 2008). The *hao* gene encoding for the hydroxylamine oxidoreductase has been used to target the bacterial community involved in anammox process (Jentten *et al.*, 2009; Penton *et al.*, 2006) (Figure 1.4).

1.1.4 Microbial communities in arctic soil

Microbial diversity in arctic soils and more widely in Polar Regions and high altitude regions was considered until recently as low (Heal, 1999; Hodkinson & Wookey, 1999), based on the analogy with plant and animal diversity which decreases with increases in latitude and altitude. However, recent studies showed that the bacterial community diversity (i.e. phylotypes richness and diversity) in arctic soils is similar or higher than in other biomes such as boreal forest, tropical forest, temperate forest, grassland, desert, or prairie (Neufeld & Mohn, 2005; Fierer & Jackson, 2006; Lauber *et al.*, 2009; Chu *et al.*, 2010). Different DNA-based methods have been used to determine the bacterial diversity in arctic soils, such as serial analysis of ribosomal sequence tags (Neufeld & Mohn, 2005), terminal restriction length polymorphism analysis (Fierer & Jackson, 2006), but also the latest generation of sequencing: pyrosequencing (Lauber *et al.*, 2009; Chu *et al.*, 2010; Bell *et al.*, 2011), showing the consistency of these results. The diversity of the fungal community was also found to be high in arctic soil, although it was not directly compared to other ecosystems. Wallenstein *et al.* (2007) found in soil samples from Low Arctic tundra (Toolik Lake, Alaska) 6 different phyla, with 19 different orders for the two dominant phyla (i.e. Ascomycetes and Basidiomycetes). The bacterial community involved in N fixation, was investigated via the N-cycling functional gene *nifH* in High Arctic tundra soil from Cambridge Bay (Canada), and its diversity was found to be similar to that from a tropical forest in Venezuela (17 and 19 different phylotypes, respectively), and even higher than a uncultivated temperate pasture from North America which had 11 different phylotypes (Izquierdo & Nüsslein, 2006). Despite the extreme environmental conditions in the Arctic, soil bacterial and fungal community diversities are not negatively affected.

1.1.4.1 Bacterial community in arctic soil

Until recently, only a few studies have investigated microbial community diversity/composition in arctic soils. Nemergut *et al.* (2005) highlighted the lack of knowledge about the bacterial community in arctic soils, indicating that only ~0.2% of bacterial 16S rRNA gene sequences from soil deposited in Genbank originated from arctic tundra soil at the time of their study. Since Nemergut *et al.* (2005), there has been increasing interest in studying microbial communities in arctic soils, probably helped by the International Polar Year 2007-2008. Thus in 2012, 1.1% of the bacterial 16S rRNA gene sequences from soil that were deposited in Genbank originated from arctic tundra soil, indicating a clear increase in the knowledge of bacterial communities in arctic tundra soil (Table 1.1). The bacterial 16S rRNA gene sequences deposited in GenBank from arctic soil up to April 2012, represented 9.5% of all the sequences from soil (Table 1.1), and the actual number of sequences originating from arctic soil (i.e. 55612) is underestimated, as the sequences from Genbank do not include all the sequences obtained by pyrosequencing (Lauber *et al.*, 2009; Chu *et al.*, 2010), but 83.7% of the Arctic soil sequences were from a single study using pyrosequencing (Bell *et al.*, 2011).

Table 1.1: Contribution (%) of bacterial and archaeal 16S rRNA gene sequences and fungal 18S rRNA gene and ITS region sequences from the Arctic soil and Arctic tundra soil, to the total number of sequences from soil samples, deposited in the Genbank nucleotide database[1] up to the 5th of April 2012. The percentage of contribution and the actual number of sequences (between brackets) are given.

	Arctic soil	Arctic tundra soil
16S rRNA Bacteria	9.5% (55612)	1.1% (6195)
16S rRNA Archaea	0.7% (217)	0.05% (16)
18S rRNA Fungi	6.9% (1785)	6.8% (1793)
ITS Fungi	5.8% (2765)	1.8% (873)

[1] http://www.ncbi.nlm.nih.gov/

Hence, Chu *et al.* (2010) obtained 107,879 sequences of the bacterial 16S rRNA gene from 47 samples across 29 sites over the High Arctic region, but represented only 0.02% of the pyrosequencing sequences deposited in the Metagenomics RAST[2] server (Meyer *et al.*, 2008) used by the authors (percentage calculated from the freely available sequences for public use).

Despite the increasing number of studies investigating bacterial communities in arctic soils, understanding of the extent to which bacterial diversity in the Arctic region is specific or differ from other ecosystems remain limited. Hence, 96.3% of the bacterial 16S rRNA gene sequences deposited in GenBank from arctic soil are characterised as uncultured bacteria without further phylogenetic assignment (Figure 1.5). The absence of phylogenetic assignment may indicate that some of these sequences (i.e. 53 541) are from new organisms, and potentially specific to arctic ecosystems, as it has been already reported by early DNA-based study in the Arctic (Neufeld & Mohn, 2005). However, 87% of these sequences were from the pyrosequencing analysis deposited by Bell *et al.* (2011) that were assigned in their study, indicating the limitation of GenBank to give accurate phylogenetic assignment. Nevertheless, from the sequences with a phylogenetic assignment, the bacterial diversity was found to be dominated by Proteobacteria (39.4%), especially the β, α and γ Proteobacteria, then the Actinobacteria (19.0%), Acidobacteria (10.3%) and Cyanobacteria (9.2%; Figure 1.5). This distribution of the dominant bacteria phylum/group was similar to that found by Chu *et al.* (2010) and Bell *et al.* (2011) using pyrosequencing analysis, although the dominance between the class of Proteobacteria differed, and Acidobacteria were more abundant than Actinobacteria for both studies.

1.1.4.2 Archaeal community in arctic soil

In contrast, the archaeal community in arctic soils has received far less attention than the bacterial community. Only 0.7% of the archaeal 16S rRNA gene sequences deposited in GenBank from soil originated from arctic soils (Table 1.1). Moreover, only 0.05% of the archaeal 16S rRNA gene sequences originate from arctic tundra soil, and

[2] http://metagenomics.anl.gov/?page=Home

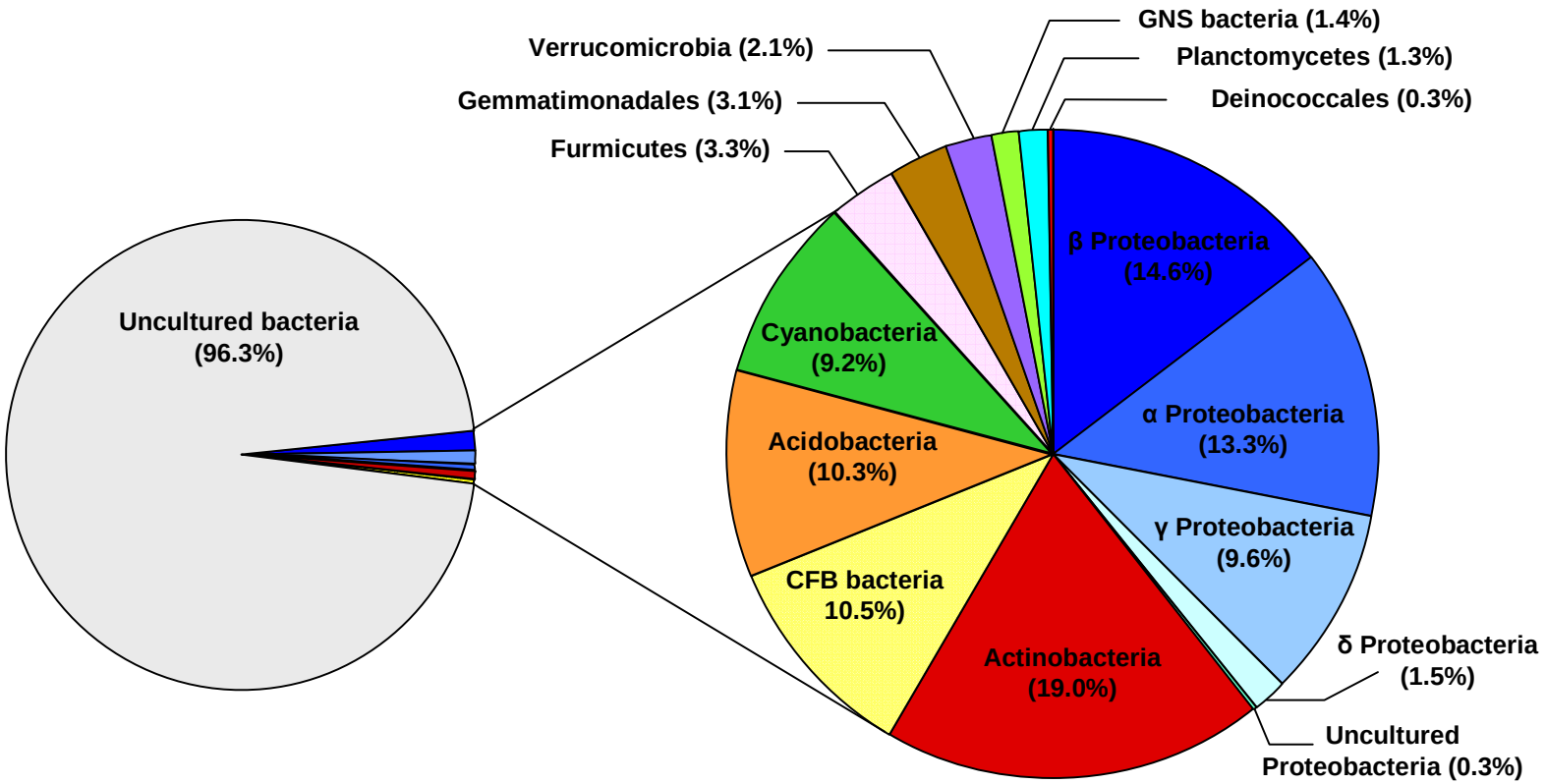

Figure 1.5: Distribution of phyla and orders from the bacterial 16S rRNA gene sequences originating from arctic soil that were deposited in Genbank nucleotide database up to 5th of April 2012. The total number of sequences was 55 612. The percentages correspond to the proportion of each phyla/order to the total number of sequences (i.e. 55 612) or to the total number of sequences with a phylogenetic assignment (i.e. 2071). CFB bacteria correspond to Cytophaga-Flavobacteria-Bacteroides bacterial group. GNS bacteria correspond to Green non-sulphur bacterial group.

correspond to 16 sequences coming from a single study in Low Arctic tundra (Chu *et al.*, 2011). Most of the studies investigating the archaeal community have focused on permanently wet ecosystems, such as acidic wetland (Wilhelm *et al.*, 2011) and peat (Høj *et al.*, 2006), representing 90.8% of the ecosystems studies (Figure 1.6 A). This is explained by the particular interest in the archaeal methanogenic community present in these wet ecosystems, and the fact that CH_4 emissions from arctic wetland represents nearly 6% of the total global CH_4 emissions sources (Høj *et al.*, 2005). CH_4 is an important greenhouse gas, and in the context of climate change, arctic emissions could increase. Thus, several studies have investigated the archaeal methanogenic community in arctic wet ecosystems and permafrost (Høj *et al.*, 2005; 2006; Ganzert *et al.*, 2007; Metje & Frenzel, 2007; Rooney-Varga *et al.*, 2007; Høj *et al.*, 2008). Hence, the number of archaeal methanogenic 16S rRNA gene sequences from peat and permafrost deposited in GenBank up to April 2012 was 192.

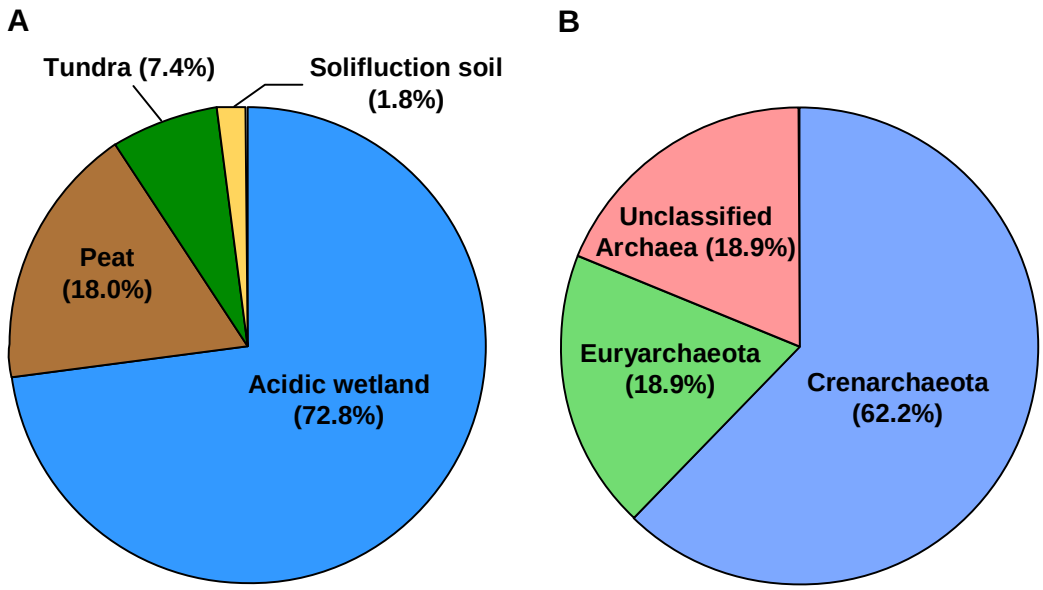

Figure 1.6: Distribution of **A)** different arctic ecosystems, and **B)** different phyla of the archaeal 16S rRNA gene sequences originating from arctic soil that were deposited in Genbank nucleotide database up to 5th of April, 2012**.** The sequences originated from 4 studies investigating different soils: acidic wetland (Wilhelm *et al.*, 2011), peat (Høj *et al.*, 2006; Barott and Lipson, unpublished), tundra (Chu *et al.*, 2011) and solifluciton soil (Høj *et al.*, 2006). The percentages correspond to the proportion of each ecosystems A) or phyla B) based on the total number of sequences (i.e. 217).

However, the limited knowledge of the archaeal community from non-permanently wet ecosystems does not enable determination of the actual archaeal diversity, their potential functions and their importance in arctic ecosystems. From the 217 archaeal 16S rRNA gene sequences retrieved from GenBank, 62.2% were related to Crenarchaeota, and Euryarchaeota and unclassified archaea both represented 18.9% of the sequences (Figure 1.6 B). Interestingly, all the Crenarchaeota sequences were not assigned beyond the class Thermoprotei, and for Euryarchaeota sequences, only 9 and 5 sequences were assigned to the order Methanomicrobiales and Methanosarcinales (Wilhelm *et al.*, 2011). The absence of phylogenetic assignment may indicate that the sequences are from new organisms that are potentially specific to arctic ecosystems. Thus, more studies are needed to investigate the entire archaeal community in order to evaluate its diversity and its ecological significance.

1.1.4.3 Fungal community in arctic soil

The fungal community in the Arctic has been studied more than the archaeal community but far less than the bacterial community. Approximately 6.9% of the fungal 18S rRNA gene sequences and 5.8% of the ITS region sequences from soil deposited in GenBank up to April 2012 originated from arctic soil, representing in total for both gene/region 4550 sequences (Table 1.1). Nearly 100% of the fungal 18S rRNA gene sequences were from arctic tundra soil, but from only two studies (Table 1.1), one accounting only for 0.8% of the Arctic tundra soil sequences (Chu *et al.*, 2011) and another one accounting for 99.2% of the sequences (Wallenstein *et al.*, 2007). However, only 1.8% of the fungal ITS sequences from soil deposited in GenBank were from arctic tundra soil, apparently coming from a single study which was not freely accessible, which did not allow confirmation of the origin of these sequences. Another 814 fungal ITS region sequences from arctic soil were from arctic tundra, coming from a single study for nearly 100% (Geml *et al.*, 2012). About 24.8% of the fungal ITS region from arctic soil were related to the boreal forest (Taylor *et al.*, 2007; 2008; Geml *et al.*, 2009), and in GenBank about 2406 sequences of the ITS region were from arctic forest and sometimes came from different studies than those found for arctic soil (Bent *et al.*,

2011). In GenBank, 7240 sequences from the fungal ITS region originated from the Arctic, showing that looking for sequences using "Soil" lead to an underestimation of the real number of sequences/studies in the Arctic. Using "Arctic root", 1089 sequences of the ITS region were found in GenBank, related to studies mainly investigating ectomycorrhizal fungi (Milne *et al.*, 2006; Bjorbækmo *et al.*, 2010; Fujiyoshi *et al.*, 2011). The distribution of sequences of the fungal ITS regions and 18S rRNA gene in GenBank, showed that only a few studies have investigated soil from arctic tundra (Wallenstein *et al.*, 2007; Chu *et al.*, 2011; Geml *et al.*, 2012), and that many studies focused on ectomycorrhizal fungi in the Arctic (Milne *et al.*, 2006; Fujimura *et al.*, 2007; Bjorbækmo *et al.*, 2010; Fujiyoshi *et al.*, 2011; Walker *et al.*, 2011; Geml *et al.*, 2012). Thus, despite the importance of saprotrophic fungi to recycle soil organic matter, the knowledge of this community in the Arctic is likely to be limited.

Nevertheless, based on the fungal ITS region sequences deposited in GenBank from arctic soil, fungal diversity was dominated by two phyla, the Basidiomycetes and Ascomycetes, accounting for ~40% and ~20% of the sequences, respectively (Figure 1.7). The dominance of these two phyla was also found by Wallenstein *et al.* (2007) in Low Arctic tundra, where these two phyla accounted for more than 80% of the fungal 18S rRNA gene sequences, with the Basidiomycetes accounting for more than 50%. The fungal ITS region sequences showed high diversity of at the order level (Figure 1.7), but the dominant order and classes differed from those identified by Wallenstein *et al.* (2007), with the exception of the order Agaricales which was also found to be also dominant.

Microbial communities involved in the N-cycle have been investigated in arctic regions using N-cycling functional genes as proxies to the different processes of the N-cycle (see section 1.3.2). Hence, the presence of different N-cycling functional genes was confirmed in arctic soils, such as: *nifH* genes encoding for N fixation were found within different arctic tundra soils (Deslippe *et al.*, 2005; Deslippe & Egger, 2006; Izquierdo & Nüsslein, 2006; Walker *et al.*, 2008); *amoA* genes encoding the first step of

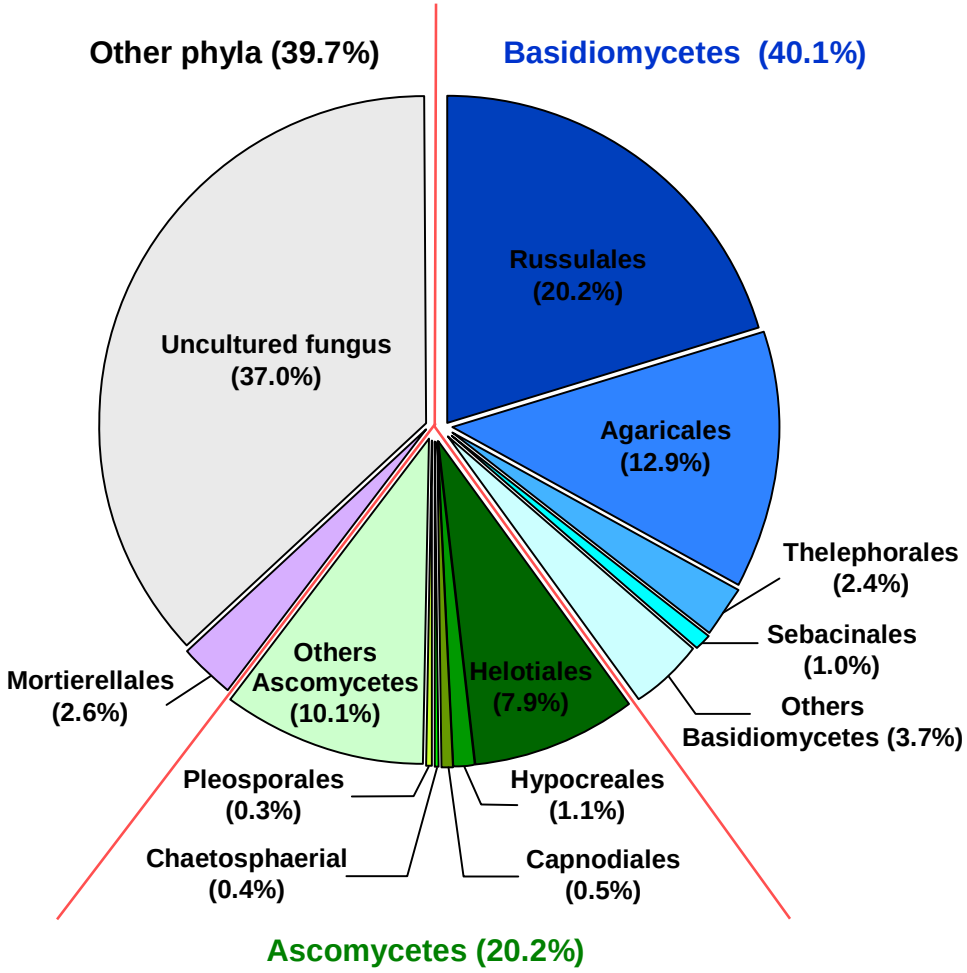

Figure 1.7: Distribution of phyla and orders of the fungal ITS region sequences originating from arctic soils that were deposited in Genbank nucleotide database up to 5th of April 2012. The percentages correspond to the proportion of each phyla/order to the total number of sequences (i.e. 2794).

nitrification were investigated in wet sedge meadow (Ma *et al.*, 2007; Siciliano *et al.*, 2009), permafrost (Yergeau *et al.*, 2010), dwarf shrub tundra (Lamb *et al.*, 2011); and different functional genes involved in denitrification were investigated in arctic tundra soil, such as *nirK*, *nirS* (Siciliano *et al.*, 2009; Yergeau *et al.*, 2010) and *nosZ* gene (Ma *et al.*, 2008; Walker *et al.*, 2008; Siciliano *et al.*, 2009; Yergeau *et al.*, 2010; Lamb *et al.*, 2011). However, the diversity of these different N-functional genes remains largely unknown. Thus, only 43 *nifH* gene sequences (Deslippe & Egger, 2006; Izquierdo & Nüsslein, 2006; Wartiainen *et al.*, 2006), 16 bacterial *amoA* gene sequences, and 7 *nosZ* gene sequences (Ma *et al.*, 2007) were found in GenBank to be related to arctic soils and

no other functional genes (i.e. *amoA* archaea, *nxrA*, *napA*, *narG*, *nirK*, and *nirS* genes) have been found from arctic soils.

Overall, the knowledge of microbial community diversities (i.e. bacteria, archaea fungi, N-functional genes) in arctic region remains limited.

1.5 Effects of N deposition

The effects of N addition have been studied in many terrestrial ecosystems, focusing on N fate and budget in soil, and responses of plant, microorganisms and soil invertebrates. N addition refers to two different types of studies simulating either N fertilisation or N deposition. The main difference between N fertilisation and N deposition is the rate of N addition which is higher for N fertilisation and the form of the N addition (e.g. solid or liquid, and NPK or NH_4NO_3). Defining the rate of N addition for both types is directly related to the site studied, as N deposition varied from 1 kg N ha^{-1} yr^{-1} to above 50 kg N ha^{-1} yr^{-1} depending on the location. Thus, the use of 50 kg N ha^{-1} yr^{-1} can be considered as representing "N fertilisation" in the Arctic while it could be considered as representing "N deposition" in temperate forest. Thus, throughout the thesis, the distinction will be made between N deposition and N fertilisation based, for each ecosystem/location discussed, on the background of atmospheric N deposition and on the type of N addition.

1.5.1 Effect of N deposition on soil and plant

The response of terrestrial ecosystems to N deposition changes with ecosystem characteristics and the amount of deposition. The N status of the ecosystem, soil texture, rate of deposition, precipitation and extent of plant cover directly influences the ecosystem response (Matson *et al.*, 2002). The ecosystem response can be studied using the "N saturation" concept, which is defined as ecosystem condition where "availability of mineral N exceeds the combined nutritional demands of plant and microbes" (Ågren & Bosatta, 1988; Aber *et al.*, 1989). N saturation involved a succession of ecosystem changes in response to N input. In N limited ecosystems, such as temperate forests

(Vitousek & Howarth, 1991), firstly N is retained by an increase in biomass (plant and microbial) - assuming N is limiting and thus increases biomass - until N inputs exceed the ability of this biomass to retain N. Then the ecosystem loses its N into solution or via gaseous fluxes. Ecosystems that are not N limited, such as most tropical forests, are likely to lose N more readily (Matson *et al.*, 1999). Furthermore, leaching of N can occur before N saturation. Other nutrients (e.g. P) can also limit biomass growth, so N is not always limiting.

Leaching of N can be accelerated by many factors such as precipitation events, snowmelt, climate, topography, soil texture and plant cover (Fenn *et al.*, 1998; Matson *et al.*, 2002). Moreover, N leaching can leach counter-ions. Thus, NO_3^- leaching and its negative charge can remove positively charged minerals (e.g. calcium, magnesium and potassium), decreasing soil fertility (Vitousek *et al.*, 1997). N deposition can lead to soil acidification, by changing the balance between proton-producing (i.e. nitrification, plant assimilation and NO_3^- immobilisation) and proton consuming (i.e. denitrification, plant assimilation and NH_4^+ immobilization) processes, and NO_3^- leaching is also an important process within soil acidification.

N deposition also affects the composition and diversity of plant communities. Decreases in plant richness (e.g. vascular plant and bryophytes) in semi-natural and natural ecosystems such as grassland and heathland, due to N deposition have been found in Europe (Bobbink *et al.*, 1998; Stevens *et al.*, 2004; Suding *et al.*, 2005; Duprè *et al.*, 2010; Maskell *et al.*, 2010; Phoenix *et al.*, 2012).

1.5.2 Effect of N deposition on microbial communities

Microbial biomass was found to either decrease (DeForest *et al.*, 2005; Schmidt *et al.*, 2004; Wallenstein *et al.*, 2006), increase (Waldrop *et al.*, 2004) or not change (Gallo *et al.*, 2004) in response to N deposition. Nevertheless, Treseder (2008), in a meta-analysis of 29 N addition studies, found a decrease of ~15% of microbial biomass which decreased more under high N addition. For example, Deforest *et al.* (2004) estimated a microbial biomass decrease of ~18% in a temperate forest soil amended with 30 kg NO_3^- ha^{-1} yr^{-1}. The bacterial biomass did not decrease significantly after N

deposition (DeForest *et al.*, 2005; Treseder, 2008) although increases or decreases in biomass of specific bacterial taxa occurred (Nilsson *et al.*, 2007; Högberg *et al.*, 2007; Nemergut *et al.*, 2008). Fungal biomass seems to decrease with N addition (Frey *et al.*, 2004; Treseder, 2004; Högberg *et al.*, 2007), although Treseder (2008) did not observe an overall significant decrease with N addition in a meta-analysis. Fungi seem to be more sensitive to N additions than bacteria (Frey *et al.*, 2004). The decrease of mycorrhizal fungi may explain part of the microbial biomass decline (Treseder, 2004). Ectomycorrhizal and arbuscular mycorrhizal fungi biomass decreased with N addition (Lilleskov *et al.*, 2002; Frey *et al.*, 2004; Waldrop *et al.*, 2004; Nilsson *et al.*, 2007). Indeed, an increase in N availability for plants can result in a reduction of C allocated to mycorrhizal fungi (Treseder, 2004). However, decreases of mycorrhizae cannot alone explain these microbial biomass decreases. Microbial, bacterial and fungal biomass alone are not sufficient to assess the effects of N deposition and it is important to focus on microbial guilds to understand which microorganisms and functions change and why. Moreover, several techniques were used to assess microbial biomass, such as PLFA profiling (Deforest *et al.*, 2004; Gallo *et al.*, 2004; Högberg *et al.*, 2007; Nilsson *et al.*, 2007), chloroform fumigation (Schmidt *et al.*, 2004; Waldrop *et al.*, 2004) or culture and cell count techniques (Frey *et al.*, 2004), which can give different results on the same samples.

Microbial activity can increase, decrease or remain unchanged after N addition. These changes depend on the activities studied and seem to be ecosystem-specific (Waldrop *et al.*, 2004). In some studies an overall decrease of microbial activity has been observed (Schmidt *et al.*, 2004). N addition reduced microbial activity and thus microbial respiration. Several studies found a decrease of CO_2 emissions after N additions (Bowden *et al.*, 2004; Frey *et al.*, 2004; Schmidt *et al.*, 2004; Wallenstein *et al.*, 2006) and Treseder (2008) in a meta-analysis found a significant decline of CO_2 emissions occurring with decreasing microbial biomass. Thus, a reduction in soil CO_2 emissions due to N addition indicates a potential decrease in microbial biomass and/or activity. N addition was found to reduce ligninolitic enzyme activity in soil by the reduction of phenol oxidase and peroxidase enzyme activity produced by white-rot fungi (Carreiro *et al.*, 2000; Deforest *et al.*, 2004; Frey *et al.*, 2004; Gallo *et al.*, 2004;

Waldrop *et al.*, 2004; Sinsabaugh *et al.*, 2005). Conversely, cellulase, phosphatase and glucosidase activity increased after N addition within the soil and litter (Carreiro *et al.*, 2000; Saiya-Cork *et al.*, 2002; Gallo *et al.*, 2004; Sinsabaugh *et al.*, 2005). Sinsabaugh *et al.* (2005) proposed that oxidative enzymatic activities (e.g. phenol oxidase) decrease and hydrolytic enzymatic activities (e.g. cellulase) increase in response to N addition, increasing decomposition of labile organic matter (cellulose) and decreasing decomposition of complex organic matter (lignin). These changes in microbial activities can be explained by changes in microbial community composition. Waldrop *et al.* (2004) proposed that N additions would shift microbial community composition from fungi to less efficient bacteria.

Both changes in microbial community structure and diversity (Egerton-Warburton & Allen, 2000; Lilleskov *et al.*, 2002; Frey *et al.*, 2004; Waldrop *et al.*, 2004; Nilsson *et al.*, 2007; Nemergut *et al.*, 2008) and an absence of changes in structure and diversity (Gallo *et al.*, 2004; Robinson *et al.*, 2004; Deforest *et al.*, 2005) have been found after N addition. The use of different techniques, such as phospholipids fatty acid (PLFA) profiling, DNA sequencing, with different resolution levels may partly explain these differences. Moreover microbial distribution within the soil is not homogeneous, with different microbial communities in different soil horizons (e.g. Hartmann *et al.*, 2009) and different soil fractions (Ranjard & Richaume, 2001). Most studies have sampled within different horizons of soil and sometimes in soil litter. Some studies have sampled the top 0-5 cm of soil (Nilsson *et al.*, 2007; Nemergut *et al.*, 2008), others the top 0-10 cm (Frey *et al.*, 2004; Waldrop *et al.*, 2004), 0-20 cm (Gallo *et al.*, 2004) or across different horizons (Deforest *et al.*, 2004). All these studies assessed the microbial community structure at different scales which are likely to represent different habitats for microorganisms and more importantly within different ecosystems.

In contrast to the bacterial and fungal communities, extremely little is known about the response of archaeal communities to N deposition despite the major role of archaea in ammonia oxidation (Leininger *et al.*, 2006; Nicol & Schleper, 2006; Nicol *et al.*, 2008). Nemergut *et al.* (2008) have shown that the archaeal to bacterial ratio decreased by ~20 % after N addition in alpine tundra, highlighting the sensitivity of archaeal communities to N addition. Similarly, little is known on the effect of N

deposition on microbial communities involved in soil N cycling. N availability influences the balance between microbial communities involved in N processes. N fixation, a relatively energy-intensive process (Vitousek *et al.*, 2002), decreased after N addition (Vitousek *et al.*, 2002; Compton *et al.*, 2004). In contrast, nitrification increased in N amended soil (Fisk & Schmidt, 1996), whilst bacterial ammonia monoxygenase (*amoA*) gene abundance (i.e. oxidizing NH_4^+), also increased after N fertilization (Compton *et al.*, 2004). In contrast, the archaeal community, comprising a large part of NH_4^+ oxidation, decreased in *amoA* gene abundance (He *et al.*, 2007), diversity (Gattinger *et al.*, 2007) after N addition. Nitrifying archaeal communities may be more sensitive to N addition than bacteria (e.g. due to changes in pH) or out-competed by bacteria (Nemergut *et al.*, 2008). N additions, also increased denitrification rates, and shifts in the denitrifying community occurred (Enwall *et al.*, 2005). N availability clearly drives shift between N processes driven by different microorganisms. However, our understanding of the effects of N deposition on the whole soil microbial N cycling community remains limited.

1.5.3 Effects of N deposition on arctic ecosystems

Arctic tundra plant communities have shown sensitivity to N addition. Hence, the biomass of vascular plants can increase with nutrient additions, whilst bryophyte and lichen biomass decreases (Gordon *et al.*, 2001; Van Wijk *et al.*, 2004). In contrast, the understanding of microbial community response to N deposition is still limited, despite the key role played by the microbial community in biogeochemical cycles.

Several studies have investigated the response of microbial communities to N additions in the Arctic, and the results of the main studies are summarised in Table 1.2 for the fungal community and Table 1.3 for the bacterial community. However, most studies simulated N fertilisation rather than N deposition, using high rates of N addition such as 100 kg N ha^{-1} yr^{-1}, and addition of N, P and K simultaneously. Moreover, some studies applied N and other nutrients in solid form (e.g. pellets) reducing the homogeneous distribution of nutrients in soil (Urcelay *et al.*, 2003; Clemmensen *et al.*, 2006; Deslippe *et al.*, 2011). The length of some experiment lasted for more than a

decade, leading to an extremely high total N load, such as 1250 kg N ha^{-1} over 15 years (Rinnan *et al.*, 2007). Nitrogen fertilisation was originally used in the Arctic to simulate increase in nutrient availability due to increases in soil mineralisation rates in response to warming (Hobbie, 1996). However, recent plot scale experiments showed that N fertilisation and soil warming do not have the same effect on bacterial, fungal and ectomycorrhizal communities (Rinnan *et al.*, 2007; Deslippe *et al.*, 2011) and sometimes opposite effects. Thus, results from N fertilisation studies in the Arctic cannot be used as a proxy for the impact of warming on soil microbial communities. On the 12 studies summarised in Table 1.2 and 1.3, only 2 studies can be considered as simulating N deposition (Robinson *et al.*, 2004; Stapleton *et al.*, 2005), by using a low rate of N addition (i.e. 5 or even lower kg N ha^{-1} yr^{-1}) and by adding only N. Neither of these studies used DNA-based methods to investigate the response of microbial communities to N deposition enabling targeting of a higher proportion of the microbial community and targeting the bacterial, archaeal and fungal community separately.

Despite the differences between N deposition and N fertilisation, and the differences in rate, form and duration of N addition, the results from studies investigating the response of the microbial community to N addition showed some similar trends. The response of the fungal community to N addition was more widely studied than the bacterial community, with a particular emphasis on mycorrhizal fungi. Fungal diversity, including the ectomycorrhizal diversity seems to be reduced by N addition (Woodin, 1997; Robinson *et al.*, 1998; Deslippe *et al.*, 2011), but saprotrophic fungi diversity and richness were not found to be affected by N addition (Robinson *et al.*, 2004). Fungal biomass was generally found to increase with N additions in arctic soil, which could be related to an increase of saprotrophic fungi (Deslippe *et al.*, 2011), although Schmidt *et al.* (2000) found a decrease in total fungal biomass. Roots colonisation by ectomycorrhizal fungi was found either to decrease (Urcelay *et al.*, 2003), or to not change after N addition (Clemmensen *et al.*, 2006; Deslippe *et al.*, 2011).

Bacterial community structure seems to be affected by N addition in the Arctic (Schmidt *et al.*, 2000; Rinnan *et al.*, 2007), although Lamb *et al.* (2011) did not find any changes. Changes in bacterial community structure were sometimes related to changes

in the dominance from Gram-negative bacteria to Gram-positive bacteria (Table 1.3). However, changes in bacterial/microbial biomass or abundance are inconsistent, although Rinnan *et al.* (2007) found an increase in bacterial abundance in the organic horizon only (0-5 cm depth) in subarctic heath, and Stapleton *et al.* (2005) an increase in bacterial abundance in High Arctic tundra but only after the first year of N application and not the second year. Only a few studies have investigated the microbial activity *in situ* after N addition finding different results (Table 1.3).

Despite the importance of archaeal community in the first step of nitrification, there have been no studies that have investigated their response to N deposition in the Arctic. Moreover, Nemergut *et al.* (2008) found that archaeal community abundance and diversity was negatively affected by N addition in alpine tundra in Colorado Rocky Mountains. Similarly, only two studies have investigated the response of N-functional genes to N addition in the Arctic. Deslippe *et al.* (2005) found no effect of N fertilization (i.e. 10 kg N ha^{-1} yr^{-1}, NPK, 1 year of treatment) on the structure of the *nifH* community but a significant increase (~3.7 times) in nitrogen fixation activity between 19 and 35 days post fertilisation in High Arctic. Lamb *et al.* (2011) did not find any significant change in the structure and abundance of bacterial *amoA*, Crenarchaeal *amoA* and *nosZ* genes after 15 years of NPK addition (see Table 1.3) at the same site as Deslippe *et al.* (2005).

Overall, the response of the different microbial communities (i.e. bacterial, archaeal, fungal and N-functional guild) to N deposition is largely unknown and requires research to determine the impact of N deposition on microbial communities in arctic regions.

1.6 Research objectives

The High Arctic tundra is a nutrient poor ecosystem, receiving chronic and perhaps, more importantly, acute episodic nitrogen deposition, during which a high percentage of annual N deposition is deposited in few days (Hodson *et al.*, 2005; 2010; Kühnel *et al.*, 2011). Thus, acute N deposition can represent significant N inputs into this N scarce ecosystem. Furthermore, N deposition is occurring

Table 1.2: Main results found in the literature investigating the response of the fungal community structure and abundance to N addition (i.e. N fertilisation and N deposition) in plot-scale experiments in arctic regions. The studies are classified between N fertilisation and N deposition, and by increasing rate of N addition. Some studies also investigated the response to warming, shading or water addition, but only the treatments focusing on N addition were shown. When studies used N and P/K treatments separately and concomitantly, only the results related to N addition were shown. = indicates no changes in bacterial community; ≠ indicates changes in fungal community; ↑ indicates increase in bacterial abundance or activity; ↓ indicates decrease in bacterial abundance or activity.

N addition type	Rate & form of N addition (kg N ha^{-1} yr^{-1})	Length of N addition	Structure Diversity	Abundance Biomass	Soil sampling depth (cm)	Location	Reference
N fertilisation	10		↓ fungal diversity	↓ mycorrhizal colonisation		Svalbard	Woodin (1997)
	50 NPK	4 yr		↓ fungal PLFA abundance	0-10	Abisko (Sweden)	Schmidt *et al.* (2000)
	50 NH_4NH_3 + KH_2PO_4 + KCl	5 yr	↓ fungal diversity (not significant)	↑ fungal colonies	Dead leaves	Ny-Ålesund (Svalbard)	Robinson *et al.* (1998)
	100 NH_4NH_3 P_2O_5	3 yr		↓ ~50% ectomycorrhizal colonisation	Roots	Toolik Lake (Alaska)	Urcelay *et al.* (2003)
	100 NPK	6 yr		↑ ergosterol concentration	Upper horizon	Abisko (Sweden)	Ruess *et al.* (1999)

N addition type	Rate & form of N addition (kg N ha^{-1} yr^{-1})	Length of N addition	Structure Diversity	Abundance Biomass	Soil sampling depth (cm)	Location	Reference
N fertilisation	100 NH_4NH_3 + KH_2PO_4/P_2O_5 + KCl	6, 14 yr		↑ ergosterol litter, 0-5 cm ↑ ectomycorrhizal mycelia production	Roots, litter, 0-5, 5-10, and > 10	Abisko (Sweden)	Clemmensen *et al.* (2006)
	100 NH_4NH_3 + KH_2PO_4 + KCl	14 yr		↑ ergosterol: 40% 0-5 cm, 31% 0-10 cm ↑ fungal PLFA: 16% 0-5 cm, 5% 0-10 cm	0-5 5-10	Abisko (Sweden)	Rinnan *et al.* (2007)
	100 NH_4NH_3 + P_2O_5	18 yr	↓ ectomycorrhizal diversity	= root tip colonisation by ectomycorrhizal ↑ proportion of saprotrophic	Roots	Toolik Lake (Alaska)	Deslippe *et al.* (2011)
N deposition	5, 50 NH_4NH_3	1 yr	= saprotrophic richness, = saprotrophic diversity		Organic & mineral soil	Ny- Ålesund (Svalbard)	Robinson *et al.* (2004)

Table 1.3: Main results found in the literature relating to the response of bacterial community structure abundance and activity to N addition (i.e. N fertilisation and N deposition) in plot-scale experiments in arctic regions. The studies are classified between N fertilisation and N deposition, and by increasing rate of N addition. Some studies also investigated the response to warming, shading or water addition, but only the treatments focusing on N addition were shown. When studies used N and P/K treatments separately and concomitantly, only the results related to N addition were shown. = indicates no changes in bacterial community; ≠ indicates changes in bacterial community; ↑ indicates increase in bacterial abundance or activity; ↓ indicates decrease in bacterial abundance or activity.

N addition type	Rate & form of N addition (kg N ha^{-1} yr^{-1})	Length of N addition	Structure Diversity	Abundance Biomass	Activity	Soil sampling depth (cm)	Location	Reference
N Fertilisation	2, 10 NPK	15 yr	= structure (DGGE)			Upper horizon	Nunavut (Canada)	Lamb *et al.* (2011)
	37.5 NH_4NH_3 Na_2HPO_4	2 yr		= microbial biomass	= soil respiration	0-12	Zackenberg (Greenland)	Illeris *et al.* (2003)
	50 NPK	4 yr	≠ in microbial structure (PLFA)	= bacterial PLFA ↑ Gram+ Gram- ratio		0-10	Abisko (Sweden)	Schmidt *et al.* (2000)
	100 NH_4NH_3 + H_2PO_4 + KCl	15 yr	≠ in bacterial structure (PLFA)	↑ 22% bacterial PLFA in 5-10 cm ↑ Gram+ Gram- ratio		0-5 5-10	Abisko (Sweden)	Rinnan *et al.* (2007)
N deposition	1, 5 NH_4^+ or NH_3^-	2 yr		↑ abundance with NH_4^+	↑ bacterial production with NH_4^+ addition	0-3	Ny- Ålesund (Svalbard)	Stapleton *et al.* (2005)

simultaneously with climate change, influencing these systems that are constrained by extreme climatic conditions. Hence, N deposition in High Arctic tundra might be an important driver of the soil microbial communities, which dominate the N-cycle, and may change microbial community structure, diversity, abundance and activity.

The overall aim of this PhD was to determine the response of microbial communities to acute atmospheric N deposition events in High Arctic tundra soil. The specific objectives of this study were to:

1) Determine variation of bacterial, archaeal and fungal communities structure and abundance within different soil horizons, and over time.

2) Determine the environmental drivers of the bacterial, archaeal and fungal communities within High Arctic tundra soil.

3) Determine the response of bacterial, archaeal and fungal communities structure and abundance to atmospheric N deposition within different soil horizons in High Arctic tundra soil.

4) Determine the response to N deposition of the microbial communities directly involved in the different processes of the N-cycle.

To address these objectives, a plot scale experiment (established in summer 2009 on the High Arctic tundra at Ny-Ålesund, Svalbard) and a microcosm experiment were used to simulate acute N deposition on High Arctic tundra soil. Soil samples from the organic and mineral horizons were taken over time. Firstly, changes in soil characteristics (e.g. soil water content, soil pH, total N) were measured for both soil horizons over time. Secondly, variation in microbial communities (i.e. bacterial, archaeal, fungal and N-functional guilds) structure, abundance and diversity were investigated using a DNA-based approach, from soil samples of the organic and mineral horizons.

The objectives of this study were addressed in the different results chapters (i.e. 3 to 6) of this thesis. These chapters are in preparation or have been submitted for publication and/or have been presented at scientific conferences (see Appendix 1.1). The outline of the results chapter is as follows:

Chapter 3: "Short-term variability of bacterial, archaeal and fungal community structure and abundance within High Arctic tundra soil horizons". This chapter assesses the variation in structure and abundance of microbial communities in the organic and mineral soil horizons from the plot experiment, at the end of the summer in 2009, and highlight the potential environmental drivers of the microbial communities (objectives 1 and 2).

Chapter 4: "Impacts of acute nitrogen deposition on the structure and abundance of microbial communities within High Arctic tundra soil". This chapter assesses the variation in the structure and abundance of microbial communities (i.e. bacterial, archaeal and fungal) in response to simulated acute atmospheric N deposition at the plot-scale experiment (objective 3).

Chapter 5: "Distribution of N-cycling functional genes within High Arctic tundra soil". This chapter assesses the presence of the microbial N-functional guilds in the organic and mineral soil horizons and their potential response to atmospheric N deposition (objectives 1 and 4).

Chapter 6: "A microcosm experiment to evaluate the impact of precipitation and nitrogen deposition on the structure and abundance of microbial communities in different soil horizons of High Arctic tundra". A microcosm experiment was used in this chapter to assess the specific response of microbial communities within the organic and mineral horizons to the same N deposition event, with same amount of N and same increase in soil water content (objectives 2 and 3).

This PhD was part of a multidisciplinary European project named NSINK[3], studying the enrichment of High Arctic terrestrial and aquatic ecosystems by reactive atmospheric nitrogen from low latitude emission centres. This project allowed collaboration with several PhD/Postdoctoral fellows and especially Sonal Choudhary, PhD student at the University of Sheffield (supervised by Dr Gareth Phoenix) working on the same plot experiment and focusing on the response of plant community to N deposition.

[3] http://nsinkproject.group.shef.ac.uk/NSINK/Home.html

Chapter 2: Materials & Methods

The plot experiment at Leirhaugen, before the first N application, the 21st of August 2009.

2.1 Materials

2.1.1 Study site

The research site was located at Leirhaugen (78º55'231"N, 11º49'819"E), 1.95 km to the South West of Ny-Ålesund in Svalbard, High Arctic (Figure 2.1). Plant cover was composed mainly of bryophytes (43%), *Salix polaris* Wahlend (32%) and lichens (16%) (S. Choudhary, personal communication; Figure 2.2). The soil comprised an organic horizon (1 – 5 cm) over a mineral horizon.

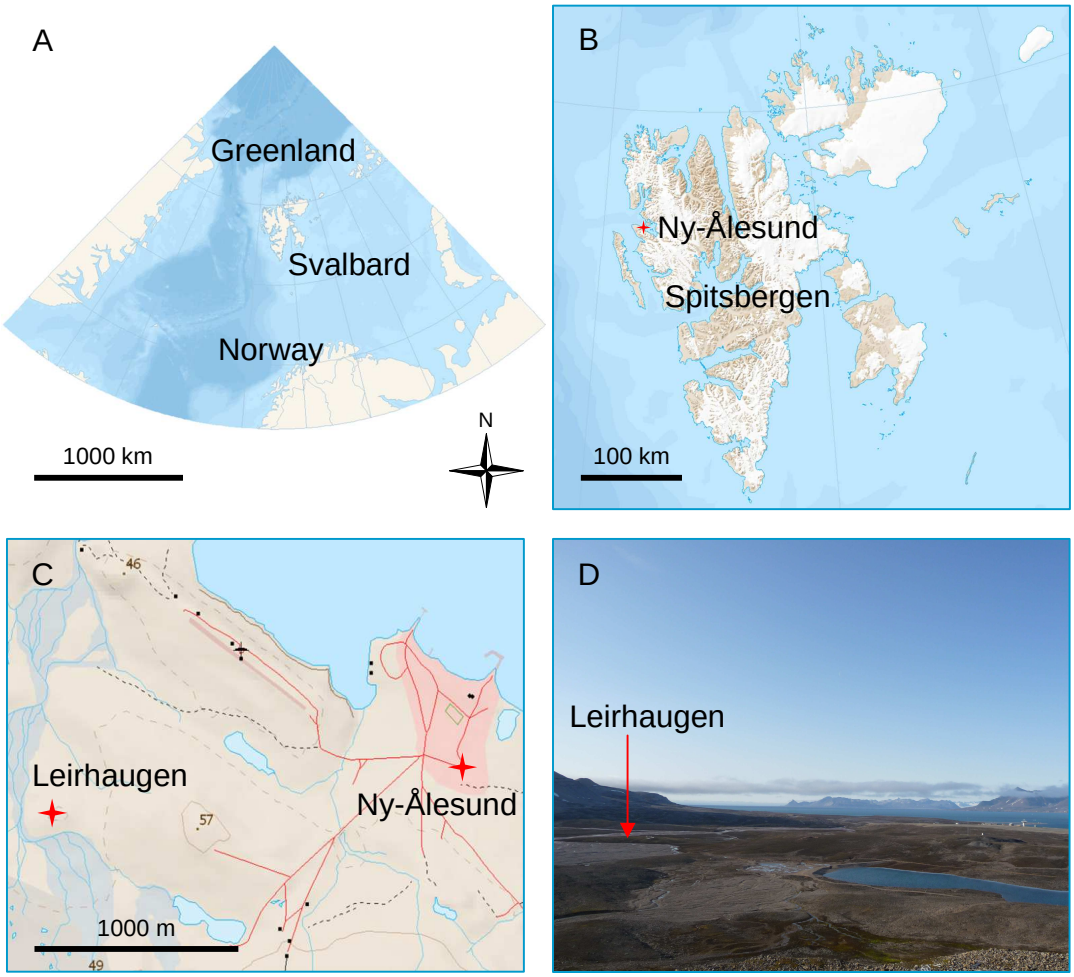

Figure 2.1: Map of Svalbard archipelago (A, B) and, map and photo of Leirhaugen study site (C, D). Map image from Norwegian Polar Institute[4].

[4] http://eivind.npolar.no/Geocortex/Essentials/Web/viewer.aspx?Site=svbk_v01_no&ReloadKey=True

2.1.2 Bacterial stains and plasmids

Clone library construction involved the use of the bacteria *Escherichia coli* (One Shot® TOP10 Chemically competent cells) with the pCR®4-TOPO plasmid (Invitrogen, Paisley, UK).

2.1.3 Buffer and solutions

Tris acetate EDTA (TAE) buffer solution (50x stock solution) was used to make agarose gel (see section 2.2.5.3):
2 M Tris
1 M glacial acetic acid
0.05 M EDTA (pH = 8.0)

2.1.4 Media

The following media were used for clone library construction (see section 2.2.5.5). The preparation of the media resulted in mixing the following chemicals in deionized water, then autoclaving:

Luria-Bertina (LB) Broth: Bactotryptone (1% w/v), NaCl (1% w/v) and Yeast extract (0.5% w/v).

Luria-Bertina (LB) Agar: Bactotryptone (1% w/v), NaCl (1% w/v) and Yeast extract (0.5% w/v), Agar No. 1 (1.5% w/v; Lab M, Bury, UK).

SOC Media: Bactotryptone (2% w/v), Yeast extract (0.5% w/v), 10 mM NaCl, 2.5 mM KCl, 10 mM $MgSO_4$ and 20 mM Glucose.

2.1.5 Chemicals

X-Gal (5-Bromo-4-chloro-3-indolyl-β-D-galactoside) was used for clone library construction at 80 µg ml^{-1} (see section 2.2.5.5). A stock solution (40 mg ml^{-1}), dissolved in dimethylformamide, was stored in a light-proof tube at -20 ºC.

Ampicillin was used for clone library construction at 50 µg ml^{-1} (see section 2.2.5.5). A stock solution (50 mg ml^{-1}), dissolved in sterile water, was stored at -20 ºC.

2.1.6 Oligonucleotide primers

Oligonucleotide primers used in this study are detailed in Table 2.1.

Table 2.1: Oligonucleotide primers.

Gene target (organisms)	Primer Pair	Primer sequences (5' – 3')	Primer reference
16S rRNA (bacteria)	FAM-63F* 1389R	[6-FAM] CAGGCCTAACACATGCAAGTC ACGGGCGGTGTGTACAAG	Osborn *et al.* (2000) Marchesi *et al.* (1998)
16S rRNA (bacteria)	Eub338 Eub518	ACTCCTACGGGAGGCAGCAG ATTACCGCGGCTGCTGG	Lane (1991) Muyzer *et al.* (1993)
16S rRNA (archaea)	FAM-Arch109F* Arch958R	[6-FAM] ACKGCTCAGTAACACGT YCCGGCGTTGAMTCCAATT	DeLong (1992) DeLong (1992)
16S rRNA (archaea)	Parch519F Arch1060R	CAGCMGCCGCGGTAA GGCCATGCACCWCCTCTC	Øvreas *et al.* (1997) Reysenbach & Pace (1995)
ITS (fungi)	FAM-ITS1F* ITS4	[6-FAM] CTTGGTCATTTAGAGGAAGTAA TCCTCCGCTTATTGATATGC	Gardes & Bruns (1993) White *et al.* (1990)
ITS (fungi)	ITS1F 5.8S	TCCGTAGGTGAACCTGCGG CGCTGCGTTCTTCATCG	Gardes & Bruns (1993) Vilgalys & Hester (1990)

* Oligonucleotide primers fluorescently labelled at the 5' end with 6'carboxyfluorescein (6-FAM) dye, used for T-RFLP analysis.

Genomic target (organisms)	Primer Pair	Primer sequence (5’ – 3’)	Primer reference
nifH	nifH3 nifH4	ATRTTRTTNGCNGCRTA TTYTAYGGNAARGGNGG	Zehr & McReynolds (1989) Zehr & Macdonald (1989)
nifH	nifH(for A) nifH(rev)	GCIWTITAYGGNAARGGNGG GCRTAIABNGCCATCATYTC	Widmer *et al.* (1999) Widmer *et al.* (1999)
amoA (archaea)	amo111F amo643R	TTYTAYACHGAYTGGGCHTGGACATC TCCCACTTWGACCARGCGGCCATCCA	Treusch *et al.* (2005) Treusch *et al.* (2005)
amoA (bacteria)	amoA-1F amoA-2R	GGGGTTTCTACTGGTGGT CCCCTCKGSAAAGCCTTCTTC	Rotthauwe *et al.* (1997) Rotthauwe *et al.* (1997)
nxrA	F1norA R1norA	CAGACCGACGTGTGCGAAAG TCYACAAGGAACGGAAGGTC	Poly *et al.* (2008) Poly *et al.* (2008)
16S rRNA gene (*Nitrobacter spp.*)	Nitro-1198F Nitro-1423R	ACCCCTAGCAAATCTAAAAAACCG CTTCACCCCAGTCGCTGACC	Graham *et al.* (2007) Graham *et al.* (2007)
nirS	NirS1F NirS6R	CCTAYTGGCCGCCRCART CGTTGAACTTRCCGGT	Braker *et al.* (1998) Braker *et al.* (1998)

Genomic target (organisms)	Primer Pair	Primer sequence (5' – 3')	Primer reference
nirS	nirSHeme832F nirSHeme1606R	TACCACCCCGAGCCGCGCGT AGKCGTTGAACTTKCCGGTCGG	Yan *et al.* (2003) Yan *et al.* (2003)
nirK	nirKCopper583F nirKCopper909R	TCATGGTGCTGCCGCGKGACGG TCATGGTGCTGCCGCGKGACGG	Yan *et al.* (2003) Yan *et al.* (2003)
narG	narG1960F narG2659R	TAYGTSGGSCARGARAA TTYTCRTACCABGTBGC	Philippot *et al.* (2002) Philipot *et al.* (2002)
napA	napAv66 napAv67	TAYTTYYTNHSNAARATHATGTAYGG DATNGGRTGCATYTCNGCCATRTT	Flanagan *et al.* (1999) Flanagan *et al.* (1999)
nosZ	nosZ661b nosZ1773	CGGYTGGGGSMWKACCAA ATRTCGATCARYTGNTCRTT	Nogales *et al.* (2002) Nogales *et al.* (2002)
Clone inserts in vector pCR®4-TOPO	T3 T7	ATTAACCCTCACTAAAGGGA TAATACGACTCACTATAGGG	Messing (1983) Messing (1983)

2.2 Methods

2.2.1 Acute N deposition simulation 2009 – 2010

A plot experiment was established on Leirhaugen (Svalbard) in July 2009. Twenty five plots (1.5 × 1.5 m) having a similar plant cover were set up across a flat landscape with an inclination of 1-10% per plot (Figure 2.2, 2.3, 2.4; Appendix 2.1, 2.2). Acute N deposition was simulated by the addition of N in solution into water over 2-4 days period, to mimic acute nitrogen N deposition events (Hodson *et al.*, 2005; 2010; Kühnel *et al.*, 2011).

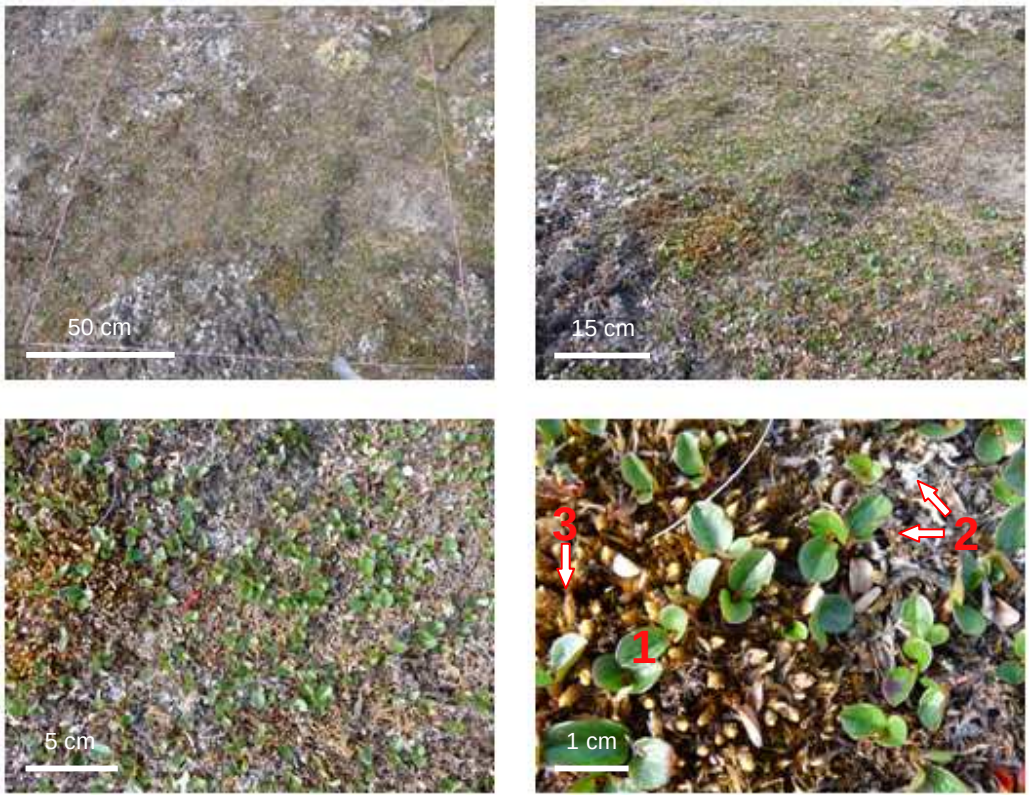

Figure 2.2: Photos of plot 4 (12 kg N ha^{-1} yr^{-1} treatment; 7th of July 2010). Numbers show the main plants groups/species: 1) *Salix polaris*, 2) lichens, 3) mosses.

In 2009, five different treatments (n = 5, allocated to plots chosen randomly) were applied to investigate the impact of: i) low ~pH 4, ii) N addition and ~pH 6, iii) N addition and low ~pH 4, iv) at different N addition rates of 0.4 and 4 kg N ha^{-1} yr^{-1} (See Table 2.2; Figure 2.3). N was applied as a solution, using tape water from NERC Arctic

research station (in 2009 and 2010), of ammonium nitrate with a pH adjusted to 4 when required by nitric acid (60%). Five plots were used as control plots, and received only water (~pH 6). The different solutions were applied with a watering can, over 2 days (21st and 22nd of August 2009), one time a day, representing 2.5 l per plot for each application (Figure 2.5). The total amount of N applied was split equally between each application. Thus the total amount of N was reached after the second N application.

Treatments were repeated in 2010, with adjustments of two treatments to test responses of microbial communities to high N loading. 0.4 kg N ha^{-1} yr^{-1} ~pH 6 plots were converted into 12 kg N ha^{-1} yr^{-1} ~pH 4 plots (see Table 2.2; Figure 2.4). To reduce sampling effort in the short field season, the plots which received previously (in 2009) water of ~pH 4 were no longer used for this PhD. These plots were used by S. Choudhary (see section 1.6, Chapter 1) and divided in two parts: one half received sodium nitrate and the other half ammonium chloride, both at a rate of 4 kg N ha^{-1}, ~pH 4. The adjustments of these plots, which initially investigated the impact of N addition with ~pH 6 and ~pH 4 only, were possible because the use of solution with different pH did not change the soil pH. In 2010 all N applications were made using solution of ^{15}N-dual labelled ammonium nitrate (99% labelled $^{15}NH_4^+$ $^{15}NO_3^-$; SerCon, Crewe, UK), enabling the fate of the nitrogen added within the soil to be followed. The applications were done over four days, from the 15th of July to the 18th of July 2010, using 2.5 l of solution per day per plot. The total amount of solution applied was 10 l per plot, and the amount of N added was split equally between the different applications. Thus the total amount of N was reached after the last application.

Table 2.2: Treatments (n = 5) applied in 2009 and 2010 on plot experiment established at Leirhaugen in 2009 (Svalbard.).

Year	2009	2010
Treatments	Control + Water: Water ~pH 6	Control + Water: Water ~pH 6
	0.4 kg N ha^{-1} ~pH 4	0.4 kg N ha^{-1} ~pH 4
	4 kg N ha^{-1} ~pH 4	4 kg N ha^{-1} ~pH 4
	0.4 kg N ha^{-1} ~pH 6	12 kg N ha^{-1} ~pH 4
	Water: ~pH 4	NO_3^- / NH_4^+ 4 kg N ha^{-1} ~pH 4*

* Plots receiving this treatment were not used in 2010 in this PhD.

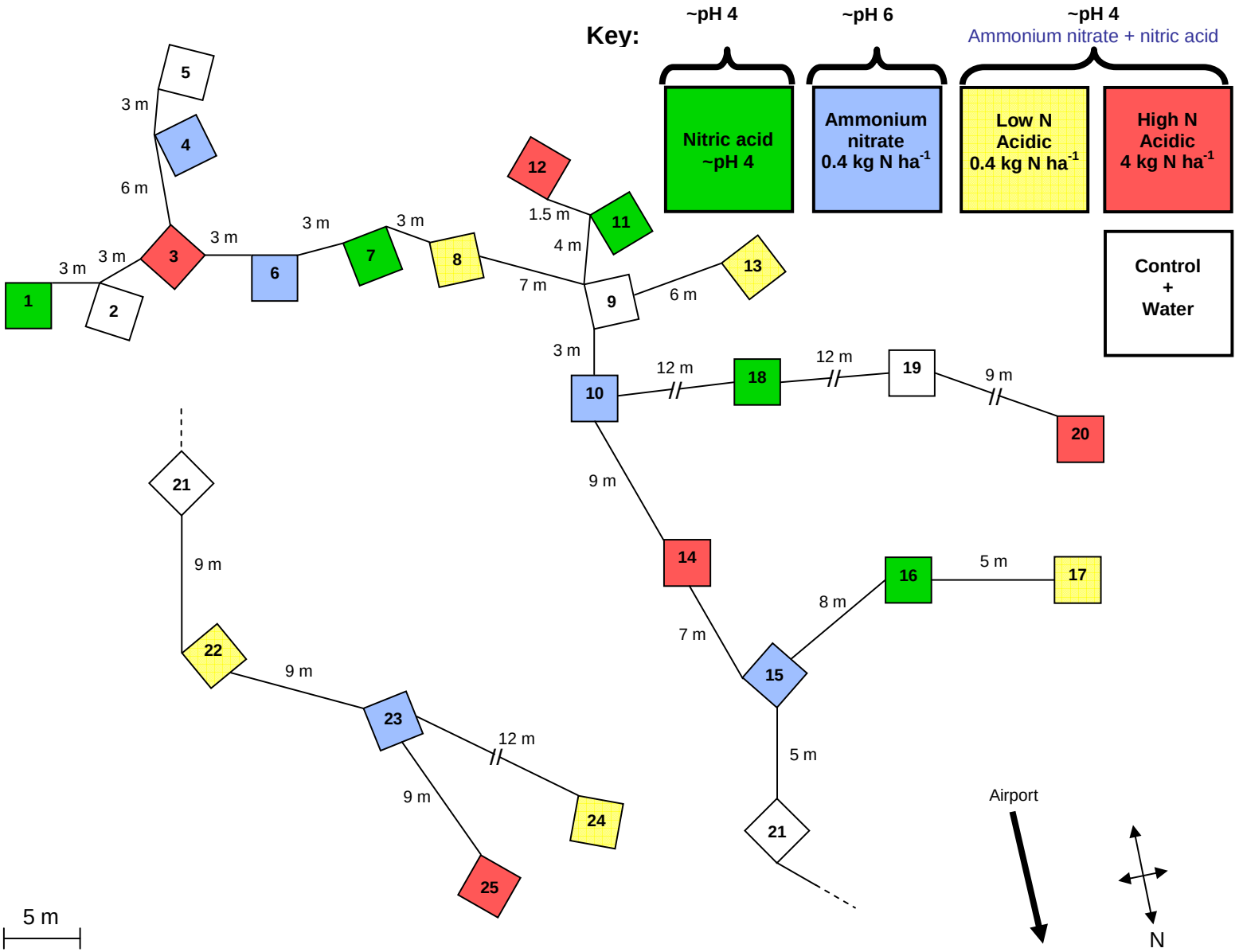

Figure 2.3: Map and treatments of the plot experiment in 2009 at Leirhaugen. Treatments of plots are as indicated in the key.

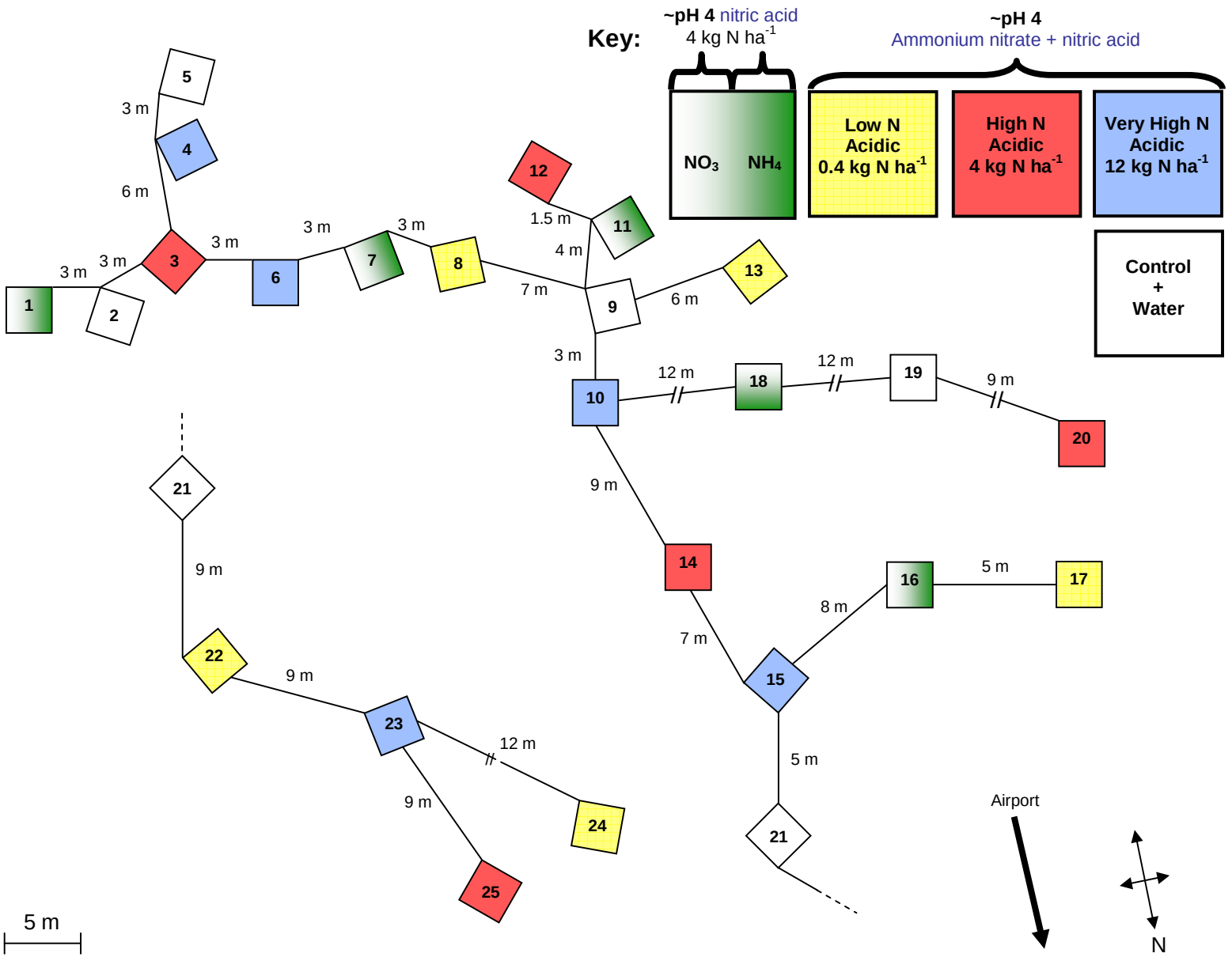

Figure 2.4: Map and treatments of the plot experiment in 2010 at Leirhaugen. Treatments of plots are as indicated in the key.

2.2.2 Soil sampling 2009 and 2010

The soil from the plots was randomly sampled within vegetated area of the plots at multiple time intervals (Figure 2.5; 2.6), using a knife disinfected between each soil sampling, with the soil placed into a sterile plastic bag and transported to the field laboratory. In the field laboratory the samples were stored at 4 ºC until processing within the same day of sampling. From the organic and mineral horizons separately, ~1 g of soil was collected with a sterile spatula and transferred into 1.5 ml tubes and stored at -20 ºC, for subsequent DNA extraction in Sheffield. Then, different amounts of soil from organic and mineral horizons were weighed separately for the different physico-chemical analyses (see section 2.2.4). After the initial soil sample processing, the remaining soil was returned back to the corresponding plot and sampling hole in order to reduce the ecological impact of soil sampling.

Soil samples of 5 × 5 cm to a depth of 10 cm were taken in 2009 from all of the plots. The soil samples were taken at multiple time intervals: before the first N application (Day-2); before the second N application (Day-1); and 1, 4 and 7 days after the last N application (Day+1, Day+4 and Day+7, respectively; Figure 2.5 A).

In 2010, the soil samples were taken at different time intervals than when sampled in 2009: 2 days before the first N application the (Day-6); after the second N application (Day -3); and 1, 4, 7, 21 and 35 days after the last N application (Day+1, Day+4, Day+7, Day+21 and Day+35, respectively; Figure 2.5 B). As in 2009, the size of soil samples for 2010 was 5 × 5 cm to a depth of 10 cm, except for Day+ 1, Day+7 and Day+21 for which the size of the sample was 10 × 10 cm down to a depth of 10 cm. Larger soil samples were taken for these sampling dates because more soil analyses were performed and the plant cover was studied by S. Choudhary, (see section 1.6, Chapter 1). Soil samples were also taken outside of the plots in 2009 and 2010 for all the date of sampling, to use as “pristine” control samples (five samples per day of sampling).

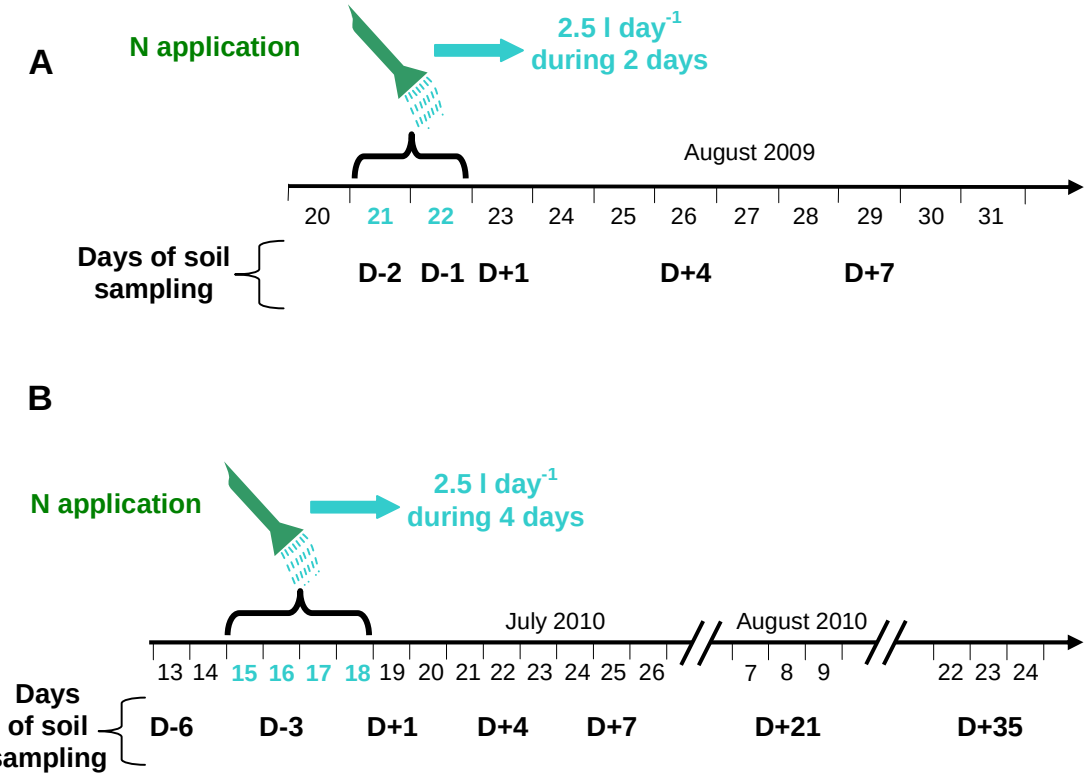

Figure 2.5: N application and days of sampling: **A** during August 2009, **B** during July and August 2010 at the plot experiment located at Leirhaugen.

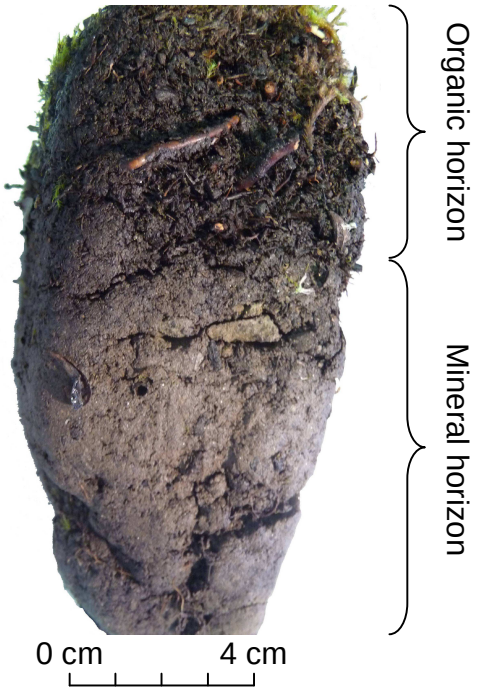

Figure 2.6: Example of a representative soil sample (5 × 5 × 10 cm) taken in 2009 at Leirhaugen, showing the organic and mineral horizons. Scale bar as indicated.

2.2.3 Microcosms experimental design

A microcosm experiment was performed in 2010 (12^{th} – 26^{th} of August) to determine the impact of N addition on microbial communities within the organic and mineral soil horizons separately.

The soil samples used for the microcosm experiment were taken within three different areas outside the plots, four soil samples (10 × 10 × 10 cm soil core) per area (12 soil core in total), on the 7^{th} of August 2010. The organic and mineral horizons from each sample were separated by hand and each horizon sample was sieved at 2 mm to remove stones and roots. Then, the four replicates of each soil horizon per area were pooled together to form composite 2 mm sieved soil samples. In total, three composite soil samples from the organic horizon and three composite soil samples from the mineral horizon were obtained. The soil samples where maintained at the temperature of incubation (7 ºC) for five days prior the beginning of the microcosm experiment.

The microcosms consisted of a sterile Falcon tube (50 ml) containing 8 g of organic or mineral soil (Figure 2.7). The soil sample within each tube was compacted to obtain a final bulk density of 0.53 and 1.07 for the organic and mineral horizon, respectively. All the composite samples received different N treatments, resulting in three replicates per treatments for the organic and mineral horizon: control microcosms (no water addition; **C**), control + water (~pH 6; **C+W**), 0.4 kg N ha^{-1} (~pH 4; **0.4N**) and 12 kg N ha^{-1} (~pH 4; **12N**). The different N additions were made with a solution of unlabelled NH_4NO_3 with pH adjusted to 4 by nitric acid (60%). The amount of water used for the treatments represented 50% of the soil water content; 2.3 ml and 1.3 ml of deionized water for 8 g of organic and mineral horizon, respectively. The microcosms were incubated in the dark at 7.47 ºC ± 0.36 (n = 33), this being a similar temperature to the soil taken from the tundra for the main plot experiment.

The composite soil samples were sampled at the beginning of the experiment and used as reference (Day0). The microcosms were destructively sampled at multiple time intervals: 1, 7 and 14 days after N addition (Day+1, Day+7 and Day+14, respectively).

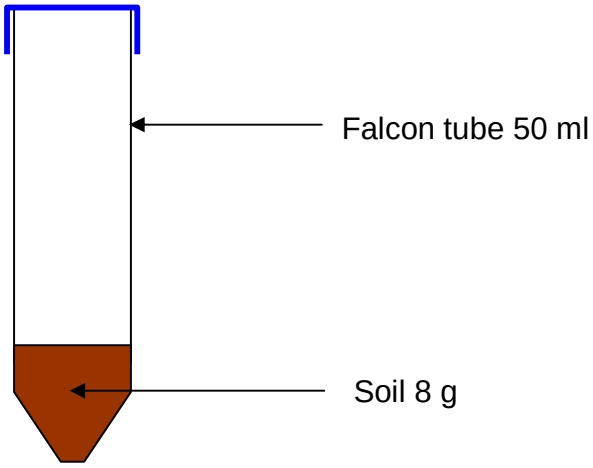

Figure 2.7: Experimental design of a microcosm.

2.2.4 Soil physico-chemical analysis

2.2.4.1 Soil characteristics

Soil moisture and pH were measured on fresh soil from the organic and mineral soil horizons for the different plot and microcosm treatment and at different dates of sampling, within the day or immediately following the day of sampling. Ten ml of deionized water was added to 1 g of soil, the solution was vortexed for 10 s, then left to settle for 1 min before pH measurement (Robinson *et al.*, 2004). The soil moisture was measured using 2 - 5 g of soil from the plots in 2009, 10 - 20 g of soil from the plots in 2010 and ~3 g of soil from the microcosm experiment. The samples were oven-dried at 40 °C for 72 h in pre-weighed plastic bags, and reweighed after cooling in a desiccator containing silicate. Soil moisture was expressed as a percentage of soil wet weight.

2.2.4.2 Soil total C, organic C, total N, inorganic N and ^{15}N

Soil organic C, total N content and ^{15}N enrichment were measured on the same soil samples used for the soil moisture measurements. After the soil moisture measurement, the soil samples were ground (< 200 µm) and analysed using an isotope ratio mass spectrometer (ANCA GSL 20-20, PDZ Europa, Cheshire, UK). The soil

carbonate content was not detectable, thus when the total C content was measured we assumed that the total C was equal to the organic C, based on the following equation:

$$\text{Total C} = \text{Inorganic C} + \text{Organic C}$$

Inorganic N (NH_4^+ and NO_3^-) was extracted from 2 g of fresh soil for the 2010 plots and microcosms soil samples by horizontal shaking with 20 ml of KCl (2 M) for 1 h. The solution was filtered (paper filter, Wathman 44, ø 110 cm, retention 3 µm) and the extract was stored at -20 °C and returned to the UK for $N\text{-}NH_4^+$ and $N\text{-}NO_3^-$ analysis by continuous flow colorimetry (Kamphake *et al.*, 1967; Krom, 1980) with an auto-analyser (FIA-flow2 nutrients analyzer, Burkard Scientific Ltd, Uxbridge, UK).

2.2.5 Molecular biology methods

2.2.5.1 Extraction of soil DNA

DNA was extracted from 0.25 g of soil using the PowerSoil® DNA isolation kit (Mo-Bio laboratories, Carlsbad, CA, USA) following the manufacturer's instructions. DNA was eluted with 100 µl of nuclease-free water (Ambion, Warrington, UK). DNA extracts were stored at -80 °C.

2.2.5.2 PCR amplification

Specific genes were amplified from the DNA extract, by PCR. The amplifications were performed in 2 different 50 µl mixtures using one of two *Taq* DNA polymerases (Qiagen and Bioline) used for different PCR amplifications (see Table 2.3). The first reaction mixture (50 µl) contained 1× reaction buffer, 100 µM of each dNTP, 0.15 µM of each oligonucleotide primer (Table 2.1, 2.3), 1.25 U of *Taq* DNA polymerase (Qiagen, Crawley, UK) and 1 µl of DNA template. For some reaction mixtures, 10 µl of Q solution (Qiagen, Crawley, UK) or BSA (400 ng μl^{-1}; Promega,

Madison, USA) were added instead of water (see Table 2.3) to improve the DNA amplification.

The second reaction mixture (50 µl) contained 1× reaction buffer, 1 mM of $MgCl_2$, 50 µM of each dNTP, 0.2 µM of each oligonucleotide primer (Table 2.1, 2.3), 2.5 U of *Taq* DNA polymerase (Bioline, London, UK) and 1 µl of DNA template. The PCR reactions were carried out in an ABI 2720 thermal cycler (Applied Biosystems, Warrington, UK) using different cycling conditions, detailed in Table 2.3, in relation to each oligonucleotide primer pair used.

The PCR amplification of functional genes (e.g. *nifH* or *amoA*) needed improvement in order to obtain PCR products of the right size (bp) and concentration. Thus, similar processes of PCR investigation were used for all the functional genes. Firstly, the PCR assays were performed on soil samples from the organic and mineral soil horizons, taken from the plots in 2009 and 2010 (control samples, control + water plots and 12 kg N ha^{-1} yr^{-1} plots) at the different dates of sampling, and also from the microcosm experiment. Secondly, the PCR were performed using the Bioline or the Qiagen *Taq* DNA polymerase, with and without BSA and, with and without Q solution (only for Qiagen). Different *Taq* DNA polymerases differ in their efficiency of DNA amplification in relation to the DNA concentration, purity and sequences being targeted. BSA is widely used to improve amplification of functional genes because it reduces the effects of inhibitory compounds on the PCR (Kreader, 1996), and Q-solution can improve the amplification of GC-rich templates but can also inhibit PCR amplification (Ralser *et al.*, 2006). At the beginning of the PCR assays, 50 cycles of PCR was used for the amplification to increase the probability of obtaining amplification products, and then cycle numbers were subsequently reduced. Finally, the annealing temperature (T_a) for each primer set was chosen from the literature and calculated by subtracting 5 ºC from the average of the melting temperature (T_m) of both primer pairs. Then, gradient PCR was performed to determine the best T_a for each set of primers. A positive control for the *amoA* gene (bacteria and archaea) was used throughout the different *amoA* gene PCR amplification. The positive control was obtained from DNA sequenced of the *amoA* gene (bacteria and archaea) from cryoconite holes particles taken in Antarctica (provided by Dr K. Cameron).

Table 2.3: PCR cycling conditions used for different oligonucleotide primer pairs.

Gene target (organisms)	Primer Pair	*Taq* polymerase	PCR cycling conditions (temperature in ºC, and time in s or min)					Expected PCR amplicon size (bp)
16S rRNA (bacteria)	FAM-63F* 1389R	Qiagen + Q[a]	94 2 min	30 cycles: 94 30 s	57 45 s	72 1.30 min	72 10 min	1326
16S rRNA (archaea)	FAM-Arch109F* Arch958R	Qiagen + Q	95 45 s	35 cycles: 95 45 s	55 1 min	72 1.30 min	72 10 min	849
ITS region (fungi)	FAM-ITS1F* ITS4	Bioline	95 5 min	35 cycles: 95 30 s	55 30 s	72 1 min	72 10 min	200-1000
nifH	nifH3 nifH4	Qiagen	95 2 min	50 cycles: 95 1 min	55 1 min	72 1 min	72 2 min	472
nifH	nifH(for A) nifH(rev)	Qiagen	95 5 min	40 cycles: 94 1 min	48 1 min	72 1 min	72 10 min	464

* Oligonucleotide primers fluorescently labelled at the 5’ end with FAM dye, used for T-RFLP analysis.
[a] Q indicates when Q solution was added to the PCR mixture for PCR performed using Qiagen *Taq* DNA polymerase (see text for details).

Gene target (organisms)	Primer Pair	*Taq* polymerase	PCR cycling conditions (temperature in ºC, and time in s or min)					Expected PCR amplicon size (bp)
amoA (archaea)	amo111F amo643R	Qiagen + BSA[b]	94 1 min	50 cycles: 94 1 min	61 1.30 min	72 1.30 min	72 10 min	557
amoA (bacteria)	amoA-1F amoA-2R	Qiagen + BSA	95 5 min	7 cycles[TD]: 94 1 min	61-58 1.30 min	72 1 min		491
				33 cycles: 94 1 min	58 1.30 min	72 1.30 min	72 10 min	
nxrA	F1norA R1norA	Qiagen + Q	94 5 min	40 cycles: 94 1 min	49 1 min	72 1 min	72 5 min	322
Nitrobacter spp.	Nitro-1198F Nitro-1423R	Qiagen + Q	95 10 min	40 cycles: 94 20 s	58 1 min	72 40 s	72 5 min	225
nirS	NirS1F NirS6R	Qiagen	95 7 min	50 cycles: 95 1 min	50 1 min	72 1 min	72 10 min	890

[b] BSA indicates that BSA was added to the PCR mixture for PCRs performed using Qiagen *Taq* DNA polymerase (see text for details). [TD] Touch Down PCR cycling: the temperature was reduced by 0.5 ºC each cycle.

Gene target (organisms)	Primer Pair	*Taq* polymerase	PCR cycling conditions (temperature in ºC, and time in s or min)					Expected PCR amplicon size (bp)
nirS	nirSHeme832F nirSHeme1606R	Qiagen	94[c] 2 min	35 cycles 94 30 s	 60 1 min	 72 1 min	72 7 min	774
nirK	nirKCopper583F nirKCopper909R	Qiagen + Q	94[c] 5 min	40 cycles 94 30 s	 60 1 min	 72 1 min	72 7 min	326
narG	narG1960F narG2659R	Qiagen + Q	94 5 min	8 cycles[TD] 94 1 min	 59-55 1 min	 72 1.30 min		650
				30 cycles 94 1 min	 55 1 min	 72 1.30 min	72 7 min	
napA	napAv66 napAv67	Qiagen + Q	94 2 min	40 cycles 94 1 min	 50 1 min	 72 2 min	72 2 min	338
nosZ	nosZ661b nosZ1773	Qiagen + BSA	94 5 min	40 cycles 94 30 s	 56 1.30 min	 72 2 min	72 10 min	1112

[c] A “hotstart” at 80 ºC for 30 s was used before the first denaturation step.

2.2.5.3 Gel electrophoresis

DNA extractions and PCR products were visualised by loading 5 µl of DNA extract or PCR products into 0.8 - 2% (w/v) agarose gels, made up in 1x TAE buffer with 50-100 ng ml^{-1} of ethidium bromide. Products were run alongside 5 µl of a Hyperladder (I or IV) molecular weight marker (Bioline, London, UK). Gels were run at 60-90 V for 60 – 120 min in relation to the gel size and percentage of agarose. Gels were visualized under ultraviolet light at 302 nm, to assess the DNA presence and size (bp) of PCR products.

2.2.5.4 PCR product purification

PCR products were purified in order to remove primers and dNTPs prior to DNA fingerprinting analysis using the QIAquick® PCR purification kit (Qiagen, Crawley, UK) following manufacturer's instructions. The purified PCR product was eluted in 50 µl of nuclease-free water (Ambion, Warrington, UK).

PCR products obtained during the clone library constructions (section 2.2.5.5) were purified using SureClean (Bioline, London, UK). Briefly, equal volumes, of the PCR product, and of the SureClean solution was added to each sample in a 96 wells plate, quickly vortexed, and incubated at room temperature for 15 min. The plate was then centrifuged at 3,500 rpm for 35 min. The solution was removed by inversion and centrifuged for 1 min at 1,000 rpm. Twice the original PCR volume of ethanol 70% was added to each well, quickly vortexed, and centrifuged at 3,500 rpm for 35 min. The solution was removed by inversion and centrifuged for 1 min at 1,000 rpm. The purified PCR product was resuspended in 20 µl of nuclease-free water (Ambion, Warrington, UK)

2.2.5.3 Fingerprinting methods

Variation in microbial community structure between different soil samples was investigated by different fingerprinting methods namely: Terminal Restriction Fragment

Length Polymorphism (T-RFLP; Liu *et al.*, 1997; Osborn *et al.*, 2000) for bacterial and archaeal communities; and Automated Ribosomal Intergenic Spacer Analysis (ARISA; Ranjard *et al.*, 2001) for the fungal community.

T-RFLP fingerprinting method assesses the variability in length of terminal restriction fragments (T-RFs). Briefly, 16S rRNA genes from bacterial or archaeal communities were amplified by PCR using labelled primer with the fluorescent dye 6'carboxyfluorescein (6-FAM) at the 5' end of the forward oligonucleotide primer (see Table 2.1). The PCR products were digested using a restriction enzyme, which cleaved at a specific restriction site present one or more times along the sequence amplified by PCR. The T-RFs amplified, were size separated by capillary electrophoresis and detected via the presence of the 5' fluorescent label.

ARISA fingerprinting method assesses the variability in length of the internal transcribed spacer (ITS) between the small 18S and large 28S subunit rRNA genes, including the 5.8S rRNA gene (Ranjard *et al.*, 2001). Briefly, ITS regions were amplified by PCR using labelled primer with the fluorescent dye (6-FAM) at the 5' end of the forward primer (see Table 2.1). The fragments amplified, were size separated by capillary electrophoresis and detected via the presence of the 5' fluorescent label.

2.2.5.3.1 T-RFLP

Purified fluorescently labelled PCR products (10 µl) were digested with 10 U of the restriction enzyme AluI and 1x restriction enzyme buffer (Roche, Hertfordshire, UK) in a total volume of 15 µl at 37 ºC for 3 h. The same restriction enzyme AluI was used to digest PCR products targeting bacterial or archaeal communities. Five µl of the digests were desalted using a precipitation step with 0.25 µl of glycogen (20 mg ml^{-1}) and 75 µl of 0.3 mM $MgSO_4.7H_2O$ in 70% ethanol. The solution was briefly vortexed and incubated at room temperature for 15 min, then centrifuged at 4,000 rpm for 30 min. The solution was removed by inversion and centrifuged for 1 min at 1,000 rpm. The pellet was resuspended in 5 µl of nuclease-free water (Ambion, Warrington, UK). For PCR products with low yield, double the amount of PCR product (10 µl) and reagents were used for the desalting step following the same protocol. Desalted products (0.5 or 1 µl)

were mixed with formamide containing 0.5% ROX-labelled GS500 internal size standard (see Figure A2.3.1, Appendix 2.3; Applied Biosystems, Warrington, UK) in a total volume of 10 µl. Digested products were denatured at 94 ºC for 3 min, transferred immediately onto ice, and samples were electrophoresed on an ABI 3730 PRISIM® capillary genetic analyser using POP7 polymer (Applied Biosystems, Warrington, UK). An initial injection voltage of 2 V and 5 or 10 s of injection time was used. 10 voltage ramps were performed with 20 s voltage interval steps before reaching the final electrophoresis run voltage of 15 V. The total electrophoresis run was 20 min.

2.2.5.3.2 ARISA

Ten µl of the purified fluorescently labelled PCR products were desalted using a precipitation step with 0.5 µl of glycogen (20 mg ml^{-1}) and 150 µl of 0.3 mM $MgSO_4.7H_2O$ in 70% ethanol. The solution was briefly vortexed and incubated at room temperature for 15 min, then centrifuged at 4,000 rpm for 30 min. The solution was removed by inverting and centrifugation for 1 min at 1,000 rpm. The pellet was resuspended in 5 µl of nuclease-free water (Ambion, Warrington, UK). Between 0.5 and 2 µl of desalted products were mixed with formamide containing 0.5% ROX-labelled GS2500 internal size standard (see Figure A2.3.1, Appendix 2.3; Applied Biosystems, Warrington, UK) in a total volume of 10 µl. Digested products were denatured at 94 ºC for 3 min, transferred immediately onto ice, and samples were electrophoresed on an ABI 3730 PRISM® capillary genetic analyser using POP7 polymer (Applied Biosystems, Warrington, UK). An initial injection voltage of 2 V and 5 or 10 s of injection time was used. 10 voltage ramps were performed with 20 s voltage interval steps before reaching the final electrophoresis run voltage of 15 V. The total electrophoresis run was 1 h.

2.2.5.3.3 Data analysis

The T-RFLP and ARISA profiles obtained with the sequencer were analysed using GeneMapper® v3.7 software (Applied Biosystems, Warrington, UK). The program

output was an electropherogram for each sample and a spreadsheet giving fragment sizes, peak size and peak height. The size, in nucleotides, of each peak of the electropherogram was estimated by comparison with the internal size standard (GS500 ROX and GS2500 ROX, for T-RFLP and ARISA, respectively). Terminal restriction fragments of between 50 and 500 nucleotides and with peak heights of ≥ 50 fluorescence units were included in the analysis. Fragments between 200 and 1000 bp and with peak heights of ≥ 100 fluorescence units were included for the ARISA analysis. The T-RFLP and ARISA profiles expressed as peak area (i.e. area between the peak outline and the *x* axis) were aligned using the T-Align software (Smith *et al.*, 2005). T-RFs and ARISA fragments with a relative abundance of < 0.5% of the total percentage area, were removed from subsequent analyses.

The richness of the microbial communities per sample was expressed as the total number of T-RFs for the bacterial and archaeal communities, and the total number of ARISA amplicons for the fungal community. The microbial communities evenness was calculated using the Shannon diversity index (*H'*) using the following equation (Shannon, 1948):

$$H' = \sum_{i=1}^{S} p_i \ln(p_i)$$

where *pi* represents the relative abundance of the T-RF *i*. The richness and evenness index, described as non-reliable index to assess the real bacterial diversity base on T-RFLP data (Blackwood *et al.*, 2007), were used as a relative diversity index of the microbial communities, to describe potential differences in T-RFLP and ARISA profiles.

2.2.5.4 Microbial communities abundance

Variation in the abundance of bacteria, archaea, fungi and of functional genes between different soil horizons, over time and in response to simulated episodic nitrogen N deposition events was investigated using quantitative PCR (Q-PCR) (Becker *et al.*, 2000; Suzuki *et al.*, 2000; Takai & Horikoshi, 2000). Q-PCR method investigates abundance of specific taxonomic or functional groups within an environment by

quantifying the targeted sequence numbers (e.g. 16S rRNA gene for bacteria and archaea) during each cycle of the PCR amplification via the measurement of the fluorescence released by the sequence amplified (Smith & Osborn. 2009). Then, the sequence number is calculated using a dilution series of the targeted sequence for which the initial number of gene is known, to calculate a standard curve. The quantification of the sequence via their fluorescence was performed using the SYBR Green detection (Wittwer *et al.*, 1997). The fluorescent dye SYBR Green is used in the PCR mixture and emits fluorescence only when it binds to double strand DNA. Thus, an increase in fluorescence is related to an increase in sequence synthesis and the sequence numbers can be determined by comparison with the fluorescence of the standard curve.

2.2.5.4.1 Q-PCR standard curve construction

Standards were constructed from environmental samples from field plot experiment (2009 and 2010 soil sampling) and from the microcosm experiment. The construction of the standards was performed using PCR products for each target gene that were amplified separately from the organic and mineral horizons of the soil sample. PCR products were then pooled together (i.e. from the organic and mineral horizons) to allow the creation of a dilution series from which a standard curve could be generated. For the plot experiment (2009 and 2010), the standards of the bacterial, archaeal and fungal community were constructed from the organic and mineral horizons of the soil sample taken immediately external to the plots and which are considered as “pristine” controls, prior to N application in 2009 (i.e. Day-2) and 2010 (i.e. Day-6).

For the microcosm experiment, the standards of the bacterial, archaeal, and fungal community were constructed, from the organic and mineral horizon separately, from a replicate of the no water addition treatment (see Chapter 6) sampled at the beginning of the incubation (i.e. Day0). To quantify bacterial *amoA* genes, the standard was constructed from the organic and mineral horizons separately from replicate three of the no water addition treatment one day after the beginning of the incubation (i.e. Day+1), from which strong PCR products were amplified (see Figure 6.7, chapter 6).

The targeted genes were amplified from the different soil samples selected for the standards, by PCR. The amplifications were performed in 50 µl mixtures that contained 1× reaction buffer, 100 µM of each dNTP, 0.15 µM of each oligonucleotide primer (Table 2.1, 2.4), 1.25 U of *Taq* DNA polymerase (Qiagen, Crawley, UK) and 1 µl of DNA template. The PCR reactions were carried out in an ABI 2720 thermal cycler (Applied Biosystems, Warrington, UK) using the same cycling conditions as were to be used for Q-PCR, detailed in Table 2.4, except that each PCR was completed by a final extension at 72 ºC for 7 min (i.e. bacteria and fungi) or 10 min (i.e. archaea and *amoA* bacteria). PCR products (i.e. 50 µl) were visualised by gel electrophoresis (agarose gel 0.8% w/v) stained with ethidium bromide and bands were excised from the gels and extracted using the QIAquick® Gel Extraction Kit (Qiagen, Crawley, UK) following the manufacturer's instructions to purify the PCR products. The DNA concentration from each band extracted was quantified in triplicate using a NanoDrop spectrophotometer (NanoDrop 8000 Spectrophotometer Thermo Scientific, Wilmington, USA). The absorbance 260/280 ratio was also measured to assess the purity of the gel extraction (A 260/280 ratio of 1.8 indicates pure DNA).

For each gene, the standards created, for each microbial community and experiment, from the organic and mineral horizon were pooled together to obtain one composite standard per microbial community and experiment which could be used as a standard for soil samples from the organic and mineral horizons. The average of the six quantification measurement per standard (i.e. three from the organic and three from the mineral horizons) was used as the DNA concentration for each standard. Then, the gene number was calculated using the following equation:

$$\text{Gene number} = \frac{6.023 \times 10^{23}\ (\text{copies mol}^{-1}) \times \text{concentration of standard (g µl}^{-1})}{\text{MW (g mol}^{-1})}$$

where 6.023×10^{23} is Avogadro's constant, MW is the molecular weight of the targeted gene obtained by multiplying the number of base pair of the gene of interest (see Table 2.4) by the molecular weight of double strain DNA (660 Da per base pair).

For each standard, a dilution series was created. For the 2009 plot experiment, a tenfold dilution series used for the bacterial and archaeal communities varied between 10^9 to 10^2 gene number μl^{-1} while for the fungal community the standard curve ranged from 10^8 to 10^2 gene number μl^{-1}. The standard curve (tenfold dilution series) used for the 2010 plot experiment for the bacterial and fungal communities ranged between 10^7 to 10^4 gene number μl^{-1}, while for the archaeal community the standard curve ranged from between 10^5 to 10^2 gene numbers μl^{-1}. For the microcosm experiment, the standard curve used for the bacterial and archaeal communities ranged between 10^9 to 10^2 gene number μl^{-1} while for the *amoA* bacteria the standard curve ranged between 10^7 to 10^3 gene number μl^{-1}.

2.2.5.4.2 Q-PCR amplification

The standard curve and the "no template control" (NTC) were amplified in triplicate in the same plate as the environmental samples. The Q-PCR amplification were performed in 25 µl mixtures containing 12.5 µl of QuantiFast® SYBR® Green PCR MasterMix (Qiagen, Crawley, UK), 9 µl of nuclease-free water (Ambion, Warrington, UK), 1.25 µl of each primer (10 µM) and 1 µl of DNA template. The Q-PCR reaction were carried out in an CFX96™ Real-Time System (Bio-Rad, Hemel Hempstead, UK) using different cycling conditions, detailed in Table 2.4, for each primer pair. The gene numbers of the samples were determined automatically using the Bio-Rad CFX Manager™ software which calculated the threshold cycle (C_t) values. To assess the quality of each amplification, the NTC C_t value was given, and the following standard curve descriptors were given: linear regression coefficient (r^2), the *y*-intercept value and the amplification efficiency (*E*) (Smith *et al.*, 2006). The SYBR Green detection method used for Q-PCR is not specific to the gene of interest with the potential for the detection of non-specific double stranded PCR products in the Q-PCR. Thus, if non-specific product or primer dimers are synthesised during the Q-PCR, this will lead to an overestimation of the gene of interest or an estimation of a non-targeted product. To assess the specificity of the Q-PCR amplification, a melting curve analysis (increase of

temperature from 72 ºC to 95 ºC by 0.5 ºC for 5 s) was performed at the end of each Q-PCR amplification (Ririe *et al.*, 1997).

Table 2.4: Q-PCR conditions used for the different oligonucleotide primer pairs.

Gene target (organisms)	Primer Pair	PCR cycling conditions (temperature in ºC, and time in s or min)				Expected PCR amplicon size (bp)*
			40 cycles			
16S rRNA (bacteria)	Eub338 Eub518	94	94	50	72	200
		3 min	30 s	45 s	30 s	
			40 cycles			
16S rRNA (archaea)	Parch519F Arch1060R	95	95	57	72	541
		3 min	30 s	45 s	45 s	
			40 cycles			
ITS regions (fungi)	ITS1F 5.8S	94	94	50	72	~300
		3 min	30 s	45 s	30 s	
			40 cycles			
amoA (bacteria)	amoA-1F amoA-2R	95	94	58	72	491
		5 min	1 min	1.30 min	1.30 min	

* Expected fragment sizes for bacterial 16S rRNA gene and ITS regions are as predicted by Fierer *et al.*, 2005. (NB. the length of the ITS region varies between different fungal strains). Expected fragment size for archaeal 16S rRNA gene is obtained by calculating the difference of the sequence position of each primer (Øvreas *et al.*, 1997; Reysenbach & Pace, 1995). Expected fragment size for *amoA* genes are as predicted by Rotthauwe *et al.* (1997).

2.2.5.5 Clone library and sequencing

Clone library construction and sequencing were done to determine if some PCR products from soil samples corresponded to the microorganisms that were targeted to amplify and to assess the diversity of these communities. Thus, the PCR products of bacterial 16S rRNA gene, fungal ITS regions, and functional genes (e.g. *amoA* Bacteria, *nxrA*) were investigated by cloning and sequencing.

2.2.5.5.1 Clone library construction and sequencing

Unpurified PCR products were ligated into PCR®4-TOPO vector and transformed into One Shot® TOP10 chemically competent *E. coli* cells (Invitrogen, Paisley, UK) following the manufacturer's instruction. Briefly, 1 µl of PCR®4-TOPO vector (Invitrogen, Paisley, UK), 2 µl of PCR product, 1 µl of salt solution and 2 µl of nuclease-free water (Ambion, Warrington, UK) were mixed with the ligation mix at room temperature for 15 min. Then, the ligation mix (6 µl) was added to a tube of One Shot® TOP10 chemically competent *E. coli* cells (Invitrogen, Paisley, UK), and incubated on ice for 15 min, then placed in a 42 °C water bath for 30 s and transfer on ice immediately for 2 min. 250 µl of SOC media was added and the mixture was shaken horizontally (~12.5 rpm) at 37 °C for 1 h. Transformants were selected on Luria-Bertani (LB) agar plates containing ampicillin (50 mg ml^{-1}) and X-gal (40 mg ml^{-1}) following overnight incubation at 37 °C. White colonies were picked and transferred into 100 µl of LB broth containing ampicillin (50 mg ml^{-1}) and incubated overnight at 37 °C. 1 µl of the culture was used to amplify the insert by PCR using the T7 and T3 primers (see Table 2.1) in a 25 µl reaction mixture using Bioline *Taq* DNA polymerase (See section 2.2.5.2 PCR amplification) following the same PCR cycling condition used for the original PCR (i.e. 16S rRNA or ITS region PCR). The PCR products were purified using SureClean (Bioline, London, UK) (See section 2.2.5.4 PCR purification). The purified PCR products were fluorescently labelled using the BigDye® Terminator v3.1 Cycle Sequencing Kit (Applied Biosystems, Warrington, UK). The reaction mixture (20 µl) contained 4 µl of sequencing buffer, 0.4 µM of T7 oligonucleotide, 0.5 µl of BigDye

mix and 4 µl of purified PCR products. The reactions were carried out in an ABI 2720 thermal cycler (Applied Biosystems, Warrington, UK) using an initial denaturation at 94 ºC for 2 min, followed by 25 cycles of 94 ºC for 15 s, 55 ºC for 15 s, and 60 ºC for 4 min, followed by a final step at 60 ºC for 5 min. The sequencing products were desalted using a precipitation step with 75 µl of 0.3 mM $MgSO_4.7H_2O$ in 70% ethanol. The solution was briefly vortexed and incubated at room temperature for 15 min, then centrifuged at 3,500 rpm for 30 min. The solution was removed by inverting and centrifugation for 1 min at 1,000 rpm. The pellet was resuspended in 10 µl of formamide. Products were denatured at 94 ºC for 3 min, quickly transferred to ice, and samples were electrophoresed on an ABI 3730 PRISM® capillary DNA genetic analyser with POP7 polymer (Applied Biosystems, Warrington, UK) using a 2 volt and injection time for 5 s and 10 voltage ramps were used with 20 s intervals before reaching the final electrophoresis run voltage of 15 V.

2.2.5.5.2 Analysis of sequence libraries

Sequences were edited using ChromasPro (version 1.5[5]). Edited sequences were compared to the GenBank database using the Basic Local Alignment Search Tool for nucleotide (BLASTn) of the National Centre for Biotechnology Information (NCBI) (Altschul, 1991). The most closely related (top BLAST hit) was recorded for each sequence.

2.2.6 Statistical analysis

2.2.6.1 Physico-chemical analysis

Physico-chemical data were analysed by ANOVA or non-parametric test using R version 2.11.1 (R Development Core Team (2010). R: A language and environment for statistical computing) to test any significant differences in total C, total N, ^{15}N, NO_3^-, NH_4^+, soil water content, C/N ratio and soil pH between: i) the organic and mineral

[5] http://www.technelysium.com.au/ChromasPro.html

horizon, ii) over time, iii) and in response to simulated episodic nitrogen deposition events. The normality of the models residues and homoscedasticity of data were checked, prior to statistical analysis and when both of these conditions were not met, the Kruskal-Wallis non-parametric test was instead used (Kruskal & Wallis, 1952). When significant effects were found by ANOVA, the detail of the effect (e.g. if a significant change over time was found, between which time interval this change happened) was investigated using the Tukey HSD test (Tukey, 1953).

Similarities between the samples based on the environmental variables (i.e. soil water content, soil pH, total C, total N, C/N and ^{15}N) were presented by principal component analysis (PCA) using the PRIMER software (V6, PRIMER-E Ltd, Plymouth, UK). Before the analysis, all of the variables were presented using pairwise scatter plots to visualise the variables which were not evenly distributed. These variables were log transformed (log + 0.1 transformation were done because some values were equal to zero) to avoid the effect of extreme outliers samples on the PCA. Then, all the variables were normalised. For the 2009 soil samples, the environmental variables were not log-transformed. The NH_4^+ and NO_3^- soil concentration were included for the 2010 analysis, and the ^{15}N and NO_3^- were log transformed.

In order to investigate potential differences between soil horizons, over time and in response to simulated episodic nitrogen deposition events, based on the environmental variables, a non-parametric permutation-based test: ANOSIM (analysis of similarity; 20 000 permutations available; PRIMER V6; Clarke & Green, 1988) were performed on similarity matrices of all the environmental variables after transformation and normalisation, constructed using the Euclidean distance method (Clarke, 1993). Two-way ANOSIM analysis was used to compare factors against another one. When more than two factors influenced the data set, each factor was tested separately against the combination of the others factors. Thus, to test the influence on soil horizons, a two-way ANOSIM was performed comparing the factor “soil horizons” against the combination of the factors “days of sampling” and “N addition”. For the influence of “days of sampling” and “N addition”, a two-way ANOSIM was performed for the organic and mineral horizon separately comparing the “days of sampling” *versus* “N addition”. The ANOSIM analyses give the significance levels, i.e. *P* value, and R value, i.e. the strength

of the factors on samples. R values close to one indicate a high separation between groups (e.g. between organic and mineral horizons), while R values close to zero indicate a low group separation.

2.2.6.2 Fingerprinting statistical analysis

All data analysis from the fingerprinting method was performed using the PRIMER software (V6, PRIMER-E Ltd, Plymouth, UK). To analyse the T-RFLP and ARISA profiles datasets, the total peak area intensity for each profile was normalised across peaks (i.e. each peak intensity was divided by the total peak intensity of each sample). Data from the T-RFLP or ARISA matrices were then square root transformed and similarity matrices were constructed using the Bray-Curtis method (Clarke *et al.*, 2006). Similarities between samples were displayed using non-metric multi-dimensional scaling (nMDS) plots. Each nMDS plot was presented with a positive 2D Stress value. The 2D Stress value indicated the mismatch between the rank similarity matrices and the nMDS 2D representation. A 2D Stress value close to 0 indicated an excellent representation in 2D. Values above 0.2 indicated a weak 2D representation, suggesting that the data were more spread in 3 dimensions.

Similarly to the environmental variables, the potential significant effect of different factors (i.e. soil horizons, over time and in response to simulated episodic nitrogen deposition events) on microbial community structures was tested using two-way and one-way ANOSIM analysis (analysis of similarity; 20 000 permutations available) on the similarity matrices obtained using the Bray-Curtis method. Two-way ANOSIM was used to compare two factors simultaneously, and one-way ANOSIM to investigate the influence of one factor (i.e. treatment effect: e.g. control + water *vs.* 12 kg N ha^{-1} yr^{-1} plots). The significance levels, i.e. *P* value, and R value, i.e. the strength of the factors on samples were determined.

2.2.6.3 Microbial communities abundance analysis

Microbial communities abundance were analysed by ANOVA or non-parametric test to investigate any significant differences between soil horizons, over time and in response to simulated episodic nitrogen deposition events. The same statistical approach as used for the physico-chemical analysis was used (see section 2.2.6.1).

2.2.6.4 Correlation between environmental variables, microbial communities structure and abundance

The relationship between microbial community structures and environmental variables was first visualised by superimposing the values of one environmental variable by different disk size on the nMDS plots. Secondly, the relationship was tested by performing correlation analysis between the similarity matrices of the T-RFLP or ARISA profiles obtained using the Bray-Curtis method and the matrices of the environmental variables (i.e. total C, N, ^{15}N, NO_3^-, NH_4^+, C/N ratio, soil water, and soil pH) obtained using the Euclidean distance (Clarke & Ainsworth, 1993). The RELATE test from the PRIMER software was used to performed the analysis, which is a permutation-based test (rank correlation method: Spearman, 999 permutations) giving the significance levels of the correlation, i.e. *P* value, and the correlation strengths, i.e. Spearman coefficient ρ. The ρ value varies between zero and one, a ρ value close to one indicates a strong correlation between the environmental variable and the microbial community structure. The correlations were performed between the entire community structure matrices or a part of it (e.g. on the samples from the organic horizon) and matrices based on one or all environmental variables.

Correlations between the microbial abundance and the environmental variables were investigated by a similar approach than for the microbial community structure using the RELATE test. The microbial abundance data was square root transformed and normalised for each community (i.e. bacteria, archaea or fungi) and a similarity matrix was constructed using Euclidean distance. These matrices were correlated to the

environmental variables matrices obtained using Euclidean distance. The *P* value and the ρ value were obtained for each correlation.

In order to investigate relationships between microbial communities, correlations were performed between the different microbial community structures or abundances and between the microbial community structure and abundance. The RELATE test from the PRIMER software was used by correlating the different similarity matrices define previously for the microbial community structure and abundance.

Chapter 3: Short-term variability of bacterial, archaeal and fungal community structure and abundance within High Arctic tundra soil horizons

Bayelva river catchment, Leirhaugen hill (middle), and Austre Brøggerbreen (bottom left) and Vestre Brøggerbreen (bottom right) glaciers the 3rd of August 2010.

3.1 Introduction

Arctic tundra ecosystems cover nearly 5% of the land on earth (Nemergut *et al.*, 2005). They are characterised by long winters and short summers, low nutrient (N and P) availability and short seasonal growth periods for plants (Shaver & Chapin, 1980). These characteristics of arctic ecosystems make them particularly sensitive to environmental change (Robinson *et al.*, 1995; Van Wijk *et al.*, 2004). Most climate models predict an increase of temperature, and precipitation for polar regions (Anisimov and Fitzharris, 2001; IPCC, 2007). As a consequence of the particular characteristics of arctic tundra and the threats that it encounters, changes in the diversity, abundance and activity are expected for its plant and the microbial communities (ACIA, 2005). Many studies have investigated the impact of temperature increase (Chapin *et al.*, 1995; Van Wijk, Clemmensen, *et al.*, 2004) or nutrient additions (Gordon *et al.*, 2001; Tye *et al.*, 2005) on arctic tundra ecosystems, which have shown a clear sensitivity to these environmental changes, for example through increases in plant biomass and/or plant community composition (Chapin *et al.*, 1995; Shaver *et al.*, 2001; Gordon *et al.*, 2001; Van Wijk *et al.*, 2004). Additionally, a number of recent studies have considered impacts of environment change on tundra microbial communities (Deslippe *et al.*, 2005; Walker *et al.*, 2008; Lamb *et al.*, 2011).

Rinnan *et al.* (2007) showed, using a 15 year plot experiment on subarctic tundra, that fertilisation (NPK addition, 100, 26 and 90 kg ha^{-1} N yr^{-1}, respectively) led to an increase of 25 - 36% in microbial biomass (especially fungal and Gram-positive bacteria biomass), whilst warming and shading led to a reduction in the relative abundance of fungi in comparison to the bacterial community. Microbial community structure, assessed by Phospholipid Fatty Acids analysis (PLFA), changed with fertilisation (explained by increase in abundance of Gram-positive bacteria and fungi), and to a lesser extent with warming and shading. All of these changes were more pronounced within the top 0-5 cm soil than in 5-10 cm layer. Other studies have investigated the archaeal (e.g. Høj *et al.*, 2005; 2006; 2008), bacterial (Neufeld *et al.*, 2004; Neufeld & Mohn, 2005; McMahon *et al.*, 2011) and fungal (Robinson *et al.*, 2004; Fujimura *et al.*, 2007) communities in arctic tundra soil. Robinson *et al.* (2004) showed

that the diversity of fungal communities, determined by a culture-dependant method, was higher in organic soil than in mineral soil, explaining that this spatial distribution was probably related to the higher C and nutrient content in the organic soil. They did not find any significant temporal variation in fungal assemblages over the course of a summer season. However, McMahon *et al.* (2011) and Høj *et al.* (2008) found differences over time (i.e. between season and over summer, respectively) in bacterial and archaeal community structure, respectively. Archaeal community composition, especially of methanogenic groups and of Group 1.3b of Crenarchaeaota was positively influenced by soil water regime (i.e. soil water input and output) whilst low temperatures selected for non-methanogenic archaea (Høj *et al.*, 2006; 2008). These studies suggest that the microbial communities do not respond similarly between different soil layers or over time, and that members of the three different microbial domains are not influenced by the same environmental drivers, which is of particular interest when aiming to understand the impact of global and nutrient changes within arctic tundra.

Despite the remote location of the Arctic, it is susceptible to receipt of episodic atmospheric nitrogen deposition events resulting from polluted air masses that travel from lower latitudes to the Arctic with minimal dispersal (Hodson *et al.*, 2005; 2010; Kühnel *et al.*, 2011). Hodson *et al.*, (2005; 2010) found that acute N deposition events can occur, in which 40% of the annual atmospheric N input can be deposited as acidic rainfall (~pH 4) in less than one week, highlighting events which could potentially impact upon the Arctic tundra ecosystems (see Chapter 1). In Alpine tundra in the Colorado Rocky Mountains, Nemergut *et al.* (2008) showed that archaeal, bacterial and fungal communities responded differently in relation to N deposition (115 kg N ha^{-1} over ten years). Bacterial and fungal communities shifted with N addition. Bacterial sequences (16S rRNA genes) related to Verrucomicrobia disappeared from N amended soil, while relative abundance of Bacteriodetes and Gemmatimonadetes increased by 3.8 and 2.5 times, respectively, in N amended soil. Similarly, fungal sequences (LSU rRNA genes) related to the Ascomycota increased in relative abundance by 30% in N-amended soil while Basidiomycota decreased. The archaeal to bacterial relative abundance declined from 20% to less than 1% between control and N amended soils.

In the context of global change and N deposition, it is important to understand the environmental drivers of the different microbial communities (i.e. abundance, activity, diversity and structure), in order to predict their responses to anthropogenic activities. However, little is known about the ecology of the different microbial communities in arctic tundra soil. Moreover, none of the previous studies have investigated the structure of all three microbial domains together, relating the communities to the environmental drivers. Thus, the aims of this study were to investigate variation in the structure and abundance of soil microbial communities (i.e. archaeal, bacterial and fungal) i) between the organic and mineral soil horizons, ii) over time, and iii) in response to simulated elevated episodic nitrogen deposition and to relate such changes to the main environmental drivers of the microbial community.

To address these objectives a plot scale experiment was established on the High Arctic tundra at Ny-Ålesund (Svalbard) in summer 2009 to simulate acute N deposition by the application of NH_4NO_3 solution of ~pH 4 at nitrogen application rates of 0.4 and 4 kg N ha^{-1} yr^{-1} (see section 2.2.1). Soil samples from the organic and mineral horizons were taken over 9 days within each plot. Changes in soil characteristics (i.e. soil water content, soil pH, total C and total N content) were measured for both soil horizons over time (see section 2.2.4). Variation in archaeal and bacterial community structure was assessed by Terminal Restriction Fragments Length Polymorphism (T-RFLP), and for the fungal community by Automated Ribosomal Intergenic Spacer Analysis (ARISA) (see section 2.2.5.3). The abundance of the different microbial communities was determined by Quantitative PCR (Q-PCR) (see section 2.2.5.4).

3.2 Results

3.2.1 Soil chemical characteristics

The soil water content of the organic horizon (63.2% ± 6.1, n = 149) was significantly higher (χ^2 = 195.9, df = 1, $P < 2.2x10^{-16}$) than in the mineral horizon (41.7% ± 11.8, n = 150) across the treatments and over time (Figure 3.1). The pH of the mineral horizon was significantly (χ^2 = 36.7, df = 1, $P = 1.4x10^{-9}$) higher (6.6 ± 0.25, n =

150) than in the organic horizon (6.4 ± 0.19, n = 149). The addition of water to the different plots did not significantly increase the soil water content or reduce the pH of either soil horizons or over time ($P > 0.05$, ANOVA) (Figure 3.2).

Total C and N soil contents were significantly higher (F = 112.2, F = 74.0, df = 1, $P = 4.8 \times 10^{-14}$, $P = 3.2 \times 10^{-11}$, respectively) in the organic than in the mineral horizon (~2.7 and 2 times higher for total C and N, respectively). However, total C and N did not change significantly between the control + water and 4 kg N ha^{-1} yr^{-1} treatments or over time ($P > 0.05$, ANOVA) (Figure 3.3). The mean total C content for the organic and mineral horizons across all sampling plots and time points was 15.1% ± 4.2 and 5.4 ± 3.0%, respectively; while the mean total N content was 0.98% ± 0.20 and 0.49% ± 0.23 soil for the organic and mineral soil horizons across all sampling plots and time points, respectively (n = 30). Similarly, the mean C/N ratio was ~1.3 times significantly higher (F = 135.2, df = 1, $P = 1.97 \times 10^{-15}$) in the organic than in the mineral horizons across all sampling plots and time points (Figure 3.3). However, the C/N ratios for both soil horizons were significantly higher (~1.6 times; $P < 0.001$, Tukey HSD) before N application (Day-2) than 1 and 7 days post treatment (Figure 3.3).

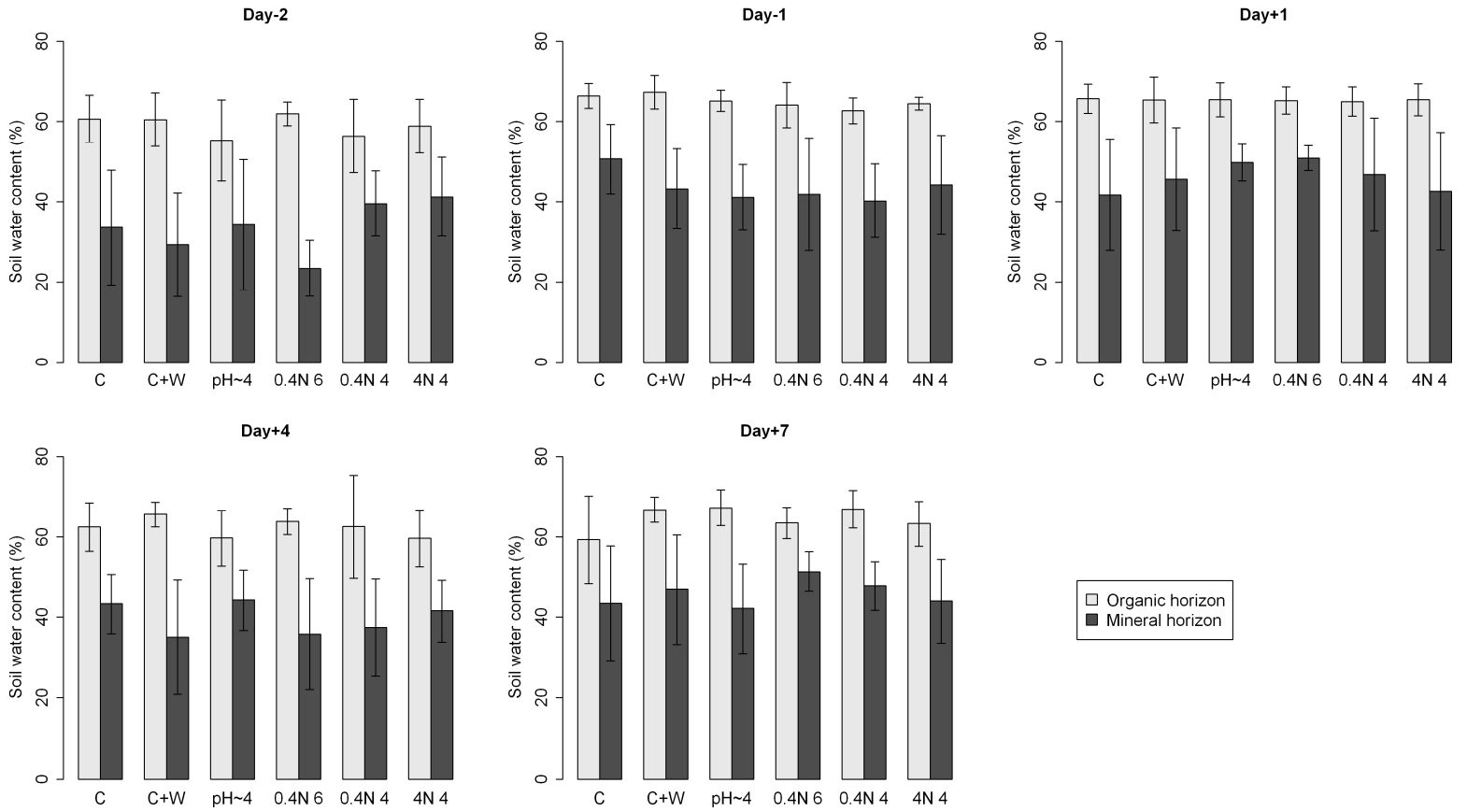

Figure 3.1: Variation in soil water content (%) between organic and mineral soil horizons, over time and in response to simulated episodic nitrogen deposition events. Plots were established and sampled in summer 2009. **Day-2**: before N application; **Day-1**: just after the first N application; **Day+1**: one day after N application; **Day+4**: four days after N application; **Day+7**: seven days after N application; **C**: Control plots; **C+W**: control + water plots; **pH~4**: water ~pH 4 plots; **0.4N 6**: 0.4 kg N ha^{-1} yr^{-1} ~pH 6 plots; **0.4N 4**: 0.4 kg N ha^{-1} yr^{-1} ~pH 4 plots; **4N 4**: 4 kg N ha^{-1} yr^{-1} ~pH 4 plots. Means values ± standard deviation (n = 5) are shown. Significant ($P < 0.001$) differences between the organic and mineral horizons were found.

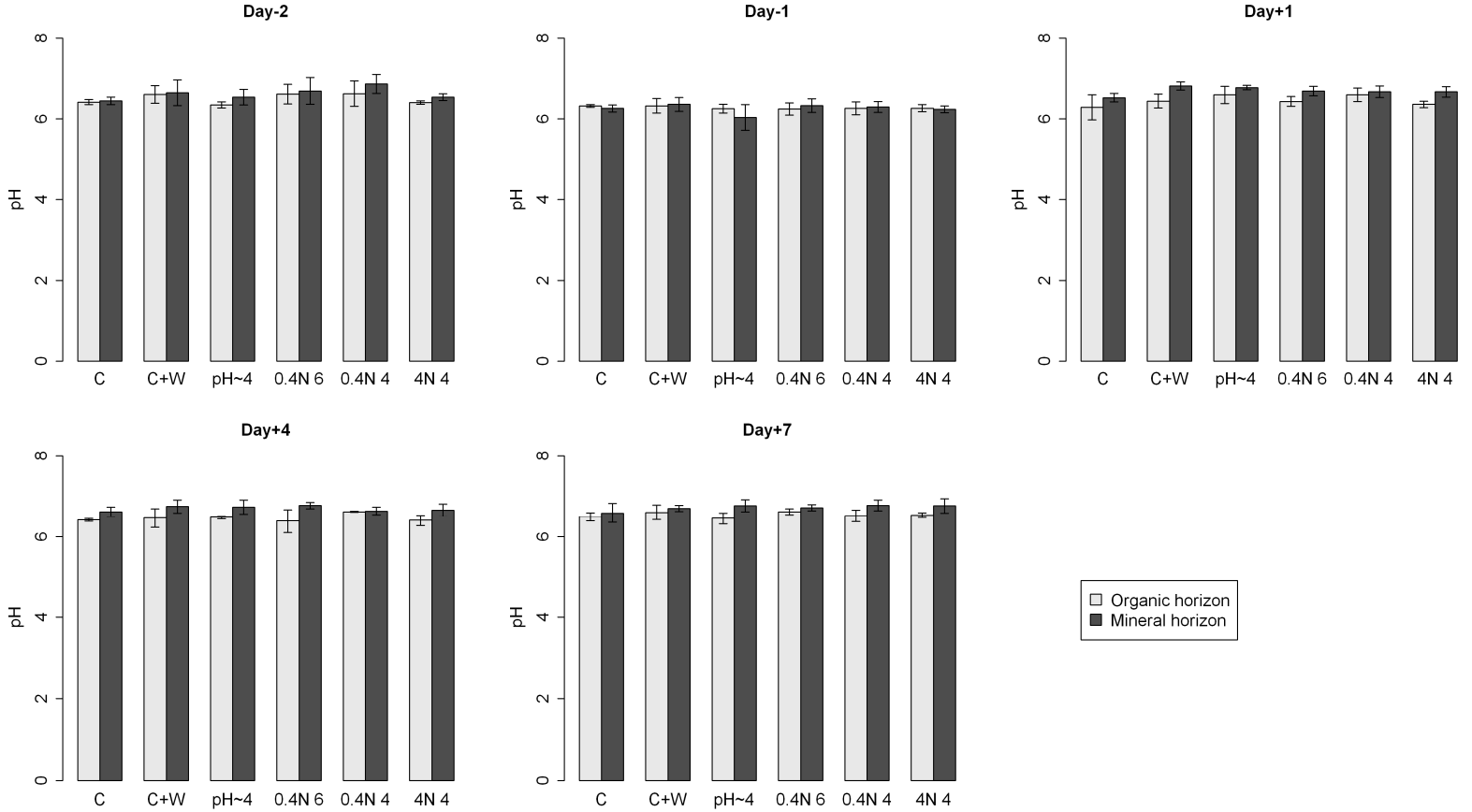

Figure 3.2: Variation in soil pH between organic and mineral soil horizons, over time and in response to simulated episodic nitrogen deposition events. Plots were established and sampled in summer 2009. **Day-2**: before N application; **Day-1**: just after the first N application; **Day+1**: one day after N application; **Day+4**: four days after N application; **Day+7**: seven days after N application; **C**: Control plots; **C+W**: control + water plots; **pH~4**: water ~pH 4 plots; **0.4N 6**: 0.4 kg N ha^{-1} yr^{-1} ~pH 6 plots; **0.4N 4**: 0.4 kg N ha^{-1} yr^{-1} ~pH 4 plots; **4N 4**: 4 kg N ha^{-1} yr^{-1} ~pH 4 plots. Means values ± standard deviation (n = 5) are shown. Significant ($P < 0.001$) differences between the organic and mineral horizons were found.

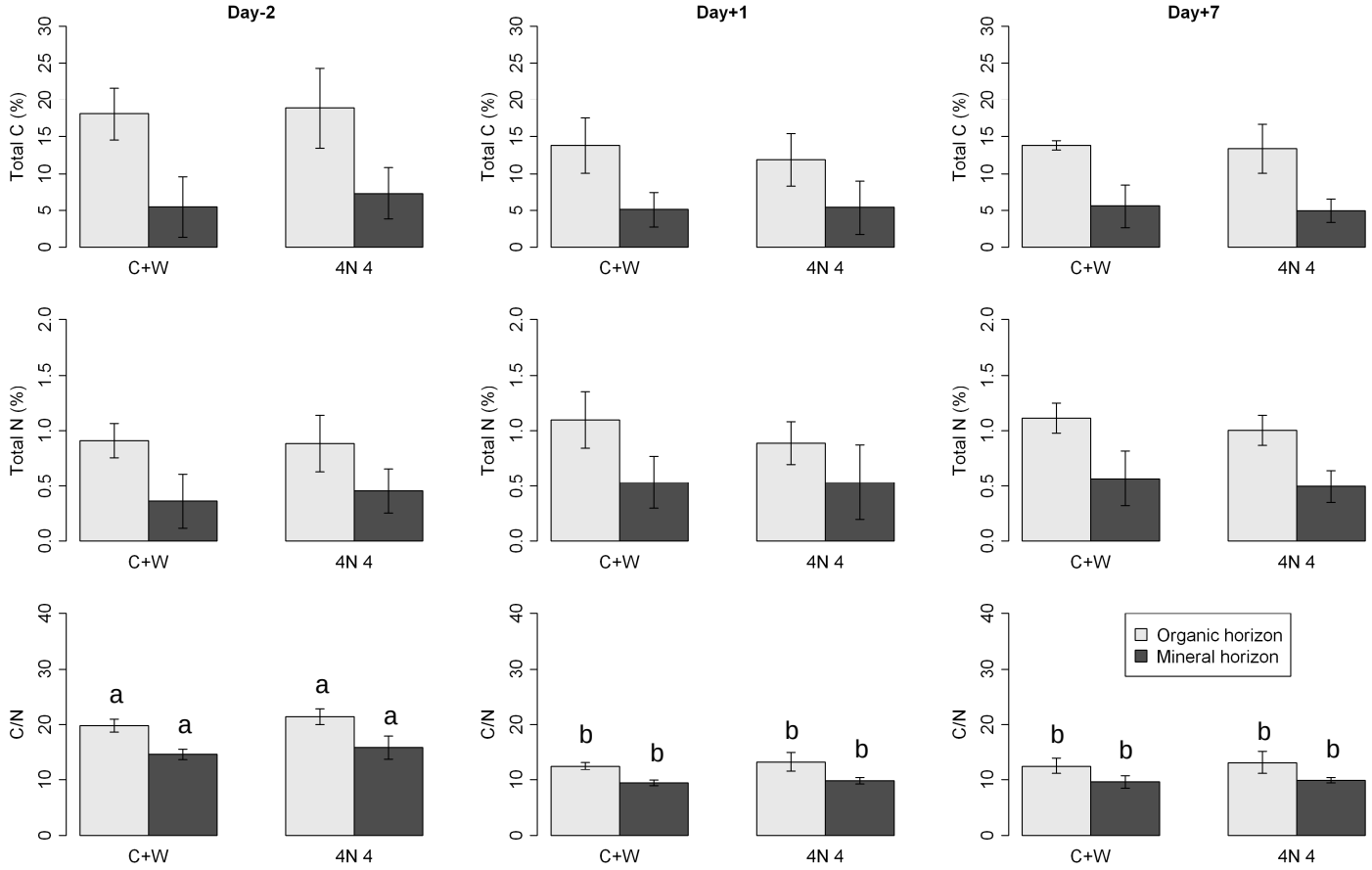

Figure 3.3: Variation in total C (%), total N (%) content and C/N ratio between organic and mineral soil horizons, over time and in response to simulated episodic nitrogen deposition events. Plots were established and sampled in summer 2009. **Day-2**: before N application; **Day+1**: one day after N application; **Day+7**: seven days after N application; **C+W**: control + water plots; **4N 4**: 4 kg N ha^{-1} yr^{-1} ~pH 4 plots. Means values ± standard deviation (n = 5) are shown. Significant ($P < 0.001$) differences in C, N and C/N ratio between the organic and mineral horizons were found. Different letters indicate significant ($P < 0.001$) difference in C/N ratio over time for a specific soil horizon and treatment.

Principal component analysis (PCA) was conducted on all of the environmental variables (total C, total N, ^{15}N, C/N ratio, soil water content and soil pH) to investigate differences and changes of environmental conditions between soil horizons, over time and in response to simulated episodic nitrogen deposition events. The first two principal components explained 85.1% of the data (PC1 = 58.8%, PC2 = 26.3%; Figure 3.4). Samples from the organic and mineral horizons showed significant differences (ANOSIM: $P = 0.00005$, R = 0.71; Figure 3.4 A; Table 3.1) along the PC1 axis, which was mainly explained by soil water content, total N and C content (Figure 3.4 D). However, the soil water content and the total N content were highly inter-correlated (Pearson correlation coefficients = 0.92), thus the influence of these two variables cannot be distinguished (Figure 3.4, D). The influence of the time (days of sampling) was explained on the PC2 axis (Figure 3.4 B), where significant differences (ANOSIM: $P \leq 0.001$) were found between Day-2 *vs.* Day+1 and Day-2 *vs.* Day+7 for both soil horizons (see Table 3.1). These differences were mainly driven by the soil C/N ratio, ^{15}N enrichment (see Appendix 3.1 for the ^{15}N enrichment detail) and soil pH on the PC2 axis (Figure 3.4 D). No significant differences (ANOSIM: $P > 0.4$) were found between the samples from the control + water and 4 kg N ha^{-1} yr^{-1} plots (Figure 3.4 C; Table 3.1).

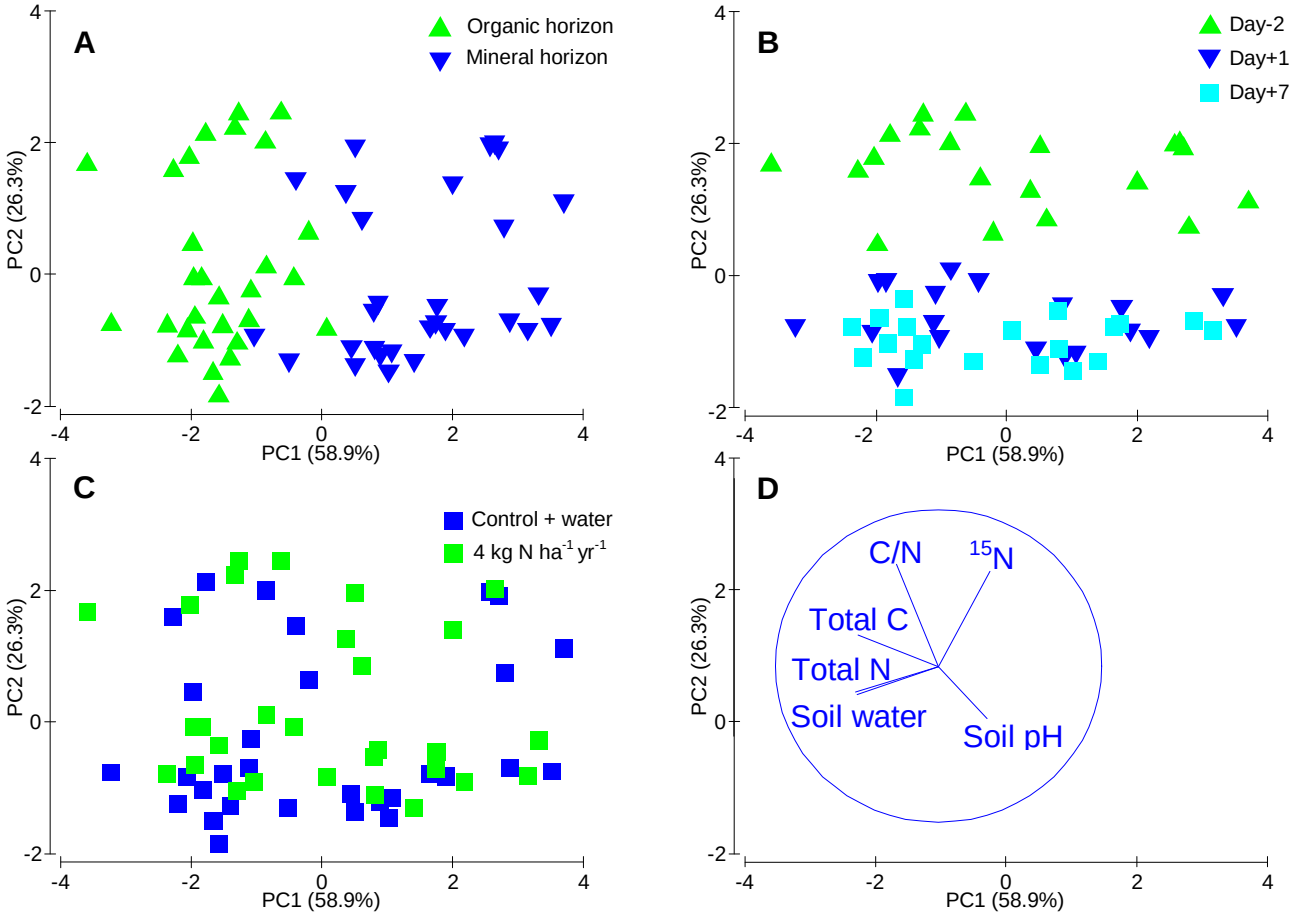

Figure 3.4: PCA of the environmental variables (i.e. total C, total N, ^{15}N, C/N ratio, soil water content and soil pH) during summer 2009 in the organic and mineral horizons from the control + water and 4 kg N ha^{-1} yr^{-1} ~pH 4 plots, before N application (Day-2) and, 1 and 7 days after N application (Day+1, Day+7 respectively). **A**: Plot showing the influence of soil horizons on the environmental variables; **B**: Plot showing the influence of time (sampling days) on the environmental variables; **C**: Plot showing the influence of simulated episodic N deposition event on the environmental variables; **D**: Plot showing the vectors driving the separation of environmental variables on the PCA plots.

Table 3.1: Two-way ANOSIM of the similarity matrix based on the environmental variables (i.e. total C, total N, ^{15}N, C/N ratio, soil water content and soil pH) between: organic and mineral horizon; different days of sampling for the organic and the mineral horizons samples; and in response to simulated episodic nitrogen deposition (control + water (**C+W**) and 4 kg N ha^{-1} yr^{-1} ~pH 4 plots). **Day-2**: before N application; **Day+1**: one day after N application; **Day+7**: seven days after N application. The R values and *P* values are given. Significant values at $P < 0.05$ are shown in bold text.

Soil horizon	Factors compared	R values	*P* values
	Organic *vs.* Mineral	**0.71**	**0.00005**
Organic	Day-2 *vs.* Day+1	**0.87**	**0.00006**
	Day-2 *vs.* Day+7	**0.90**	**0.00006**
	Day+1 *vs.* Day+7	0.13	0.13
Mineral	Day-2 *vs.* Day+1	**0.54**	**0.0002**
	Day-2 *vs.* Day+7	**0.69**	**0.0001**
	Day+1 *vs.* Day+7	-0.072	0.78
Organic	C+W *vs.* 4 kg N ha^{-1} yr^{-1}	0.005	0.43
Mineral	C+W *vs.* 4 kg N ha^{-1} yr^{-1}	-0.007	0.49

3.2.2 Variation in soil microbial community structure

3.2.2.1 DNA extraction

DNA was extracted from soil samples of the organic and mineral horizons taken in summer 2009 within the plots which received: water (Control+Water: C+W) or 4 kg N ha^{-1} yr^{-1} (4N 4). The DNA extractions were performed on three dates of sampling: before N application (D-2), and after one and seven days following N application (D+1 and D+7, respectively), these being 60 soil samples in total. Extractions of DNA were then visualised on agarose gels showing that the DNA was successfully isolated from all 60 soil samples (Figure 3.5). The agarose gels of the DNA extractions showed consistently that more DNA was extracted from the mineral horizon than from the organic horizon based on DNA band intensity (Figure 3.5).

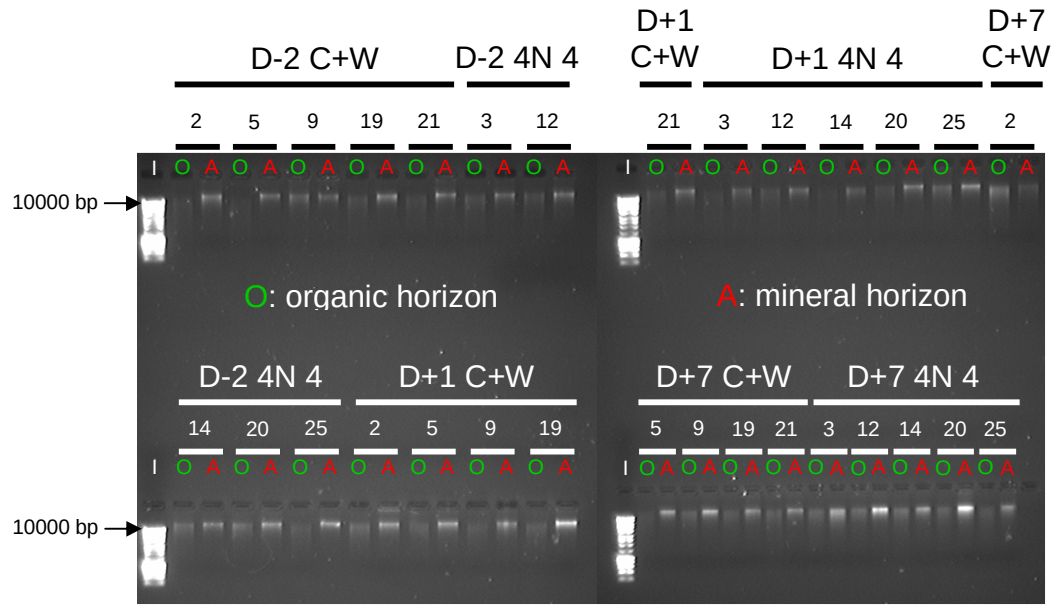

Figure 3.5: Agarose gels electrophoresis (0.8% agarose) of DNA extractions from soil samples of the organic (**O**) and mineral (**A**) horizons from the 2009 plots. DNA was extracted from the soil samples of the control + water (**C+W**) and 4 kg N ha^{-1} yr^{-1} ~pH 4 (**4N 4**) plots; before N application (**D-2**), and 1 and 7 days after N application (**D+1**, **D+7**, respectively). Numbers above the lanes, indicate plot numbers. The Hyperladder™ I (Bioline, London, UK; **l**) was used as a size standard.

3.2.2.2 PCR amplification of bacterial and archaeal 16S rRNA genes, and fungal internal transcribed spacer (ITS) regions

The presence of bacteria was investigated by the amplification of the 16S rRNA gene by PCR from the 60 DNA extractions. Agarose gel electrophoresis showed that PCR products were amplified for all the DNA extractions (Figure 3.6). The intensity of PCR products from the mineral horizon was generally stronger than for those from the organic horizon across the different dates of sampling and treatments, which was consistent with DNA band intensities seen in Figure 3.5. However, sometimes the organic horizon presented similar (e.g. plot 2 D-2 C+W; Figure 3.6) or even higher band intensity (e.g. plots 3 and 12, D-2 4N 4; Figure 3.6).

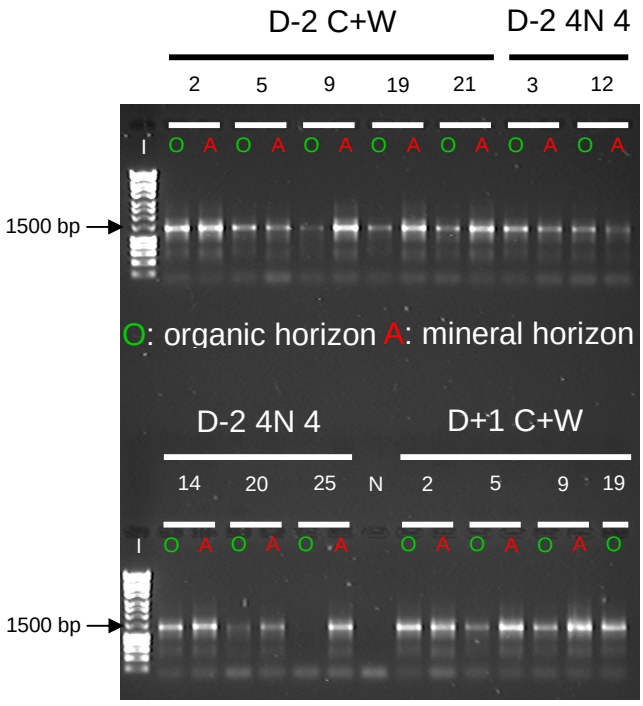

Figure 3.6: Agarose gel electrophoresis (0.8% agarose) of representative PCR amplifications of the bacterial 16S rRNA gene from soil samples of the organic (**O**) and mineral (**A**) horizons from the 2009 plots. **C+W**: control + water plots; **4N 4**: 4 kg N ha^{-1} yr^{-1} ~pH 4 plots; **D-2**: before N application; **D+1**: 1 day after N application; **N**: PCR negative control. The numbers above the lanes, indicate the plot number. The Hyperladder™ I (Bioline, London, UK; **I**) was used as a size standard.

The presence of archaea in the soil was investigated by PCR amplification of the 16S rRNA gene from the 60 DNA extractions. Agarose gel electrophoresis (Figure 3.7) showed that PCR products were amplified from all of the DNA extractions from the mineral horizon but from only 20 DNA extracts from the organic horizon (Figure 3.7). The intensity of archaeal PCR products from the mineral horizon were stronger than those amplified from the organic horizon. The band intensity of PCR products from both soil horizons decreased over time of sampling (Figure 3.7). This decrease in band intensity over time was more pronounced for the organic horizon than for the mineral horizon. Consequently, the archaeal PCR products from the organic horizon after one and seven days of N application were mostly of a too low yield to subsequently perform T-RFLP.

The presence of fungi was investigated by the amplification of the ITS region by PCR from the 60 DNA extractions. PCR products were obtained from all of the 60 samples (e.g. Figure 3.8). In contrast to the DNA extractions and 16S rRNA gene PCR products from bacteria and archaea, the fungal ITS PCR products from the organic horizon often were of a higher intensity than of those from the mineral horizon (Figure 3.8). However, the intensity of ITS PCR products from both horizons showed high variability. The fungal PCR products consisted of one or more bands varying in size between 600 - 1500 bp (Figure 3.8). In order to confirm that these different bands were fungal ITS sequences, a small clone library was generated from the product amplified from the soil sample from the mineral horizon of plot 12 (4 kg N ha^{-1} yr^{-1} ~pH 4) sampled seven days after N application, as it included bands ranging from ~600 - 1500 bp in size (Figure 3.9).

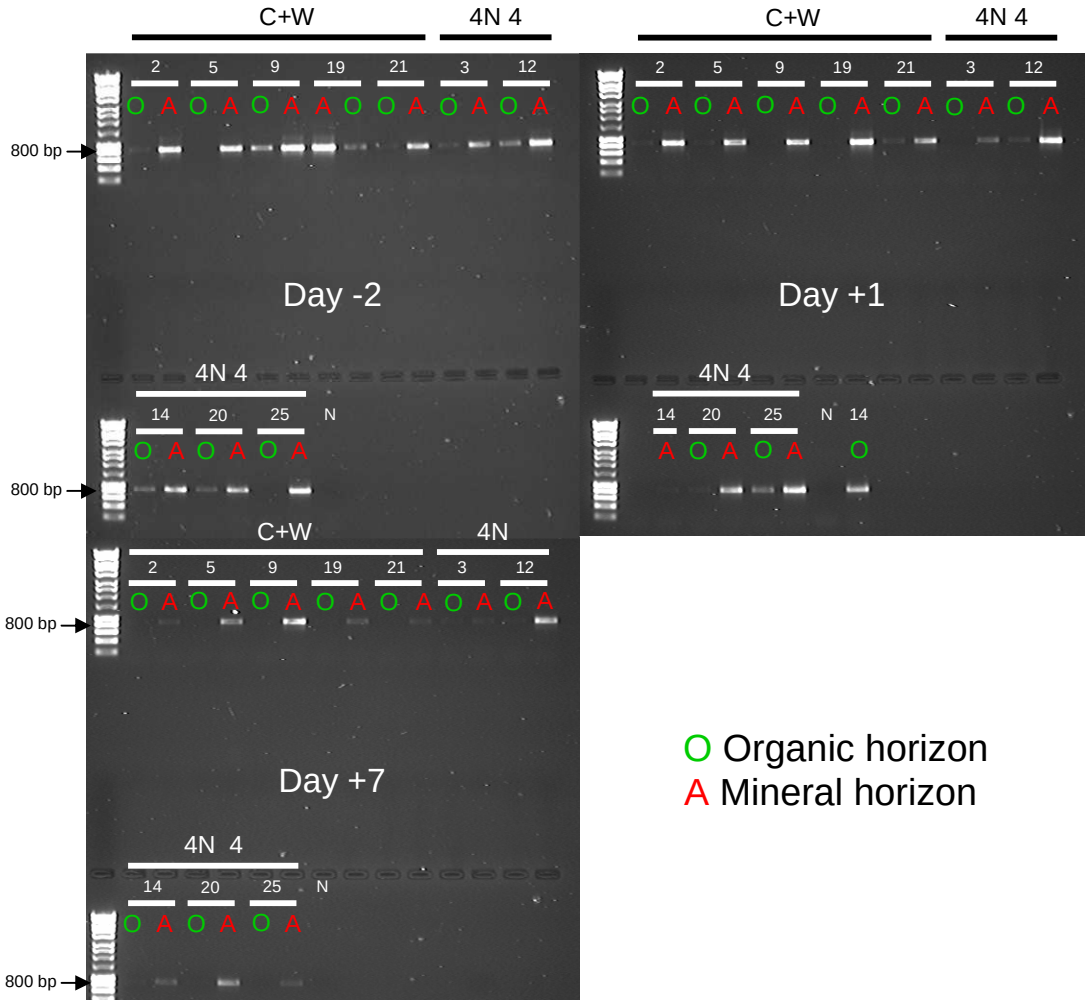

Figure 3.7: Agarose gel electrophoresis (0.8% agarose) of PCR amplifications of the archaeal 16S rRNA gene from soil samples of the organic (**O**) and mineral (**A**) horizons from the 2009 plots. **C+W**: control + water plots; **4N 4**: 4 kg N ha^{-1} yr^{-1} ~pH 4 plots; **D-2**: before N application; **D+1**: 1 day after N application; **N**: PCR negative control. The numbers above the lanes, indicate the plot number. The Hyperladder™ I (Bioline, London, UK; **I**) was used as a size standard.

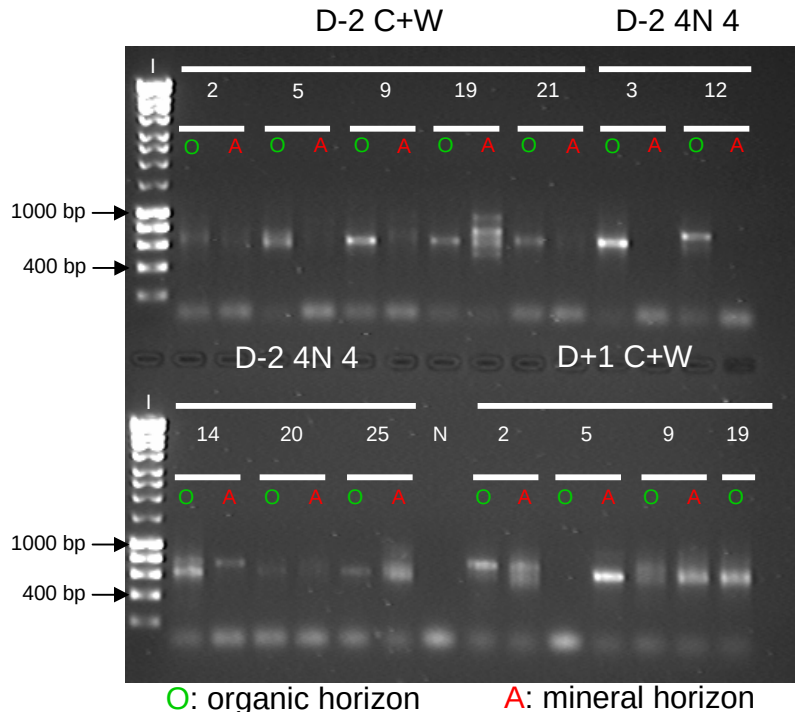

Figure 3.8: Agarose gel electrophoresis (1% agarose) of representative PCR amplifications of the fungal ITS region from soil samples of the organic (**O**) and mineral (**A**) horizons from the 2009 plots. **C+W**: control+water plots; **4N 4**: 4 kg N ha^{-1} yr^{-1} ~pH 4 plots; **D-2**: before N application; **D+1**: 1 day after N application; **N**: PCR negative control. The numbers above the lanes, indicate the plot number. The Hyperladder™ I (Bioline, London, UK; **l**) was used as a size standard.

23 ITS sequences were generated and BLASTn was used to compare these sequences to the GenBank database. All 23 sequences were related to ITS regions from fungi (Table 3.2). In addition, all of the sequences were most closely related to sequences from members of the phylum Ascomycota, except one sequence which was most closely related to an *incertae sedis* phylum (Mucoromycotina). One sequence could not be assigned to any phylum. Ascomycetes-related sequences were mainly assigned to the class Leotiomycetes (83%) of which 65% of sequences were most closely related to sequences from the order Heliothales. 22% of the sequences were assigned to uncultured ectomycorrhizal fungi. The ITS sequences were mainly most closely related to those from fungi in forest (e.g. beech, maple or boreal soils but also from Alpine grassland (*Mortierellacaea sp.*) and Chinese Alpine meadow ecosystems (*Cordyceps crassispora*). The sequences assigned to the Heliothales fungi shared a very

high percentage of identity (98-100%) to sequences in the database, but assignment covered a low percentage of the sequences (17-28%). However, the unique sequences generally presented a high percentage of identification covering a high percentage of the sequence.

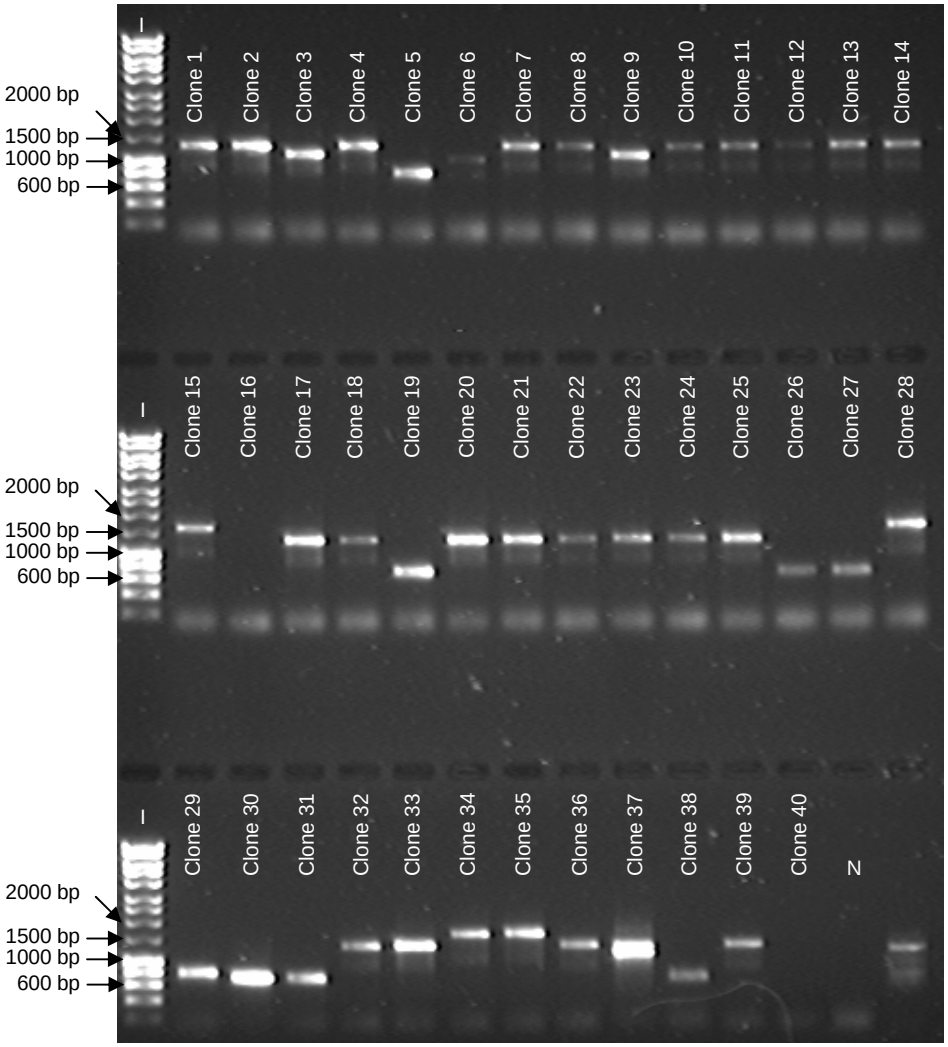

Figure 3.9: Agarose gel electrophoresis (0.8% agarose) of inserts amplified using T7 and T3 oligonucleotide primers from a clone library of PCR–amplified fungal ITS. The clone library was constructed from the soil sample of the mineral horizon of plot 12 (4 kg N ha^{-1} yr^{-1} ~pH 4, Day+7). **N**: PCR negative control. The Hyperladder™ I (Bioline, London, UK; **I**) was used as a size standard.

Table 3.2: Identification of fungal ITS sequences in arctic tundra soil fungal communities. Sequences were identified by BLASTn comparison to the GenBank database. Fungal ITS sequences were amplified from the mineral horizon of plot 12 (4 kg N ha^{-1} yr^{-1}, ~pH 4) sampled seven days post treatment. The clone numbers refer to clones shown in Figure 3.9.

Clone numbers	Closest related sequence	Accession number	Origin (ecosystem)	Phylum	Class	Order	% Identity	% coverage
1, 2, 4, 7, 10, 13, 14, 17, 19, 24, 31, 32, 39	Uncultured *Helotiales* clone LTSP_EUKA_P4J12	FJ553817.1	Forest stand	Ascomycota	Leotiomycetes	Heliotiales	98 - 100	22, 28, 28, 22, 17, 27, 29, 22, 28, 27, 21, 27, 24
5	*Mortierellaceae sp.* QLF105	FJ02503.1	Alpine grassland	*incertae sedis* (Mucoromycotina)	-	-	99	93
11	Uncultured ectomycorrhizal fungus DNA sequence	FM999525.1	Beech maple forest	-	-	-	77	63
12, 22	*Pezicula sp.* strain CBS778.95	AF141187.1	-	Ascomycota	Leotiomycetes	Heliotiales	79	47, 46
15, 27, 33, 34	Uncultured ectomycorrhiza (Leohumicola) clone LTSP_EUKA_P5I10	FJ554099.1	Forest stand	Ascomycota	Leotiomycetes	-	78	51, 50, 53, 48
18	Uncultured Ascomycota clone AhedenD29	FJ475721.1	Boreal Forest	Ascomycota	-	-	98	91
30	*Cordyceps crassispora*	AB067714.1	Chinese Alpine meadow	Ascomycota	Sordariomycetes	Hypocreomycetidae	99	91

3.2.2.3 Variation in structure of the bacterial, archaeal and fungal communities

Complex T-RFLP profiles were generated from the bacterial and archaeal communities, comprising a total of 149 and 128 different terminal restriction fragments (T-RFs), respectively (Figure 3.10; 3.11). Each individual profile was comprised of an average of 37 and 26 T-RFs for bacteria and archaea, respectively. ARISA profiles, of the fungal community, were also complex, with a total of 377 different amplicons identified (Figure 3.12). However, the numbers of distinct amplicons varied between 2 and 43 per sample with 23 amplicons in average, highlighting considerable variability of ARISA profiles between the samples. No significant ($P > 0.05$, Tukey HSD) differences were found for taxon richness (i.e. total number of T-RFs or ARISA amplicons) either for bacterial, archaeal or fungal communities between the organic and mineral horizons, over time or between control + water and 4 kg N ha^{-1} yr^{-1} plots (data not shown). Similarly, there were no significant differences in Shannon diversity index within the bacterial, archaeal and fungal communities, between the organic and mineral horizons, over time or between control + water and 4 kg N ha^{-1} yr^{-1} plots (data not shown).

nMDS plots were generated from the T-RFLP and ARISA profiles of all of the soil samples from the soil horizons, different dates of sampling and from the control + water and 4 kg N ha^{-1} yr^{-1} plots (Figure 3.13). The same nMDS plots (except for the archaea) were used to show: i) the influence of soil horizons on microbial community structure, ii) the influence of days of sampling on microbial community structure, and iii) the influence of simulated episodic N deposition event on microbial community structure. For each nMDS plots the 2D stress was given, indicating the quality of the representation (see section 2.2.6.2). The 2D stress values for the nMDS plots of the bacterial and archaeal community structure were close or equal to 0.2, indicating a good to weak 2D representation. For the nMDS plots of the fungal community, the 2D stress was equal to 0.26, indicating that the nMDS 2D plots do not give a good representation of the fungal community structure, which is better explained in 3 dimensions. Thus, the interpretation of the fungal nMDS with a high 2D stress should be done with caution.

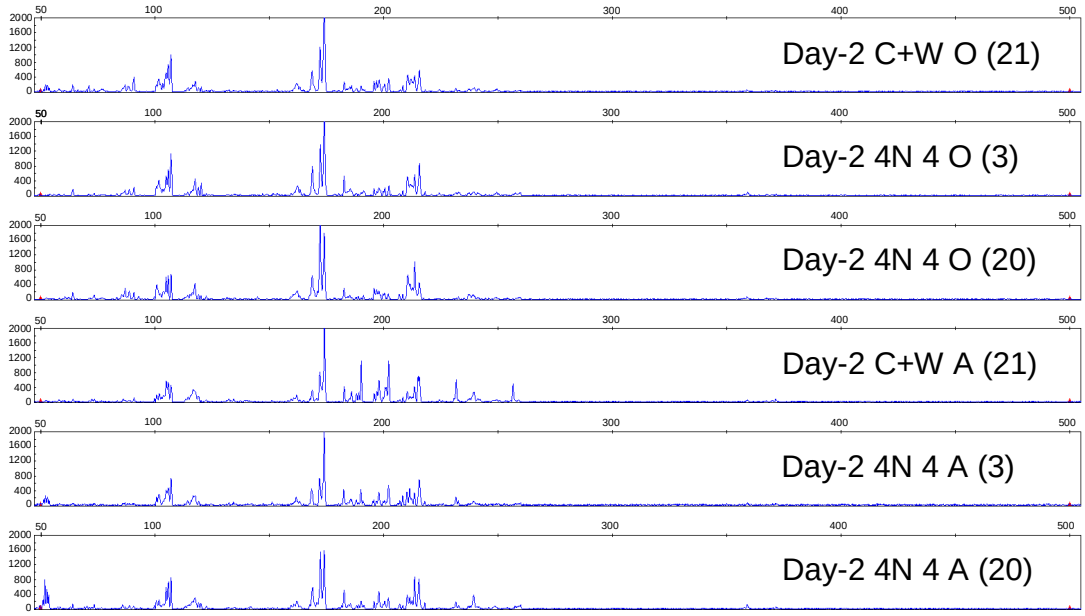

Figure 3.10: Representative T-RFLP profiles from the AluI digestion of bacterial 16S rRNA gene PCR products from the organic (**O**) and the mineral (**A**) horizons of soil samples taken before the N application (**Day-2**) within the control + water plots (**C+W**) and from the 4 kg N ha^{-1} yr^{-1} ~pH 4 plots (**4N 4**). The plot number is indicated in brackets. The *x* axis corresponds to the size of T-RFs (nucleotides) and the *y* axis corresponds to the relative fluorescence (arbitrary units) of each T-RFs.

The potential influence of geographical location of the individual plots across the experimental site upon the structure and abundance of bacterial, archaeal and fungal communities was investigated using the RELATE test from the PRIMER software to perform correlation analysis between similarity matrices of each microbial community structure (obtained using Bray-Curtis method) and a similarity matrix based on plot location (obtained using Euclidian distance; see Appendix 2.1). The structure and abundance of bacterial, archaeal and fungal communities were not significantly ($P > 0.1$) correlated to the location of plots for either the organic or mineral soil horizons over time. Only the fungal community structure at Day+7 within the organic horizon showed a significant correlation to the location of plots (R = 0.40, $P = 0.008$). Therefore, the

geographical location of plots within the experimental site was not a key driver of bacterial, archaeal and fungal community structure and abundance. Consequently, any differences in the structure and/or abundance of microbial communities reflect ecological variability between soil horizons, over time and in response to acute N deposition.

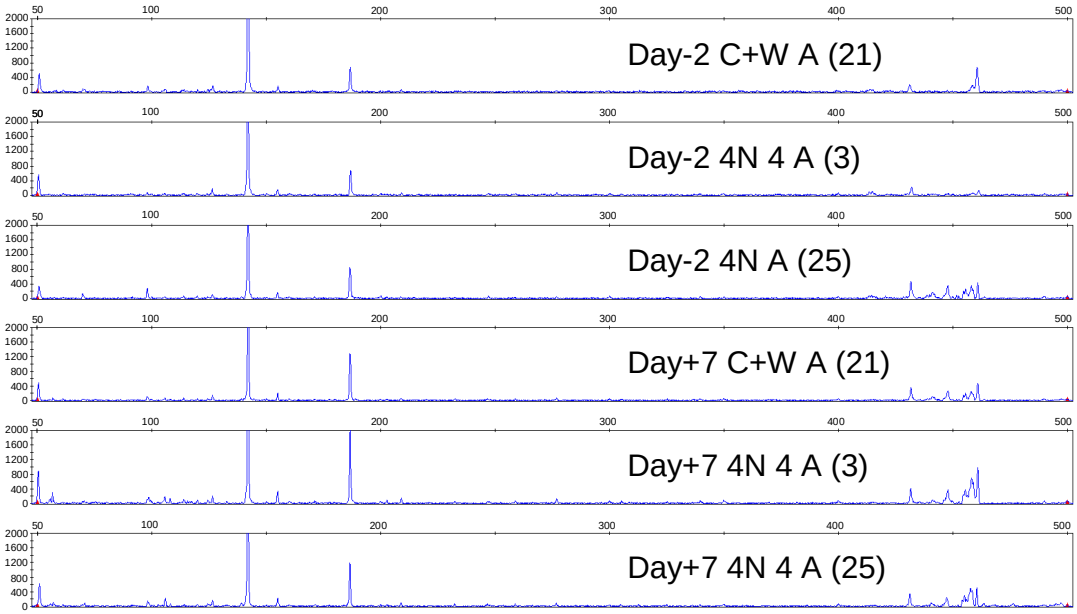

Figure 3.11: Representative T-RFLP profiles from the AluI digestion of archaeal 16S rRNA gene PCR products from the mineral horizon (**A**) of the soil samples taken before (**Day-2**) and seven days (**Day+7**) after the N application within the control + water plots (**C+W**) and the 4 kg N ha^{-1} yr^{-1} ~pH 4 plots (**4N 4**). The plot number is indicated in brackets. The *x* axis corresponds to the size of T-RFs (nucleotides) and the *y* axis corresponds to the relative fluorescence (arbitrary units) of each T-RFs.

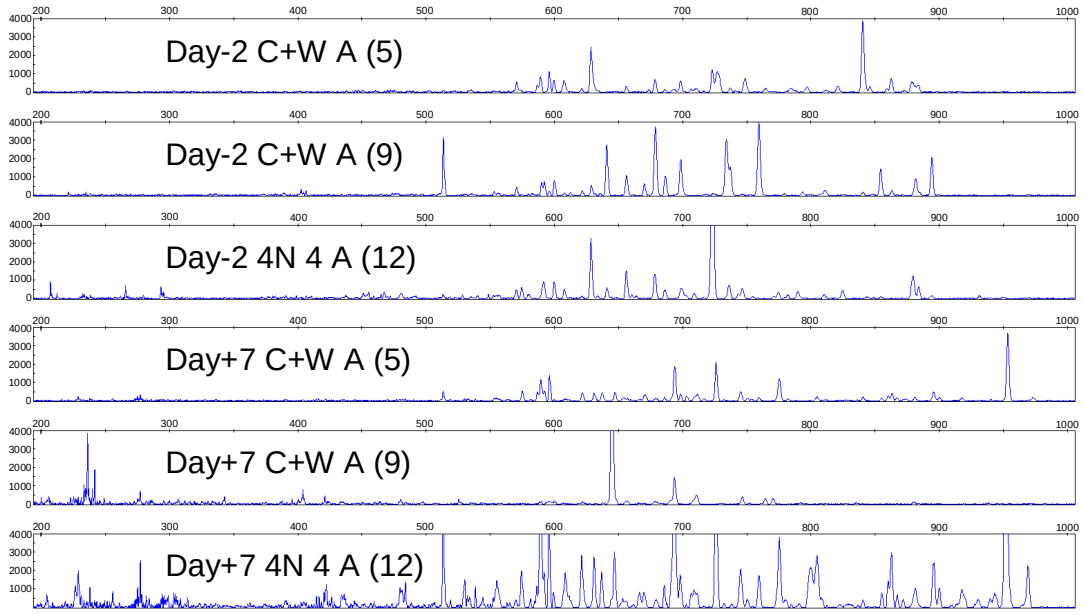

Figure 3.12: Representative ARISA profiles of the fungal ITS region PCR products from the mineral horizon (**A**) of the soil samples taken before (**Day-2**) and seven days (**Day+7**) after the N application within the control + water plots (**C+W**) and the 4 kg N ha^{-1} yr^{-1} ~pH 4 plots (**4N 4**). The plot number is indicated in brackets. The *x* axis corresponds to the size of ARISA amplicons (nucleotides) and the *y* axis corresponds to the relative fluorescence (arbitrary units) of each T-RFs.

The first objective of the study was to investigate variation in community structure between different soil horizons. ANOSIM and nMDS plots analysis generated from the T-RFLP profiles of the bacterial communities revealed significant differences (P = 0.00005) between the organic and the mineral soil horizons (Figure 3.13 A; Table 3.3). ANOSIM analysis (R = 0.55; Table 3.3) indicated a strong separation of the communities present in the organic and mineral horizons. In the organic soil horizon, archaeal 16S rRNA gene PCR products were obtained from seven samples (from ten) at Day-2, and from only three samples at Day+1, and from no samples at Day+7. Thus, the ANOSIM and nMDS analysis between the archaeal community from the organic and mineral horizons were performed only on the Day-2 (Figure 3.13 A). The archaeal community showed significant differences (P = 0.005) between organic and mineral horizon soils (R = 0.38; Table 3.3). The ARISA profiles obtained for the fungal community were not significantly different (P = 0.08) between the organic and mineral horizon (Figure 3.13 A; Table 3.3).

The second objective was to investigate the change of the microbial communities over time. The bacterial community structure of the organic horizon changed over time, but community structure did not change over time within the mineral horizon (Figure 3.13 B; Table 3.3). Within the organic horizon, the bacterial community structure was significantly different ($P = 0.046$) between Day-2 and Day+7 (R = 0.17; Table 3.3). The difference between Day-2 and Day+7 could not be seen on the 2D nMDS plot (2D stress 0.17; Figure 3.13 B), but was only visible on 3D nMDS plot (data not shown). The effect of time on the archaeal community was assessed only for the mineral horizon, as 16S rRNA genes were amplified over time, mainly from the mineral horizon. The archaeal community structure of the mineral horizon changed through time, with significant differences ($P = 0.03$) in the communities between Day-2 *vs.* Day+1, and Day-2 *vs.* Day+7 ($P = 0.007$), but no significant difference between Day+1 *vs.* Day+7 (Figure 3.13 B, Table 3.3). The R statistic was higher between Day-2 *vs.* Day+7 than Day-2 *vs.* Day+1 (R = 0.39 and R = 0.16, respectively). Similarly, the structure of the fungal community in the mineral horizon differed significantly (R = 0.29; $P = 0.009$) between Day-2 *vs.* Day+7, but did not differ between the other two sampling dates (Figure 3.13 B, Table 3.3). However, the fungal community of the organic horizon did not significantly change over time ($P < 0.05$; See Table 3.3).

The third objective was to investigate the impact of acute N deposition simulation upon microbial community structure. The addition of N did not have any significant effect on the bacterial community structure in either the organic or mineral horizons ($P = 0.68$, $P = 0.43$, respectively; Figure 3.13 C; Table 3.3). As for the effect of days of sampling, the archaeal community structure between the control and the N treatment was assessed for the mineral horizon only. The archaeal community structure of the mineral horizon was not significantly influenced by the N addition ($P = 0.54$). Similarly, the structure of the fungal communities in both organic and mineral horizons were not significantly ($P = 0.91$, $P = 0.43$, respectively) influenced by the N addition (Figure 3.13; Table 3.3).

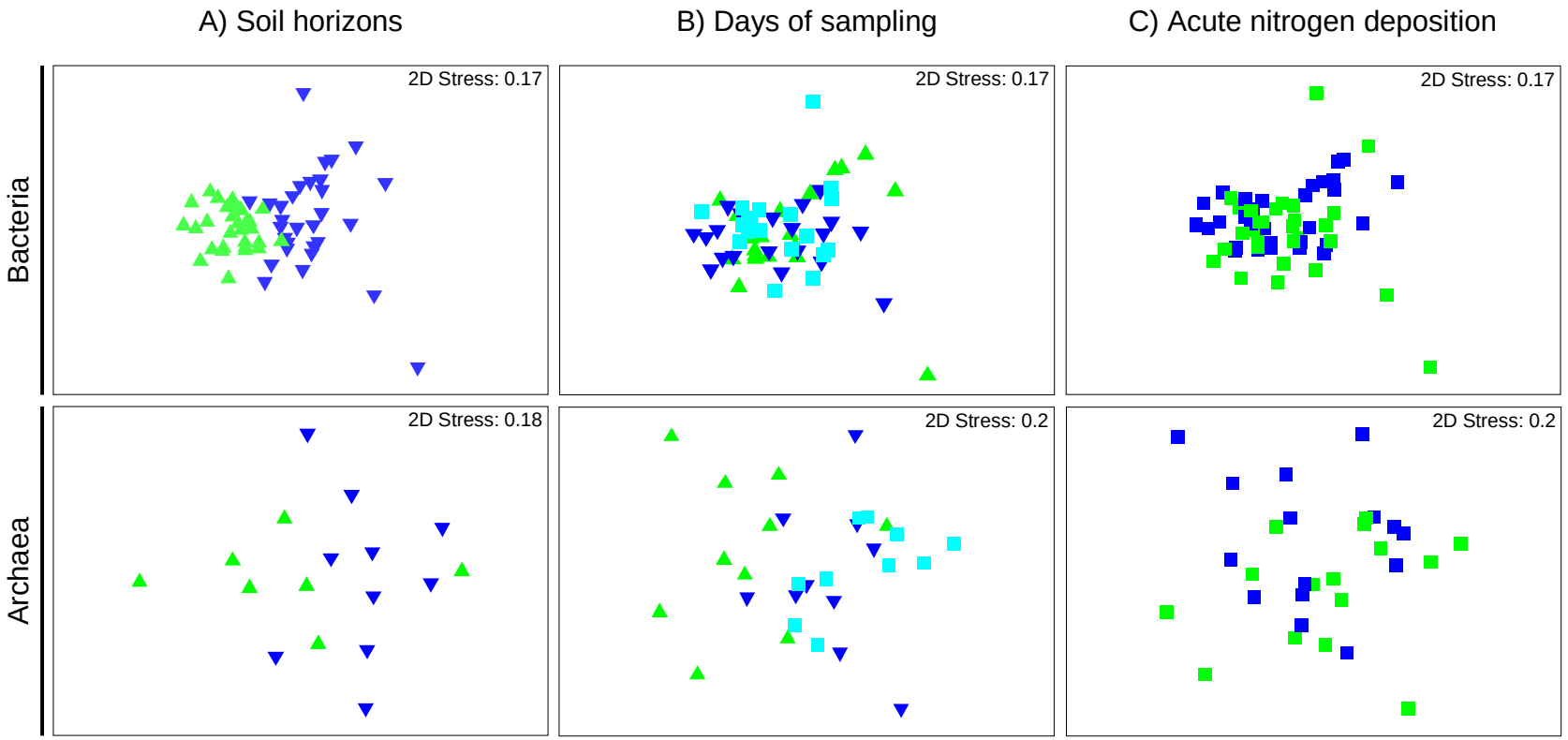
A) Soil horizons
B) Days of sampling
C) Acute nitrogen deposition
Bacteria
Archaea
2D Stress: 0.17
2D Stress: 0.17
2D Stress: 0.17
2D Stress: 0.18
2D Stress: 0.2
2D Stress: 0.2

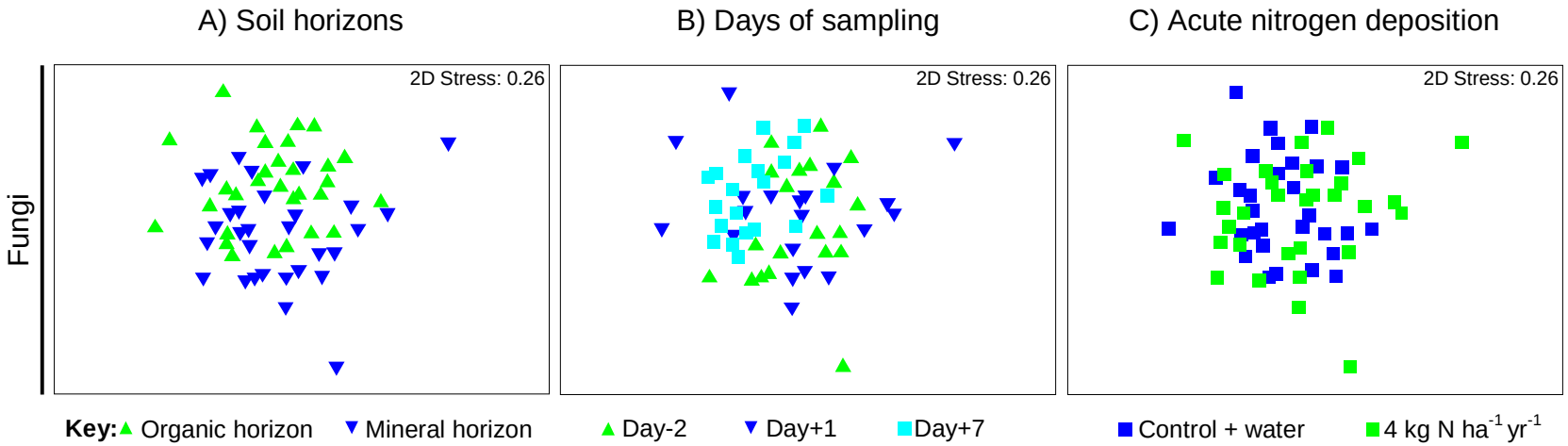

Figure 3.13: nMDS plots of the bacterial, archaeal and fungal community structures between organic and mineral soil horizons, over time and in response to simulated episodic N deposition events from soil samples taken from the organic and mineral horizons in the control + water and 4 kg N ha^{-1} yr^{-1} ~pH 4 plots, before N application (Day-2) and, 1, and 7 days after N application (Day+1, Day+7 respectively). **A**: plots showing the influence of soil horizons on microbial community structure; **B**: plots showing the influence of the sampling day on microbial community structure; **C**: plots showing the influence of simulated episodic N deposition event on microbial community structure. nMDS plot of the archaeal community structure between organic and mineral horizons was obtained from Day-2 soil samples only. nMDS plots of the archaeal community structure between the days of sampling and the treatments were obtained from the mineral horizon only. Soil horizons, days of sampling and treatments are as indicated in the key. The 2D stress is given for each nMDS plot.

Table 3.3: Two-way ANOSIM of the archaeal, bacterial and fungal community structures between: organic and mineral horizons; different days of sampling for the organic and mineral horizons samples; and in response to simulated episodic nitrogen deposition for the organic and mineral horizons (control + water (**C+W**) and 4 kg N ha^{-1} yr^{-1} ~pH 4 plots). **Day-2**: before N application; **Day+1**: one day after N application; **Day+7**: seven days after N application. The R values and the significance level (in brackets) are given. Significant values at $P < 0.05$ are shown in bold text.

Soil horizons	Factors compared	Bacteria	Archaea	Fungi
	Organic *vs.* Mineral	**0.55 (0.00005)**	**0.38 (0.005)**[†]	0.09 (0.08)
Organic	Day-2 *vs.* Day+1	0.13 (0.084)	-	-0.02 (0.53)
	Day-2 *vs.* Day+7	**0.17 (0.046)**	-	0.04 (0.35)
	Day+1 *vs.* Day+7	0.13 (0.092)	-	0.02(0.39)
Mineral	Day-2 *vs.* Day+1	0.01 (0.40)	**0.16 (0.03)**	0.002 (0.48)
	Day-2 *vs.* Day+7	0.01 (0.38)	**0.39 (0.007)**	**0.29 (0.009)**
	Day+1 *vs.* Day+7	-0.09 (0.86)	0 (0.41)	0.18 (0.053)
Organic	C+W *vs.* 4 kg N ha^{-1} yr^{-1}	-0.04 (0.68)	-	-0.11 (0.91)
Mineral	C+W *vs.* 4 kg N ha^{-1} yr^{-1}	0.005 (0.43)	-0.02 (0.54)	-0.01(0.43)

[†] R and *P* value calculated using data from Day-2 samples only (see text for details)

3.2.3 Variation in microbial community abundance within soil

Variation in the abundance of bacteria, archaea and fungi abundance was investigated by Q-PCR from the soil samples of the control + water and 4 kg N ha^{-1} yr^{-1} plots from the organic and mineral horizons, taken at Day-2, Day+1 and Day+7 (60 samples). Microbial abundances were obtained from all of the soil samples (Figure 3.14), except from one sample for the bacteria (sample: mineral horizon of the 4 kg N ha-1 yr^{-1} plot 20 at day+7) and one sample for the archaea (sample: mineral horizon of the 4 kg N ha^{-1} yr^{-1} plot 14 at day+7). Bacteria, archaea and fungi were significantly ($P < 0.05$, Kruskal-Wallis) more abundant in the mineral than in the organic horizon (Figure

3.14). These microbial communities from the mineral horizon showed more variability than those from the organic horizon, but on average the mineral horizon had 2.9, 4.5 and 1.7 times more bacterial and archaeal 16S rRNA gene numbers, and fungal ITS region numbers respectively than in the organic horizon. Abundance of bacterial 16S rRNA gene numbers did not significantly ($F = 0.79$, $df = 2$, $P = 0.46$) change over time in the organic horizon. However, the bacterial 16S rRNA gene abundance in the mineral horizon increased by 2.7 times between Day-2 and Day+7, but the increase was not significant, despite a low P value ($\chi^2 = 5.07$, $df = 2$, $P = 0.079$). Archaeal 16S rRNA gene abundance did not show any significant ($F < 3$, $df = 2$, $P > 0.05$) change over time for both horizons, but the mineral horizon showed high variability in abundance over time. In contrast, abundance of fungal ITS amplicons increased over time in the organic and mineral horizons of 2.7 and 3.5 times, respectively. The increase in fungal ITS abundance in the organic horizon was close to significant ($\chi^2 = 4.9$, $df = 2$, $P = 0.086$), while the increase in fungal ITS abundance in the mineral horizon was significant ($\chi^2 = 10.5$, $df = 2$, $P = 0.0053$). Abundance of bacterial, archaeal and fungal rRNA or ITS numbers were not significantly influenced by the N addition for any soil horizon or date of sampling (Figure 3.14).

3.2.4 Relationship between microbial community structures, abundance and environmental variables

3.2.4.1 Correlations with microbial community structure

Bacterial community structure for both soil horizons was significantly correlated ($P = 0.001$) to all of the environmental variables except C/N ratio ($P = 0.23$; Table 3.4). The soil water content was the most strongly correlated to the bacterial community structure ($\rho = 53$), then the total N and total C also showed strong correlations ($\rho = 0.43$ and 0.33, respectively). Then, the soil ^{15}N enrichment and soil pH showed weaker correlation to the structure of bacteria ($\rho = 0.23$ and 0.22, respectively). The bacterial community structure was significantly but weakly correlated to bacterial 16S rRNA gene abundance ($P = 0.009$, $\rho = 0.17$).

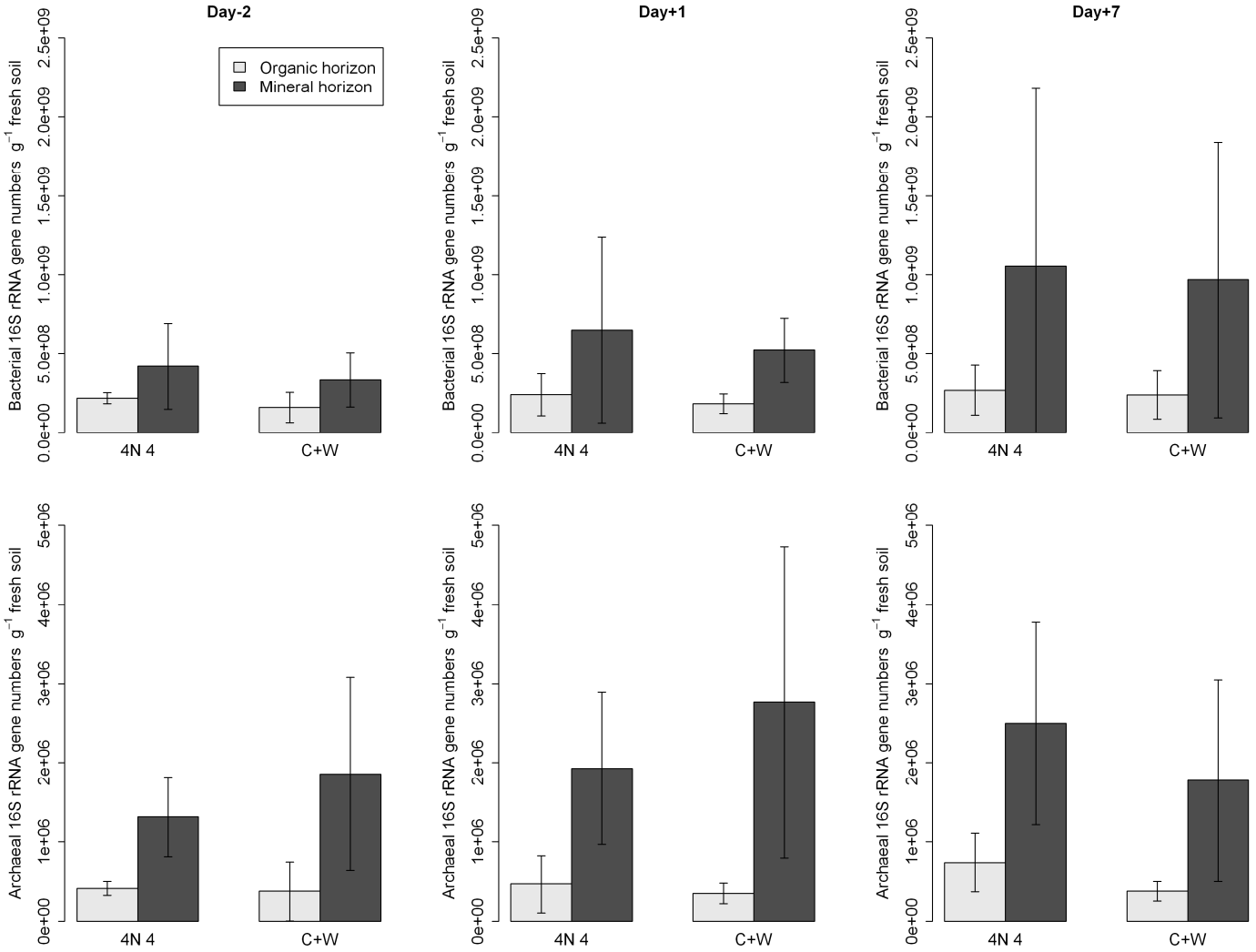
Day-2
Day+1
Day+7
Organic horizon
Mineral horizon
Bacterial 16S rRNA gene numbers g-1 fresh soil
Archaeal 16S rRNA gene numbers g-1 fresh soil
0.0e+00
5.0e+08
1.0e+09
1.5e+09
2.0e+09
2.5e+09
0e+00
1e+06
2e+06
3e+06
4e+06
5e+06
4N 4
C+W

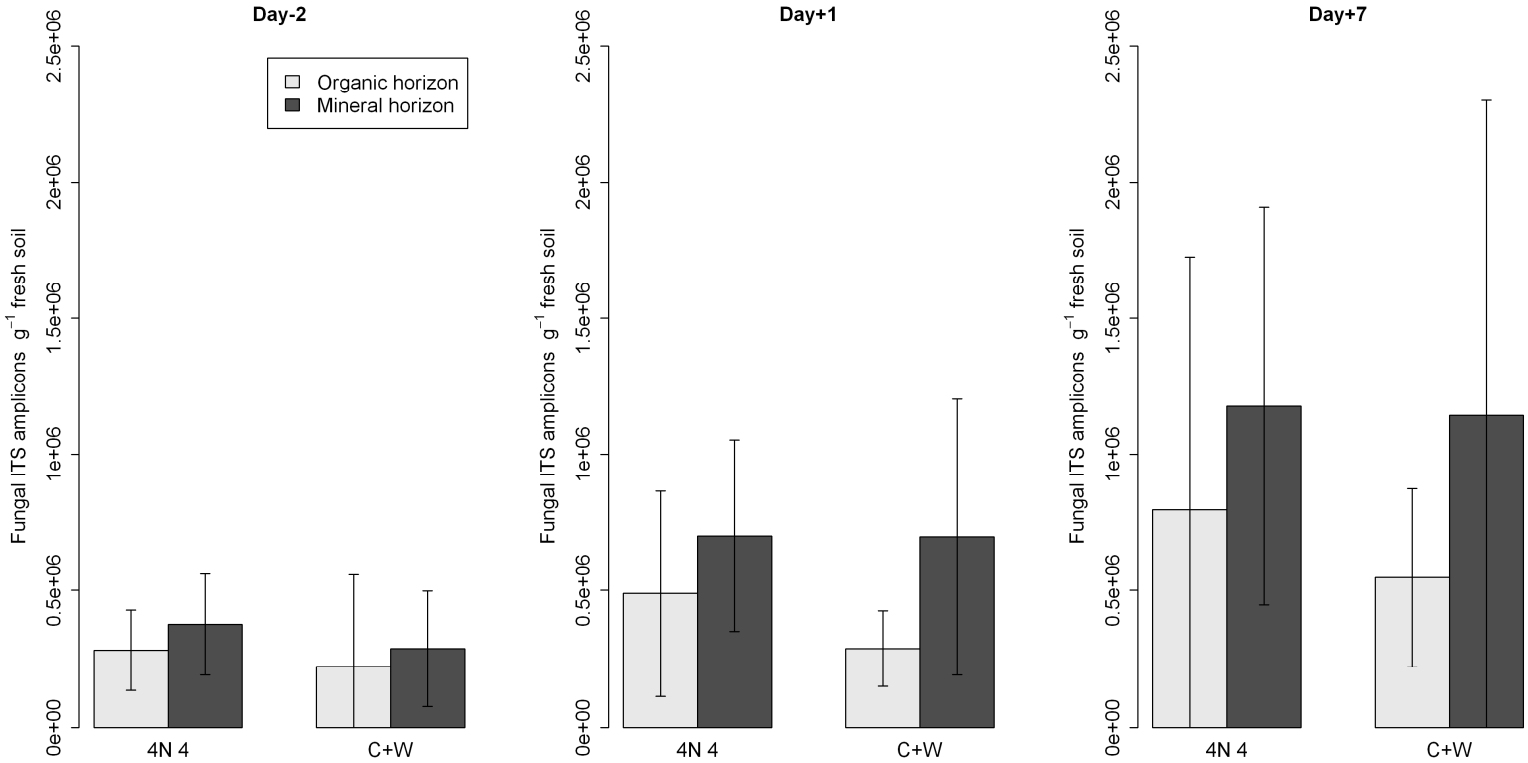

Figure 3.14: Variation in bacterial and archaeal gene abundance (16S rRNA gene numbers g^{-1} fresh soil) and fungal abundance (ITS amplicons g^{-1} fresh soil) between organic and mineral soil horizons, over time and in response to simulated episodic nitrogen deposition events. Plots were established and sampled in summer 2009. **Day-2**: before N application; **Day+1**: one day after N application; **Day+7**: seven days after N application; **C+W**: control + water plots; **4N 4**: 4 kg N ha^{-1} yr^{-1} ~pH 4 plots. Means values ± standard deviation (n = 5, except when mentioned in the text) are shown. Gene numbers were calculated from the standard curve: bacteria: r^2 = 0.991, y (intercept) = 36.48, *E* (amplification efficiency) = 94.2%, NTC C_t = 29.4; archaea: r^2 = 0.995, y = 36.95, *E* = 85.9%, NTC C_t = 32.4; fungi: r^2 = 0.899, y = 32.76, *E* = 138.5%, NTC C_t = 37.3. Significant ($P < 0.05$) differences between organic and mineral horizons for the three communities were found. Significant ($P = 0.0053$) increase of the fungal abundance over time in the mineral horizon was found.

When the correlations were performed on the organic and mineral horizons separately, only the C/N ratio was weakly correlated to the organic bacterial community structure ($P = 0.04$, $\rho = 0.14$). Whereas, the mineral bacterial community structure show significant good correlations ($P \leq 0.034$) to the soil water and total N content ($\rho = 0.31$ and 0.27, respectively) and weaker correlation to the ^{15}N enrichment and soil pH ($\rho =$ 0.24 and 0.16, respectively).

The archaeal community structure from both soil horizons was only investigated at Day-2 (see section 3.2.2.2) and showed significant correlation only to the C/N ratio ($P = 0.01$, $\rho = 0.23$) but a strong correlation with the archaeal abundance at Day-2 ($P = 0.003$, $\rho = 0.30$). The archaeal community structure of the organic horizon was not significantly ($P > 0.05$) correlated to any environmental variables (and archaeal abundance) despite a nearly significant correlation with the soil pH ($P = 0.06$, $\rho = 0.50$). However, the correlations between environmental variables and organic archaeal community structure were performed only on seven soil samples at Day-2. In contrast, the archaeal community structure of the mineral horizon showed significant ($P \leq 0.009$) correlation to the C/N ratio, total C, soil pH and ^{15}N. The C/N ratio and total C showed the strongest correlations ($\rho = 0.25$ and 0.24, respectively) with the mineral archaeal community structure while the soil pH and ^{15}N showed lower correlations to the archaeal community ($\rho = 0.20$, 0.19, respectively).

The fungal community structure of both soil horizons was extremely weakly correlated to the total N, ^{15}N and soil water content ($\rho = 0.10$, 0.10 and 0.09, respectively). No significant correlations ($P > 0.05$) were found between the fungal community of the organic or mineral horizons and the environmental variables or fungal abundance.

The fungal community structure was significantly correlated to the bacterial community structure ($P = 0.025$, $\rho = 0.25$) but not to the archaeal community structure and no significant correlation was found between bacterial and archaeal community structure ($P > 0.3$).

3.2.4.2 Correlations with microbial community abundance

Bacterial abundance was significantly ($P \leq 0.024$) correlated to all of the environmental variables except to the ^{15}N enrichment and C/N ratio (Table 3.5). In contrast to the bacterial community structure, the correlations for the bacterial abundance were not strong, with ρ varying between 0.11 and 0.16. When the bacterial correlations were investigated on the organic and mineral horizons separately, only the total C was significantly correlated to the structure of the organic horizon bacterial community ($P = 0.05$, $\rho = 0.17$).

Archaeal abundance showed different correlations than see for the archaeal structure, with significant ($P \leq 0.03$) and strong correlation to all of the variables except the ^{15}N enrichment. The soil water content, total C and total N showed strong correlations ($\rho = 0.40$, $\rho = 0.37$. $\rho = 0.34$, respectively) while the soil pH and C/N ratio showed low correlations ($\rho \leq 0.14$). When the archaeal abundance at Day-2 was correlated to the environmental variables, similar results to those of the archaeal community structure at Day-2 was found (data not shown). Thus, the C/N ratio was significantly correlated to the archaeal abundance at Day-2 ($P = 0.016$, $\rho = 0.25$) and at a lesser extent to the total C content ($P = 0.038$, $\rho = 0.19$). Archaeal abundance within the organic or mineral horizons was not significantly ($P > 0.1$) correlated to any environmental variables.

Fungal abundance was poorly correlated to any of the environmental variables. Only the total C and the C/N ratio were significantly correlated ($P = 0.039$, 0.035, respectively) to fungal abundance. Between the fungal abundance from the organic or mineral horizons, only the community from the mineral horizon showed significant ($P = 0.024$) correlations, with the soil water content and the ^{15}N enrichment. These significant correlations were stronger than the ones for the overall fungal community (Table 3.5).

The abundance of the three microbial groups showed significant correlations between them ($P = 0.001$), with a strong correlation between abundance of bacteria and archaea ($\rho = 0.46$), then between abundance of bacteria and fungi ($\rho = 0.32$) and between abundance of archaea and fungi ($\rho = 0.25$).

Table 3.4: Correlations of the microbial (bacterial, archaeal and fungal) community structure and environmental variables or microbial (bacterial, archaeal and fungal) community abundance within both soil horizons or within a specific soil horizon, obtained using the RELATE test from PRIMER software. The ρ values and the significance level (in brackets) are given. Significant values at $P < 0.05$ are shown in bold text.

Microbial community	Water	pH	Total C	Total N	^{15}N	C/N ratio	Abundance
Bacteria	**0.53 (0.001)**	**0.22 (0.001)**	**0.33 (0.001)**	**0.43 (0.001)**	**0.23 (0.001)**	0.03 (0.23)	**0.17 (0.009)**
Bacteria organic	-0.04 (0.65)	0.01 (0.46)	-0.03 (0.58)	0.042 (0.29)	0.06 (0.18)	**0.14 (0.04)**	0.10 (0.12)
Bacteria mineral	**0.31 (0.001)**	**0.16 (0.034)**	0.12 (0.13)	**0.27 (0.003)**	**0.24 (0.006)**	0.002 (0.47)	0.14 (0.12)
Archaea*	0.01 (0.45)	0.08 (0.26)	0.10 (0.17)	0 (0.47)	0.01 (0.47)	**0.23 (0.01)**	**0.30 (0.003)**
Archaea organic*	0.06 (0.37)	0.50 (0.06)	-0.15 (0.75)	-0.02 (0.76)	-0.03 (0.53)	0.22 (0.17)	0.04 (0.41)
Archaea mineral	0.09 (0.097)	**0.20 (0.005)**	**0.24 (0.009)**	0.05 (0.233)	**0.19 (0.0014)**	**0.25 (0.007)**	0.15 (0.45)
Fungi	**0.09 (0.038)**	0.09 (0.314)	0.09 (0.027)	**0.10 (0.01)**	**0.10 (0.015)**	0.03 (0.243)	- 0.08 (0.947)
Fungi organic	-0.12 (0.95)	0.12 (0.093)	0.034 (0.36)	-0.025 (0.62)	0.03 (0.34)	-0.01 (0.55)	-0.08 (0.83)
Fungi mineral	-0.08 (0.94)	-0.01 (0.52)	-0.09 (0.86)	-0.10 (0.94)	0.01 (0.44)	0.09 (0.17)	-0.04 (0.68)

* ρ and *P* value calculated using data from Day-2 samples only (see text for details)

Table 3.5: Correlations of the microbial (bacterial, archaeal and fungal) community abundance and environmental variables within both soil horizons or within a specific soil horizon, obtained using the RELATE test from PRIMER software. The ρ values and the significance level (in brackets) are given. Significant values at $P < 0.05$ are shown in bold text.

Microbial community	Water	pH	Total C	Total N	^{15}N	C/N ratio
Bacteria	**0.12 (0.024)**	**0.11 (0.018)**	**0.16 (0.003)**	**0.11 (0.014)**	-0.06 (0.9)	0.09 (0.066)
Bacteria organic	0.01 (0.42)	0.12 (0.111)	**0.17 (0.05)**	-0.01 (0.50)	-0.05 (0.75)	-0.02 (0.55)
Bacteria mineral	0.06 (0.19)	0.05 (0.28)	-0.04 (060)	0.004 (0.39)	0.08 (0.18)	-0.03 (0.60)
Archaea	**0.40 (0.001)**	**0.14 (0.003)**	**0.37 (0.001)**	**0.34 (0.001)**	0.05 (0.15)	**0.10 (0.031)**
Archaea organic	0.07 (0.21)	-0.07 (0.71)	0.09 (0.20)	-0.04 (0.64)	0.06 (0.19)	0.005 (0.42)
Archaea mineral	0.06 (0.15)	0.09 (0.12)	-0.10 (0.50)	0.06 (0.19)	0.01 (0.41)	-0.05 (0.68)
Fungi	0.07 (0.094)	0.03 (0.24)	**0.09 (0.039)**	0.05 (0.12)	-0.05 (0.89)	**0.10 (0.035)**
Fungi organic	0.03 (0.34)	0.02 (0.42)	0.12 (0.12)	-0.05 (0.99)	-0.01 (0.46)	0.07 (0.15)
Fungi mineral	**0.15 (0.024)**	0.09 (0.12)	0.04 (0.30)	0.11 (0.096)	**0.18 (0.024)**	0.02 (0.37)

3.3 Discussion

3.3.1 Changes in microbial communities with soil horizons

The soil physico-chemical characteristics showed clear differences between the organic and mineral horizon over time (Figure 3.1 – 3.4; Table 3.1). The organic and mineral horizons showed distinct environmental conditions, with different nutrient contents, water availability and soil pH, that are likely to influence microbial community structure, abundance and activity. Thus, both soil horizons represented different environment/habitats for the microbial communities. Moreover, the environmental conditions were dynamic, even over the short period of time of the study (9 days), which could lead to microbial community changes (i.e. abundance, activity and structure) over time.

3.3.1.1 Bacterial and archaeal communities structure

The structure of both bacterial and archaeal communities were different between the organic and mineral horizons (Figure 3.13; Table 3.2), and both bacteria and archaea showed much higher abundances in the mineral than in the organic horizon (Figure 3.14). Several studies have found variation of bacterial and archaeal communities structure and abundance in relation to soil horizons or soil depths in a variety of ecosystems such as, forest (Fritze *et al.*, 2000; Ekelund *et al.*, 2001; Pesaro & Widmer 2002; Kemnitz *et al.*, 2007; Hartmann *et al.*, 2009), grassland (Fierer *et al.*, 2003), acidic peatlands (Cadillo-Quiroz *et al.*, 2006), high altitude tropical forest (Fierer *et al.*, 2011), but also in polar regions in subarctic heath (Rinnan *et al.*, 2007) and arctic tundra (Wallenstein *et al.*, 2007). The bacterial community structure was correlated to the environmental variables, mainly to the soil water content, N and C content, with soil water content the dominant driver. Arctic tundra ecosystems are characterised as a dry ecosystem, receiving relatively low precipitation over the summer period. Over the sampling period (9 days), the tundra received ~6 mm of rain (Appendix 3.2), and only 46 mm over July and August 2009 (ecologically, these systems are classes as “polar

semi-deserts"). Thus, soil water is likely to be an important variable regulating the bacterial community structure. Despite soil water content being 1.5 times higher in the organic than in the mineral horizon, the volumetric water content (calculated by multiplying the average soil water content by the soil density) was ~3 times higher in the mineral than in the organic horizon. Thus, more water was available in the mineral horizon than the organic horizon. The bacterial community structure of the organic horizon is likely to be affected and regulated by change in water regime over time.

Soil N content was also strongly correlated to the structure of the bacterial community. However, the total N content was inter-correlated to the soil water content making the influence of these two factors difficult to distinguish. Nevertheless, effects of these two factors are interconnected as the water content can determine soil N availability, and so both of these two factors may play an important role in regulating the bacterial community structure. The C content, has been shown previously to be a dominant driver of the bacterial communities in different soil horizons (Zhou *et al.*, 2002; Fierer *et al.*, 2003; LaMontagne *et al.*, 2003; Hansel *et al.*, 2008). In this study, the total C content also showed a strong correlation with the bacterial community structure. Thus, the high C content of the organic horizon might select for copiotrophs/r-strategist bacteria able to grow rapidly under nutrient rich conditions, while the mineral horizon might select for oligotrophs/K-strategist bacterial communities characterised by a slow growth rate, but able to grow under C-poor conditions (Fierer *et al.*, 2007). However, copiotrophs communities are characterised as "highly sensitive to environmental stress" (Fierer *et al.*, 2007), conditions more likely to occur in the organic horizon, where the soil water content will be directly influenced by precipitation and where the soil temperature variation can be large over day. Moreover, copiotroph communities are supposed to show high variability in abundance (Fierer *et al.*, 2007), but the bacterial abundance of the organic horizon (Figure 3.14) was constant over time, whereas within the mineral horizon, bacterial abundance increased over time. Thus, further research is needed to investigate whether the copiotrophs/r-strategist and oligotrophs/K-strategist theory can be related to bacterial community structure or abundance within the organic and mineral horizon of High Arctic tundra soil.

Soil pH is considered as a key environmental factor influencing bacterial community composition (Fierer & Jackson, 2006; Lauber *et al.*, 2009; Rousk *et al.*, 2010). Despite the low difference in soil pH between the organic and mineral horizons (pH difference ~0.2), there was a significant correlation between pH and bacterial community, although the correlation was not as strong as for the water, N or C content.

In contrast to the bacterial community, the archaeal community structure of both soil horizons were not or only weakly correlated to the environmental conditions prior to N application. Thus, other environmental variables such as temperature, O_2, organic C or N and P, could explain the different archaeal community structures between the soil horizons. Høj *et al.* (2008) showed that temperature affects archaeal community structure in High Arctic peat located a few km from the experimental site studied here. Despite an important difference in soil water content and availability between the organic and mineral horizons (Figure 3.1), the archaeal community structure were not influence by soil water content, which contrasts with the study by Høj *et al.* (2006). This difference is likely due to the sites studied by Høj *et al.* (2006) which had a high water gradient (water content ~40 – 800%) and whilst the sites close to our experiment were peats and permanently wet. In acidic forest soils, changes in archaeal community composition with soil depths have been related to changes in C content (Pesaro & Widmer, 2002; Kemnitz *et al.*, 2007), while soil pH was shown to regulate the abundance and diversity of Group 1.1c Crenarchaeota in acidic forest soils but also within moorland and grassland (Lehtovirta *et al.*, 2009). However, the archaeal community structure within the soil horizons of this current study were not related to nutrient content (i.e. C and N) or soil pH. The archaeal community structure from both soil horizons was investigated only prior to N application, which limits the possibility to correlate the community structure and the environmental variables.

3.3.1.2 Bacterial and archaeal communities abundance

The bacterial and archaeal abundance was much higher in the mineral than the organic horizons, especially for archaea which were ~4.5 times more abundant in the mineral horizon (Figure 3.14). These results are in contrast to many previous studies that

mainly show a decrease of the microbial biomass with soil depths (Fritze *et al.*, 2000; Taylor *et al.*, 2002; Fierer *et al.*, 2003; LaMontagne *et al.*, 2003; Agnelli *et al.*, 2004; Hartmann *et al.*, 2009). Many studies have shown that bacterial community abundance decreased with soil depths/horizons (Fritze *et al.*, 2000; Ekelund *et al.*, 2001; Taylor *et al.*, 2002; Fierer *et al.*, 2003; Kemnitz *et al.*, 2007). Only Ekelund *et al.* (2001) found a higher bacterial biomass at 42.5 cm depth than at the soil surface and in a wet peaty spruce forest. For archaea, only a few studies have investigated the variation of archaeal abundance with soil depths, showing either a decrease in abundance, no difference or an increase in total archaeal or specific groups abundance with soil depth (Cadillo-Quiroz *et al.*, 2006; Leininger *et al.*, 2006; Kemnitz *et al.*, 2007). This difference with prior bacterial and archaeal research might first be explained by the different ecosystems investigated, ranging from forest soil (Fritze *et al.*, 2000; Ekelund *et al.*, 2001; Agnelli *et al.*, 2004; Kemnitz *et al.*, 2007), agricultural fields (Taylor *et al.*, 2002), Mediterranean grassland (Fierer *et al.*, 2003; LaMontagne *et al.*, 2003) for the bacterial communities, and acidic peatland (Cadillo-Quiroz *et al.*, 2006) and forest (Kemnitz *et al.*, 2007) for the archaeal communities. Secondly, a wide range of soil depths/horizons was investigated, from the soil surface up to 300 cm deep, while this study has focused on the organic horizon (~0-5 cm) and the mineral horizon (~5-10 cm). Despite the wide range of soil depths investigated, when similar soil depths to this study were considered, a clear decrease in bacterial abundance was found (Fritze *et al.*, 2000; Ekelund *et al.*, 2001; Fierer *et al.*, 2003; Kemnitz *et al.*, 2007), whereas archaeal abundance did not change or slightly increased at similar soil depths (Kemnitz *et al.*, 2007). Another explanation of these differences is that different methods were used to estimate the microbial abundance, such as substrate-induced respiration (SIR), DNA concentration, chloroform-extractable microbial biomass, bacterial count, bacterial culture and phospholipids fatty acids (PLFA). Only a few studies used the same methods to this study (Cadillo-Quiroz *et al.*, 2006; Kemnitz *et al.*, 2007), although Q-PCR is considered as one of the best method to accurately estimate microbial abundance in soil (Smith & Osborn, 2009, for a review).

Potential methodological biases could explain the difference of our results with the literature. The organic horizon showed a high organic matter (OM) content (e.g.

roots, leaves, stem) which can release humic acids during DNA extraction. Humic acids are known to inhibit PCR (Smalla *et al.*, 1993; Tebbe & Vahjen, 1993) and subsequently Q-PCR, leading to a potential decrease in amplified DNA template abundance and a likely decrease in the number of T-RFs and ARISA amplicons. However, T-RFLP and ARISA profiles from both soil horizons were complex (section 3.2.2.3) and did not show differences in T-RF and ARISA richness or relative abundance, indicating that PCR inhibitors did not explain the differences found between microbial communities structure and abundance. Moreover, the DNA extraction kit (i.e. PowerSoil® DNA isolation kit) included a DNA purification step, reducing the co-extraction of humic acids with DNA. Another methodological bias could be related with the DNA extraction between the soil horizons. The extractions of DNA showed clearly that the soil samples from the mineral horizon contained more DNA than the organic horizon (Figure 3.4). The low DNA content in the organic horizon could be explained by a different DNA extraction efficiency between the soil horizons related to the different soil structure. However, the same DNA extraction kit was used, and DNA of both soil horizons were extracted simultaneously. Finally, the melting curve analysis performed after each Q-PCR to investigate the specificity of the amplification, showed that the bacterial and archaeal community were specifically amplified (Appendix 3.3). Thus, the results of the microbial community abundances (and also structures) are indeed likely to be a true reflection of High Arctic tundra soil in relation to the specific environmental conditions within the organic and mineral horizons.

Bacterial abundance showed a significant correlation with the total C content, water content, pH and total N content (Table 3.5). However, these correlations were not strong ($\rho < 0.16$), but highlighted similar driver to those found for the bacterial structure, which were confirmed by the significant correlation between bacterial community structure and abundance. Other environmental variables might explain the high bacterial abundance in the mineral horizon. A simple explanation could be that the mineral horizon contained more microhabitats (and space) allowing the bacteria and also the archaea to grow. Indeed, the mineral horizon showed a much higher soil density than the organic horizon. Moreover, soil porosity mainly made of micropores, likely to be the case in the mineral horizon, protect bacteria and archaea against predation by protozoa

(Ranjard & Richaume, 2001, for a review). In contrast, the archaeal community abundance showed strong correlation with water content ($\rho = 0.40$), total C ($\rho = 0.37$), total N ($\rho = 0.34$) and to a lesser extent to the soil pH and C/N ratio ($\rho \leq 0.14$). Little is known about the drivers controlling archaeal abundance in soil but these results show that the archaeal abundance is regulated by the water and nutrient content/availability and is probably highly sensitive to environmental changes. The environmental variables measured in this study, explained well the variability of the archaeal abundance but not archaeal community structure. However, the relationship between archaeal community structure and environmental variables was assessed only at Day-2, while for the archaeal abundance was investigated for the whole sampling period. When the archaeal abundance at Day-2 was correlated to the environmental variables, similar results to those found for the archaeal community structure were found. Thus, the C/N ratio was significantly correlated to the archaeal abundance ($\rho = 0.25$, $P = 0.016$) and to a lesser extent to the total C content ($\rho = 0.19$, $P = 0.038$). Moreover archaeal structure and abundance showed a strong correlation at Day-2 ($\rho = 0.30$, $P = 0.003$) indicating that similar environmental variables might regulate archaeal community structure and abundance, and a longer time scale investigation for the archaeal community structure is needed to highlight the key environmental drivers. The fact that bacterial and archaeal community abundances are likely regulated by similar environmental drivers is confirmed by the strong correlation between the abundance of the two communities ($\rho = 0.46$, $P = 0.0001$).

3.3.1.3 Fungal community

Fungal community structure did not show significant differences between soil horizons. Similarly, Hartmann *et al.* (2009) did not find significant differences in eukaryotic community structure between organic and mineral horizons (located under the organic horizon) of a forest, using the same method as used in this study (i.e. ARISA) but using a different primer pair. They described the eukaryotic community as heterogeneous and better represented in 3D, which is similar to the results herein in which a high 2D stress value was obtained for the fungal nMDS (Figure 3.13),

indicating a highly variable community better represented in 3D. In contrast, Robinson *et al.* (2009) found the fungal community structure of a grassland soil to be significantly different between the surface (1-2 cm) and subsurface (14-15 cm) soil, using the same primer pair as used in this study (i.e. ITS1F-FAM / ITS4) but using a different method (i.e. T-RFLP). The absence of difference between soil horizons is perhaps explained by the fungal mycelia, which probably were present in both soil horizons, especially at the border between them (Landeweert *et al.*, 2003). Moreover, Robinson *et al.* (2009) investigated difference in fungal community structure between soil depths at a 12 cm interval, whereas this study investigated soil horizons adjacent to each other. When ANOSIM was performed between soil horizons for each time point separately, the fungal community structure was nearly significantly different ($R = 0.16$, $P = 0.08$) at Day+7. Moreover, fungal community structure changed only in the mineral horizon over time and the increase of fungal abundance over time was greater in the mineral horizon than in the organic horizon. Thus, different fungal communities inhabited the organic and mineral horizon, or different environmental variables regulated the fungal communities in relation to their location in different soil horizon. Despite the continuum of the mycelium between the organic and mineral horizon, investigating the fungal community within both soil horizons is important to understand: the dynamic and the variables regulating the fungal community, and probably the response of the fungal community to environmental changes such as global warming or N deposition.

Fungal community abundance showed different results than were found for fungal community structure (Figure 3.14). Fungal abundance was greater in the mineral than in the organic horizon, as found for the bacteria and archaea, despite a high variability in fungal abundance which is in agreement with variability in the community structure. Similarly to the archaeal and bacterial abundance, this result contrasts with previous studies, which reported a decrease in fungal community biomass with soil depth (Berg *et al.*, 1998; Fritze *et al.*, 2000; Ekelund *et al.*, 2001; Taylor *et al.*, 2002; Fierer *et al.*, 2003; Rinnan *et al.*, 2007; Brockett *et al.*, 2012). In addition to the differences between ecosystems and soil depths discussed earlier for the archaeal and bacterial communities, the method used in this study might also explain discrepancies with past studies. To the best of our knowledge, no studies have investigated fungal

abundance in different soil horizons using Q-PCR. Several methods have previously been used such as ergosterol concentration (Rinnan *et al.*, 2007), hyphal length (Berg *et al.*, 1998; Ekelund *et al.*, 2001), or PLFA (Fritze *et al.*, 2000; Fierer *et al.*, 2003; Brockett *et al.*, 2012). Estimation of fungal abundance/biomass represents a challenge, due to the potential presence of wide mycelium from a single individual, several nuclei within a single hypha and hypha distribution within the soil. Thus, the higher fungal abundance in the mineral horizon can be related either to widespread distribution of a small number of fungi or to limited distribution of a larger number of fungal hypha. The use of the Q-PCR method to quantify fungal abundance can also be problematic when targeting the ITS region due to the high variability of this region's size, which may bias the accurate quantification of abundance (see Appendix 3.3).

Fungal community structure and abundance were weakly correlated with a few environmental variables (Table 3.4). The absence of clear patterns and the high heterogeneity within the fungal community structure, might explain the absence of a strong correlation. However, fungal abundance showed differences between soil horizons which could not be explained by the environmental variables measured. Other environmental variables could also influence the fungal community abundance such as O_2, CO_2 (Landeweert *et al.*, 2003) or predation which has been found to select for the distribution of two basidiomycetes in different soil horizons (Newell, 1984).

The clone library of the fungal community based on the ITS1, 5.8S and ITS2 regions related the sequences to saprotrophs, mycorrhizal, ectomycorrhizal and even parasitic fungi. The order Helotiales dominated the fungal community, which are characterised as saprotrophs and ericoid mycorrizhae fungi (Cairney & Ashford 2002; Wang *et al.*, 2006, Binder, *et al.*, 2006), able to colonize soils with low nutrient content. This order was reported to colonize roots of arctic tundra Ericaceae plant *Cassiope tetragona* (Walker *et al.*, 2011), which is present around Ny-Ålesund but was not found within any of the plots. Thus, the Heliotiales fungi were more likely to be saprotrophs than ericoid mycorrhizae. However the percentage of coverage between sequences was low for the Heliotiales fungi, especially for the more abundant sequence (uncultured Heliotiales clone) which showed on average a coverage of 25%. This low coverage of the sequence might be explained by sequence insertion within the ITS region, which

have been reported to occur as 200 bp insertions in the ITS1 region (Vrålstad, 2004). The coverage of the total Heliotiale sequence (uncultured Heliotiales clone) was ~200 bp. The ecosystem distribution of the sequences identified in this study were related to those from fungi already reported as being present in the Arctic, such as the Heliotiales, but also to fungi from Alpine grassland and meadow. Thus, the occurrence of sequences from other cold environments highlights the fungal adaptation to these conditions (Robinson, 2001). It is interesting to notice that *Cordyceps crassispora* identified herein, is a parasitic fungus on larvae of Lepidoptera, endemic to the Alpine high mountains of China (Zang, 1990). However, more studies are needed to identify the presence of this fungus and of a potential host in the High Arctic tundra ecosystem.

3.3.2 Dynamics of microbial communities

Bacterial, archaeal and fungal communities were dynamic over the short sampling period (9 days) at the end of the summer and showed different patterns between communities, in relation to their location in different soil horizons and different environmental variables regulated these communities.

Bacterial abundance increased over time only in the mineral horizon but this variation was not correlated to any environmental variables indicating the possible influence of others variables, such as temperature (decrease of ~2.5 ºC between Day-2 and Day+7) or decreasing predators abundance. Jonasson *et al.* (1999) did not find fluctuation in microbial biomass over the growing season in subarctic tundra. However, they pooled the first 10 cm of the soil despite the presence of distinct soil layers (Rinnan *et al.*, 2007) which may therefore explain the absence of changes in microbial biomass, highlighting the importance of investigating microbial communities in both soil horizons separately. Stapleton *et al.* (2005) found an increase of bacterial biomass (measured by counting) in the organic horizon between mid-July and mid-August 2002 at a study site located ~2 km north from our site. However, this increase was not found in 2001 within the same period of time, indicating that changes in bacterial abundance within the organic horizon over the summer period might not be consistent between years: this might explain the absence of bacterial abundance change in the organic horizon.

Bacterial community structure did not change over time, except in the organic horizon but the low R value (0.17) indicated a poor separation between Day-2 and Day+1. McMahon *et al.* (2011) found significant changes in bacterial community structure over time investigated by T-RFLP within tundra soil in Alaska. However, changes in bacterial structure occurred between a much longer time interval, June to August. Similarly, Wallenstein *et al.* (2007) found significant changes via 16S rRNA gene sequencing between the pre-freeze and post-thaw period in different arctic tundra soils. The absence of changes in bacterial community structure in our study could be explained by the short-period of time investigated. However, we can conclude that the bacterial community structure seems to be insensitive to environmental changes over a short-period of time at the end of the summer, which is in contrast to variation in bacterial abundance.

Little is known about the archaeal community in arctic soils, in term of temporal variation and the environmental variables regulating it. Most prior studies have focused on the methanogenic community in arctic wetlands (Wartiainen *et al.*, 2003; Høj *et al.*, 2005; 2006; Ganzert *et al.*, 2007; Metje & Frenzel 2007; Rooney-Varga *et al.*, 2007; Høj *et al.*, 2008) but very few studies have investigated the entire archaeal community in arctic soils (Høj *et al.*, 2005; 2006; 2008). The archaeal community structure in the mineral horizon showed the greatest changes over the short period of the experiment in comparison to the bacterial and fungal community (Figure 3.13; Table 3.3). The total soil C content and C/N ratios were highly correlated to changes in archaeal community structure in the mineral horizon, showing that a decrease in total C content and significant ($P < 0.001$) decrease in C/N ratio represent an important driver of archaeal community structure. Thus, in the mineral horizon archaeal community structure was regulated by different environmental variables to those influencing the bacterial community structure. Høj *et al.* (2005) also found changes in archaeal community structure investigated by DGGE analysis between July and August, in a peat soil located ~2 km north east from the site. Changes in archaeal community structure were not followed by changes in the abundance in the mineral horizon, despite some fluctuation in abundance (Figure 3.14). Within the organic horizon, the archaeal 16S rRNA gene could not be amplified to enable T-RFLP analysis at Day+1 and Day+7 (Figure 3.7),

which indicated a dramatic decrease in the abundance of the archaeal community. However, when the archaeal community abundance was investigated by Q-PCR, the archaea were detected within all the samples and no trends towards decreased abundance at these time points were found. Detection of archaeal DNA by Q-PCR within all the samples from the organic horizon is not surprising as the Q-PCR method is highly sensitive, and is able to detect low gene numbers (Smith & Osborn, 2009). These differences may be a consequence of the use of different primer pairs. Different primers pairs were used because short sequences are better for amplification by Q-PCR to obtain more accurate estimates of abundance (Smith & Osborn, 2009). Thus, different archaeal populations were potentially amplified by the primers used for T-RFLP and Q-PCR. However, when each primer was compared to archaeal 16S rRNA gene sequences within the ribosomal database project (v10) using the Probe Match tool (Cole *et al.*, 2009), all the primers were related to Crenarchaeota and Euryarchaeota sequences or similar class and order.

Fungal community structure changed over time only in the mineral horizon, as was similarly found for the archaeal community. However, temporal variation could not be correlated to any of the environmental variables measured. Robinson *et al.* (2004) did not find a significant effect of sampling time on the fungal assemblages within tundra soil located ~5 km to the west of our site, despite soil sampling taking place between the end of June and beginning of August. However, the culture-dependant method used by Robinson *et al.* (2004) to investigate the fungal community is likely to explain the absence of significant difference over time. In contrast, Wallenstein *et al.* (2007) found significant differences in the 18S SSU rRNA gene clone libraries from different soil samples of arctic tundra in Alaska taken in August 2004 and June 2005 and related these changes to different organisms being adapted to different seasons. However, the current study showed that changes in fungal community structure and abundance can happen over a short period of time. The study took place at the transition between summer to autumn, during which time environmental conditions change considerably, such as decreases in daily temperature, increase in the diurnal oscillation in air temperature, and plant senescence. Nemergut *et al.* (2005) described this period within Alpine tundra as characterised by important changes in microbial communities, dominated by changes in

the fungal community that are able to decompose recalcitrant organic matter. Despite, important difference between alpine and arctic tundra, the changes found in fungal community structure in the mineral horizon and the increase of fungal abundance in both soil horizons might be related to these changes in environmental conditions during the transition from summer to autumn.

3.3.3 Responses of microbial communities to acute nitrogen deposition

The archaeal, bacterial and fungal community structure and abundances were not affected by the N or water addition with low pH within both soil horizons over time. The addition of water with low pH did not detectably change the soil water content or the soil pH. Thus, no changes in the microbial community structures and abundances may be expected from the water addition or soil pH.

Several studies similarly also found no effect of N addition on arctic tundra soil microbial communities. Robinson *et al.* (2004) did not find any change of the microfungal diversity and richness after two years of N addition at higher N rates than this study (i.e. 5 and 50 kg N ha^{-1} yr^{-1}) at an experimental site located ~5 km to the west of this site. Recently, no changes have been found in the bacterial community structure, investigated by DGGE analysis, in a Canadian arctic tundra, despite N additions at rate of 100 and 500 kg ha^{-1} yr^{-1} of NPK fertilizer for nearly 15 years (Lamb *et al.*, 2011). Schmidt *et al.* (2000) did not find changes in the microbial biomass investigated by PLFA after four years of N addition which represented a total N load of 400 kg N ha^{-1}, but the bacterial community structure (PLFA) was significantly affected by fertilisation. Other studies have showed significant responses of microbial communities to N addition. Decreases in ectomycorrhizal richness and structure were reported along an N deposition gradient (Lilleskov *et al.*, 2001; 2002), but also increases in fungal biomass were found (Rinnan *et al.*, 2007). Changes of bacterial community structure (PLFA) and increases in bacterial biomass were also found (Rinnan *et al.*, 2007). Nearly nothing is known about the response of the archaeal community to N deposition. Only Nemergut *et al.* (2008) have found a dramatic decrease in archaeal abundance investigated by Q-PCR after N addition of 115 kg N ha^{-1} over ten years in alpine tundra. However, the response

of microbial communities in alpine tundra might differ significantly from High Arctic tundra and the use of urea for the N addition may explain the difference with the results from this study.

It is extremely difficult to compare the results herein to the prior literature as many studies have simulated N fertilisation instead of N deposition. Common N addition rates of 10, 50 kg N ha^{-1} yr^{-1} have been used (e.g. Schmidt *et al.*, 2000; Robinson *et al.*, 2004; Rinnan *et al.*, 2007) up to 100 and 500 kg NPK ha^{-1} yr^{-1} (Lamb *et al.*, 2011). Moreover, N application occurred over several years leading to total N additions of 100 kg N ha^{-1} over 2 years (Robinson *et al.*, 2004), 400 kg N ha^{-1} over 4 years (Schmidt *et al.*, 2000) or 1250 kg N ha^{-1} over 15 years (Rinnan *et al.*, 2007). The low rate of N application used in this study was perhaps not enough to reach the critical load of the tundra ecosystem, under which ecosystem changes do not occur (Jefferies & Maron, 1997). Only a few studies used similar N rates, such as 1 and 5 kg N ha^{-1} yr^{-1} used to investigate microbial responses of N deposition in arctic tundra (Robinson *et al.*, 2004; Stapleton *et al.*, 2005). Stapleton *et al.* (2005) found an increase in bacterial biomass 44 days after N application of 5 kg N-NH_4 ha^{-1}. Thus, a longer period of sampling post N application might be needed for the microbial community to significantly respond to N application. Some researchers have hypothesised that the response of microbial communities structure to environmental changes, such as N addition or warming can take decades (Rinnan *et al.*, 2007; Walker *et al.*, 2008; Lamb *et al.*, 2011). However, we found that the microbial community structure and abundance are dynamic over short-periods of time in the summer period and are probably able to respond rapidly (i.e. within the summer period) to environmental changes.

Factors others than the N addition rate or the soil sampling duration could explain the absence of a microbial response to N addition. The small amount of water used for the N application (~1.1 mm m^{-2} per application) may not be enough to allow N to pass through the plant cover and reach both soil horizons, as the plant cover was dominated by mosses (~43%), and lichens (~16%). Some precipitation occurred during the second N application (~ 4 mm) and one day after N application (~1 mm), which might allow N to reach the top soil horizon (Appendix 3.2). Finally, the N application (and first sampling) started at the end of the summer period, whereas all the studies

investigating the impact of N deposition on soil microbial communities of arctic tundra started N application mainly in June and sampled the soil from July to the middle of August at the latest (Robinson *et al.*, 1998; Robinson *et al.*, 2004; Stapleton *et al.*, 2005; Rinnan *et al.*, 2007). The average ambient temperature in August 2009 was 4 ºC, whereas July showed an average of 6 ºC and included the highest temperature recorded for 2009 summer (i.e. > 10 ºC). Despite, an ambient temperature of 7 ºC on the second day of N application, the temperature dropped to 1.3 ºC three days after N application, and was 2.6 ºC at Day+7 (Appendix 3.2). Thus, soil N content/availability might not represent a significant driver of the microbial communities in High Arctic tundra soil ecosystem at the end of the summer period, but the low ambient temperature might be a strong driver of microbial communities.

3.4 Conclusions

This study show that the Arctic tundra soil with different soil horizons cannot be considered as a single unit in terms of its microbial communities, but as different soil compartments within the wider soil ecosystem. Different soil horizons had different environmental characteristics but also differences in structure and abundance of bacterial, archaeal and fungal communities. The environmental conditions differentially influenced the microbial communities, which responded and evolved over a short period of time differently within the soil horizons. Thus, soil water, C and N content regulated the bacterial community structure and abundance and also the archaeal community abundance, while the archaeal community structure requires further investigation to determine its key environmental driver. Despite, common drivers between bacteria and archaea, the main drivers and the strength of their influence vary greatly between communities. Thus, the archaeal community seems to be highly sensitive to change in environmental variables (i.e. water, C and N content), whilst the fungal community was not regulated by the environmental variables measured. In contrast to prior literature, all of the microbial communities (i.e. bacteria, archaea and fungi) showed higher abundance in the mineral than in the organic horizons, highlighting the fact that the mineral horizon

in arctic tundra soil might represent a more suitable environment for microbial communities with more abundant and dynamic communities.

Investigating the response of microbial communities to environmental changes, such as soil warming or N deposition, only within one soil horizon could lead to an under-estimation of the real impact of these changes to the microbial communities and limit our understanding of the factors regulating these communities. This observation is unlikely just to be limited to arctic tundra soil since many studies have found different microbial communities within different soil horizons (Berg *et al.*, 1998; Fritze *et al.*, 2000; Ekelund *et al.*, 2001; Pesaro & Widmer 2002; Taylor *et al.*, 2002; Fierer *et al.*, 2003; Rinnan *et al.*, 2007; Kemnitz *et al.*, 2007; Robinson *et al.*, 2009; Hartmann *et al.*, 2009; Brockett *et al.*, 2012)

No significant influence of N deposition on the microbial communities was found in this study. This can be explained either by the fact that N is not the main limiting nutrient in this soil but other nutrient (such as P) are limiting, or since low rates of N addition were used and low amount of water were added to the plots. In subsequent chapters, further studies are described that assess the impact of N deposition over the summer period on High Arctic tundra soil microbial communities, by using ^{15}N-labelled $^{15}NO_3$$^{15}NH_4$, to enable the presence and amount of N applied to the plots to be determined within both soil horizons. Furthermore, microbial communities involved in the different step of the N-cycling (such as, N-fixation, nitrification and denitrification) are investigated, in terms of the structure and abundance of the different N-functional genes, such as *nifH* for N-fixation, *amoA* for ammonia oxidation and *nirK* and *nirS* for denitrification.

Chapter 4: Impacts of acute nitrogen deposition on the structure and abundance of microbial communities within High Arctic tundra soil

Steinflåstupet cliffs at Stuphallet the 8th of August 2010.

4.1 Introduction

Atmospheric nitrogen deposition represents one of the major inputs of reactive N (Nr) to terrestrial ecosystems (Galloway *et al.*, 2004). Although most arctic regions are geographically isolated from major anthropogenic activities, Nr is deposited on these pristine ecosystems. For example the Nr content of the Greenland ice cap has doubled since the industrial revolution (Laj *et al.*, 1992; Fischer *et al.*, 1998). Arctic N deposition is estimated to range from 1 – 5 kg N ha^{-1} yr^{-1} across arctic regions but can reach up to 10 kg N ha^{-1} yr^{-1} in Northern Norway, Northern Alaska and in the Taymir Peninsular in Russia (Woodin, 1997) and even up to 20 kg N ha^{-1} yr^{-1} adjacent to human activities in the Kenai Peninsula inat the border of subarctic in Alaska (Lilleskov *et al.*, 2001; 2002). Moreover, increased melting of the Arctic sea ice in summer is likely to lead to a seasonally ice-free Arctic Ocean (Serreze *et al.*, 2007) which will potentially considerably increase Arctic Ocean maritime transports which is an important source of Nr produced from the combustion of fossil fuel. Arctic ecosystems are also susceptible to episodic atmospheric N deposition resulting from polluted air masses that travel rapidly from lower latitudes to the Arctic with mineral dispersal (Hodson *et al.*, 2005; 2010; Kühnel *et al.*, 2011). Acute N deposition events can occur, in which 40% of the annual atmospheric N input can be deposited as acidic rainfall in less than one week (Hodson *et al.*, 2005; 2010). Although that annual N deposition is low in the Arctic, acute N deposition events represent an important part of the annual N-input, and might significantly affect these nutrient-limited, and especially N-limited, ecosystems (Henry & Svoboda 1986; Chapin *et al.*, 1995). Arctic tundra plant communities have shown sensitivity to N addition with increases in plant biomass or decreases in lichen cover (Jonasson *et al.*, 1999; Gordon *et al.*, 2001). However, the response of the microbial community to N deposition is still unclear, despite the key role played by the microbial community in biogeochemical cycles.

Of the studies that have been undertaken, microbial communities have shown different responses to N addition in arctic or subarctic ecosystems. However, most prior studies have not investigated the response of microbial communities to N deposition but rather to N fertilisation, as they used high rates (e.g. 50 kg N ha^{-1} yr^{-1}; Schmidt *et al.*,

2000) of NPK fertiliser addition (e.g. Schmidt *et al.*, 2000; Rinnan *et al.*, 2007; Lamb *et al.*, 2011). Rinnan *et al.* (2007) found in subarctic heath that the bacterial community structure was significantly affected and that bacterial biomass increased after 15 years of NPK addition (total N addition 1250 kg N ha^{-1}). Schmidt *et al.* (2000) also found, at the same location as Rinnan *et al.* (2007), that bacterial community structure was affected after 4 years of NPK addition (total N addition 400 kg N ha^{-1}) but bacterial biomass was not affected. In contrast, Lamb *et al.* (2011) did not find any effect on bacterial community structure despite 15 years of NPK addition at rates of 100 and 500 kg ha^{-1} yr^{-1} in the tundra in Alaska. Simulation of N deposition in High Arctic showed increase in bacterial biomass and microbial activity after 2 years of low NH_4-addtion rate (5 kg N ha^{-1} yr^{-1}; Stapleton *et al.*, 2005). Similarly, the fungal community showed different responses to N addition. N fertilisation studies showed increased in fungal biomass (Ruess *et al.*, 1999; Clemmensen *et al.*, 2006; Rinnan *et al.*, 2007) or decrease (Schmidt *et al.*, 2000). The ectomycorrhizal community was found to be negatively affected by N fertilisation, with decrease in diversity (Deslippe *et al.*, 2011) and decrease in ectomycorrhizal colonisation (Urcelay *et al.*, 2003), although roots colonisation by ectomyccorhizal fungi was also found to not be affected by N fertilisation (Deslippe *et al.*, 2011). Lilleskov *et al.* (2002) showed that N deposition changed ectomycorrhizal structure and richness in boreal forest in Alaska near the subarctic boundary. In contrast, Robinson *et al.* (2004) simulated N deposition in High Arctic semi-desert ecosystem did not find any changes in the microfungal community after 2 years of NH_4NO_3 addition at rates of 5 and 50 kg N ha^{-1} yr^{-1}. Surprisingly no studies have investigated the response of the archaeal community to N deposition in arctic soils, despite the major role of archaea in ammonia oxidation (Leininger *et al.*, 2006; Nicol & Schleper 2006; Nicol *et al.*, 2008).

Given the prevalence of NPK studies or high dose rates, the real impact of Nr deposition to microbial communities remains unclear; despite the potential threat that acute N deposition events represent for arctic ecosystems. Furthermore, the impact of N addition on microbial communities over the entire summer has been rarely investigated and no studies have investigated the responses of bacteria, archaea and fungi simultaneously, making it difficult to evaluate the overall effect of N addition on the

microbial community. Finally, recent studies showed that different microbial communities inhabit different soil horizons in arctic tundra, and are likely to respond differently to N deposition (Rinnan *et al.*, 2007; Chapter 3). Thus, the main objective of this study was to investigate variation in the structure and abundance of the soil microbial communities (i.e. archaeal, bacterial and fungal) in response to acute atmospheric N deposition events in different soil horizons over the summer period in High Arctic tundra.

In 2009 a plot scale experiment was established in High Arctic to simulate N deposition and to investigate the response of the microbial communities to the N added (Chapter 3). No significant effects of the N deposition were found on the microbial community (Chapter 3). However, the N deposition simulation took place at the end of the summer period, for a short period of time (9 days), which might explain the absence of effects on microbial communities. At the beginning of the growing season the microbial communities might be more active, and longer period of time might be needed for the microbial community to respond to N addition. Moreover, the low rates of N added and the low amount of water used for the application, were maybe not enough to affect the communities and to reach the different soil horizons due to the plant cover dominated by bryophytes.

Thus, in order to investigate the impact of N deposition upon the microbial communities, acute N deposition was simulated in summer 2010, at the plot experiment established on the High Arctic tundra at Ny-Ålesund (Svalbard) in 2009, by the application of ^{15}N-labelled $^{15}NH_4{}^{15}NO_3$ (99% labelling) solution combined with a ~pH 4 at nitrogen application rates similar than in 2009: 0.4, 4 kg N ha^{-1} yr^{-1}, and higher: 12 kg N ha^{-1} yr^{-1} (see section 2.2.1, Chapter 2). ^{15}N-labelling of the NH_4NO_3 enabled the fate of the N applied within the different soil horizons to be followed over time. Soil samples from the organic and mineral horizons were taken over the summer period (over a 27 day period) from all of the plots and the soil characteristics (total C, N, ^{15}N, NO_3^- and NH_4^+ content, soil water and soil pH) were determined for both soil horizons over time. The potential influence of N deposition on the structure of archaeal and bacterial communities was assessed by Terminal Restriction Fragments Length Polymorphism (T-RFLP) analysis, and changes in the fungal community were assessed by Automated

Ribosomal Intergenic Spacer Analysis (ARISA). Variation in the abundance of the different microbial communities was determined by Quantitative PCR (Q-PCR).

4.2 Results

4.2.1 Soil chemical characteristics

4.2.1.1 Soil pH, soil water content, total C, total N and C/N

The soil water content of the organic horizon (57.2% ± 5.7, n = 180) was significantly higher (χ^2 = 232.8, df = 1, $P < 2.2x10^{-16}$) than in the mineral horizon (37.2% ± 10.3, n = 179) overall across the treatments and over time (Figure 4.1), while the soil pH was significantly (χ^2 = 228.6, df = 1, $P < 2.2x10^{-16}$) higher in the mineral horizon (7.3 ± 0.26, n = 179) than in the organic horizon (6.6 ± 0.31, n = 180) overall. The addition of water adjusted to ~pH 4 did not affect the soil pH and the soil water content for either soil horizon or over time, except in the mineral horizon between the dry control and 12 kg N ha^{-1} yr^{-1} plots one day after N application, where the soil water content was significantly higher ($P < 0.05$, Tukey HSD) in the 12 kg N ha^{-1} yr^{-1} plots.

The total C content was significantly higher (χ^2 = 121.8, df = 1, $P < 2.2x10^{-16}$) in the organic horizon (16.2% ± 4.5, n = 85) than in the mineral horizon (5.9% ± 2.7, n = 85) overall across the treatments and over time (Figure 4.3). However, no significant ($P > 0.05$, Tukey HSD) differences were found between the different time points or between treatments for both soil horizons. Similarly, the total N content was significantly higher (F = 402.6, df = 1, $P < 2.2x10^{-16}$) in the organic horizon (1.09% ± 0.19, n = 85) than in the mineral horizon (0.52% ± 0.20, n = 85) overall across the treatments and over time (Figure 4.4), but no significant ($P > 0.05$, Tukey HSD) difference were found between time points or between treatments. The C/N ratio was significantly higher (χ^2 = 43.6, df = 1, $P < 3.9x10^{-11}$) in the organic horizon (~1.3 times higher) than in the mineral horizon (except at Day-6 and Day+1 for the C+W and 12N plots, respectively; Figure 4.5). The C/N ratio changed significantly (χ^2 = 45.0, df = 4, $P = 3.9x10^{-9}$) over time in both soil horizons. Thus, the 12 kg N ha^{-1} yr^{-1} plots showed a

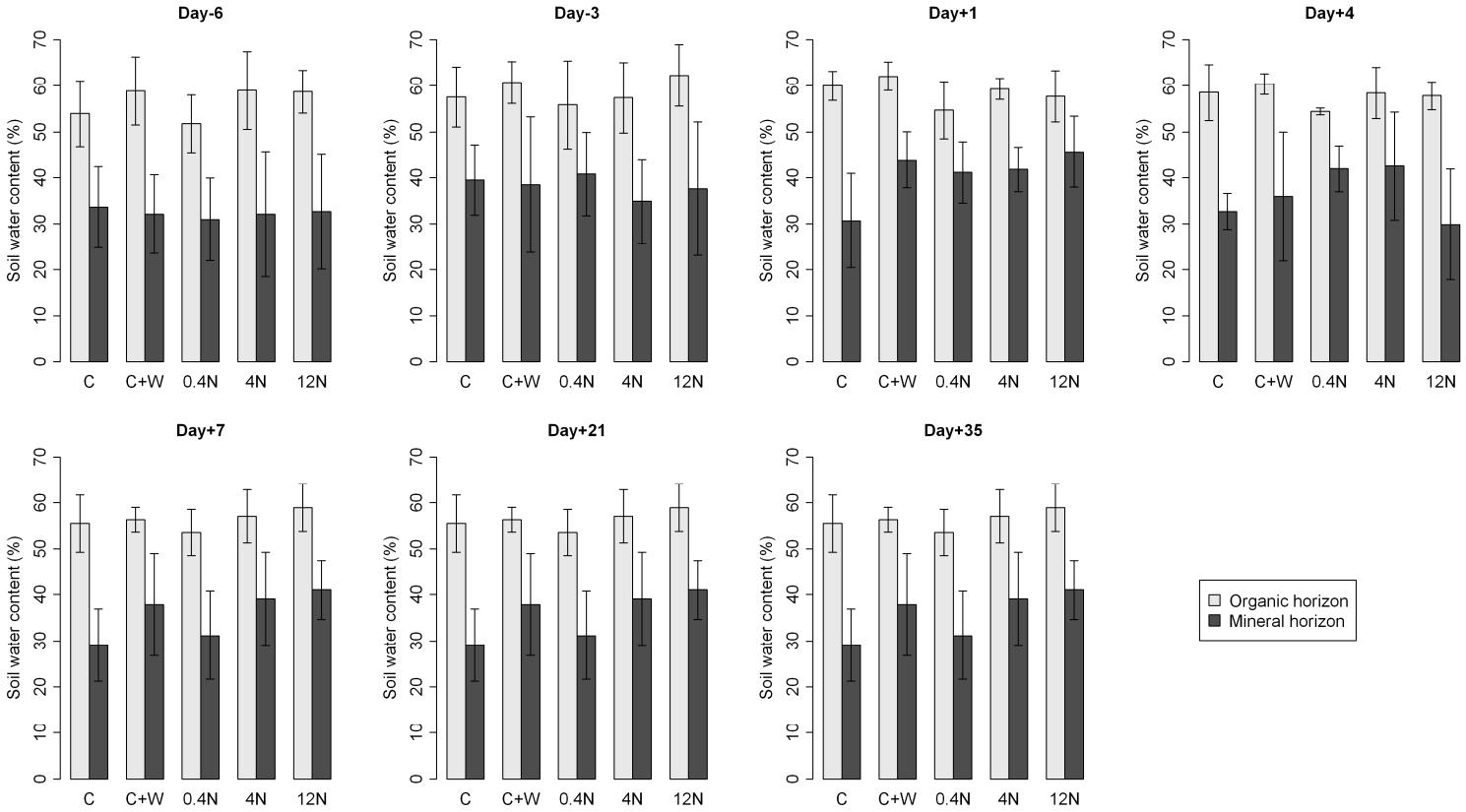

Figure 4.1: Variation in soil water content (%) between organic and mineral soil horizons, over time and in response to simulated episodic N deposition events. Plots were established in 2009 and subjected to simulated N deposition events in 2009 and 2010, and sampled in summer 2010 (see section 2.2.1). **Day-6**: two days before N application; **Day-3**: just after 50% of N application was completed; **Day+1**: one day after total N application; **Day+4**: four days after total N application; **Day+7**: seven days after total N application; **Day+21**: twenty-one days after total N application; **Day+35**: thirty five days after total N application; **C**: Control plots; **C+W**: control + water plots; **0.4N**: 0.4 kg N ha^{-1} yr^{-1} ~pH 4 plots; **4N**: 4 kg N ha^{-1} yr^{-1} ~pH 4 plots; **12N**: 12 kg N ha^{-1} yr^{-1} ~pH 4 plots. Means values ± standard deviation (n = 5) are shown. Significant ($P < 0.001$) differences between organic and mineral horizons were found.

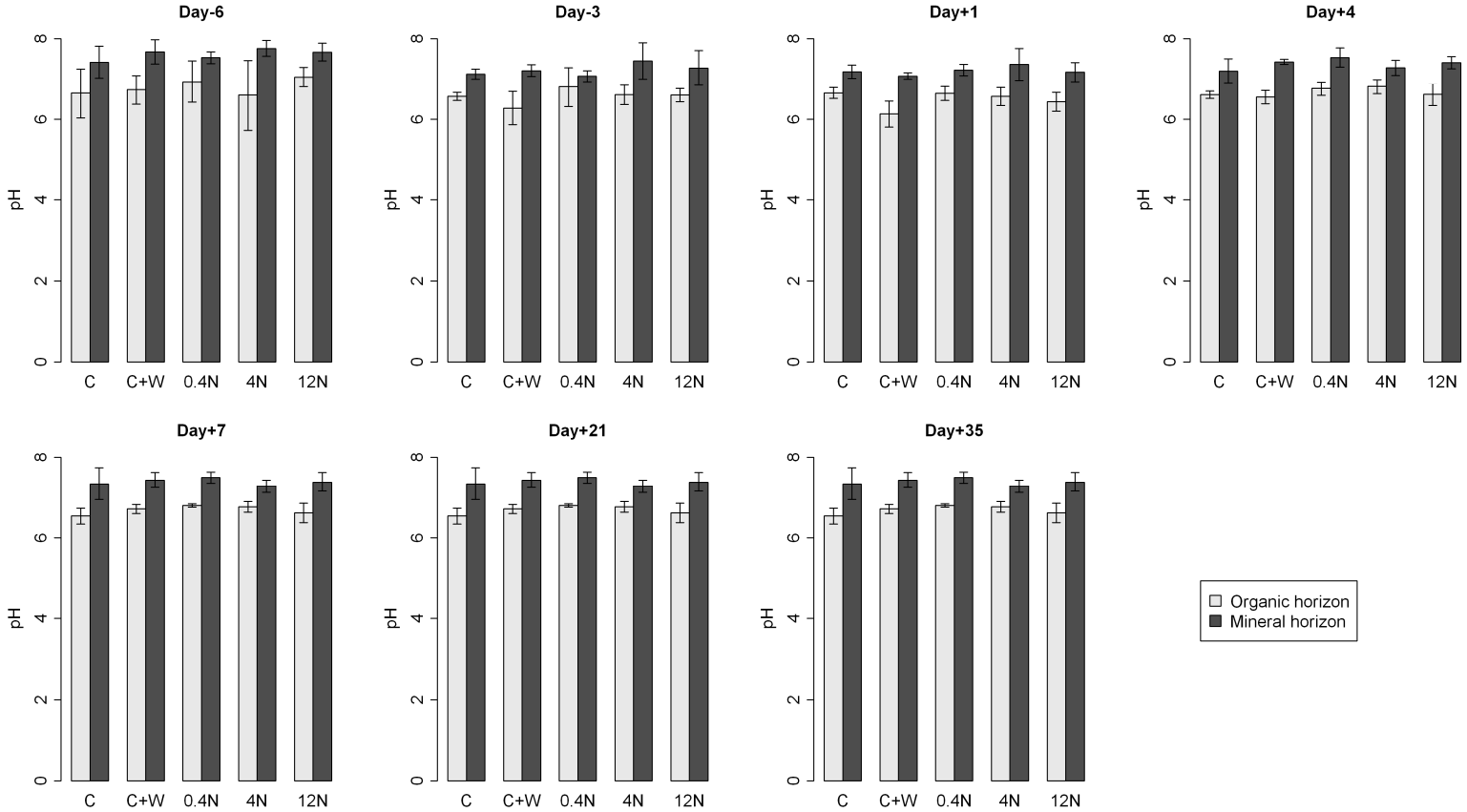

Figure 4.2: Variation in soil pH between organic and mineral soil horizons, over time and in response to simulated episodic N deposition events. Plots were established in 2009 and subjected to simulated N deposition events in 2009 and 2010, and sampled in summer 2010 (see section 2.2.1). **Day-6**: two days before N application; **Day-3**: just after 50% of N application was completed; **Day+1**: one day after total N application; **Day+4**: four days after total N application; **Day+7**: seven days after total N application; **Day+21**: twenty-one days after total N application; **Day+35**: thirty five days after total N application; **C**: Control plots; **C+W**: control + water plots; **0.4N**: 0.4 kg N ha^{-1} yr^{-1} ~pH 4 plots; **4N**: 4 kg N ha^{-1} yr^{-1} ~pH 4 plots; **12N**: 12 kg N ha^{-1} yr^{-1} ~pH 4 plots. Means values ± standard deviation (n = 5) are shown. Significant ($P < 0.001$) differences between organic and mineral horizons were found.

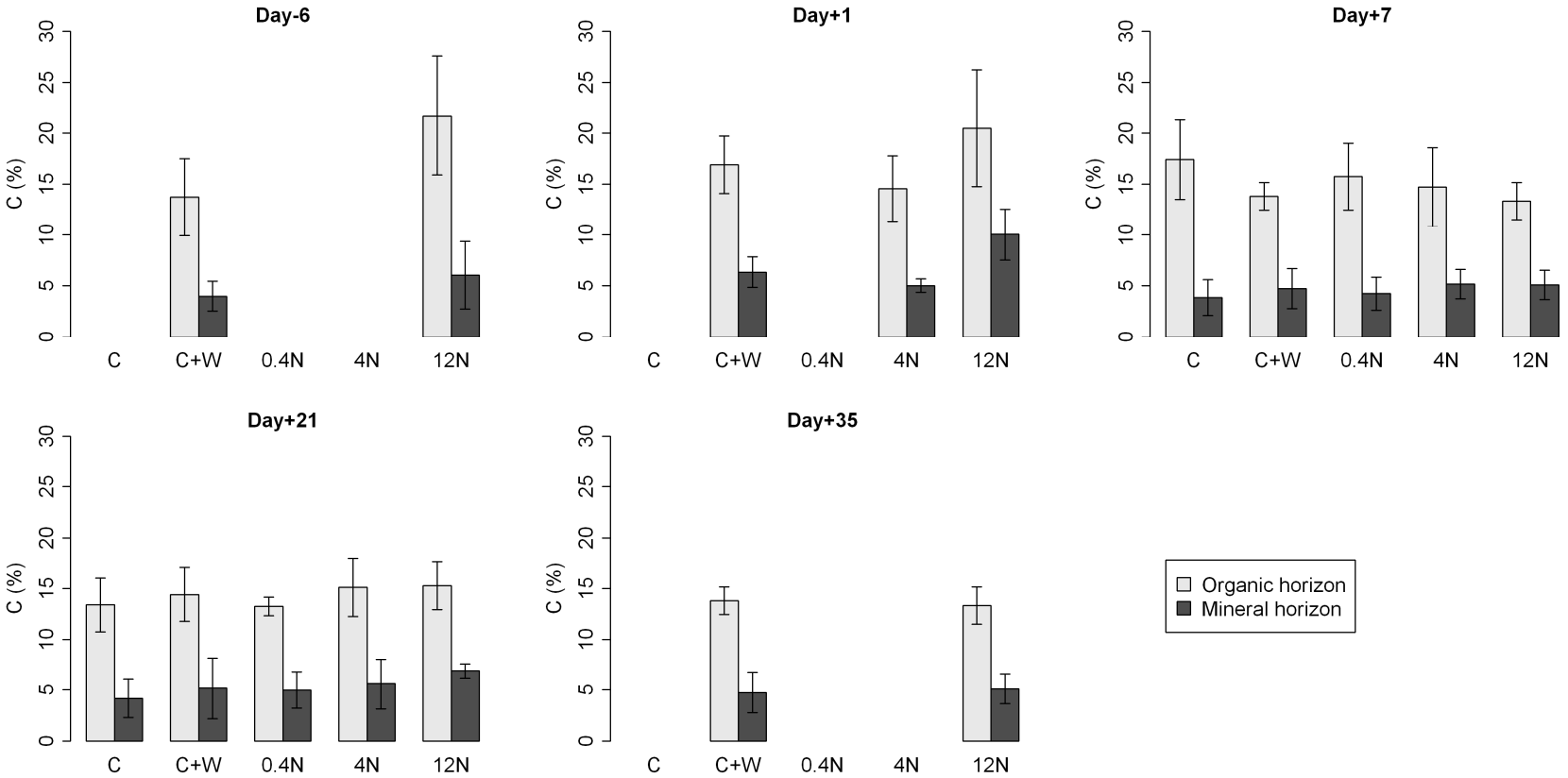

Figure 4.3: Variation in soil total C content (%) between organic and mineral soil horizons, over time and in response to simulated episodic N deposition events. Plots were established in 2009 and subjected to simulated N deposition events in 2009 and 2010, and sampled in summer 2010 (see section 2.2.1). **Day-6**: two days before N application; **Day+1**: one day after total N application; **Day+7**: seven days after total N application; **Day+21**: twenty-one days after total N application; **Day+35**: thirty five days after total N application; **C**: Control plots; **C+W**: control + water plots; **0.4N**: 0.4 kg N ha^{-1} yr^{-1} ~pH 4 plots; **4N**: 4 kg N ha^{-1} yr^{-1} ~pH 4 plots; **12N**: 12 kg N ha^{-1} yr^{-1} ~pH 4 plots. Means values ± standard deviation (n = 5) are shown. Where bars are absent, measurements were not determined. Significant ($P < 0.001$) differences between organic and mineral horizons were found.

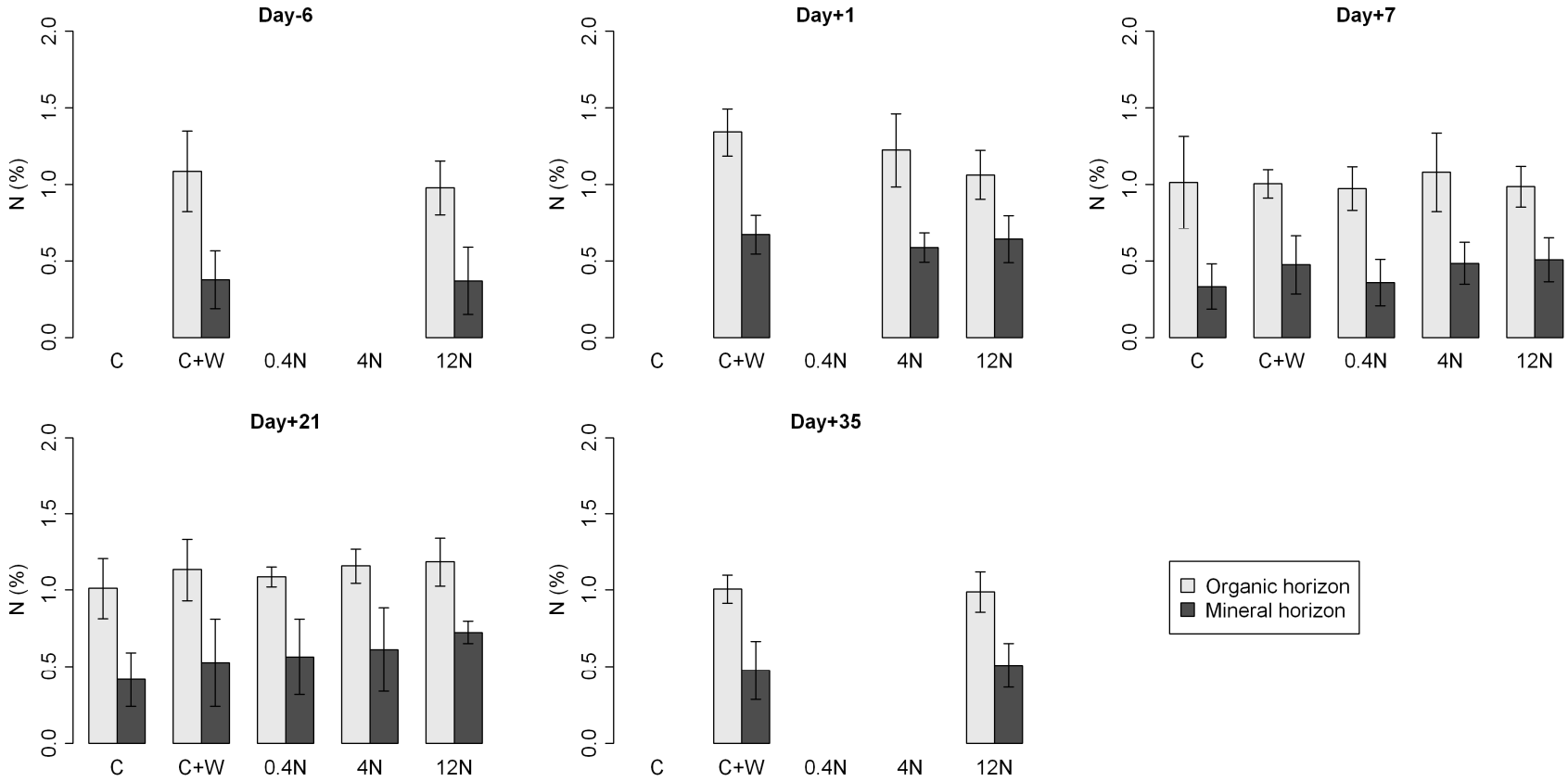

Figure 4.4: Variation in soil total N content (%) between organic and mineral soil horizons, over time and in response to simulated episodic N deposition events. Plots were established in 2009 and subjected to simulated N deposition events in 2009 and 2010, and sampled in summer 2010 (see section 2.2.1). **Day-6**: two days before N application; **Day+1**: one day after total N application; **Day+7**: seven days after total N application; **Day+21**: twenty-one days after total N application; **Day+35**: thirty five days after total N application; **C**: Control plots; **C+W**: control + water plots; **0.4N**: 0.4 kg N ha^{-1} yr^{-1} ~pH 4 plots; **4N**: 4 kg N ha^{-1} yr^{-1} ~pH 4 plots; **12N**: 12 kg N ha^{-1} yr^{-1} ~pH 4 plots. Means values ± standard deviation (n = 5) are shown. Where bars are absent, measurements were not determined. Significant ($P < 0.001$) differences between organic and mineral horizons were found.

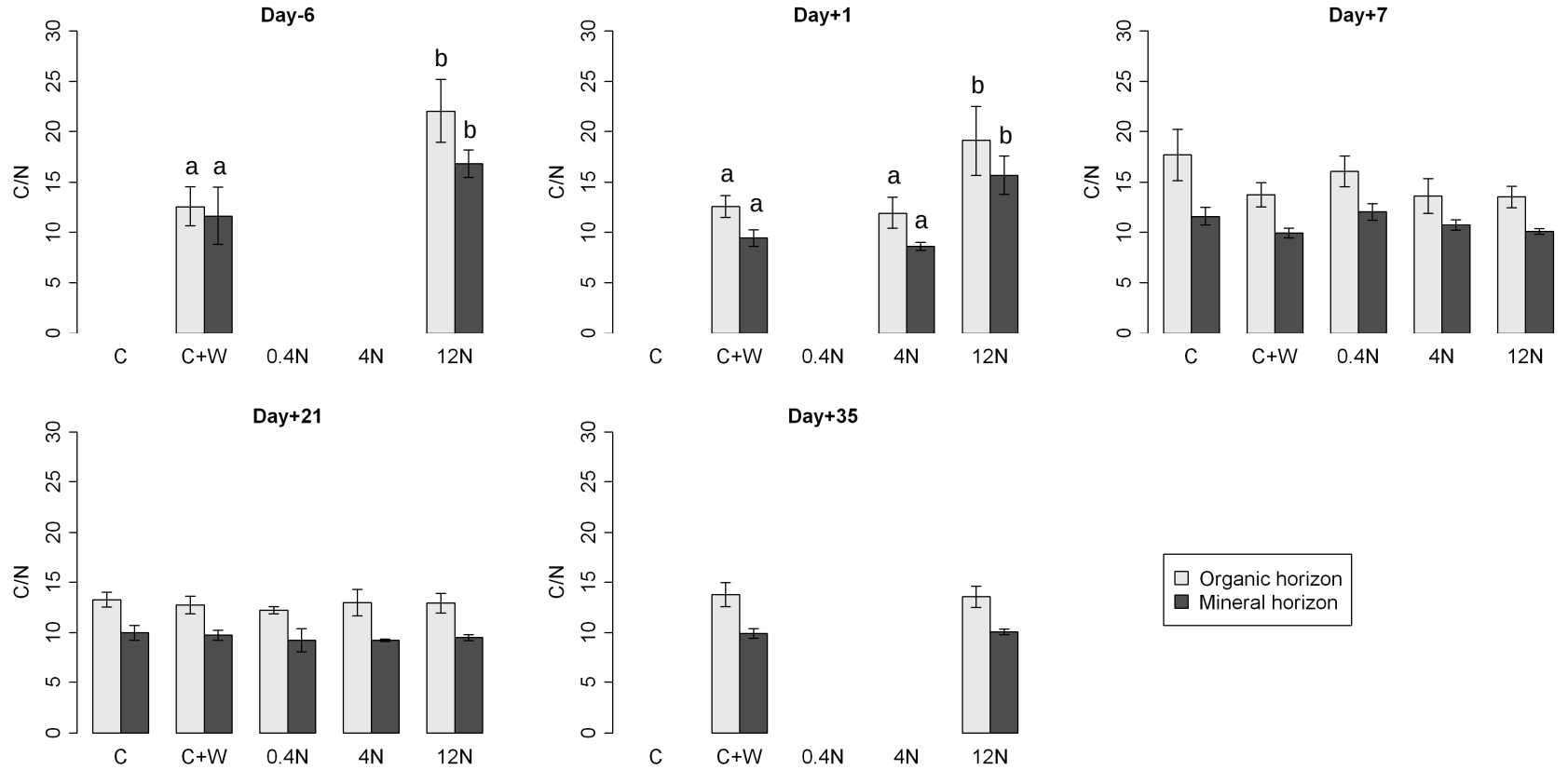

Figure 4.5: Variation in soil C/N ratio between organic and mineral soil horizons, over time and in response to simulated episodic N deposition events. Plots were established in 2009 and subjected to simulated N deposition events in 2009 and 2010, and sampled in summer 2010 (see section 2.2.1). **Day-6**: two days before N application; **Day+1**: one day after total N application; **Day+7**: seven days after total N application; **Day+21**: twenty-one days after total N application; **Day+35**: thirty five days after total N application; **C**: Control plots; **C+W**: control + water plots; **0.4N**: 0.4 kg N ha^{-1} yr^{-1} ~pH 4 plots; **4N**: 4 kg N ha^{-1} yr^{-1} ~pH 4 plots; **12N**: 12 kg N ha^{-1} yr^{-1} ~pH 4 plots. Means values ± standard deviation (n = 5) are shown. Where bars are absent, measurements were not determined. Significant ($P < 0.001$) differences between organic and mineral horizons were found. Different letters indicate significant ($P < 0.001$) difference between treatments for a specific soil horizon at Day-6 or Day+1 (no significant differences were found for the other dates).

decrease of the C/N ratio between Day-6, Day+1 and Day+7 (decrease of ~1.6 times for both horizons between Day-6 and Day+7). The 12 kg N ha^{-1} yr^{-1} plots had a significantly ($P < 0.001$, Tukey HSD) higher C/N ratio than the control + water plots and 4 kg N ha^{-1} yr^{-1} plots at Day+1 (and at Day-6 for the control + water plots) for both horizons, but no significant differences ($P > 0.05$, Tukey HSD) were found for the later time points (Day+7, Day+21 and Day+35).

4.2.1.2 Fate of ^{15}N in soil

The use of ^{15}N-labelled NH_4NO_3 (99% labelling) allowed the fate of the N applied on each plot to be followed and to determine whether the N applied reached the different soil horizons for each N addition rate. One day after N applications, the 4 kg N ha^{-1} yr^{-1} and 12 kg N ha^{-1} yr^{-1} plots showed significant ($P < 0.05$) ^{15}N enrichment in comparison to the control and control + water plots, mainly in the organic horizon and to a lesser extent in the mineral horizon (Figure 4.6). The organic horizon of the 4 kg N ha^{-1} yr^{-1} and 12 kg N ha^{-1} yr^{-1} plots had ^{15}N enrichment that were ~1.14 and ~2.01 times higher than in the control + water plots, respectively. However, the organic horizon of the 12 kg N ha^{-1} yr^{-1} plots exhibited high variability in ^{15}N enrichment. Only small increases in the ^{15}N enrichment in the mineral horizon of the 12 kg N ha^{-1} yr^{-1} and 4 kg N ha^{-1} yr^{-1} were found (1.05 and 1.01 times higher than in the control + water, respectively). The 0.4 kg N ha^{-1} yr^{-1} plots did not show significant ^{15}N enrichment over time for either soil horizon, although the values were, in general, higher in comparison to the control + water plots.

The ^{15}N enrichment of the 4 kg N ha^{-1} yr^{-1} and 12 kg N ha^{-1} yr^{-1} plots significantly ($P < 0.05$, Kruskal-Wallis) changed over time. Within the organic horizon from the 12 kg N ha^{-1} yr^{-1} plots, ^{15}N enrichment decreased by 19% at Day+7 in comparison to Day+1, and by 14% at Day+21 in comparison to Day+7, but increased by 11% at Day+35. In contrast, the ^{15}N enrichment in the mineral horizon of the 12 kg N ha^{-1} yr^{-1} plots increased by 7% between Day+1 and Day+35. Seven days after N application, the 4 kg N ha^{-1} yr^{-1} plots showed a small decrease (3%) in ^{15}N enrichment in the organic horizon,

which increased (9%) at Day+21. The ^{15}N enrichment of the mineral horizon in the 4 kg N ha^{-1} yr^{-1} plots slightly decreased (3%) between Day+1 and Day+21.

4.2.1.3 Inorganic N in soil (NO_3^- and NH_4^+)

Soil NO_3^- concentration did not show any significant ($\chi^2 = 0.56$, df = 1, $P = 0.45$) difference between the organic and mineral horizons before N addition (mean 0.36 ± 0.34 mg kg^{-1} soil at day-6, n = 48). Only the 12 kg N ha^{-1} yr^{-1} plots showed significant difference in NO_3^- concentration between the organic and mineral horizons over time ($\chi^2 = 5.99$, df = 1, $P = 0.014$; Figure 4.7). One day after N addition, the 12 kg N ha^{-1} yr^{-1} plots showed an increase in the NO_3^- concentration in both soil horizons, and NO_3^- concentration in 12 kg N ha^{-1} yr^{-1} plots was significantly ($\chi^2 = 5.54$, df = 1, $P = 0.019$) different to the control + water plots for the organic horizon at Day+1 (Figure 4.7). The organic horizon of the 12 kg N ha^{-1} yr^{-1} plots had a higher (but not significant; $\chi^2 = 2.53$, df = 1, $P = 0.12$) NO_3^- concentration (16.15 ± 17.06 mg kg^{-1} soil, n = 5) than the mineral horizon (0.85 ± 1.89 mg kg^{-1} soil, n = 5) at Day+1. Seven days after N addition, the NO_3^- concentration of the 12 kg N ha^{-1} yr^{-1} treatment decreased within both soil horizons (organic: 1.3 ± 1.85, mineral: 0.20 ± 0.22 mg kg^{-1} soil, n = 5) and was still decreasing twenty-one days after N addition in the organic horizon (0.6 ± 0.6 mg kg^{-1} soil, n = 5), but no significant ($\chi^2 = 0.31$, df = 3, $P = 0.96$) temporal variation was found. The plots which received 4 kg N ha^{-1} yr^{-1} showed an increase in their NO_3^- concentration at Day+21 in both soil horizons (organic: 1.2 ± 2.10, mineral: 1.46 ± 2.23 mg kg^{-1} soil, n = 5) which was not significantly ($\chi^2 = 3.98$, df = 2, $P = 0.14$) higher in comparison to the other date of sampling. The 4 kg N ha^{-1} yr^{-1} plots showed the highest NO_3^- concentration at Day+21 in comparison to the other treatments and significant ($\chi^2 = 9.1$, df = 4, $P = .04$) difference between treatments was found at Day+21.

In contrast to the NO_3^- soil concentration, the soil NH_4^+ concentration was significantly higher ($\chi^2 = 78.0$, df = 1, $P < 2.2x10^{-16}$) in the organic (5.5 ± 2.7 mg kg^{-1} soil, n = 84) than in the mineral (2.0 ± 1.2 mg kg^{-1} soil, n = 86) horizon over time (Figure 4.7). However, no significant ($P > 0.05$, Tukey HSD) differences were found between treatments or time points.

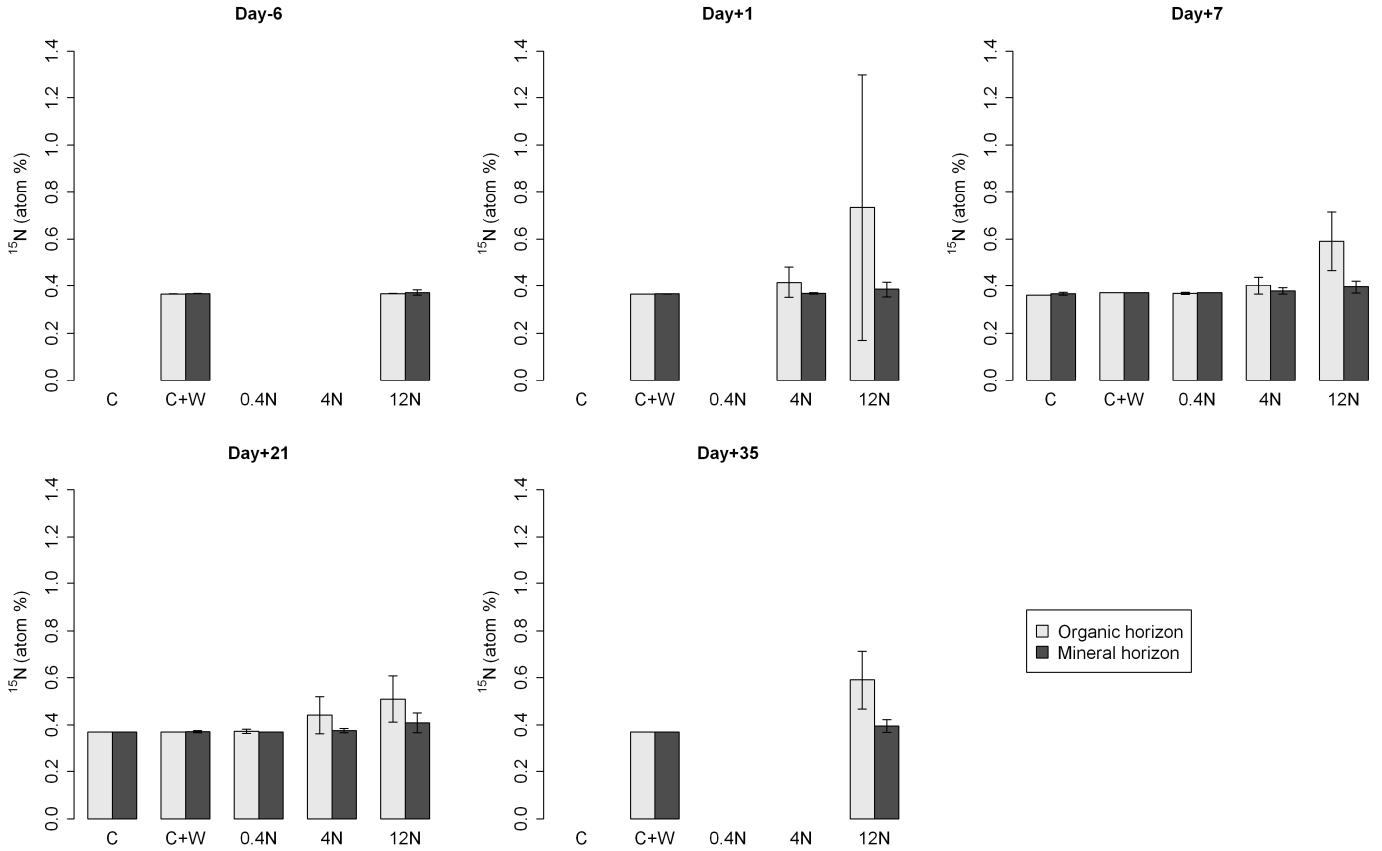

Figure 4.6: Variation in soil ^{15}N enrichment (atom %) between organic and mineral soil horizons, over time and in response to simulated episodic N deposition events. Plots were established in 2009 and subjected to simulated N deposition events in 2009 and 2010, and sampled in summer 2010 (see section 2.2.1). **Day-6**: two days before N application; **Day+1**: one day after total N application; **Day+7**: seven days after total N application; **Day+21**: twenty-one days after total N application; **Day+35**: thirty five days after total N application; **C**: Control plots; **C+W**: control + water plots; **0.4N**: 0.4 kg N ha^{-1} yr^{-1} ~pH 4 plots; **4N**: 4 kg N ha^{-1} yr^{-1} ~pH 4 plots; **12N**: 12 kg N ha^{-1} yr^{-1} ~pH 4 plots. Means values ± standard deviation (n = 5) are shown. Where bars are absent, measurements were not determined.

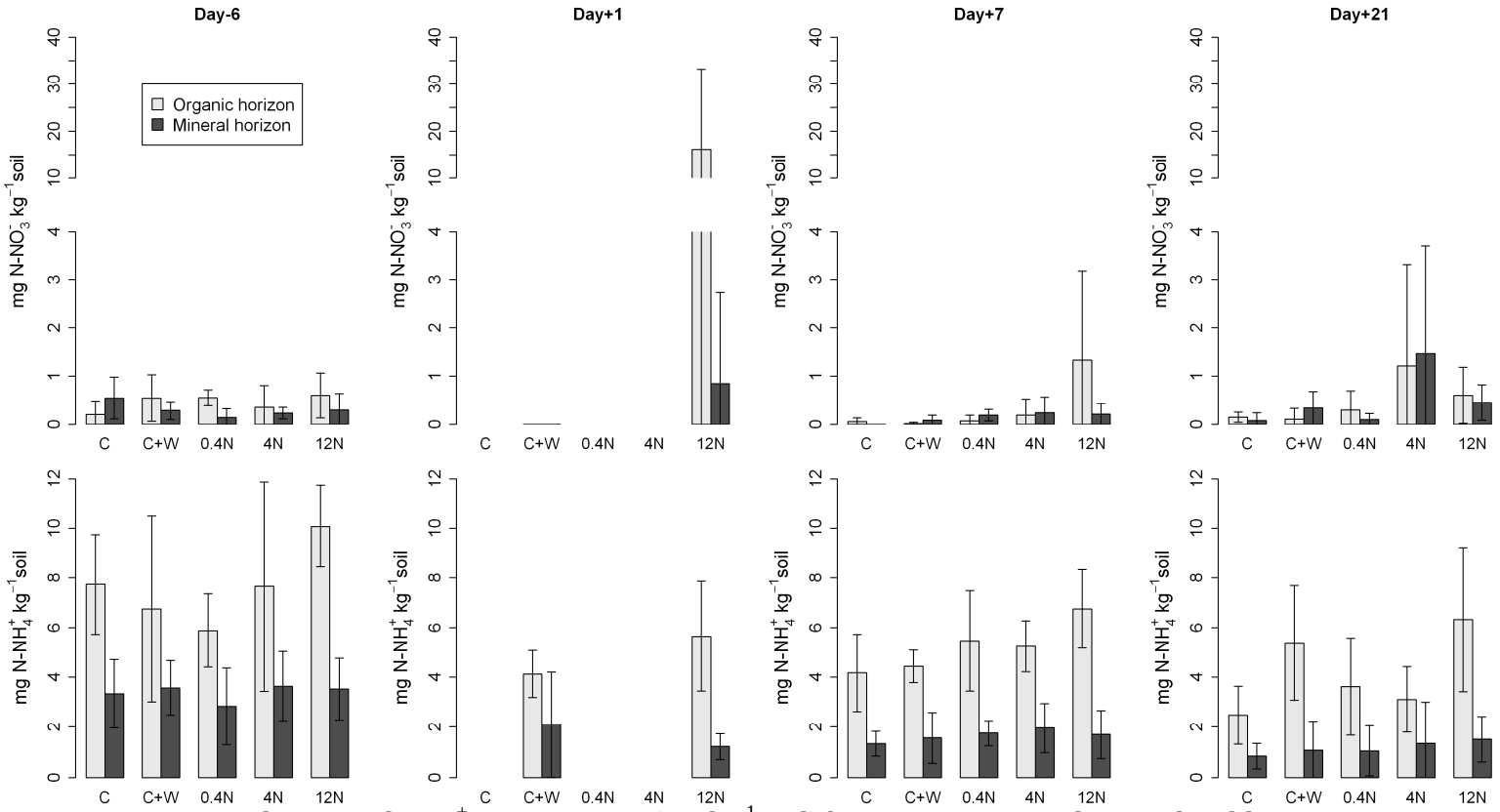

Figure 4.7: Variation in soil NO_3^- and NH_4^+ concentration (mg kg^{-1} soil) between organic and mineral soil horizons, over time and in response to simulated episodic N deposition events. Plots were established in 2009 and subjected to simulated N deposition events in 2009 and 2010, and sampled in summer 2010 (see section 2.2.1). **Day-6**: two days before N application; **Day+1**: one day after total N application; **Day+7**: seven days after total N application; **Day+21**: twenty-one days after total N application; **Day+35**: thirty five days after total N application; **C**: Control plots; **C+W**: control + water plots; **0.4N**: 0.4 kg N ha^{-1} yr^{-1} ~pH 4 plots; **4N**: 4 kg N ha^{-1} yr^{-1} ~pH 4 plots; **12N**: 12 kg N ha^{-1} yr^{-1} ~pH 4 plots. Means values ± standard deviation (n = 5) are shown. Where bars are absent, measurements were not determined. Significant ($P < 0.001$) differences in NH_4^+ concentration between organic and mineral horizons were found.

4.2.1.4 PCA of the soil environmental variables

Principal component analysis (PCA) was conducted on all of the environmental variables (i.e. total C, total N, ^{15}N, NO_3^-, NH_4^+, C/N ratio, soil water content and soil pH) to investigate differences and changes in environmental variables between soil horizons, over time and in response to simulated episodic N deposition events. The PCA explained 70.8% of the data on the PC1 and PC2 axes and 84.6% by including the third PC (PC1 = 53.4%, PC2 = 17.4%, PC3 = 13.8%; Figure 4.8). The samples from the organic and mineral horizons were significantly different (ANOSIM: R = 0.86, P = 0.00005; Figure 4.8 A; Table 4.1) with separation on the PC1 axis explained by a number of factors: soil total C, soil water and total N content, soil pH and NH_4^+ concentration (Figure 4.8 D). However, the soil water and total N content were highly inter-correlated (Pearson correlation coefficient = 0.93). Therefore, the influence of these two variables on the data cannot be distinguished. Within both soil horizons, samples from a specific date of sampling in general grouped together and all of the sampling dates were significantly different from each other ($P \leq 0.013$) for both soil horizons, except between Day+7 and Day+21 (Figure 4.8 B; Table 4.1). The R values varied between 0.25 and 0.56. The influence of date of sampling was explained on the PC2 axis mainly by NO_3^- and ^{15}N, but also on the PC3 axis by the C/N ratio and ^{15}N enrichment (Figure 4.8 D). The PCA revealed significant differences between environmental variables of the control + water plots *vs.* 12 kg N ha^{-1} y^{-1} plots for both soil horizons (Figure 4.8 C). The organic horizon showed strong significant differences between samples from the control + water and 12 kg N ha^{-1} yr^{-1} plots (P = 0.00005, R = 0.58), while the mineral horizon showed a smaller influence of N addition (P = 0.026, R = 0.15; Table 4.1). The difference between the control + water and 12 kg N ha^{-1} yr^{-1} plots were explained on the PC2 and PC3 axes by environmental variables related to N (i.e. ^{15}N, NO_3^- and the C/N ratio).

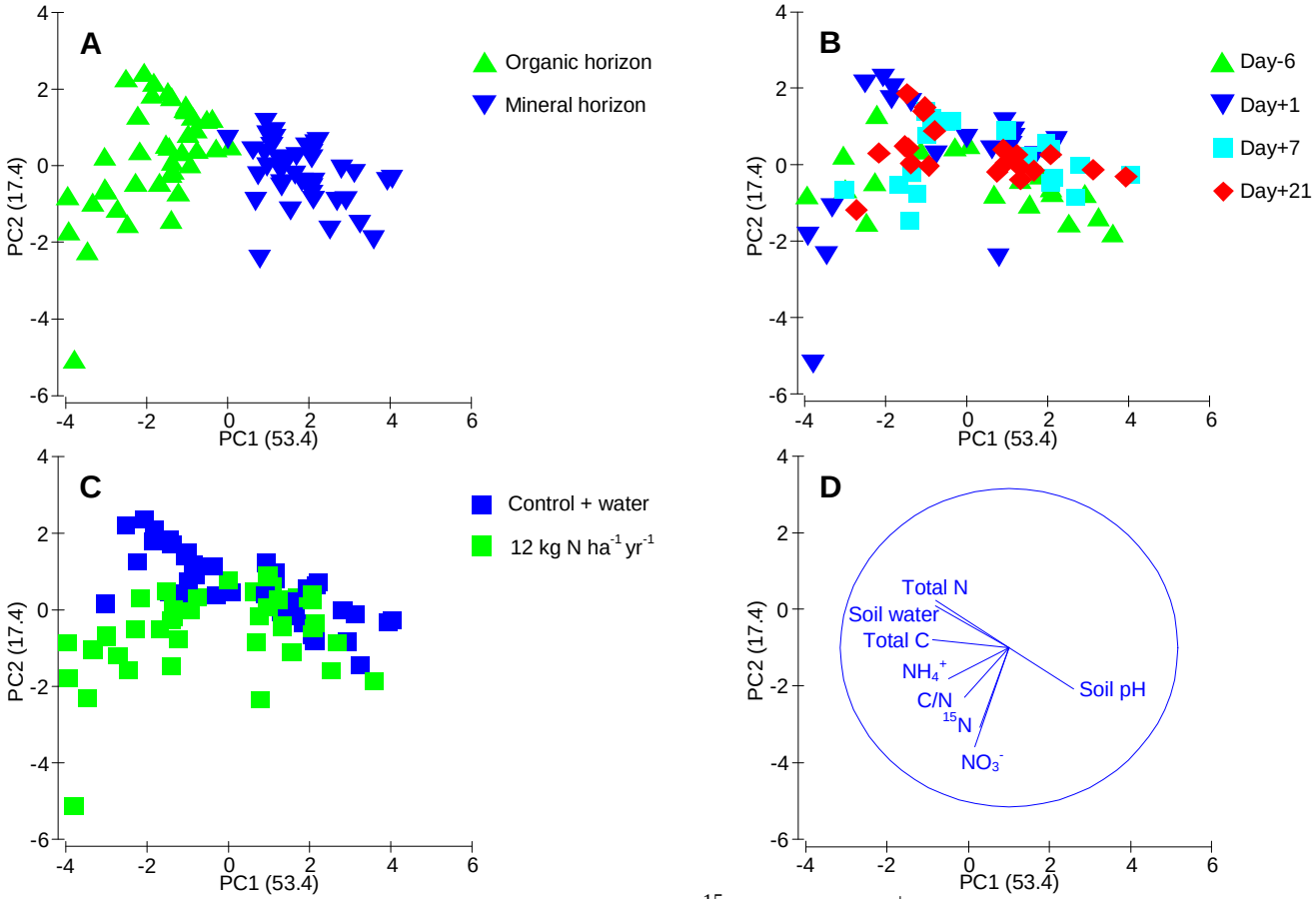

Figure 4.8: PCA of the environmental variables (i.e. total C, total N, ^{15}N, NO_3^-, NH_4^+, C/N ratio, soil water content and soil pH) during the summer 2010 in the organic and mineral horizons from the control + water and 12 kg N ha^{-1} yr^{-1} ~pH 4 plots, before N application (Day-6), and 1, 7, and 21 days after total N application (Day+1, Day+7 and Day+21, respectively). **A**: Plot showing the influence of soil horizons on the environmental variables; **B**: Plot showing the influence of time (sampling days) on the environmental variables; **C**: Plot showing the influence of simulated episodic N deposition event on the environmental variables. **D**: Plot showing the vectors driving the separation of environmental variables on the PCA plots.

Table 4.1: Two-way ANOSIM to compare differences in environment variables with respect to soil horizons (organic *vs.* mineral), time (days of sampling) and simulated episodic elevated N deposition. Analysis based on an Euclidean similarity matrix derived from the environmental variables (i.e. total C, total N, ^{15}N, NO_3^-, NH_4^+, C/N ratio, soil water content and soil pH) within soil plots (control + water (**C+W**) and 12 kg N ha^{-1} yr^{-1} ~pH 4 plots). **Day-6**: two days before N application; **Day+1**: one day after N application; **Day+7** seven days after N application; **Day+21**: twenty-one days after N application. The R values and *P* values are given. Significant values at $P < 0.05$ are shown in bold text.

Soil horizons	Factors compared	R values	*P* values
	Organic *vs.* Mineral	**0.86**	**0.00005**
Organic	Day-6 *vs.* Day+1	**0.44**	**0.0001**
	Day-6 *vs.* Day+7	**0.56**	**0.00006**
	Day-6 *vs.* Day+21	**0.44**	**0.004**
	Day+1 *vs.* Day+7	**0.53**	**0.0002**
	Day+1 *vs.* Day+21	**0.29**	**0.003**
	Day+7 *vs.* Day+21	0.03	0.302
Mineral	Day-6 *vs.* Day+1	**0.54**	**0.0002**
	Day-6 *vs.* Day+7	**0.43**	**0.0008**
	Day-6 *vs.* Day+21	**0.45**	**0.002**
	Day+1 *vs.* Day+7	**0.25**	**0.013**
	Day+1 *vs.* Day+21	**0.44**	**0.0003**
	Day+7 *vs.* Day+21	0.14	0.132
Organic	C+W *vs.* 12 kg N ha^{-1} yr^{-1}	**0.58**	**0.00005**
Mineral	C+W *vs.* 12 kg N ha^{-1} yr^{-1}	**0.15**	**0.026**

4.2.2 Variation in microbial community structure within the soil

DNA was extracted from the 80 soil samples taken during 2010 from the different soil horizons (40 samples from each horizon), from four different time points: before N application (Day-6), 1 (Day+1), 7 (Day+7) and 21 (day+21) days after N application (20 samples per date of sampling) and from the control + water and 12 kg N ha^{-1} yr^{-1} plots (40 samples from each treatment). Bacterial 16S rRNA genes were amplified by PCR from all of the samples, while archaeal 16S rRNA genes and fungal ITS regions were each amplified from 79 samples. From two samples, one for the archaeal community (sample from the organic horizon taken 21 days after N application within plot 15, which received 12 kg N h^{-1} yr^{-1}) and one for the fungal community (sample from the mineral horizon taken 7 days after N application within the control + water plot 2), the archaeal 16S rRNA gene or fungal ITS region could not be amplified or was only amplified in extremely low concentrations. Thus, variation in archaeal and fungal community structure was investigated from 79 samples, while variation in the bacterial community structure was investigated from 80 samples.

Complex T-RFLP and ARISA profiles were generated from the bacterial, archaeal and fungal communities comprising a total of 101 and 146 terminal restriction fragments (T-RFs), and 383 ARISA amplicons, respectively. On average, each bacterial and archaeal profile was comprised of 36 ± 3 (n = 80) and 27 ± 8 T-RFs (n = 79), respectively, and 22 ± 5 (n = 79) ARISA amplicons for each fungal profile.

4.2.2.1 Variation in microbial community structure between soil horizons

nMDS plots were generated from the T-RFLP and ARISA profiles of all the samples from the soil horizons, different time points and from the control + water and 12 kg N ha^{-1} yr^{-1} plots (Figure 4.9) The 2D stress is shown for each nMDS plot, indicating the relevance of the representation (see section 2.2.6.2). The nMDS plots for the bacterial and archaeal community structures have a low (< 0.2) 2D stress (except for the nMDS plot of the bacteria in the organic horizon; Figure 4.9 B) indicating a good representation of the data in two dimensions. However, the 2D stress of the nMDS plots

for the fungal community structure were higher (0.24 and 0.28; Figure 4.9), indicating that the nMDS plots were weaker representations of the variability of the data, which were better represented in three dimensions. Interpretation of the nMDS with a 2D stress higher than 0.2 should be treated with caution.

Analysis of the bacterial and archaeal community structures generated by T-RFLP, showed significant (P = 0.00005; Table 4.2) differences in community structure between the organic and mineral horizons (Figure 4.9 A). ANOSIM analysis of both bacterial and archaeal communities indicated a very strong separation between communities in the organic and mineral horizons (R = 0.70, R = 0.75, respectively). The fungal community structure also showed significant (P = 0.01) differences between the organic and mineral horizons (Figure 4.9 A), but separation of fungal communities was low (R= 0.14; Table 4.2). When ANOSIM analysis was performed on each date of sampling, no significant difference was found in the fungal community structure prior to N application (P = 0.27). After one and seven days post N application, differences in community structure were close to being significant (P = 0.059 and 0.077, respectively, R = 0.164 for both), and it was only twenty-one days after N application that differences between the communities in the two soil horizons was significant (P = 0.047, R = 0.171 Table 4.2).

No significant differences (P > 0.05, Tukey HSD) were found in T-RF richness for bacterial community and for ARISA amplicon richness for fungal communities between the organic and mineral horizons over time (data not shown). Similarly, there was no significant difference (P > 0.05, Tukey HSD) in Shannon diversity index for either bacterial or fungal communities between the organic and mineral horizons over time (data not shown). In contrast, the archaeal community showed a higher T-RF richness in the organic horizon (31 ± 6, n = 39) than in the mineral horizon (23 ± 7, n = 40) over time, but this difference was not significant (P > 0.05, Tukey HSD). The Shannon diversity index of the archaeal community was also higher in the organic horizon (2.9 ± 0.21, n = 39) than in the mineral horizon (2.4 ± 0.29, n = 40), and showed a significant difference (P < 0.05, Tukey HSD) between the organic and mineral horizons for the control + water plots at both Day-6 and Day+21 (data not shown).

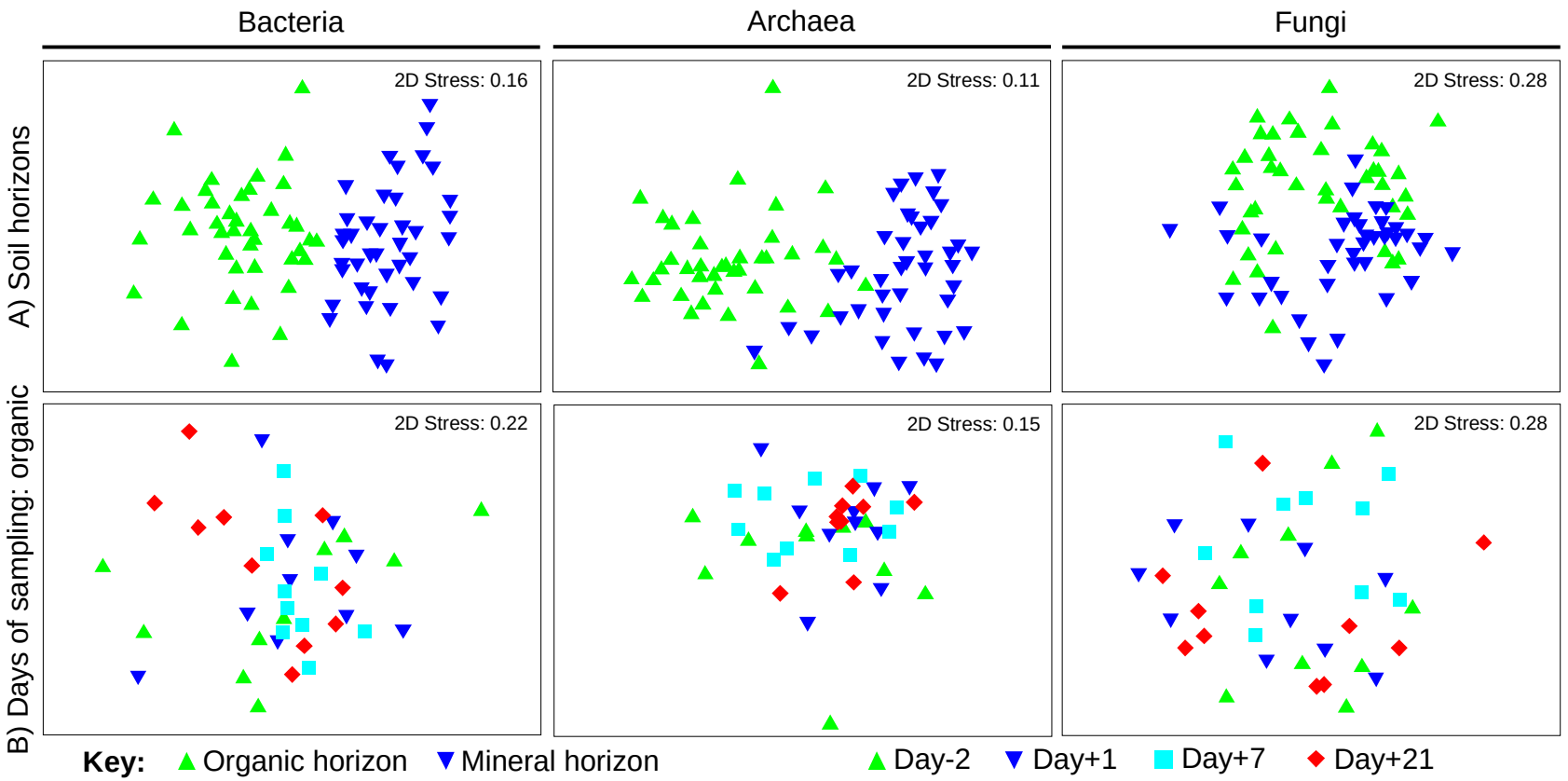
Bacteria
Archaea
Fungi
A) Soil horizons
B) Days of sampling: organic
2D Stress: 0.16
2D Stress: 0.11
2D Stress: 0.28
2D Stress: 0.22
2D Stress: 0.15
2D Stress: 0.28
Key:
Organic horizon
Mineral horizon
Day-2
Day+1
Day+7
Day+21

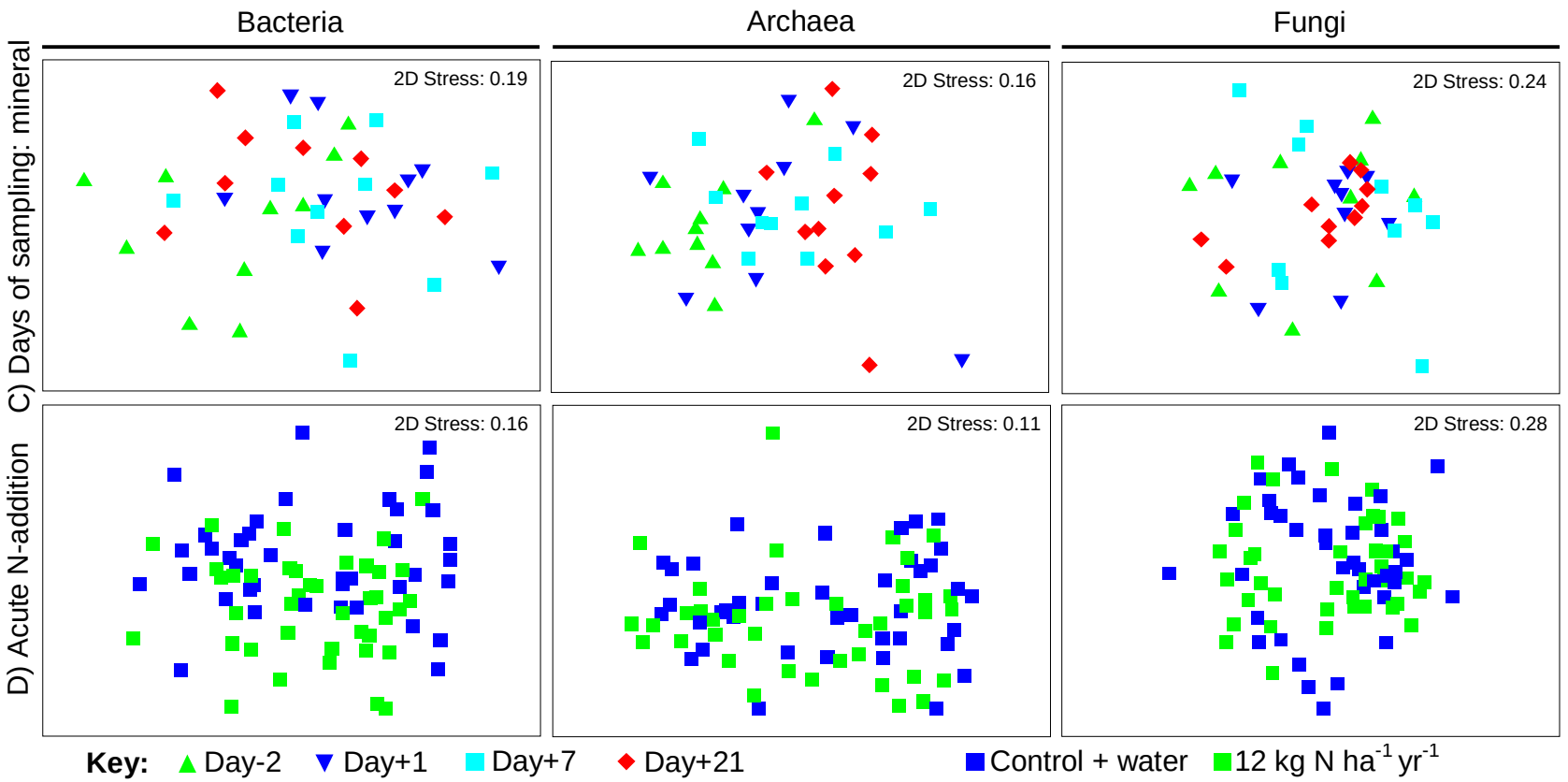

Figure 4.9: nMDS plots showing difference in structure of the bacterial, archaeal and fungal communities between organic and mineral soil horizons, over time and in response to simulated episodic N deposition events from soil samples taken from the organic and mineral horizons in the control + water and 12 kg N ha^{-1} yr^{-1} ~pH 4 plots, before N application (Day-6), and 1, 7 and 21 days after total N application (Day+1, Day+7, Day+21 respectively). **A**: plots showing the influence of soil horizons on microbial community structure; **B**: plots showing the influence of the sampling day on microbial community structure in the organic horizon; **C**: plots showing the influence of the sampling days on microbial community structure in the mineral horizon; **D**: plots showing the influence of simulated episodic N deposition event on microbial community structure. Soil horizons, days of sampling and treatments are as indicated in the key. The 2D stress is given for each nMDS plot.

Table 4.2: Two-way ANOSIM showing variation in the structure of bacterial, archaeal and fungal communities between: different time points for the organic and the mineral horizons samples; and in response to simulated episodic N deposition for the organic and mineral horizons (control + water (**C+W**) and 12 kg N ha^{-1} yr^{-1} ~pH 4 plots). The R values and the significance level (in brackets) are given. Significant values at $P < 0.05$ are shown in bold text.

Soil horizons	Factors compared	Bacteria	Archaea	Fungi
	Organic *vs.* Mineral	**0.70 (0.00005)**	**0.75 (0.00005)**	**0.14 (0.01)**
Organic	Day-6 *vs.* Day+1	-0.02 (0.55)	0.08 (0.157)	0.06 (0.28)
	Day-6 *vs.* Day+7	0.06 (0.20)	0.002 (0.435)	0.20 (0.053)
	Day-6 *vs.* Day+21	0.12 (0.13)	0.06 (0.22)	0.06 (0.26)
	Day+1 *vs.* Day+7	-0.02 (0.56)	-0.02 (0.499)	0.08 (0.23)
	Day+1 *vs.* Day+21	0.08 (0.18)	0.05 (0.239)	-0.07 (0.73)
	Day+7 *vs.* Day+21	0.11 (0.13)	-0.01 (0.481)	**0.26 (0.024)**
Mineral	Day-6 *vs.* Day+1	**0.29 (0.005)**	0.07 (0.189)	-0.05 (0.65)
	Day-6 *vs.* Day+7	0.12 (0.095)	**0.31 (0.015)**	0.14 (0.091)
	Day-6 *vs.* Day+21	0.10 (0.17)	**0.65 (0.0002)**	0.12 (0.099)
	Day+1 *vs.* Day+7	0.02 (0.39)	-0.03 (0.578)	0.15 (0.097)
	Day+1 *vs.* Day+21	0.1 (0.135)	0.15 (0.072)	-0.05 (0.677)
	Day+7 *vs.* Day+21	-0.13 (0.90)	-0.03 (0.581)	**0.24 (0.019)**
Organic	C+W *vs.* 12 kg N ha^{-1} yr^{-1}	0.02 (0.37)	-0.05 (0.75)	0.02 (0.32)
Mineral	C+W *vs.* 12 kg N ha^{-1} yr^{-1}	**0.17 (0.014)**	0.01 (0.42)	**0.12 (0.05)**

4.2.2.2 Variation in microbial community structure over time

Bacterial and archaeal community structure within the organic horizon did not significantly change over time (Figure 4.9 B, see Table 4.2). However, the fungal community in the organic horizon did show some variability over time; the fungal

community in the organic horizon was significantly different (P = 0.024) between Day+7 *vs.* Day+21 and nearly significant at $P < 0.05$ between Day-6 *vs.* Day+7 (P value = 0.053) but the group separation was low (ANOSIM, R = 0.26 and 0.20, respectively; Table 4.2).

In contrast, in the mineral horizon, variability was seen over time (Figure 4.9 C) in the structure of all three communities (bacterial, archaeal and fungal). Bacterial community structure in the mineral horizon was significantly different between Day-6 *vs.* Day+1 (R = 0.29, P = 0.005), while the fungal community was significantly different between Day+7 *vs.* Day+21 (R = 0.24, P = 0.019). The archaeal community structure showed the greatest change over time, with significant differences between Day-6 *vs.* Day+7 (P = 0.015, R = 0.31) and Day-6 *vs.* Day+21 (R = 0.65, P = 0.0002). The R values of the mineral archaeal community were higher in comparison to those from the corresponding time points for the bacterial and fungal communities and in particular with a high R value between Day-6 *vs.* Day+21 (Table 4.2). Changes in microbial community structure over time were not reflected either by differences in T-RFs richness or Shannon diversity indices, for either bacterial, archaeal or fungal communities between the different dates of sampling with respect to either soil horizon or treatment (data not shown).

4.2.2.3 Variation in microbial community structure to N deposition

The N application (i.e. 12 kg N ha^{-1} yr^{-1} plots) did not significantly ($P \geq 0.32$; Table 4.2) change the structure of bacterial, archaeal and fungal communities within the organic horizon over time (Figure 4.9 D). Similarly, the structure of archaeal community within the mineral horizon did not differ between the control + water and 12 kg N ha^{-1} yr^{-1} plots (P = 0.42). However, the structure of both the bacterial and fungal communities within the mineral horizon were significantly affected by N application (P = 0.014 and 0.05, respectively) over time but ANOSIM analysis generated low R values (R = 0.17 and 0.12, respectively). When the nMDS and ANOSIM analysis of the bacterial and fungal communities of the mineral horizon were performed separately on each date of sampling, the results show that the influence of the N application occurred

on a specific date of sampling (Figures 4.10 and 4.11; Table 4.3). Thus, fungal community structure was significantly different between the control + water and 12 kg N ha^{-1} yr^{-1} plots only after seven days post N application (R = 0.33, *P* = 0.048; Figure 4.10), although, from the soil sample of the control + water plot 2, fungal ITS sequences could not be amplified. Twenty-one days after N application, the fungal communities were no longer significantly different (R = 0.092, *P* = 0.019) between the control + water and 12 kg N ha^{-1} yr^{-1} plots. It is interesting to notice that the fungal communities within the organic horizon at Day+7 had the highest R value and the lowest *P* value (R = 0.15 and *P* = 0.19, respectively) in comparison to other sampling dates, with this value being similar to that determined for the mineral horizon at Day+21 (Table 4.3). The difference between the structure of the fungal communities in the control + water and 12 kg N ha^{-1} yr^{-1} plots in the mineral horizon at Day+7, did not result in a significant (*P* > 0.05) change in the ARISA amplicons richness or Shannon diversity index (data not shown).

Table 4.3: One-way ANOSIM showing variability in the structure of bacterial, archaeal and fungal communities between the control + water and 12 kg N ha^{-1} yr^{-1} ~pH 4 plots for the organic and mineral horizon for each day of sampling. The R values and the significance level (in brackets) are given. Significant values at *P* < 0.05 are shown in bold text.

Soil horizons	Days of sampling	Bacteria	Archaea	Fungi
Organic	Day-6	-0.06 (0.67)	-0.04 (0.55)	0.08 (0.34)
	Day+1	0.17 (0.079)	-0.15 (0.85)	-0.05 (0.62)
	Day+7	-0.12 (0.88)	0.08 (0.20)	0.15 (0.19)
	Day+21	0.08 (0.22)	-0.09 (0.86)	-0.03 (0.55)
Mineral	Day-6	0.24 (0.071)	0.10 (0.15)	-0.03 (0.56)
	Day+1	**0.37 (0.024)**	-0.06 (0.69)	0.01 (0.45)
	Day+7	0.01 (0.47)	0.04 (0.365)	**0.33 (0.048)**
	Day+21	0.06 (0.29)	-0.05 (0.60)	0.09 (0.19)

^{15}N soil enrichment was superimposed onto the nMDS plot of fungal community structure from the mineral horizon for each date of sampling (Figure 4.10) and correlation analysis was undertaken to investigate the relationship between changes in fungal community structure and ^{15}N enrichment. The soil ^{15}N enrichment of the mineral horizon clearly increased from Day+1 to Day+21 (Figure 4.10). However, no significant correlation ($P \geq 0.28$) was found between the ^{15}N enrichment and the structure of the fungal communities.

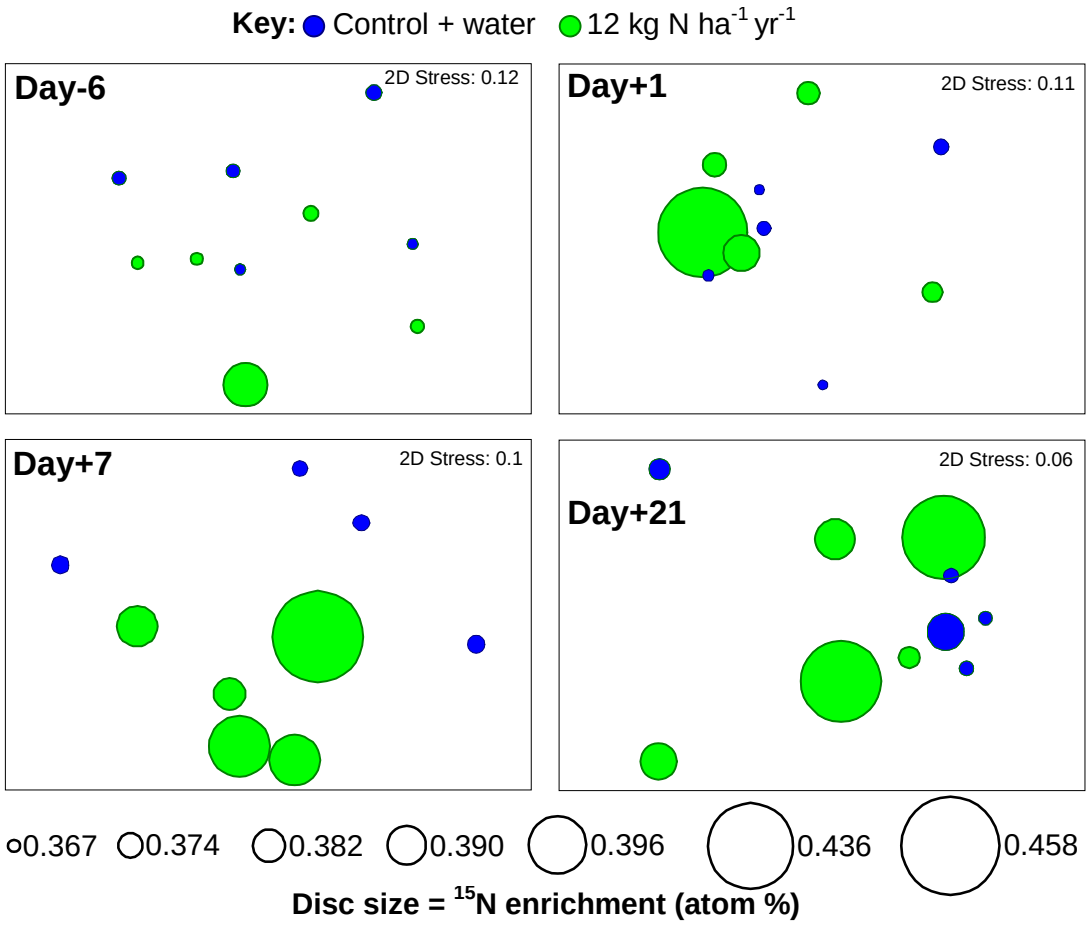

Figure 4.10: nMDS plots showing variability in fungal community structure in response to simulated episodic N deposition of the mineral horizon from the Control + Water and 12 kg N ha^{-1} yr^{-1} ~pH 4 plots (as indicated in the key), for each day of sampling: **Day-6**: two days before N application; **Day+1**: one day after N application; **Day+7**: seven days after N application; **Day+21**: twenty-one days after N application. The different sizes of discs represent variation in ^{15}N enrichment (atom %) in the soil samples. The 2D stress is given for each nMDS plot.

Bacterial community structure in the mineral horizon was significantly different between the control + water and 12 kg N ha^{-1} yr^{-1} plots, one day after N application (R = 0.37, *P* = 0.024; Figure 4.11). However, no significant differences were found at Day+7 and Day+21 (*P* = 0.47 and 0.29, respectively). Bacterial community structure in the organic horizon was close to being significantly influenced by the N application at Day+1 (R = 0.17, *P* = 0.079; Table 4.3). N application did not change either the T-RF

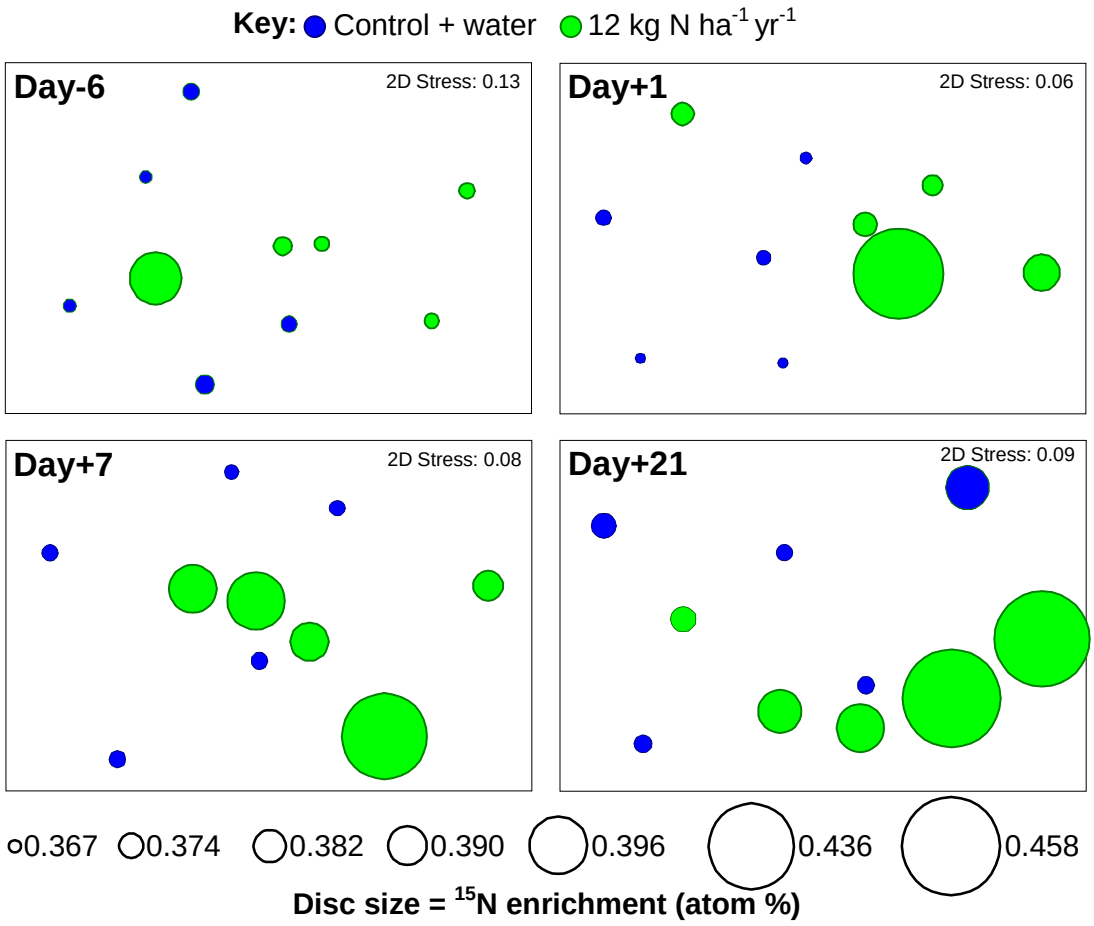

Figure 4.11: nMDS plots showing variability in bacterial community structure in response to simulated episodic N deposition of the mineral horizon from the Control + Water and 12 kg N ha^{-1} yr^{-1} ~pH 4 plots (as indicated in the key), for each day of sampling: **Day-6**: two days before N application; **Day+1**: one day after N application; **Day+7**: seven days after N application; **Day+21**: twenty-one days after N application. The different sizes of discs represent variation in ^{15}N enrichment (atom %) in the soil samples. The 2D stress is given for each nMDS plot.

richness or the Shannon diversity index between the control + water and 12 kg N ha^{-1} yr^{-1} plots for any time points within the organic or mineral horizon. Superimposing the soil ^{15}N enrichment onto the nMDS plot showing variation in bacterial community structure within the mineral horizon for each date of sampling (Figure 4.11) did not reveal any significant correlation ($P \geq 0.18$) between bacterial community structure and ^{15}N enrichment. The significant effect of N deposition on bacterial community structure at Day+1 occurred with a lower soil ^{15}N enrichment than was found by Day+7 and Day+21 (Figure 4.11).

The 12 kg N ha^{-1} yr^{-1} N application represented an extreme N deposition event to simulate N deposition, and led to significant effects upon the structure of the bacterial and fungal communities within the mineral horizon. Therefore, to investigate the response of microbial communities to a more typical N deposition event, variation in the bacterial community structure from the 4 kg N ha^{-1} yr^{-1} plots was assessed. Variation in bacterial community structure was investigated in the organic and mineral horizon, one day after N application (Figure 4.12), at which time-point there had been a significant influence in the 12 kg N ha^{-1} yr^{-1} treatment. As was seen for the bacterial community over the entire experiment (Figure 4.9A; Table 4.2), the structure of the bacterial communities in the control + water, 4 kg N ha^{-1} yr^{-1} and 12 kg N ha^{-1} yr^{-1} plots at Day+1 showed significant differences between the organic and mineral horizon (R = 0.64, P = 0.00005,). Bacterial community structure within the organic horizon from the 4 kg N ha^{-1} yr^{-1} plots did not differ significantly from the control + water and 12 kg N ha^{-1} yr^{-1} plots ($P \geq 0.30$; Table 4.4). In contrast, the bacterial community structure of the mineral horizon, showed a significant (P = 0.032) difference between the control + water and 4 kg N ha^{-1} yr^{-1} plots (Figure 4.12, Table 4.4). The R value obtained ANOSIM (R = 0.32) was lower than the one between the control + water and 12 kg N ha^{-1} yr^{-1} (R = 0.36). No significant difference were found between communities with respect to the two different N treatments in the mineral horizon (R = 0.23, P = 0.087; Table 4.4). No significant correlation was found between the bacterial community structure and the ^{15}N soil enrichment for any treatments or soil horizons ($P \geq 0.17$).

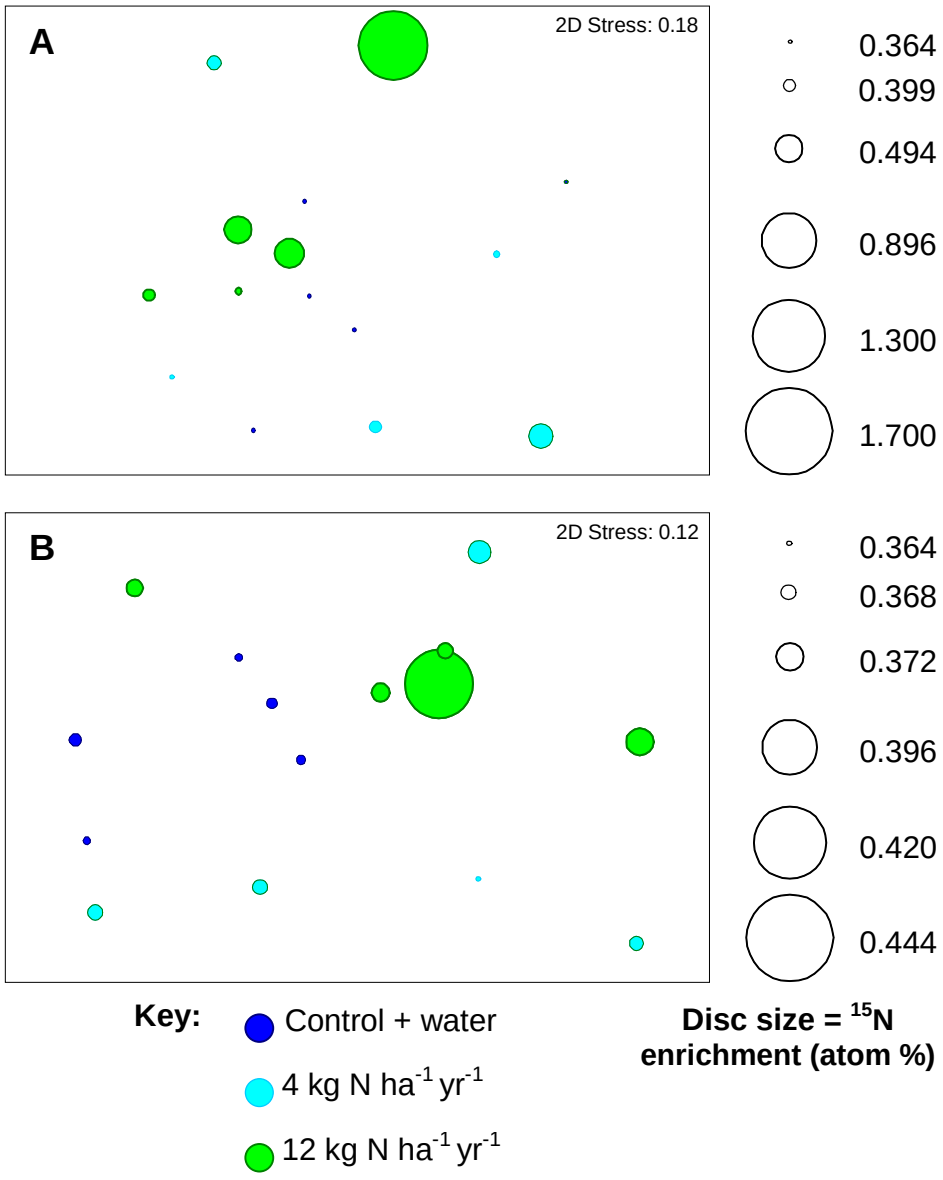

Figure 4.12: nMDS plots showing variability in bacterial community structure in response to simulated episodic N deposition from the organic (**A**) and mineral horizon (**B**), one day after N application for the Control + Water, 4 kg N ha^{-1} yr^{-1} ~pH 4 and 12 kg N ha^{-1} yr^{-1} ~pH 4 plots (as indicated in the key). The different sizes of discs represent variation in ^{15}N enrichment (atom %) in the soil samples. The 2D stress is given for each nMDS plot.

Table 4.4: One-way ANOSIM showing variability in the structure of bacterial communities between the control + water (**C+W**), 12 kg N ha^{-1} yr^{-1} ~pH 4 (**12N**) and 4 kg N ha^{-1} yr^{-1} ~pH 4 (**4N**) plots for the organic and mineral horizon one day after N application. The R values and the significance level (in brackets) are given. Significant values at $P < 0.05$ are shown in bold text.

Soil horizons	Factors compared	Bacteria
Organic	C+W *vs.* 12N	0.18 (0.071)
	C+W *vs.* 4N	-0.02 (0.60)
	12N *vs.* 4N	0.08 (0.30)
Mineral	C+W *vs.* 12N	**0.36 (0.024)**
	C+W *vs.* 4N	**0.32 (0.032)**
	12N *vs.* 4N	0.23 (0.087)

4.2.3 Variation in bacterial, archaeal and fungal abundance within soil

There were no significant differences ($P > 0.05$) in either bacterial 16S rRNA gene or fungal ITS regions abundance between the organic and mineral horizons (Figure 4.13 and 4.15). In contrast, archaeal 16S rRNA genes abundance was on average ~2.9 times and significantly ($\chi^2 = 37.2$, df = 1, $P = 1.1 \times 10^{-9}$) higher in the mineral horizon than in the organic horizon over time (Figure 4.14). Despite variability over time in the abundance of the bacteria, archaea and fungi, no significant differences ($P > 0.05$) were found over time in either soil horizons or treatments. Similarly, the bacterial, archaeal and fungal rRNA gene or ITS regions abundances were not significantly influenced by N addition for either soil horizons or date of sampling (Figure 4.13, 4.14, 4.15), even when significant changes in bacterial and fungal community structures were found.

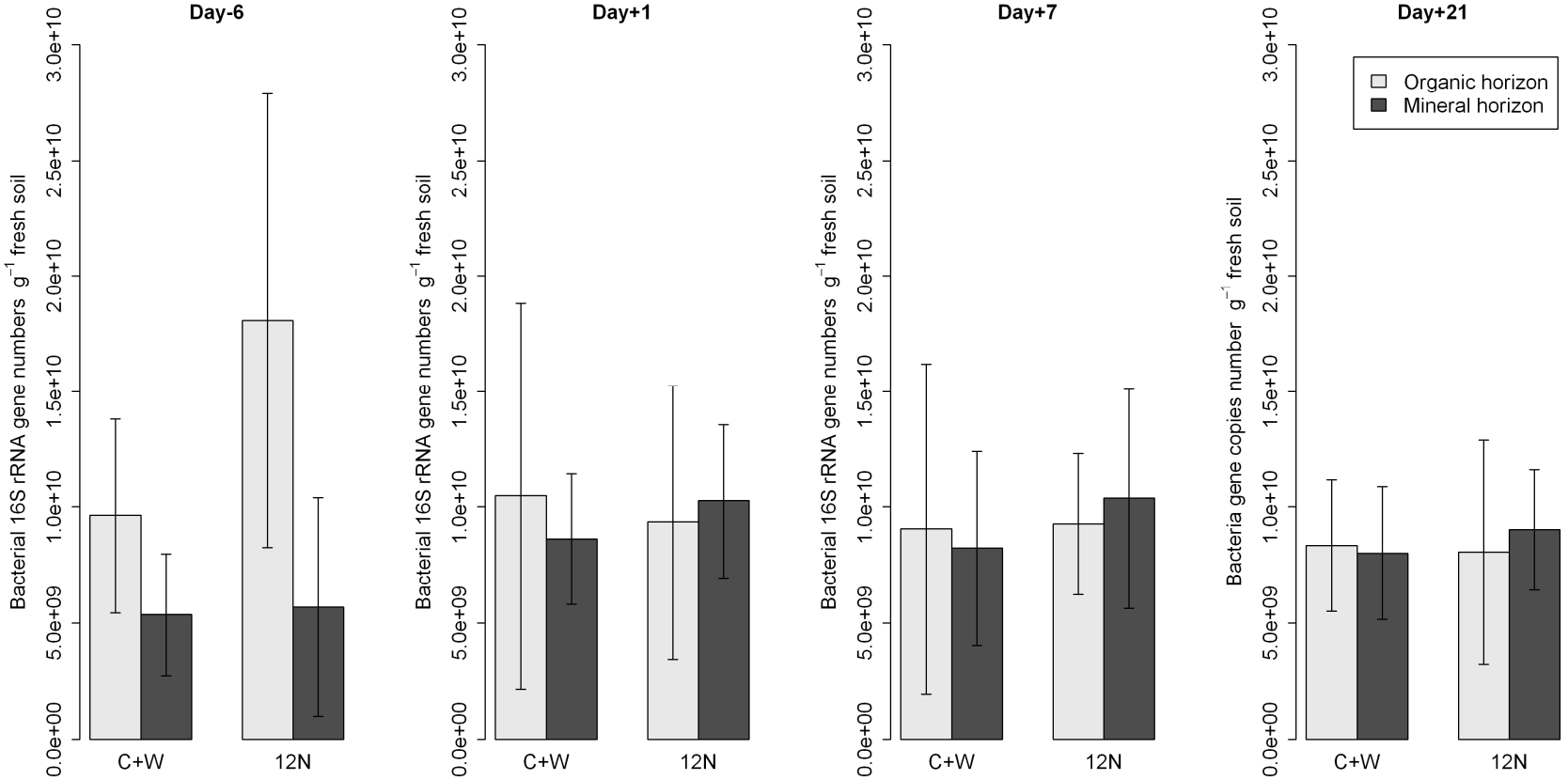

Figure 4.13: Variation in bacterial gene abundance (16S rRNA gene numbers g^{-1} fresh soil) between organic and mineral soil horizons, over time and in response to simulated episodic N deposition events. Plots were established in 2009 and subjected to simulated N deposition events in 2009 and 2010, and sampled in summer 2010 (see section 2.2.1). **Day-6**: two days before N application; **Day+1**: one day after total N application; **Day+7**: seven days after total N application; **Day+21**: twenty-one days after total N application; **C**: Control plots; **C+W**: control + water plots; **12N**: 12 kg N ha^{-1} yr^{-1} ~pH 4 plots. Means values ± standard deviation (n = 5) are shown. Gene numbers were calculated from the standard curve: $r^2 = 0.993$, y intercept = 39.66, *E* (amplification efficiency) = 88.3%, NTC $C_t = 29.5$.

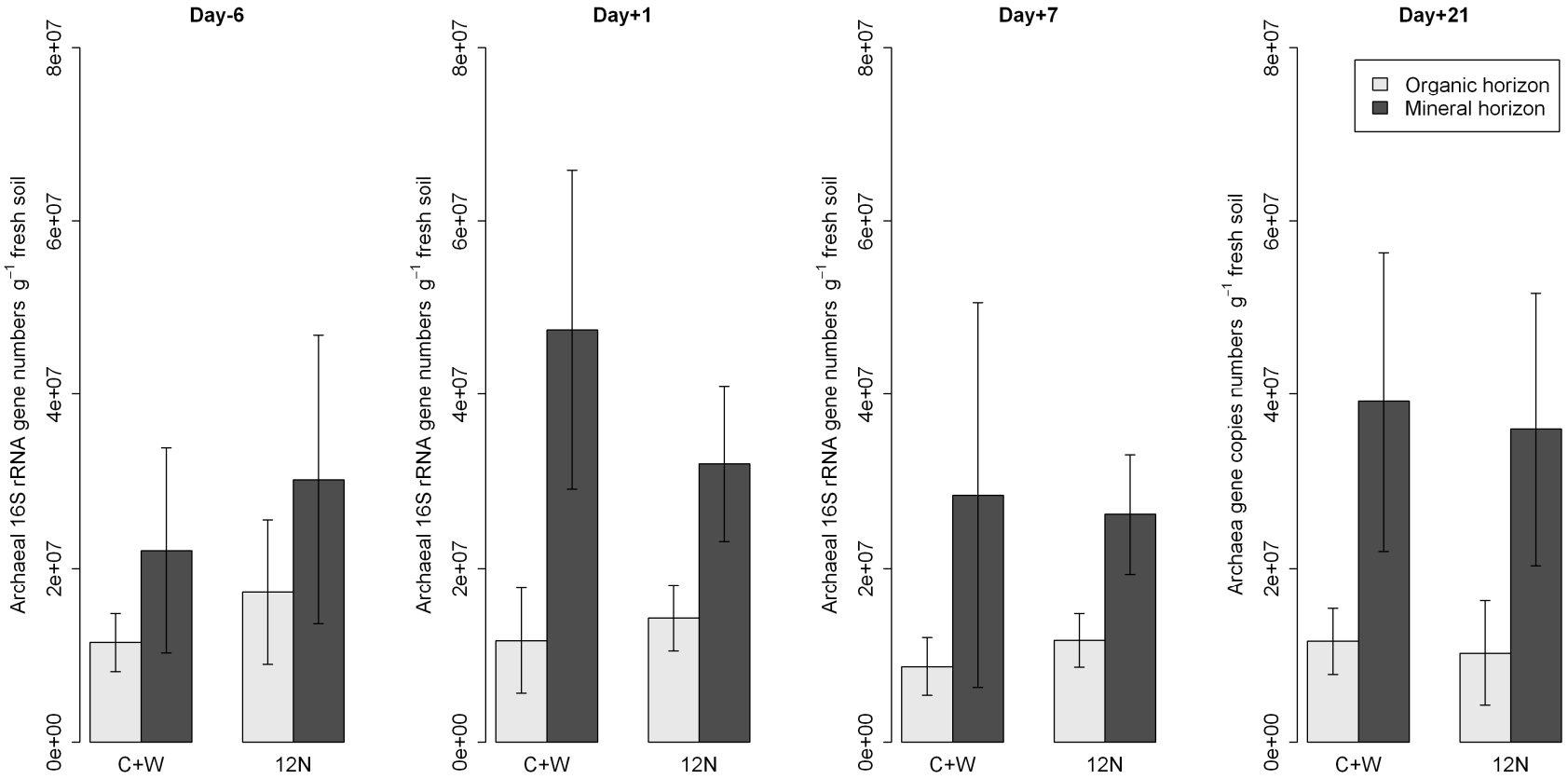

Figure 4.14: Variation in archaeal gene abundance (16S rRNA gene numbers g^{-1} fresh soil) between organic and mineral soil horizons, over time and in response to simulated episodic N deposition events. Plots were established in 2009 and subjected to simulated N deposition events in 2009 and 2010, and sampled in summer 2010 (see section 2.2.1). **Day-6**: two days before N application; **Day+1**: one day after total N application; **Day+7**: seven days after total N application; **Day+21**: twenty-one days after total N application; **C**: Control plots; **C+W**: control + water plots; **12N**: 12 kg N ha^{-1} yr^{-1} ~pH 4 plots. Means values ± standard deviation (n = 5) are shown. Gene numbers were calculated from the standard curve: $r^2 = 0.956$, y intercept = 32.18, *E* (amplification efficiency) = 140.9%, NTC C_t = 31.6. Archaea were significantly ($P < 0.001$) more abundant in the mineral than organic horizons.

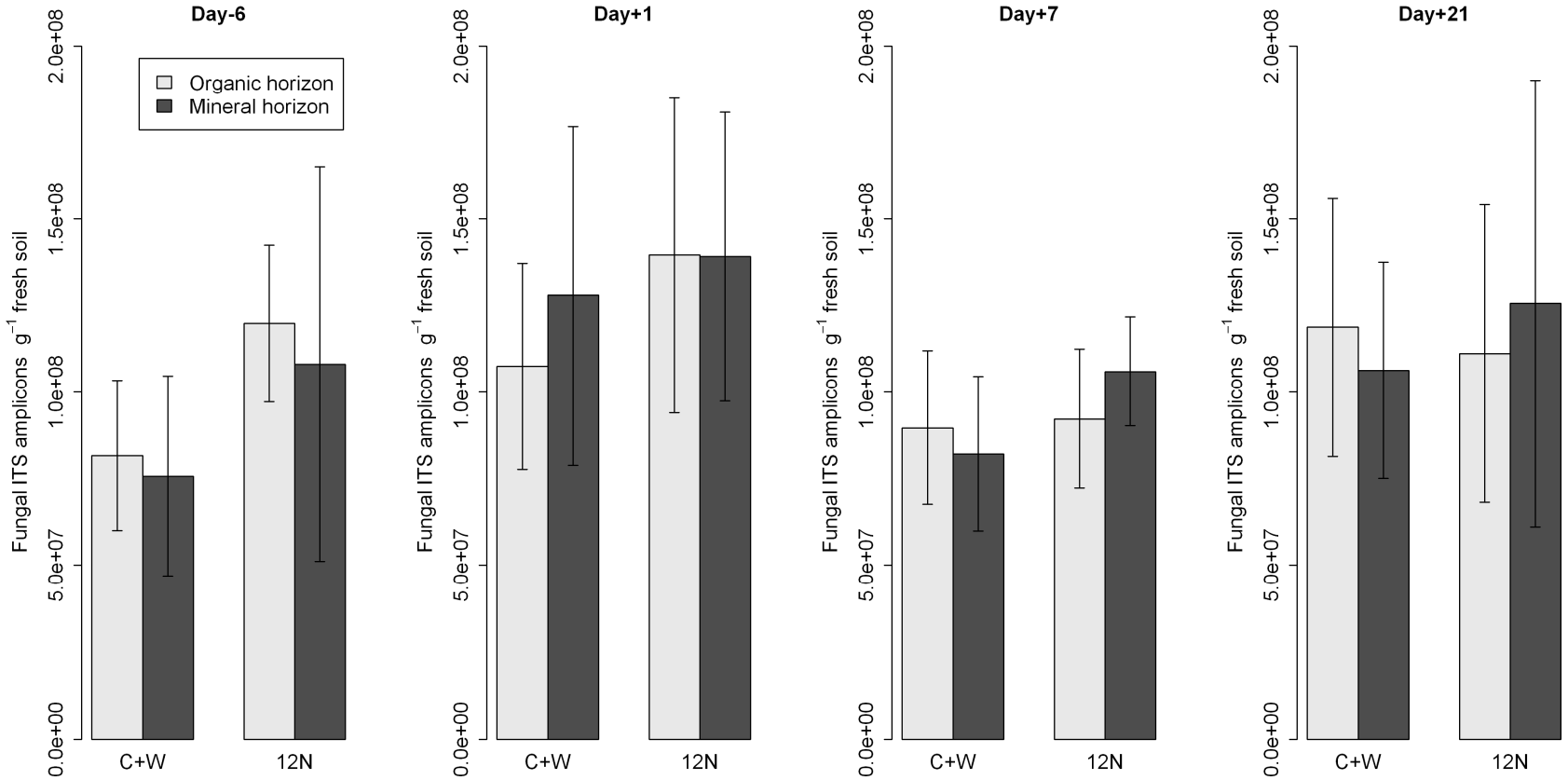

Figure 4.15: Variation in fungal abundance (ITS amplicons g^{-1} fresh soil) between organic and mineral soil horizons, over time and in response to simulated episodic N deposition events. Plots were established in 2009 and subjected to simulated N deposition events in 2009 and 2010, and sampled in summer 2010 (see section 2.2.1). **Day-6**: two days before N application; **Day+1**: one day after total N application; **Day+7**: seven days after total N application; **Day+21**: twenty-one days after total N application; **C**: Control plots; **C+W**: control + water plots; **12N**: 12 kg N ha^{-1} yr^{-1} ~pH 4 plots. Means values ± standard deviation (n = 5) are shown. Gene numbers were calculated from the standard curve: r^2 = 0.962, y intercept = 43.66, *E* (amplification efficiency) = 67.8%, NTC C_t = 34.8.

4.2.4 Relationship between microbial community, structure, abundance and environmental variables

Bacterial community structure in both soil horizons was significantly ($P \leq 0.01$) and strongly correlated to total N ($\rho = 0.40$), water content ($\rho = 0.39$), total C ($\rho = 0.38$) and soil pH ($\rho = 0.34$); and to a lesser extent to NH_4^+ concentration ($\rho = 0.28$) and weakly to the C/N ratio ($\rho = 0.11$) (Table 4.5). No significant ($P \geq 0.29$) correlation of bacterial community structure was found with ^{15}N enrichment, NO_3^- concentration and bacterial abundance. When the correlations were performed on the bacterial community structure from the organic horizon, only the NH_4^+ concentration showed significant ($P = 0.001$) and strong correlation ($\rho = 0.32$). The bacterial community structure of the mineral horizon was significantly ($P \leq 0.015$) correlated to the water content, total C and total N content, but these correlations were not as strong as for the whole bacterial community (Figure 4.5).

Archaeal community structure from both soil horizons was significantly ($P = 0.001$) and strongly correlated to the total C ($\rho = 0.48$), total N ($\rho = 0.46$), and water content ($\rho = 0.39$), soil pH ($\rho = 0.37$) and less strongly to archaeal community abundance ($\rho = 0.28$), NH_4^+ concentration ($\rho = 0.23$) and to the C/N ratio ($\rho = 0.20$). As was seen for the bacterial community structure in the organic horizon, the archaeal community of the organic horizon was significantly ($P = 0.02$) correlated to NH_4^+ concentration ($\rho = 0.19$; Table 4.5). Archaeal community structure in the mineral horizon was only significantly correlated to the soil pH ($P = 0.05$, $\rho = 0.19$).

Fungal community structure in both soil horizons was significantly ($P \leq 0.03$) but weakly, correlated to the soil pH, and total C and total N content ($\rho = 0.16$, 0.11 and 0.08, respectively; Table 4.5). When correlations were performed on the fungal community structure of the organic and mineral horizons separately, no significant ($P \leq 0.06$) correlations were found, although fungal community structure in the mineral horizon was nearly significantly ($P < 0.05$) correlated to soil pH ($P = 0.06$).

The structure of the bacterial, archaeal and fungal communities in both soil horizons were all significantly ($P = 0.001$) correlated to each other, with a strong correlation between bacteria *vs.* archaea ($\rho = 0.48$) and weak correlations between

Table 4.5: Correlations between microbial community structure and environmental variables or microbial community abundance within both soil horizons or within specific soil horizon, obtained using the RELATE test from PRIMER software. The ρ values and the significance level (in brackets) are given. Significant values at $P < 0.05$ are shown in bold text.

Microbial community	Water	pH	Total C	Total N	^{15}N	C/N ratio	NO_3^-	NH_4^+	Abundance
Bacteria	**0.39 (0.001)**	**0.34 (0.001)**	**0.38 (0.001)**	**0.43 (0.001)**	0.03 (0.29)	**0.11 (0.01)**	0.003 (0.42)	**0.28 (0.001)**	0.01 (0.39)
Bacteria organic	-0.02 (0.59)	0.06 (0.22)	-0.02 (0.53)	0.12 (0.056)	0.06 (0.29)	0.01 (0.42)	0.07 (0.16)	**0.32 (0.001)**	-0.05 (0.68)
Bacteria mineral	**0.23 (0.005)**	0.11 (0.07)	**0.17 (0.015)**	**0.19 (0.001)**	0.005 (0.47)	-0.01 (0.52)	0.01 (0.44)	0.04 (0.23)	0.09 (0.13)
Archaea	**0.39 (0.001)**	**0.37 (0.001)**	**0.48 (0.001)**	**0.46 (0.001)**	0.0 (0.52)	**0.20 (0.001)**	0.046 (0.09)	**0.23 (0.001)**	**0.28 (0.001)**
Archaea organic	-0.02 (0.61)	-0.07 (0.81)	-0.05 (0.70)	0.08 (0.15)	-0.03 (0.62)	0.004 (0.48)	-0.07 (0.81)	**0.19 (0.02)**	-0.02 (0.58)
Archaea mineral	-0.03 (0.67)	**0.19 (0.05)**	0.03 (0.33)	0.02 (0.35)	0.05 (0.26)	0.05 (0.24)	0.08 (0.11)	0.02 (0.34)	-0.09 (0.90)
Fungi	0.05 (0.13)	**0.16 (0.001)**	**0.11 (0.007)**	**0.08 (0.03)**	-0.001 0.53)	0.05 (0.11)	0.003 (0.44)	0.05 (0.13)	-0.08 (0.97)
Fungi organic	-0.01 (0.98)	0.03 (0.30)	0.02 (0.35)	-0.02 (0.67)	0.01 (0.44)	0.02 (0.37)	-0.01 (0.61)	0.11 (0.37)	-0.12 (0.99)
Fungi mineral	0.05 (0.24)	0.12 (0.06)	0.08 (0.15)	0.05 (0.22)	-0.01 (0.84)	0.07 (0.19)	-0.09 (0.93)	0.04 (0.26)	-0.03 (0.63)

Table 4.6: Correlations between microbial community abundance and environmental variables within both soil horizons or within specific soil horizon, obtained using the RELATE test from PRIMER software. The ρ values and the significance level (in brackets) are given. Significant values at $P < 0.05$ are shown in bold text.

Microbial community	Water	pH	Total C	Total N	^{15}N	C/N ratio	NO_3^-	NH_4^+
Bacteria	**0.09 (0.03)**	**0.14 (0.003)**	**0.10 (0.02)**	**0.11 (0.006)**	-0.04 (0.71)	**0.14 (0.007)**	-0.04 (0.83)	0.03 (0.27)
Bacteria organic	-0.07 (0.87)	**0.17 (0.037)**	-0.02 (0.57)	0.02 (0.39)	-0.03 (0.59)	0.07 (0.19)	-0.06 (0.76)	-0.01 (0.48)
Bacteria mineral	**0.29 (0.001)**	**0.27 (0.001)**	**0.16 (0.029)**	**0.28 (0.001)**	-0.10 (0.88)	**0.23 (0.01)**	-0.11 (1.0)	0.12 (0.06)
Archaea	**0.18 (0.001)**	**0.15 (0.001)**	**0.14 (0.001)**	**0.18 (0.001)**	-0.07 (0.93)	0.10 (0.019)	-0.5 (0.91)	**0.19 (0.001)**
Archaea organic	-0.06 (0.82)	-0.10 (0.11)	0.002 (0.45)	0.05 (0.20)	-0.04 (0.64)	0.07 (0.20)	-0.7 (0.82)	0.12 (0.06)
Archaea mineral	**0.14 (0.034)**	0.08 (0.12)	0.05 (0.22)	**0.20 (0.003)**	-0.06 (0.70)	0.07 (0.21)	-0.03 (0.65)	**0.18 (0.007)**
Fungi	**0.13 (0.007)**	0.04 (0.13)	0.02 (0.27)	0.07 (0.052)	0.07 (0.12)	0.04 (0.16)	-0.03 (0.70)	0.1 (0.36)
Fungi organic	0.04 (0.26)	-0.03 (0.65)	-0.003 (0.46)	-0.04 (0.69)	0.08 (0.20)	0.01 (0.42)	-0.04 (0.71)	0.08 (0.12)
Fungi mineral	0.10 (0.07)	**0.14 (0.026)**	-0.04 (0.74)	0.05 (0.20)	0.12 (0.08)	0.13 (0.058)	-0.01 (0.54)	0.10 (0.73)

bacteria *vs.* fungi, and fungi *vs.* archaea ($\rho = 0.16$ for both).

Bacterial abundance in both soil horizons was significantly ($P \leq 0.03$) correlated to the C/N ratio, soil pH, total N, total C and water content (Table 4.6). However, these correlations were weak, varying between 0.14 to 0.09. Bacterial abundance in the organic horizon was significantly ($P = 0.037$) but weakly correlated to soil pH ($\rho = 0.17$). In contrast, bacterial abundance in the mineral horizon was significantly ($P \leq 0.029$) correlated to water content, total N, soil pH, the C/N ratio and total C. Moreover, correlations were stronger than for the bacterial community abundance in both soil horizons, especially for water content, total N, total C and C/N ratio ($\rho = 0.29$, 0.28, 0.27 and 0.23 respectively).

Archaeal abundance in both soil horizons showed significant ($P = 0.001$) correlation with the NH_4^+, water and total N content, soil pH and total C (Table 4.6). The strength of these correlations was higher than found for the bacterial abundance from both soil horizons, with ρ values varying between 0.19 to 0.14, but still lower than those found for the archaeal structure. No significant ($P \geq 0.06$) correlations were found for the archaeal abundance in the organic horizon, although the correlation with NH_4^+ concentration was nearly significant at $P < 0.05$ ($P = 0.06$). Archaeal abundance of the mineral horizon showed significant ($P \leq 0.034$) correlations with the total N, NH_4^+ and water content with similar strengths of correlations to those found for the community from both soil horizons.

Fungal abundance in both soil horizons was significantly ($P = 0.007$) but weakly correlated to the soil water content ($\rho = 0.13$), whilst fungal abundance in the organic horizon was not significantly ($P \geq 0.12$) correlated to any variables. In the mineral horizon, fungal abundance was significantly ($P = 0.026$) correlated to soil pH ($\rho = 0.14$). The C/N ratio, water content and ^{15}N enrichment were nearly significantly correlated at $P < 0.05$ to fungal abundance in the mineral horizon. No significant ($P \geq 0.09$) correlations were found between abundance of bacteria, archaea and fungi.

4.3 Discussion

4.3.1 Vertical and temporal variation of microbial communities

The structure of bacterial, archaeal and fungal communities were all highly different between the organic and mineral horizons (Figure 4.9, Table 4.2). These differences are in agreement with the results obtained in 2009 (see Chapter 3) and other studies showing that different bacterial and fungal communities inhabit the organic and mineral horizons in subarctic tundra soil (Rinnan *et al.*, 2007; Wallenstein *et al.*, 2007). In contrast, little is known about the archaeal community in arctic soil. Thus, the results of the archaeal community (see Chapter 3), indicate clearly that different soil horizons also represent distinct environments for the archaea. The structure of both bacterial and archaeal communities were strongly correlated to the soil nutrient content (i.e. total C and N content) and soil water content (Table 4.5), variables also described as main drivers of the bacterial community structure with soil depth in other studies (Zhou *et al.*, 2002; Fierer *et al.*, 2003; LaMontagne *et al.*, 2003; Hansel *et al.*, 2008). The soil pH, considered as a key driver of bacterial community structure in soils (Fierer & Jackson 2006; Lauber *et al.*, 2009; Rousk *et al.*, 2010) and also in subarctic soil (Männistö *et al.*, 2007) was also a strong driver of the bacterial and archaeal community structure, although the difference in soil pH between the organic and mineral horizons was only 0.7 pH unit in average. Therefore, the bacterial and archaeal community structure could potentially be sensitive to any significant change in soil pH related to acute N deposition events. Although similar variables regulated the bacterial and archaeal community structure, the strength of the variables on the bacterial and archaeal community structure differed. Moreover, archaeal community structure showed a stronger relationship to the environmental variables measured than was found for bacteria. Thus, the archaeal community is likely to be more sensitive to environmental changes than the bacterial community.

Despite the high variability of the fungal community structure, which has already been observed between different soil horizons (Hartmann *et al.*, 2009), significant differences between soil horizons were found. However, the low separation (by

ANOSIM) between the fungal structure of the organic and mineral horizons (Table 4.2) indicates that fungal mycelia were probably not exclusively limited to a single soil horizon (Landeweert *et al.*, 2003; Hartmann *et al.*, 2009). Although the fungal mycelia overlap to some extent across both soil horizons, different fungal community structures were found in the soil horizons, and these also evolved differently over time and responded differently to N deposition (Figure 4.9; Table 4.2). Thus it appears that different environmental variables regulated the fungal community structure within each soil horizon. However, fungal community structure was weakly correlated to the soil pH, total C and total N. The high variability in fungal community structure might explain the weak correlations with these environmental variables, or that other variables regulated the fungal community in both soil horizons.

Bacterial, archaeal and fungal abundance did not decrease with soil depth (Figures 4.13-15) which is in contrast to the usual decrease in microbial biomass found with soil depth in others ecosystems (Fritze *et al.*, 2000; Ekelund *et al.*, 2001; Taylor *et al.*, 2002; Fierer *et al.*, 2003; LaMontagne *et al.*, 2003; Agnelli *et al.*, 2004; Hartmann *et al.*, 2009). Similar results were obtained in 2009 at the end of the summer period within the same experimental site (see Chapter 3). Bacteria were more abundant in the organic than in the mineral horizon, but only at the beginning of the experiment while archaeal abundance was always higher in the mineral horizon. Despite the sharp decrease in soil water content, total C, total N, C/N ratio and NH_4^+ from the organic to the mineral horizon, these did not strongly influence microbial abundance, although these factors are commonly considered to influence microbial biomass with soil depths (Fritze *et al.*, 2000; Fierer *et al.*, 2003). Thus, the mineral horizon represents a favourable environment for the microbial community, and especially the archaeal community in arctic tundra soil, with more microhabitats and more suitable environmental conditions for microorganisms than the organic horizon. Indeed, the mineral horizon is less likely to dry in summer than the organic horizon and the temperature is more stable in the mineral horizon, because the permafrost under the active layer buffers the soil temperature and regulates water availability (Nemergut *et al.*, 2005).

Bacterial, archaeal and fungal community structures were dynamic over time (Figure 4.9; Table 4.2). However, the temporal changes in bacterial and fungal

community structures in the mineral horizon are likely to be related to the N application, as each significant difference between dates of sampling included the day where significant influence of N deposition was found. In contrast, the archaeal community showed greater temporal changes in structure over time in the mineral horizon between the first date of sampling and the latest dates of sampling, i.e. 12 and 26 days later. Despite the temporal changes, the archaeal community structure in the mineral horizon was only correlated to the soil pH, indicating that soil pH potentially regulates archaeal structure over time. Høj *et al.* (2005) also found changes in the archaeal community structure over the summer period in a peat located ~1.5 km from our experimental site. Bacterial, archaeal and fungal abundance showed some variation over the summer but no significant trends were observed (Figures 4.13-15). Thus, changes in microbial community structure over time were not followed by changes in abundance. Stapleton *et al.* (2005) showed that changes in bacterial biomass over the summer period within the organic horizon of an arctic tundra near our site, was not consistent over two successive years. Microbial communities show variability in structure, in particular, and abundance indicating that Arctic microbial communities are dynamic over the summer period and can show high turnover rates, which is in contrast to studies hypothesizing that microbial community turnover is low in arctic soils (Rinnan *et al.*, 2007; Lamb *et al.*, 2011).

4.3.2 Fate of nitrogen within the soil

The addition of ^{15}N-labelled NH_4NO_3 shows that N reached both soil horizons and mainly the organic horizon (Figure 4.6). Despite the low rates of N deposition and amount of water used (equivalent to precipitation of ~1.1 mm per application), the N passed through the plant cover, and therefore the results of the microbial community structure and abundance can be related to the impacts of N deposition simulation on soil. The soil ^{15}N enrichment declined over time, indicating ^{15}N leaching from the organic to the mineral horizon, and also plant or microbial uptake (Gordon *et al.*, 2001; Tye *et al.*, 2005). However, N applications did not change the total N content which is to be expected given the very small addition of N the treatments represent compared to the bulk soil N (Robinson *et al.*, 2004; Tye *et al.*, 2005).

NO_3^- concentration also increased in both soil horizons for the plots receiving N (Figure 4.7). While the NO_3^- concentration decreased over time in both soil horizons in the 12 kg N ha^{-1} yr^{-1} plots, it increased in the 4 kg N ha^{-1} yr^{-1} plots. Thus, NO_3^- was either utilised by plants or reduced by microorganisms in the 12 kg N ha^{-1} yr^{-1} plots, and the release of NO_3^- from the plant cover, in the lower N addition treatments, especially in the 4 kg N ha^{-1} yr^{-1} plots, takes longer than in the 12 kg N ha^{-1} yr^{-1} plots, leading to different peaks in NO_3^- concentration over the summer in relation to the rate of N deposition. In contrast, no difference in NH_4^+ concentration was found between control and treatments (Figure 4.7). Thus, NH_4^+ was either quickly utilised by the plant community or oxidised by the microbial community. The NH_4^+ could also been tightly bound to the plant cover, organic matter and clay, leading to a significant decrease in the extraction method efficiency.

Changes in the soil water content or soil pH were not found over time despite the addition of water with low pH and NH_4NO_3 (Figure 4.1, 4.2). An absence of soil acidification or increase in soil water content after N addition was also reported in other N deposition simulations at sites located near this plot experiment (Gordon *et al.*, 2001; Robinson *et al.*, 2004). Therefore, any changes in microbial community after acute N deposition simulation are likely due to addition of NH_4NO_3, rather than to changes in water availability or soil pH.

4.3.3 Responses of microbial communities to acute N deposition event

Bacterial and fungal community structure showed a rapid response to acute N deposition simulation in the mineral horizon. While the bacterial community structure was different between the control + water plots and the 12 kg N ha^{-1} yr^{-1} plots only one day after the last N application, the response in fungal community structure occurred seven days post-application (Figure 4.10, 4.11; Table 4.3). The delay in the fungal response to N deposition is likely to be due to a slower growth rate for the fungi. Several researchers hypothesised that microbial community responses to environmental changes such as N addition or warming may take more than a decade (Rinnan *et al.*, 2007; Walker *et al.*, 2008; Lamb *et al.*, 2011). However, this study clearly shows that bacterial

and fungal community structures can be rapidly affected by the N addition and that the responses of the communities are not constant over the summer. Thus, the microbial communities show some resilience to low rates of N deposition.

The responses of the bacterial and fungal communities to N deposition occurred only in the mineral horizons (Table 4.2), showing that the different microbial communities inhabiting soil horizons are not similarly affected by N deposition and that responses of microbial communities to other environmental changes (e.g. warming, precipitation) might also be different between soil horizons. Rinnan *et al.* (2007) found the structure of the bacterial communities investigated by PLFA, within the organic and mineral horizons of subarctic heath was affected after 15 years of N addition with a total N load of 1250 kg N ha^{-1}. However, they found that the total PLFA content (i.e. bacterial and fungal PLFA) increased with fertilisation by 16% in the organic horizon but by 27% in the mineral horizon and when only the bacterial PLFA content were considered, they found a 22% increase only within the mineral horizon of the fertilised plots. Thus, the responses of microbial communities to N addition are different between soil horizons and sometimes specific to a soil horizon. Rinnan *et al.* (2007) found significant effects of fertilisation on microbial communities after 15 years of fertilisation, but previous studies found that microbial biomass C was marginally altered after 5 (Jonasson *et al.*, 1999) and 6 years (Ruess *et al.*, 1999) and there was no effect after 10 years (S Jonasson & A Michelsen, unpublished), concluding that microbial responses to N addition can take more than a decade. However, the organic and mineral horizons were pooled in the previous studies, which may explain the differences to the results of Rinnan *et al.* (2007).

This current study shows that bacterial and fungal communities can be sensitive to relatively low rate of N deposition (i.e. 12 kg N ha^{-1} yr^{-1}). Moreover bacterial community structure within the mineral horizon of the plots which received only 4 kg N ha^{-1} yr^{-1} was also affected by N deposition one day post N application (Figure 4.12). In addition, the amount of N that reached the mineral horizon is extremely low in comparison to the initial N applied and the changes of bacterial and fungal community structure did not occur at the highest soil ^{15}N enrichment (Figure 4.10, 4.11). Thus, acute

N deposition events that represent extremely low N-input are likely to have a rapid effect on the microbial communities in the mineral horizon of High Arctic tundra.

Several studies applied NPK fertiliser in arctic tundra, which does not enable the influence of a particular nutrient on the microbial communities to be distinguished (Schmidt *et al.*, 2000; Rinnan *et al.*, 2007). The use of NH_4NO_3 in this study enables attribution of effects directly to N deposition and indicates whether the bacterial and fungal communities are potentially limited by N in the mineral horizon. However, the non-continuous response of the communities indicate that other nutrients such as P or K might be limiting factors too (Madan *et al.*, 2007), or that other environmental variables regulate communities.

Bacterial, archaeal and fungal abundance was not affected by N deposition in either soil horizon (Figure 4.13-15). Schmidt *et al.* (2000) also did not find changes in the microbial biomass investigated by PLFA, despite changes in the microbial community structure after fertilisation in subarctic heaths. In this current study, changes in bacterial and fungal community structures in the mineral horizon were not followed by an increase in bacterial and fungal abundance. Therefore, specific bacterial and fungal groups were sensitive to N deposition with some of them increasing in abundance while others decreased. Ectomycorrhizal fungi have been shown to be negatively affected by N deposition (Lilleskov *et al.*, 2001; 2002) while fungal denitrifiers which seem to play an important role in the Arctic (Siciliano *et al.*, 2009) could respond positively to N deposition. The bacterial community involved in the different steps of the N-cycle (i.e. N-fixation, nitrification and denitrification) might respond differently to N deposition with a reduction of the community involved in N-fixation and increase in nitrifier abundance. However, the functional genes of the different steps of the N-cycling could not be amplified or were in low abundance (see Chapter 5). Thus, potentially other bacterial groups show some sensitivity to N deposition, such as Gram-positive bacteria shown to increase in abundance after N addition in the Arctic (Schmidt *et al.*, 2000; Rinnan *et al.*, 2007).

Microbial communities within the organic horizon were not affected by N deposition. The organic horizon contains two times more N than the mineral horizon (Figure 4.4). Thus, the microbial communities within the organic horizon are maybe not

limited by N, but by other nutrients or by environmental variables such as temperature and water availability. Moreover, competition with plant roots for N uptake is likely to be greater in the organic horizon as the root length density is ~4 times higher in the organic than in the mineral horizon (personal communication F Oulehle). And finally, root exudation, and dead roots may represent an important source of organic N for the microbial communities. However, a few studies have found changes in microbial community structure or abundance in the organic horizon of subarctic heath soils (Schmidt *et al.*, 2000; Rinnan *et al.*, 2007). These studies added N over several years leading to high total N-input, which might indicate that microbial communities from the organic horizon respond to higher rates of N-input. Bacterial community structure within the organic horizon one day post N application was nearly significantly affected by N deposition while the fungal community structure within the organic horizon seven days post N application showed the lowest *P* value and highest R value in comparison to the other dates (Table 4.3). Thus, bacterial and fungal community structures showed some sensitivity to N deposition and higher rates of N deposition are likely to affect these communities. This was confirmed for the bacterial community structure when the 4 kg N ha^{-1} yr^{-1} plots were investigated. While the bacterial community structure within the organic horizon one day post N application was nearly significantly different between the control + water and 12 kg N ha^{-1} yr^{-1} plots, no difference was found between the control + water and 4 kg N ha^{-1} yr^{-1} plots (Figure 4.12; Table 4.4). Thus, bacterial and fungal communities in the mineral horizon are sensitive to extremely low N deposition, while these communities within the organic horizon are sensitive to higher rates of N deposition.

In contrast to bacteria and fungi, the archaeal community structure did not change in response to N deposition. The archaeal community is considered an important player in ammonia-oxidation in soil (Leininger *et al.*, 2006; Nicol & Schleper 2006; Nicol *et al.*, 2008); thus changes in archaeal community structure or abundance after N addition of NH_4NO_3 could be expected. The absence of a response in archaeal community structure could be explained by a low abundance of the ammonia-oxidizing community in the soil studied, which was confirmed by the very low abundance of the *amoA* gene in the soil (functional gene for the ammonia oxidizers) obtained by PCR (see

Chapter 5). Similarly, non-suitable environmental condition could explain the absence of changes, as the archaeal ammonia oxidizers were suggested to be more active than the bacterial ammonia oxidizers in soil with low pH (i.e. 4.5) (Gubry−Rangin *et al.*, 2010). Thus, with the neutral or close to neutrality pH in the soil studied, nitrifying archaea might be out-competed by bacteria. Nemergut *et al.* (2008) found a dramatic decrease in the archaeal community abundance in an Alpine tundra following ten years of N addition for a total load of 115 kg N ha^{-1}. Behind the important differences between alpine and arctic tundra ecosystems, this might indicate that the archaeal community is sensitive to higher N input rates than used in this study, and that repeated (more frequent) acute N deposition could have an effect on the archaeal community.

4.4 Conclusions

The results of this study demonstrate that short-term acute N deposition events significantly affected the structure of the bacterial and fungal communities within the mineral horizon of High Arctic tundra. Moreover, this effect on microbial community structure can occur at low N input rates. Therefore, the microbial communities are influenced by N, but then this effect only lasts a few days, despite an increase in soil N content, indicating that other nutrients or environmental variables are also influencing factors. Overall, despite the initial responses, microbial communities in the longer term show resilience to low levels of N deposition. The absence of changes in the abundance of the bacterial and fungal communities in response to N deposition indicates that the effects on microbial community structure are related to changes in the dominance of different microbial groups rather than a global increase or decrease in abundance. In contrast, archaeal community structure and abundance was insensitive to acute N deposition events. Therefore, the absence of an effect may indicate that the archaeal community is not influenced by N but by others factors such as soil water content, C content, soil pH or temperature (Appendix 4.1).

The rapid response of the bacterial and fungal community structures to acute N deposition, show clearly that microbial communities in High Arctic tundra soil are able to respond quickly, i.e. over few days, to N deposition. Therefore, it may indicate that

microbial community responses to other environmental changes, such as climate warming and increases in precipitation that arctic ecosystems will face, may also occur rapidly. This conclusion is in contradiction to studies showing that microbial responses to global changes may take more than a decade. Moreover, the effects of N deposition on bacterial and fungal communities were found only within the mineral horizon. Thus, studies investigating the responses of microbial communities (i.e. archaea, bacteria and fungi) to global changes in arctic ecosystem should consider several dates of sampling (and early sampling after treatment) as responses of microbial communities are unlikely to be continuous, and within different soil horizons when they are present as the response of microbial communities in different soil horizons is unlikely to be similar.

Acute N deposition events could represent a significant factor influencing the microbial communities in arctic tundra ecosystems, especially if the phenomenon is repeated every year or several times a year in the future. The repeated effect of acute N deposition is unknown, but could lead to stronger changes in microbial community structure and possibly changes in microbial abundance and activity. More investigations are needed to find which bacterial and fungal groups are influenced by N deposition using e.g. using next generation sequencing methods and to repeat the simulation of acute N deposition events to assess its longer term effects. Finally, this study simulated the impact of acute N deposition events over the summer period, however the microbial communities could respond differently just after snowmelt or at different season, especially because acute N deposition can occur at any time during the year.

Chapter 5: Distribution of N-cycling functional genes within High Arctic tundra soil

View of Schetelig mountain (694 m alt.) from Ny-Ålesund the 27th of July 2009.

5.1 Introduction

The microbial N-cycling guild is one of the best described soil communities of biogeochemical cycles. Functional genes encoding for the different enzymatic activities of the N-cycle are used as proxies to enable the investigation of the microbial communities involved in the different N-cycling processes (see Chapter 1). The diazotrophs community is responsible for N-fixation which is catalysed by the nitrogenase enzyme encoded by the *nifH* gene (Zehr & McReynolds, 1989; Zehr *et al.*, 2003). The ammonium formed by N-fixation is oxidised into nitrite then nitrate via nitrification. The first step of nitrification is the oxidation of ammonia into nitrite by bacteria and archaea, which is encoded by *amo* genes (such as *amoA*) in both domains (Rotthauwe *et al.*, 1997; Treusch *et al.*, 2005). The second step of nitrification is the oxidation of nitrite into nitrate which can be investigated via the *nxrA* gene (Poly *et al.*, 2008). Then nitrate is reduced into nitrite, with this reaction catalysed by nitrate reductase proteins encoded by *narG* (Gregory *et al.*, 2000; Philippot *et al.*, 2002) and *napA* (Flanagan *et al.*, 1999) genes. The nitrite formed can be reduced through the different steps of denitrification into dinitrogen (Zumft, 1997; Throbäck *et al.*, 2004). First, nitrite is reduced to nitric oxide by the nitrite reductases encoded by *nirK* and *nirS* genes (Throbäck *et al.*, 2004). Secondly, nitric oxide is reduced to nitrous oxide via nitric oxide respiration encoded by *nor* genes (Braker & Tiedje 2003). Finally, nitrous oxide is reduced to dinitrogen, encoded by the *nosZ* gene (Scala & Kerkhof 1998). Ammonium can also be produced from nitrite via dissimilatory nitrate reduction encoded by the *nrfA* gene (Mohan *et al.*, 2004) and dinitrogen can also be produced by coupling oxidation of ammonium and reduction of nitrite via anaerobic ammonium oxidation (Penton *et al.*, 2006; Francis *et al.*, 2007).

Several previous studies have investigated the different N-functional genes in arctic tundra soil. The *nifH* community structure has been shown to be different with soil depths and between different soil size fractions within a number of arctic tundra soils (Deslippe *et al.*, 2005; Deslippe & Egger 2006; Izquierdo & Nüsslein 2006; Walker *et al.*, 2008). Deslippe *et al.* (2005) showed that the *nifH* community structure changed over the summer season and in response to soil warming (Deslippe *et al.*, 2005). Walker

et al. (2008) also found changes of the *nifH* community structure in response to warming in arctic tundra soils. Bacterial and archaeal *amoA* gene communities have also been investigated in arctic soils including wet sedge meadow (Ma *et al.*, 2007; Siciliano *et al.*, 2009), permafrost (Yergeau *et al.*, 2010), and dwarf shrub tundra (Lamb *et al.*, 2011). Bacterial *amoA* gene abundance was found to be higher in a wet sedge meadow than a raised beach in the High Arctic, and inversely the Crenarchael *amoA* gene was more abundant in raised beach soils (Siciliano *et al.*, 2009).

The different functional genes involved in denitrification have also been investigated in arctic tundra soil, including *niK* and *nirS* genes (Siciliano *et al.*, 2009) and *nosZ* gene (Ma *et al.*, 2008; Walker *et al.*, 2008; Siciliano *et al.*, 2009; Lamb *et al.*, 2011). *nosZ* and *nirK* genes abundances were found to be greater in wet sedge meadow soil than raised beach soils in High Arctic tundra, whilst the *nirS* gene was more abundant within raised beach soils (Ma *et al.*, 2007; Siciliano *et al.*, 2009). Walker *et al.* (2008) showed that *nosZ* community structure was different between High Arctic tundra soils located at the same site but with different plant cover, and that the community structure changed with soil depth and in response to warming, similarly to *nifH* community.

However, only a few studies have investigated the responses of the different N-functional guilds to global changes such as warming or N deposition. The *nifH* gene community structure was shown to be affected by warming in different arctic tundra soils (Deslippe *et al.*, 2005; Walker *et al.*, 2008). Genotype richness of the *nifH* gene was lower in warmed samples but the effect of warming was not consistent across different arctic tundra sites at Alexandra Fjord which differed by their plant cover and soil characteristics (Walker *et al.*, 2008). Similarly, Walker *et al.* (2008) showed also that *nosZ* community structure changed after 13-years of warming in arctic tundra with *nosZ* gene genotype richness tending to be lower in warmed plots. In contrast, Lamb *et al.* (2011) did not find changes in the structure or abundance of bacterial and Crenarchaeal *amoA* and *nosZ* genes after 16 years of warming and fertilisation (rates of 100 and 500 kg ha^{-1} yr^{-1} of NPK fertilizer) in the Canadian arctic. Similarly, Ma *et al.* (2007) found that the ammonia oxidising bacteria community structure were not affected by addition of ammonium sulphate, potassium sulphate or potassium formate.

Overall, the understanding of the impact of environmental changes upon microorganisms involved in N-cycling in arctic tundra soil is limited or clouded by multiple ecosystem specific responses. In the context of climate change and the potential threat that N deposition represents for arctic tundra ecosystem, it is important to know more about the N-cycling guilds and their responses to environmental changes. Thus, the objectives of this study were to investigate soil microbial (i.e. bacteria and archaea) functional guilds involved in N-cycling (e.g. N-fixation, ammonia oxidizing communities): i) between the organic and mineral soil horizons, ii) over time, and iii) in response to simulated episodic nitrogen deposition.

To investigate microbial communities involved in N-cycling, this research studied N-functional genes encoding enzymes that catalyse different steps of the N-cycle. PCR was used to screen for the presence of genes encoding different parts of the N-cycle. The following N-cycling processes were assessed through targeting their associate functional genes by PCR-based methods: N-fixation (*nifH*); nitrification: ammonia oxidizing bacteria and archaea (*amoA*), nitrite oxidation (*nxrA*, *Nitrobacter sp.*); nitrate reduction (*napA*, *narG*); denitrification: nitrite reduction (*nirK*, *nirS*), and reduction of nitrous oxide (*nosZ*). These functional genes were assessed within soil samples taken in 2009 and 2010 from the plot experiment established in 2009, simulating acute N deposition. First, the presence of each gene was investigated by PCR, and when a gene was successfully amplified, a clone library was generated to confirm whether the PCR products corresponded to the gene targeted and to investigate the diversity of the functional gene(s).

5.2 Results

The presence of nine different N-functional genes was investigated, via PCR, within soil samples from the plot experiment sampled in both summer 2009 and 2010. For each gene amplification, several PCR optimisations were assessed, to investigate the use of different primer pairs, different PCR reaction mixtures and PCR cycling conditions. The detection of each N-functional gene by PCR is summarised in Table 5.1.

Table 5.1: Amplification of functional genes from DNA isolated from soil samples from the plot experiment sampled in 2009 and 2010 from the organic and mineral soil horizons. **Red**: no gene amplification; **Orange**: amplification of multiple amplicons of different sizes (bp), with one of the amplicons being similar size to that of the gene of interest; **Green**: amplification of a single amplicon of a similar size to that of the gene of interest. **C**: clone library generated to determine if the sequence amplified was of the target gene of interest.

Functional genes		PCR amplification of target genes			
		Plots 2009		Plots 2010	
Target gene	Primer pair	Organic horizon	Mineral horizon	Organic horizon	Mineral horizon
nifH	nifH3 / nifH4				
nifH	nifH(for A) / nifH(rev)				
amoA bacteria	amoA-1F / amoA-2R				
amoA archaea	amo111F / amo643R				
nxrA	F1norA / R1norA	**C**	**C**	**C**	**C**
Nitrobacter spp. 16S rRNA gene	Nitro-1198F / Nitro-1423R	**C**	**C**		
napA	napAv66 / napAv67				
narG	narG1960F / narG2659R				
nirS	NirS1F / NirS6R				
nirS	nirSHeme832F / nirSHeme1606R				
nirK	nirKCopper583F / nirKCopper909R			**C**	
nosZ	nosZ661b / nosZ1773				

5.2.1 N fixation

The microorganisms involved in N fixation were investigated by targeting the *nifH* gene encoding for the nitrogenase enzyme, which catalyses biological dinitrogen reduction to ammonium. *nifH* genes were not detected from soil samples taken from the plot experiment in 2009 and 2010 within both soil horizons, using either gene primer pairs or using a range of different PCR conditions (Table 5.1; Figure 5.1). Different PCR reaction mixes were used (with or without: Q-solution, BSA; Figure 5.1) and different annealing temperatures were investigated by gradient PCR (data not shown), but *nifH* genes were not amplified.

5.2.2 Nitrification

Bacterial *amoA* genes were amplified by PCR from soil samples from the plot experiment taken in both 2009 and 2010. Single length PCR products were obtained of a similar size (i.e. 491 bp) to that expected for bacterial *amoA* genes when BSA were used in the PCR solution mix with Qiagen *Taq* polymerase at an annealing temperature of 60 ºC (Table 5.1; Figure 5.2). However, the intensity of the PCR products amplified from soil DNA was extremely low, despite the use of 50 cycles for the PCR (Figure 5.2). Temperature gradient PCR was used to identify the optimal annealing temperature (i.e. 58 ºC; Figure 5.2 and 5.4), to increase detection of bacterial *amoA* gene PCR products (Figure 5.3). Subsequently, PCR products were obtained from several samples at Day-6 from the control plots (soil samples taken outside the plots and used as "pristine" controls) but no PCR products were obtained from the control + water and 12 kg N ha^{-1} yr^{-1} plots at Day-6 (data not shown) and only one *amoA* gene PCR product was amplified from a plot sampled at Day+1 (Figure 5.3). Despite the improvement in PCR detection of *amoA* genes, the PCR product intensity remained low. *amoA* genes were mainly amplified from the mineral horizons.

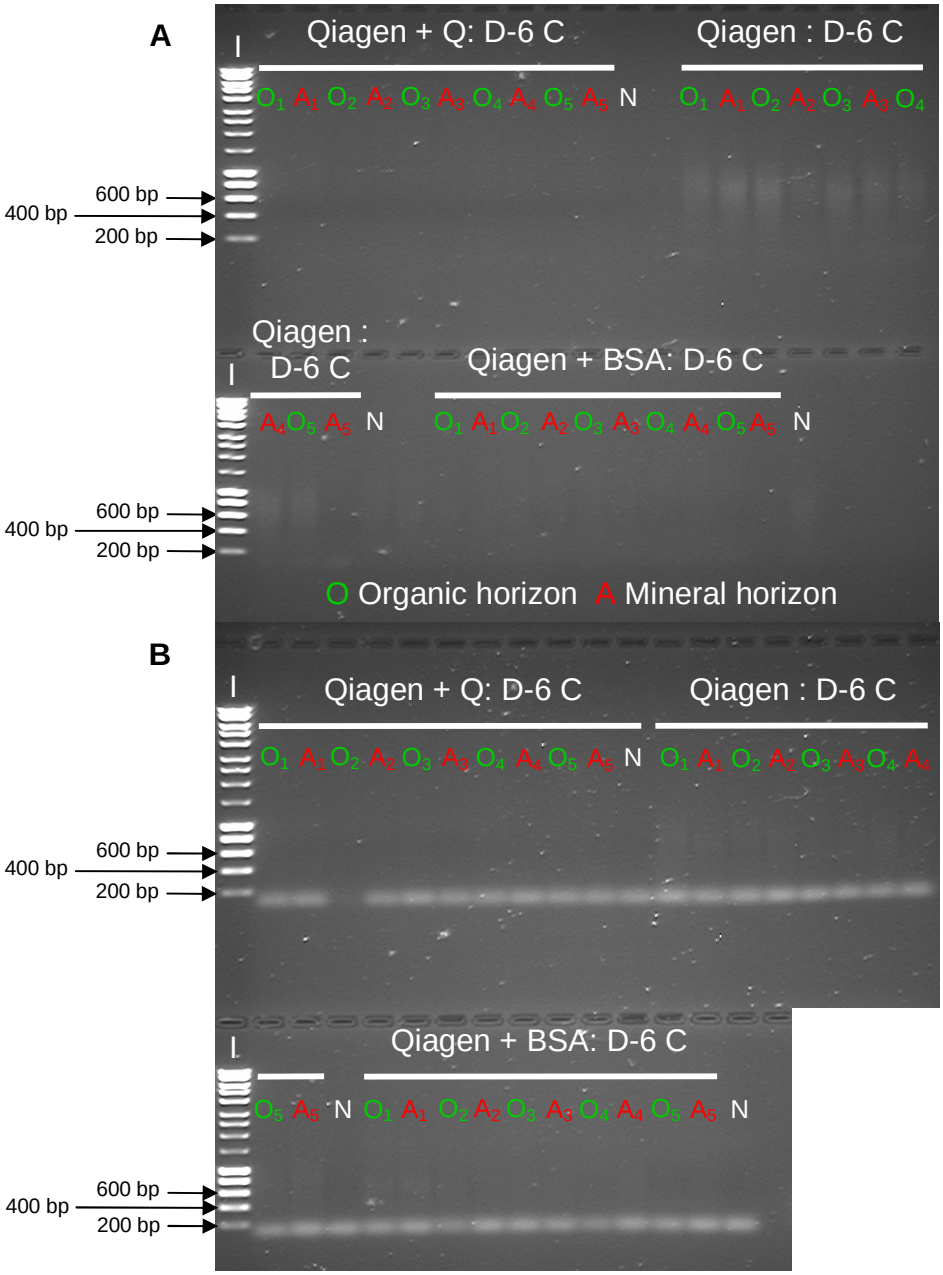

Figure 5.1: Agarose gel electrophoresis (1% agarose) of representative PCR amplifications targeting the *nifH* gene **A)** using primer pair nifH3 / nifH4 and **B)** using primer pair nifH(for A) / nifH(rev). Soil samples used were from the organic and mineral horizons taken in summer 2010 from the plot experiment. **Qiagen**: indicates the use of Qiagen *Taq* polymerase; **+Q**: indicates the use of Q-solution in the PCR solution mix; **+BSA**: indicates the use of BSA in the PCR solution mix. **D-6**: two days before N application; **C**: Control plots. **N**: PCR negative control. The numbers beside O and A indicate the soil replicate number (see section 2.2.2). The Hyperladder™ I (Bioline, London, UK; **l**) was used as a size standard.

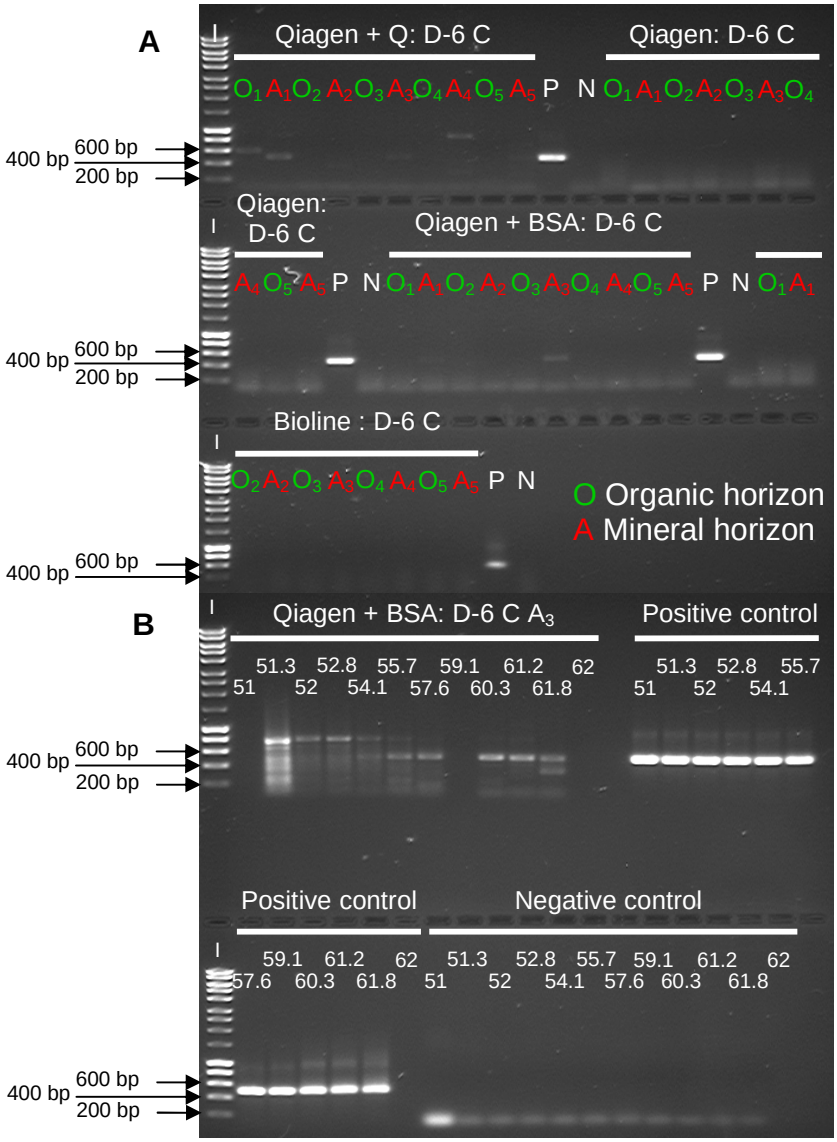

Figure 5.2: Agarose gel electrophoresis (1% agarose) of representative PCR amplifications targeting bacterial *amoA* genes **A)** using different PCR mixtures, and **B)** a temperature gradient PCR varying annealing temperature from 51 – 62 ºC. Soil samples used were from the organic and mineral horizons taken in summer 2010 from the plot experiment. **Qiagen**: indicates the use of Qiagen *Taq* polymerase; **Bioline**: indicates the use of Bioline *Taq* polymerase, **+Q**: indicates the use of Q-solution in the PCR mixture; **+BSA**: indicates the use of BSA in the PCR mixture. **D-6**: two days before N application; **C**: Control plots. **N**: PCR negative control. **P**: PCR positive control was obtained from DNA sequences of bacterial *amoA* gene from cryoconite hole particles taken in Antarctica (provided by K Cameron). The numbers beside O and A indicate the soil replicate number (see section 2.2.2). The Hyperladder™ I (Bioline, London, UK; **l**) was used as a size standard. Bacterial *amoA* gene PCRs (A and B) were performed with 50 cycles: 7 cycles of touch down (61 to 58 ºC) then 43 cycles at a constant annealing temperature (58 ºC). The PCR with different reactions mixtures were performed at an annealing temperature of 60 ºC.

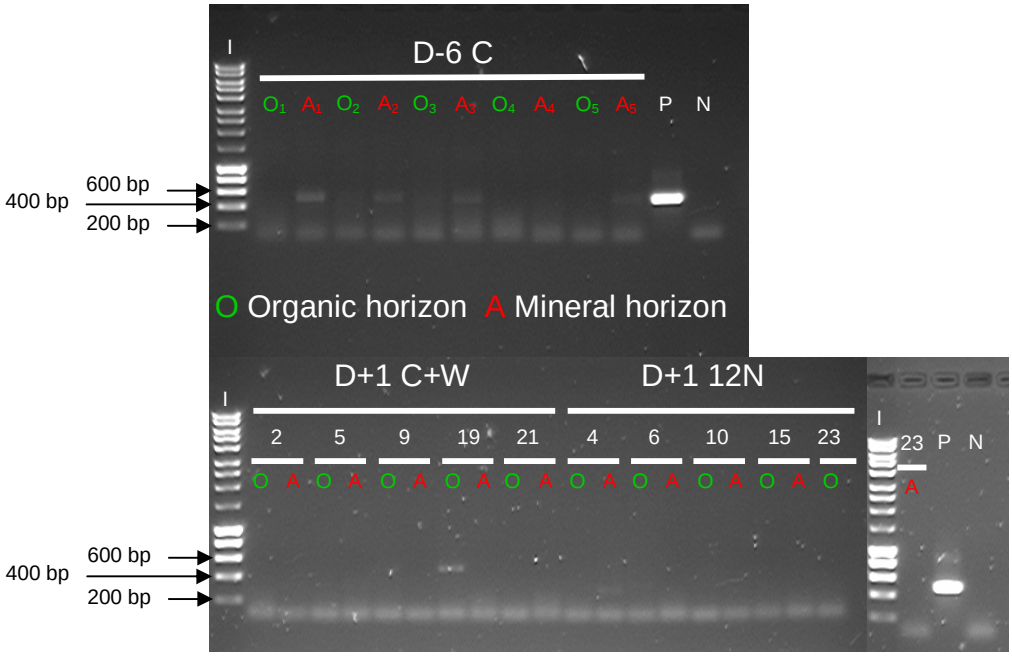

Figure 5.3: Agarose gel electrophoresis (1% agarose) of representative PCR amplifications targeting bacterial *amoA* genes from soil samples of the organic and mineral horizons taken in summer 2010 from the plot experiment. **D-6**: two days before N application; **D+1**: one day after N application; **C**: Control plots; **C+W**: control + water plots; **12N**: 12 kg N ha^{-1} yr^{-1} ~pH 4 plots. **N**: PCR negative control. **P**: PCR positive control was obtained from DNA sequenced of bacterial *amoA* gene from cryoconite holes particles taken in Antarctica (provided by K Cameron). The numbers beside O and A indicate the soil replicate number (see section 2.2.2) and the numbers above O and A indicate the plot number. The Hyperladder™ I (Bioline, London, UK; **I**) was used as a size standard. Bacterial *amoA* gene PCRs were performed with 50 cycles: 7 cycles of touch down (61 to 58 ºC) followed by 43 cycles at a constant annealing temperature (58 ºC).

PCR products of archaeal *amoA* genes were amplified more readily from multiple plots using a PCR mixture containing BSA and Qiagen *Taq* polymerase (Figure 5.4). Temperature gradient PCR did not enable improved detection specificity and intensity of PCR products (Figure 5.4). Therefore, archaeal *amoA* gene amplification generated products of multiple lengths and PCR products were only amplified from a few samples at Day-6 (Figure 5.5). The size of the different amplicons amplified was either slightly larger than or smaller than that of the positive control. PCR product intensity was generally weak despite the multiple attempts to improve the PCR, and archaeal *amoA* gene PCR products were mainly obtained from the mineral horizon, while the organic horizon did not yield single amplicons of the expected size (Figure 5.5).

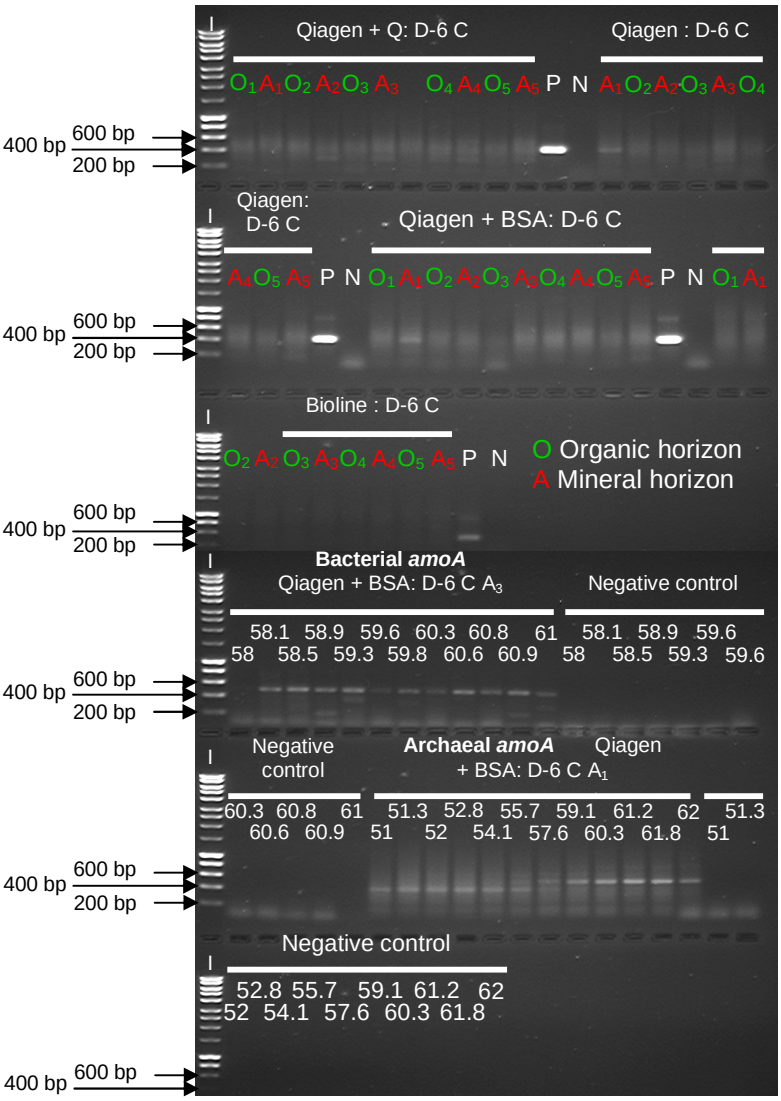

Figure 5.4: Agarose gel electrophoresis (1% agarose) of representative PCR amplifications targeting archaeal *amoA* genes **A)** using different PCR mixtures, and **B)** temperature gradient PCR of bacterial and archaeal *amoA* genes annealing temperature varying from 58-61 ºC and 51-62 ºC, respectively. Soil samples used were from the organic and mineral horizons taken in summer 2010 from the plot experiment. **Qiagen**: indicates the use of Qiagen *Taq* polymerase; **Bioline**: indicates the use of Bioline *Taq* polymerase, **+Q**: indicates the use of Q-solution in the PCR solution mix; **+BSA**: indicates the use of BSA in the PCR solution mix. **D-6**: two days before N application; **C**: Control plots. **N**: PCR negative control. **P**: PCR positive control was obtained from DNA sequences of bacterial and archaeal *amoA* gene from cryoconite hole particles taken in Antarctica (provided by K Cameron). The numbers beside O and A indicate the soil replicate number (see section 2.2.2). The Hyperladder™ I (Bioline, London, UK; **l**) was used as a size standard. Bacterial *amoA* gene PCR was conducted for 50 cycles: 7 cycles of touch down (61 to 58 ºC) then 43 cycles at a constant annealing temperature (58 ºC).

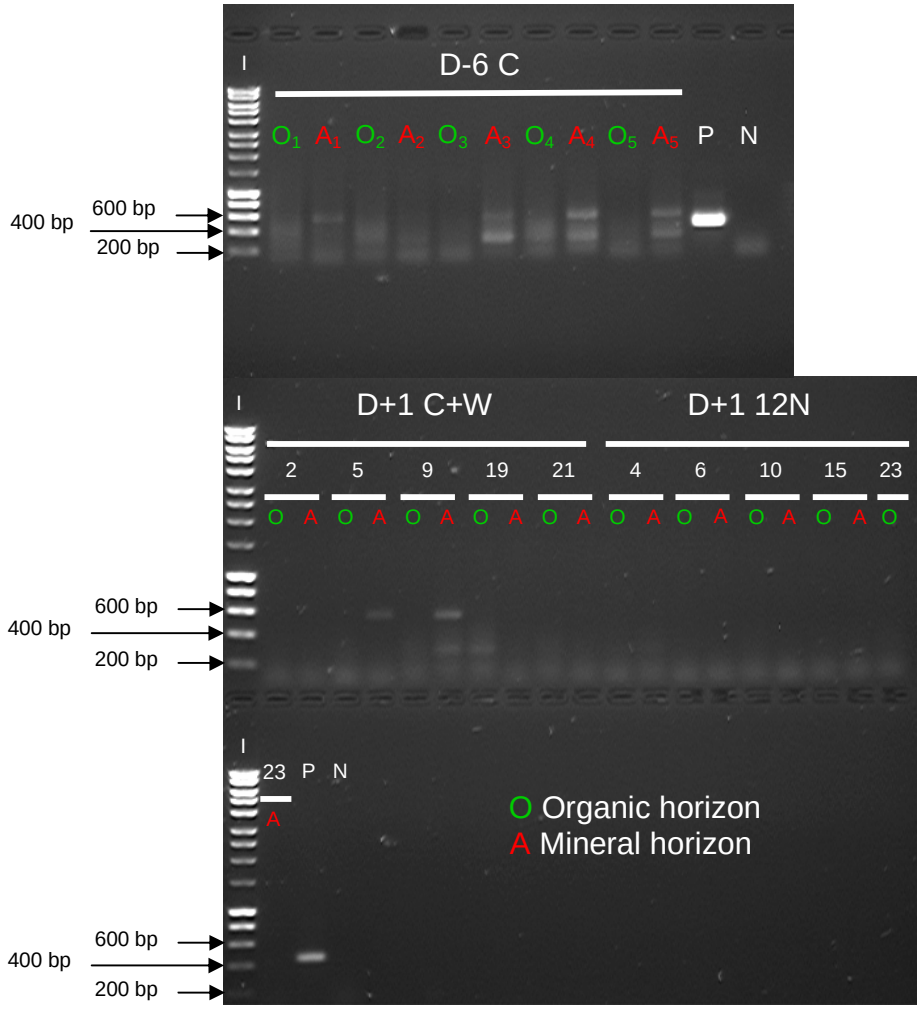

Figure 5.5: Agarose gel electrophoresis (1% agarose) of representative PCR amplifications targeting archaeal *amoA* gene from soil samples of the organic and mineral horizons taken in summer 2010 from the plot experiment. **D-6**: two days before N application; **D+1**: one day after N application; **C**: Control plots; **C+W**: control + water plots; **12N**: 12 kg N ha^{-1} yr^{-1} ~pH 4 plots. **N**: PCR negative control. **P**: PCR positive control was obtained from DNA sequences of bacterial and archaeal *amoA* gene from cryoconite hole particles taken in Antarctica (provided by K Cameron). The numbers beside O and A the soil replicate number (see section 2.2.2) and the numbers above O and A indicate the plot number. The Hyperladder™ I (Bioline, London, UK; **I**) was used as a size standard.

The oxidation of nitrite into nitrate was investigated via PCR assays targeting either *nxrA* genes or *Nitrobacter spp.* 16S rRNA genes. PCR of *nxrA* gene yielded either single or multiple PCR products (Table 5.1; Figure 5.6), which always included one amplicon of a similar size to that of the target gene of interest (i.e. 322 bp). *nxrA* genes

were amplified more often from the mineral than the organic soil horizon, as had similarly been observed for both bacterial and archaeal *amoA* genes. A small clone library was generated from *nxrA* PCR products from both soil horizons from the 12 kg N ha^{-1} yr^{-1} plots sampled at Day+1 (Figure 5.6), but the sequences subsequently generated were not related to the bacterial domain, and instead the closest related sequences were plants. Further attempts to generate clone libraries from *nxrA* gene products were not successful. PCR products of *Nitrobacter spp.* 16S rRNA genes were amplified from all of the soil samples investigated from the plot experiment in both 2009 and 2010 (Table 5.1; Figure 5.6). PCR products were of a similar size to that of the gene of interest (i.e. 225 bp). In contrast to the other genes targeting nitrification, the intensity of PCR products of *Nitrobacter spp.* 16S rRNA genes were strong and had similar intensities between the organic and mineral horizons. Several attempts to generate a clone library for *Nitrobacter spp.* 16S rRNA genes were made, but failed to produce any clones containing the gene of interest.

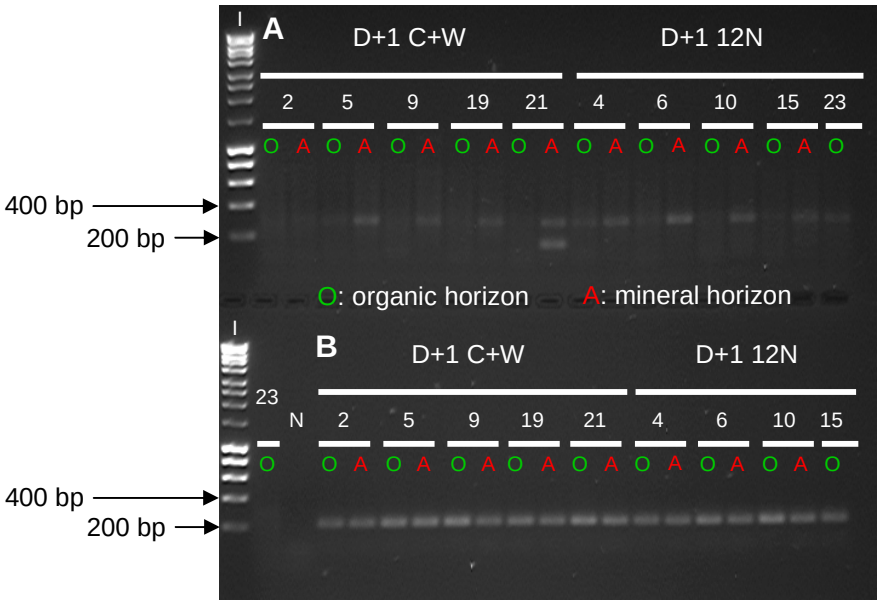

Figure 5.6: Agarose gel electrophoresis (1.5% agarose) of representative PCR amplifications targeting *nxrA* genes, **A**) and *Nitrobacter spp.* 16S rRNA genes, **B**) from soil samples of the organic and mineral horizons taken in summer 2010 from the plot experiment. **C+W**: control + water plots; **12N**: 12 kg N ha^{-1} yr^{-1} ~pH 4 plots; **D+1**: 1 day after N application; **N**: PCR negative control. The numbers above the lanes, indicate the plot number (see section 2.2.2). The Hyperladder™ I (Bioline, London, UK; **I**) was used as a size standard.

5.2.3 Denitrification

The bacterial guilds involved in the reduction of nitrate into nitrite were investigated via the amplification of *narG* and *napA* genes encoding nitrate reductase proteins. PCR products were not obtained from soil samples from the plot experiment taken either in 2009 or 2010 (data not shown)

The reduction of nitrite into nitric oxide during denitrification, was investigated via targeting of *nirS* and *nirK* genes. Amplification of *nirS* genes was performed using two different primer pairs (Table 5.1). The use of the primer pair NirS1F / NirS6R did not generate PCR products (Figure 5.7 A) from soil samples taken in 2010 from the plot experiment, despite the use of different PCR solution mixtures with or without Q-solution or BSA (data not shown). The second primer pair (nirSHeme832F / nirSHeme1606R), yielded one PCR product from one sample (Figure 5.7 B) from the mineral horizon of a similar size to that expected (i.e. 774 bp). However, no further investigation using the primer pair nirSHeme832F / nirSHeme1606R was done from soil samples of the plot experiment. PCR of the *nirK* gene yielded single size PCR products of a similar size to that expected (i.e. 326 bp), from soil samples taken in 2010 within the control plots at Day-6 (Figure 5.7 C) and also from the control + water and 12 kg N ha^{-1} yr^{-1} plots at Day-6 (data not shown). *nirK* PCR products from soil samples from both soil horizons were of a similar intensity (Figure 5.7 C). A clone library was generated from PCR products from the control plot soil samples, but despite obtaining colonies potentially containing the insert (i.e. white colonies) the amplification of the insert by PCR using the T7 and T3 primer did not yield products. No further attempts to obtain a clone library were made.

Finally, the last step of denitrification (i.e. reduction of nitrous oxide into dinitrogen) was investigated by targeting the *nosZ* gene. However, *nosZ* gene PCR products were not amplified from any of the soil samples from the plot experiment taken in 2010 (data not shown).

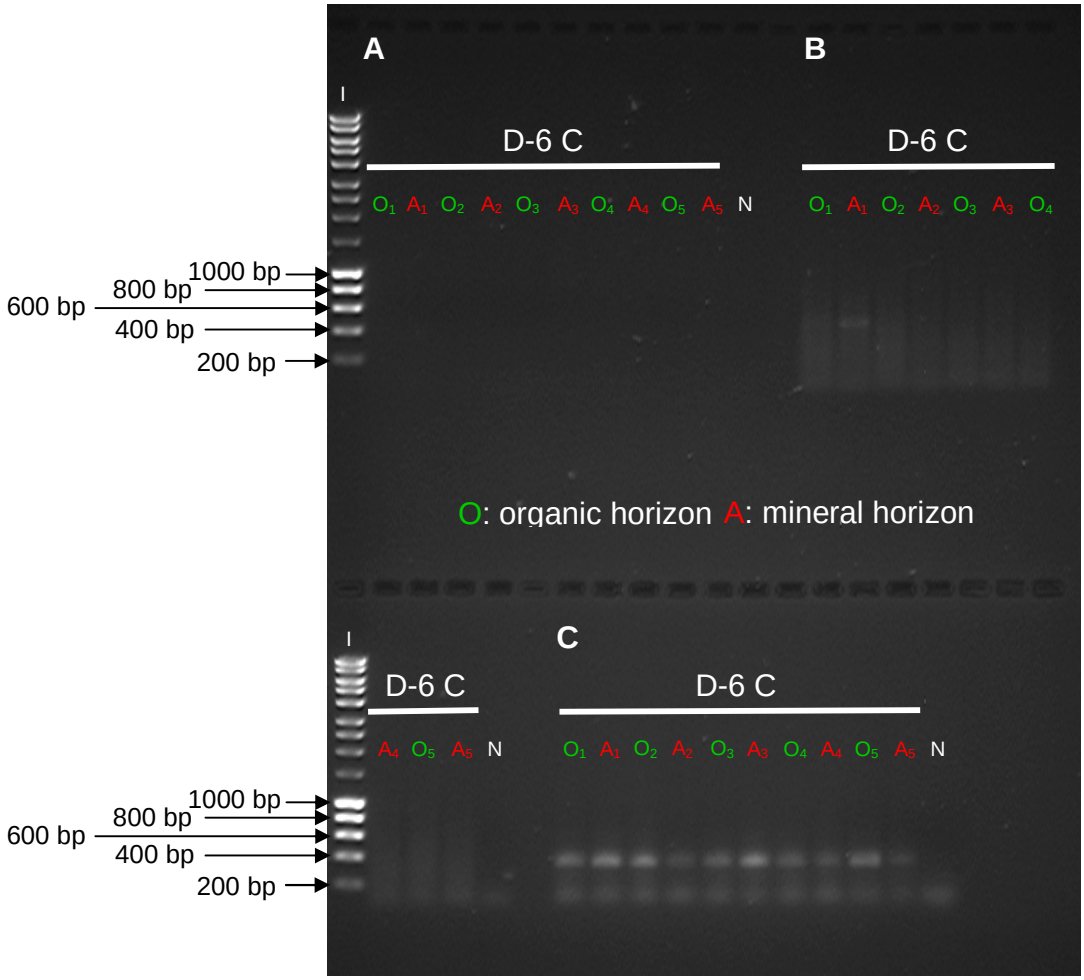

Figure 5.7: Agarose gel electrophoresis (1% agarose) of representative PCR amplifications targeting **A**) *nirS* genes amplified with primer pair NirsS1F / NirS6R, **B**) *nirS* genes amplified with primer pair nirSHeme823F / nirSHeme1606R, and **C**) *nirK* genes, from soil samples of the organic and mineral soil horizons taken in summer 2010 within pristine control (**C**) of the plot experiment. **D-6**: two days before N application. **N**: PCR negative control. The numbers beside O and A indicate the soil replicate number (see section 2.2.2). The Hyperladder™ I (Bioline, London, UK; **l**) was used as a size standard.

5.3 Discussion

Generally, most of the N-cycling functional genes were not amplified by PCR from DNA from the soil samples. Where PCR products were generated, optimisation of the PCR was required to obtain and improve PCR. Twelve different primer pairs were

used to investigate nine different N-cycling functional genes. 25% of the primer pairs used yielded a specific amplification product for the gene of interest, while a further 25% showed variables result yielding either non-specific PCR products or products of the expected size but with extremely low product intensity. 50% of the primer pairs used did not produce any amplicons despite multiple attempts at optimisation. Several factors might explain the difficulties in amplifying the different genes, including i) the primer pairs used, ii) the PCR conditions (i.e. PCR solution mixtures and PCR cycling conditions), and iii) the low abundance and the targeted genes within the soil samples investigated.

The use of different primer pairs might have enabled the amplification of the genes of interest. Deslippe *et al.* (2005; 2006) and Walker *et al.* (2008) used different primer pairs to those used in this study to investigate the *nifH* community via a half-nested PCR using Nh21F / WidNhR (Widmer *et al.*, 1999) for the primary reaction and Nh428R for the second reaction (Widmer *et al.*, 1999; Deslippe *et al.*, 2005). That assay was able to detect *nifH* genes in two studies at the same study area at Alexandra Fjord located on the northern side of Johan Peninsula on the East coast of Ellesmere Island, Nunavut, Canada (Deslippe *et al.*, 2005; Walker *et al.*, 2008). Hence the use of different primer pairs may enable the amplification of the *nifH* guild in the Leirhaugen plots of this thesis. However, Izquierdo & Nüsslein (2006) successfully amplified *nifH* genes from arctic tundra near Cambridge Bay (Canada) using the primer pair nifH3 / nifH4 (followed by a second PCR with the primer pair: nifH1 / nifH2) which was also used in this thesis's study. Despite the use of the same primer pair and PCR cycling conditions as used by Izquierdo & Nüsslein (2006), *nifH* genes could not be amplified from the Leirhaugen plots. Bacterial *amoA* genes were amplified using the same primer pair (i.e. amoA-1F / amoA-2R) as used in this study in different arctic tundra soils, showing that this primer pair is able to amplify bacterial *amo*A gene in arctic tundra soils (Siciliano *et al.*, 2009; Yergeau *et al.*, 2010; Lamb *et al.*, 2011). Only Ma *et al.* (2007) used a different primer pair to specifically target ammonia oxidizers of the *β Proteobacteria* (Kowalchuk *et al.*, 1997). In contrast, none of the more recent studies investigating the archaeal ammonia oxidizing guilds used the same primer pair as used in this study. Siciliano *et al.* (2009) used the primer pair Arch-amoAF / Arch-amoAR (Francis *et al.*,

2005) to target the archaeal *amoA* gene in arctic soil at Truelove Lowland study site on Devon Island, Nunavut, Canada. Yergeau *et al.* (2010) used the primer pair amoA19F / CrenamoA616r48x (Leininger *et al.*, 2006; Le Roux *et al.*, 2008) to investigate archaeal *amoA* genes within Canadian High Arctic permafrost soils, whilst Lamb *et al.* (2011) specifically targeted Crenarchaeal *amoA* genes using the primer pair CrenamoA23f / CrenamoA616r (Tourna *et al.*, 2008). Archaeal (and bacterial) *amoA* gene have also been amplified near Ny-Ålesund within fen peatland soils (at Solvatnet and Knudsenheia site) using newly designed primers (personal communication R. Alves). The low bacterial *amoA* genes PCR product numbers obtained is unlikely to be explained by the use of the primer pair used in this study as this primer pair has been successfully used in other studies in the Arctic. However, archaeal *amoA* genes have been amplified using a variety of primer pairs in arctic tundra soil, which might enable the amplification of *amoA* genes in the Leirhaugen plots. Similarly, the presence of *nosZ* genes have been investigated in arctic tundra soils using different primers to those used in this study such as: nosZ-F / nosZ-R (Rich *et al.*, 2003) in Nunavut, Canada (Siciliano *et al.*, 2009; Lamb *et al.*, 2011), and nosZ-F / nosZ1622R and Nos1773R (Throbäck *et al.*, 2004) in a half-nested PCR (Walker *et al.*, 2008). However, only a few studies have investigated the presence of *nirS* and *nirK* genes (Yergeau *et al.*, 2009; Siciliano *et al.*, 2009; Palmer *et al.*, 2011), and *narG* genes in arctic soil (Palmer *et al.*, 2011) and to the best of our knowledge, no studies have investigated the presence of *nxrA* genes and *Nitrobacter spp.* 16S rRNA genes in arctic soil. Thus, it is difficult to assess the ability of primer pairs to amplify these N-functional genes in arctic tundra soil.

Different PCR solution mixes and different PCR cycling conditions play a critical role in the success of any PCR amplification. Two different *Taq* polymerases were used in PCR amplifications for most of the functional genes targeted. Qiagen *Taq* more frequently enabled amplification of the different N-functional genes than Bioline *Taq* which did not amplify any of the target genes (Figure 5.2; 5.4). However, Qiagen *Taq* polymerase was not always the best *Taq* polymerase for PCR amplification, as Bioline *Taq* yielded the strongest PCR product intensity when targeting the fungal community (data not shown). Different solutions were used in the PCR mix such as Q-solution which can improve the amplification of GC-rich templates (Ralser *et al.*, 2006),

and BSA which can improve amplification of functional genes by reducing the effects of the inhibitory compounds on the PCR (Kreader, 1996). The use of Q-solution lead to the amplification of non-specific PCR products for the bacterial *amoA* gene (Figure 5.2), or inhibited the amplification of archaeal *amoA* genes (Figure 5.4) but was also able to improve PCR detection of *nirK* genes (data not shown). Similarly, BSA enabled the amplification of specific PCR products for bacterial *amoA* genes (Figure 5.2), but did not improve the amplification for some other genes including archaeal *amoA* genes (Figure 5.4), *nifH* genes (Figure 5.1) or *nirK* genes. Thus, the use of different *Taq* polymerases, Q-solution and BSA may improve the amplification of genes and it is necessary to empirically test multiple reactions contents in order to obtain and improve PCR product detection.

However in this study, the use of different PCR solutions mixes did not improve PCR product detection or improve amplification products yields for most of the genes investigated, indicating that other factors potentially influenced the efficiency of amplification. Indeed, different buffer solutions (e.g. with higher $MgCl_2$ content) or different concentrations of *Taq* polymerase and primers might potentially improve the PCR amplification. However, these different optimisations were not investigated in this study. DNA template concentration and purity are also likely to affect the PCR amplification. Thus, Ma *et al.* (2007) and Siciliano *et al.* (2009) purified DNA extracts using polyvinylpolypyrrolidone columns (Berthelet *et al.*, 1996) prior to PCR amplification of *amoA*, *nirS*, *nirK* and *nosZ* genes in arctic soils. However, DNA purification could significantly reduce the amount of DNA, which would be particularly unwanted for the DNA from a low-abundance community, (such as N-functional genes) and may lead to an underestimation of gene abundance when investigated by Q-PCR.

DNA extraction is also a key step prior to PCR which will determine DNA concentration and purity. Most of the studies investigating N-functional genes in arctic soil used UltraClean™ Soil DNA Isolation kits (Mo-Bio laboratories, Carlsbad, CA, USA) to extract DNA from soil (Deslippe *et al.*, 2005; Deslippe & Egger, 2006; Ma *et al.*, 2007; Walker *et al.*, 2008; Siciliano *et al.*, 2009). Thus, the UltraClean® Soil DNA Isolation kit could be better for the subsequent amplification of N-functional genes. However, different DNA kits/protocols were investigated prior to this study on soil

samples from subarctic shrub tundra taken in 2008 in Abisko (Sweden). PowerSoil® and UltraClean® DNA isolation kit were both tested in addition to DNA extraction using the protocol described by Griffiths *et al.* (2000). Two different protocols were investigated for the UltraClean® DNA isolation kit, following the manufacturer's instruction, which are supposed to generate different DNA extraction yields, and two protocols using different sizes of beads (i.e. first: 0.1 mm, and second: 1.4 mm, 0.1 mm and 1 bead of 4 mm) for the protocol described by Griffiths *et al.* (2000). The PowerSoil® DNA isolation kit subsequently used for field plot samples produced higher DNA extraction yields than the other kit/protocols (data not shown), which determined the choice of this DNA extraction kit in this study.

Beside the PCR mixture, the PCR cycling conditions are also important, especially the annealing temperature which determines the binding efficiency of the primers to the targeted sequence and subsequent DNA synthesis. The bacterial *amoA* gene clearly showed more samples being amplified using an annealing temperature of 58 ºC rather than 60 ºC (Figure 5.2; 5.3). However, variability between soil samples was also found with samples which were amplified better at a high temperature whilst others were amplified at a lower temperature. The studies which investigated bacterial *amoA* genes in arctic soils using the same primer pair as used in this study used different annealing temperature such as 52 ºC (Yergeau *et al.*, 2010), 54 ºC (Siciliano *et al.*, 2009) or 58 ºC (Lamb *et al.*, 2011) for Q-PCR analysis, and 55 ºC for DGGE analysis (Lamb *et al.*, 2011). Thus, it is important to empirically investigate the annealing temperature by temperature gradient PCR to choose the temperature that is specific to the gene targeted within a specific environment. However, despite the use of the same PCR cycling conditions (and trying different PCR solutions mixtures) to those used by Izquierdo & Nüsslein (2006) to investigate *nifH* genes, using the same primer pair (i.e. nifH3 / nifH4), *nifH* genes could not be amplified. Thus, the use of different PCR solution mixtures and/or PCR cycling conditions did not enable amplification of PCR products for most of the N-functional genes targeted in this study, suggesting that maybe non-methodological related issues may explain the low yields of amplification.

Such absence of amplification for several N-functional genes could be explained by the variability of abundance of these different communities over the summer. Indeed,

archaeal 16S rRNA genes could not be amplified with the primer pair FAM-Arch109F / Arch958R within soil samples of the plot experiment taken in both 2009 at Day+1 and Day+7 (see Chapter 3). However, the N-functional genes were investigated in 2009 and 2010, at different dates of sampling for each year and within both soil horizons. Thus, the fluctuation of detection of genes during the sampling period is unlikely to explain the frequent failure to detect functional genes. The absence of amplification for some functional genes is likely to be due to the low abundance of some or many of the genes within the soil. For example, the bacterial (and archaeal) ammonia oxidising community might be out-competed by plants roots for NH_4^+ leading to low growth of this community. Siciliano *et al.* (2009) showed that fungi can out-compete denitrifiers for NO_3^- in arctic soil, which may explain the weak amplification of genes involved in denitrification. Finally, amplification of N-functional genes did not increase within either soil horizons in the plots following addition of N. Thus, N addition did not seem to affect the presence and/or abundance of N-cycling functional genes.

It is interesting to note that bacterial and archaeal *amoA* genes, and *nxrA* genes yielded PCR products with a higher intensity from the mineral than the organic horizon (Figure 5.3; 5.5), while *Nitrobacter spp.* 16S rRNA genes and *nirK* genes did not show any difference in PCR product intensity between soil horizons (Figure 5.6). Walker *et al.* (2008) showed that *nifH* and *nosZ* community structures in arctic soil varied with soil depths, especially when organic and mineral horizons were clearly visible within the soil. Similarly to the bacterial, archaeal and fungal community structures and abundances (see Chapter 3 and 4), the presence and abundance of N-cycling functional genes might be strongly influenced by soil horizons in arctic tundra. However, at least the abundance of some N-cycling functional guilds (such as *nirK)* may not be influenced by the different environmental variables characterizing each soil horizon. Investigating N-functional genes within different soil horizons is important to understand the distribution within the soil of these functional guilds, and the environmental variables which drive these guilds, and subsequently to determine the responses of these communities to environmental change and consequences for N cycling.

5.4 Conclusions

Generally, most of the N-cycling functional genes were weakly amplified by PCR and required several steps of optimisations such as PCR with different primer pairs for each gene, use of different PCR mixtures (e.g. *Taq* polymerase, BSA, Q-solution) and different PCR cycling conditions. Only a few genes (i.e. bacterial *amoA*, *nxrA* genes and *Nitrobacter spp.* 16S rRNA gene, *nirK* gene) were successfully amplified but could not be sequenced to confirm the specific amplification of the gene of interest. It should be stressed that the absence of amplification did not confirm the absence or low abundance of the gene of interest within the soil. It is likely that other genes which were not amplified were present in extremely low abundance in the soil indicating that these communities are perhaps not key players within the wider microbial community and the N-cycle. Therefore, microbial communities involved in the different steps of N-cycling remain uncharacterised within these arctic tundra soils. This remains a concern, especially given the global change threats that arctic ecosystems face (e.g. warming, N deposition) which are likely to lead to changes in biogeochemical cycles. Further studies are needed to identify the N-cycling community that are present and active within these arctic tundra soil, and to identify the different microbial taxa involved in these processes.

Chapter 6: A microcosm experiment to evaluate the impact of precipitation and nitrogen deposition on the structure and abundance of microbial communities in different soil horizons of High Arctic tundra

Unidentified organism at Stuphallet the 8th of August 2010.

6.1 Introduction

Recent studies show that the structure and abundance of bacterial and archaeal communities differ between organic and mineral horizons within subarctic (Rinnan *et al.*, 2007) and High Arctic tundra soils (Wallenstein *et al.*, 2007; Chapter 3 and 4). In this thesis, archaea have been found to be 3 to 4.5 times more abundant in the mineral than in organic horizons, while bacterial abundance was also higher in the mineral than in organic horizon or equal between soil horizons (Chapter 3, 4) in High Arctic tundra soil. Wallenstein *et al.* (2007) found that the relative abundance of bacterial taxonomic groups such as Acidobacteria, Deltaproteobacteria and Firmicutes were higher in the mineral horizon, while Alphaproteobacteria and Bacteroidetes were more abundant in the organic than in mineral horizons. The presence of bacteria involved in N fixation (via the *nifH* gene) and the reduction of nitrous oxide into dinitrogen (via the *nosZ* gene) were also found to differ between organic and mineral horizons in High Arctic tundra soils, with fewer *nifH* and *nosZ* genotypes within deeper horizons (Walker *et al.*, 2008).

Change in the structure of bacterial and archaeal communities within different soil horizons were shown to vary differently over time in High Arctic tundra soils (Wallenstein *et al.*, 2007; Chapter 3 and 4). For example, the relative abundance of bacterial phyla such as Bacteriodetes increased over time in the organic horizon, while their abundance decreased within the mineral horizon, and conversely, Verrucomicrobial abundance increased in the mineral horizon and decreased in the organic horizon over time (Wallenstein *et al.*, 2007). In this current study the structure of archaeal communities showed strong changes over time only within the mineral horizon, and similarly bacterial and archaeal abundance showed variation over time only within the mineral horizon (Chapter 3 and 4). Hence, the bacterial and archaeal communities inhabiting different soil horizons seems to respond differently to environmental changes, and could potentially respond differently to global changes such as warming, N deposition or changes in precipitation that arctic ecosystems are facing.

Previously, only a few studies have investigated the response of microbial communities to warming, shading or fertilisation within different soil horizons in the subarctic (Rinnan *et al.*, 2007) and High Arctic tundra soils (Walker *et al.*, 2008).

Rinnan *et al.* (2007) found significant effect of fertilisation, shading and warming on the bacterial community structure obtained by PLFA analysis within the organic horizon, while only fertilisation significantly affected the bacterial community structure within the mineral horizon. In contrast, they found that fertilisation did not significantly affect total bacterial PLFA content within the organic horizon but that fertilisation significantly increased total bacterial PLFA content by 22% within the mineral horizon. However, the Gram-positive / Gram-negative ratio significantly increased with fertilisation only within the organic horizon. Walker *et al.* (2008) investigated the response of N-functional genes involved in N fixation (i.e. *nifH* gene) and the reduction of nitrous oxide into dinitrogen (i.e. *nosZ* gene) to warming, and found that the structure of *nifH* and *nosZ* functional guilds significantly changed following warming within upper and lower soil layers. This current study found that bacterial community structure was significantly affected by N deposition only within the mineral horizon (Chapter 4). Therefore, bacterial communities exhibit different responses to global changes within different soil horizons. Therefore, investigations of the response of microbial communities to global changes within only a single soil horizon (e.g. Deslippe *et al.*, 2005; Lamb *et al.*, 2011) may underestimate the impact of global changes upon microbial communities.

Recent studies showed that acute N deposition events, during which a high percentage of annual N deposition is deposited in few days, occur in the High Arctic and may represent a threat to arctic ecosystems (Hodson *et al.*, 2005; 2010; Kühnel *et al.*, 2011) (see section 1.2.2). Increases in annual precipitation are predicted to occur at the poles, but the effect of a potential increase in soil water content remains unclear, but may occur via melting of permafrost and early snowmelt (ACIA, 2005; see section 1.1.4). However, little is known about the effects of atmospheric N deposition and changes in precipitation regimes on High Arctic tundra ecosystem. Moreover, the different microbial communities inhabiting different soil horizons were found to be differently affected by N deposition (Chapter 4). However, it remains unknown if these different microbial communities show the same sensitivity to similar N input. Similarly, microbial communities inhabiting different soil horizons may also respond differently to increase in soil water content, and their sensitivity to similar water input might be different. Thus, the objectives of this study were to investigate the responses of the

different microbial communities (i.e. bacterial, and archaeal community and of N-cycling functional guilds) inhabiting different soil horizons (i.e. organic *vs.* mineral), to water and N addition over time.

Thus, a microcosm experiment was performed to address these objectives, enabling to use higher rate of water addition that the one used for the plot experiment and add the same amount of N within both soil horizons. Soil samples were taken in summer 2010, close to the plot experiment established in 2009 at Leirhaugen (soil was not taken from within the plots), Ny-Ålesund in the High Arctic (Svalbard). The organic and mineral horizons were separated, and sieved to remove plants roots, reducing the competition for N uptake between plant and microbial communities. The organic and mineral horizons were separately incubated within microcosms at constant temperature (7 ºC) for 14 days, after addition of either water (control + water) or NH_4NO_3 solution combined with low ~pH 4 at different nitrogen application rates: 0.4 kg N ha^{-1} yr^{-1} and 12 kg N ha^{-1} yr^{-1} (see section 2.2.3). Organic and mineral soil horizons samples were also incubated without water or N addition and used as control microcosms (Control). Microcosms were destructively sampled after 1, 7 and 14 days post treatment, and different environmental variables were measured (i.e. total C, total N, ^{15}N, NO_3^-, NH_4^+ and soil water content and soil pH). Changes in bacterial and archaeal community structure were investigated by T-RFLP analysis and in the abundance of these communities by Q-PCR. The presence, diversity and abundance of different N-functional genes involved in N fixation, nitrification and denitrification were investigated by PCR, clone library construction and Q-PCR.

6.2 Results

6.2.1 Soil characteristics

6.2.1.1 Soil water content and soil pH

The soil water content during the microcosm experiment was always significantly ($F = 1290$, $df = 1$, $P < 2.2x10^{-16}$) higher (~1.5 times higher) in the organic

than in the mineral horizon for all treatments over time (Figure 6.1 A). The control microcosms, which did not receive any water, had a soil water contents over time of 47.4% ± 2.9 and 30.7% ± 2.5 (n = 12) for the organic and mineral horizon, respectively. For all other treatments which received water including N treatments, soil water content did not vary significantly ($P > 0.05$, Tukey HSD) between treatments over time but had a significant ($P < 0.05$, Tukey HSD) higher soil water content than the control for the organic and mineral horizons, 58.1% ± 2.2 and 40.0% ± 1.7 (n = 27), respectively (Figure 6.1 A). Only the 12 kg N ha^{-1} yr^{-1} and control microcosms from the mineral horizon were not significantly ($P > 0.05$, Tukey HSD) different at Day+1 (Figure 6.1 A).

The soil pH was significantly higher ($P < 0.05$, Tukey HSD) in the mineral than in the organic horizon (pH = 7.6 ± 0.4 and 6.8 ± .07, respectively; n = 3) in the control microcosms prior to the start of the microcosm experiment (Figure 6.1 B). At Day+1, for the control and the control + water microcosms and by Day+14 in the control + water microcosms, the soil pH was again significantly higher ($P < 0.05$, Tukey HSD) in the mineral horizon than in the organic horizon (Figure 6.1 B).

The N addition at a ~pH 4 changed the soil pH of 0.4 kg N ha^{-1} yr^{-1} microcosms and especially the 12 kg N ha^{-1} yr^{-1} microcosms. The N addition significantly ($P < 0.05$, Tukey HSD) decreased the soil pH in the 12 kg N ha^{-1} yr^{-1} microcosms within both soil horizons in comparison to all the other treatments over time (Figure 6.1 B). Only the soil pH at Day+14 within the organic horizon from the 12 kg N ha^{-1} yr^{-1} and control + water microcosms were not significantly different ($P > 0.05$, Tukey HSD).

The soil pH of the 0.4 kg N ha^{-1} yr^{-1} microcosms significantly ($P < 0.05$, Tukey HSD) decreased in the mineral horizon in comparison to the control + water microcosms at Day+1, and in comparison to the control and control + water microcosms at Day+7 and Day+14 (Figure 6.1 B). However, no significant ($P < 0.05$, Tukey HSD) differences in soil pH within the organic horizon were found between the 0.4 kg N ha^{-1} yr^{-1} microcosms and the control and the control + water microcosms over time.

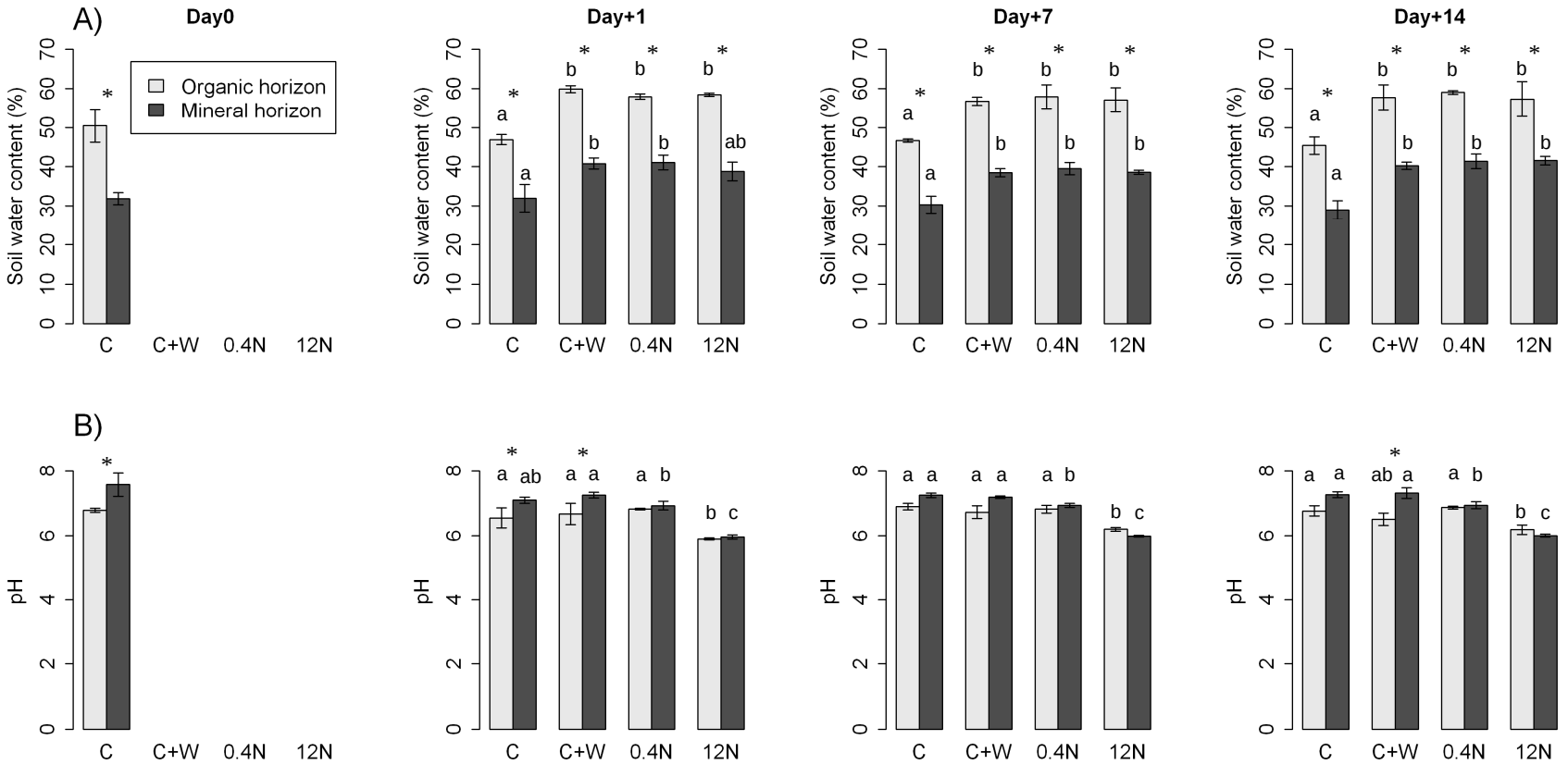

Figure 6.1: Variation in **A)** soil water content (%) and **B)** soil pH between tne organic and mineral soil horizons over time and in response to water and nitrogen addition. **Day0**: before any treatments; **Day+1**: one day after treatment; **Day+7**: seven days after treatment; **Day+14**: fourteen days after treatment; **C**: Control microcosms, **C+W**: Control + water microcosms; **0.4N**: 0.4 kg N ha^{-1} yr^{-1} ~pH 4 microcosms; **12N**: 12 kg N ha^{-1} yr^{-1} ~pH 4 microcosms. Means values ± standard deviation (n = 3) are shown.* indicates significant ($P < 0.001$) differences between the organic and mineral horizons. Different minuscule letters indicate significant ($P < 0.001$) differences between treatments for a specific soil horizon and date of sampling.

6.2.1.2 Soil C and N content

The total C and N soil content were significantly ($P < 0.01$, Tukey HSD) higher (~2.9 and ~2.4 times, respectively) in the organic than in the mineral horizons for all the treatments and date of sampling (Figure 6.2 A). The mean total C for all treatments and dates of sampling was 13.2% ± 1.2 and 4.5% ± 0.6 (n = 27) in the organic and mineral horizons respectively; while the mean total N content in the organic and in the mineral horizons was 0.99 ± 0.09% and 0.41% ± 0.06 (n = 27), respectively. The C/N ratio was in average ~1.2 times higher in the organic (13.3 ± 1.1, n = 27) than in the mineral horizon (11.0 ± 0.8, n = 27; Figure 6.2 B). The C/N ratio was not significantly ($P > 0.05$, Tukey HSD) different between soil horizons at Day0, but was significantly ($P < 0.01$, Tukey HSD) higher in the organic horizon at Day+1 for all treatments, while only the control treatment at Day+7 showed a significantly ($P < 0.05$, Tukey HSD) higher C/N ratio in the organic horizon (Figure 6.2 C). Between Day+1 and Day+7 the C/N ratio within the treatment which received N and/or water, decreased by ~15% within both soil horizons. Only the 12 kg N ha^{-1} yr^{-1} ~pH 4 microcosms showed a significant ($P < 0.01$, Tukey HSD) decrease in the C/N ratio between Day+1 and Day+7.

6.2.1.3 Inorganic N in soil (NO_3^- and NH_4^+)

The mean soil NO_3^- concentration at the beginning of the microcosm experiment (i.e. Day0) was 0.85 ± 0.18 mg N-NO_3^- kg^{-1} soil and 1.74 ± 0.22 mg N-NO_3 kg^{-1} (n = 3) in the organic and mineral horizons, respectively (Figure 6.3 A). No significant ($P < 0.05$, Tukey HSD) differences were found between control and control + water microcosms for both soil horizons or over time. The microcosms receiving N-inputs showed significantly ($P < 0.05$, Tukey HSD) higher NO_3^- concentration than in the control and control + water microcosms within both soil horizons, except for the 0.4 kg N ha^{-1} yr^{-1} microcosms at Day+7 within the organic horizon (Figure 6.3 A).

The 0.4 kg N ha^{-1} yr^{-1} microcosms had NO_3^- concentrations of 8.5 ± 1.2 N-NO_3 mg kg^{-1} soil and 6.0 ± 0.6 N- NO_3^- mg kg^{-1} soil at Day+1 in the organic and mineral horizons, respectively. The NO_3^-concentration within the organic horizon of the 0.4 kg N

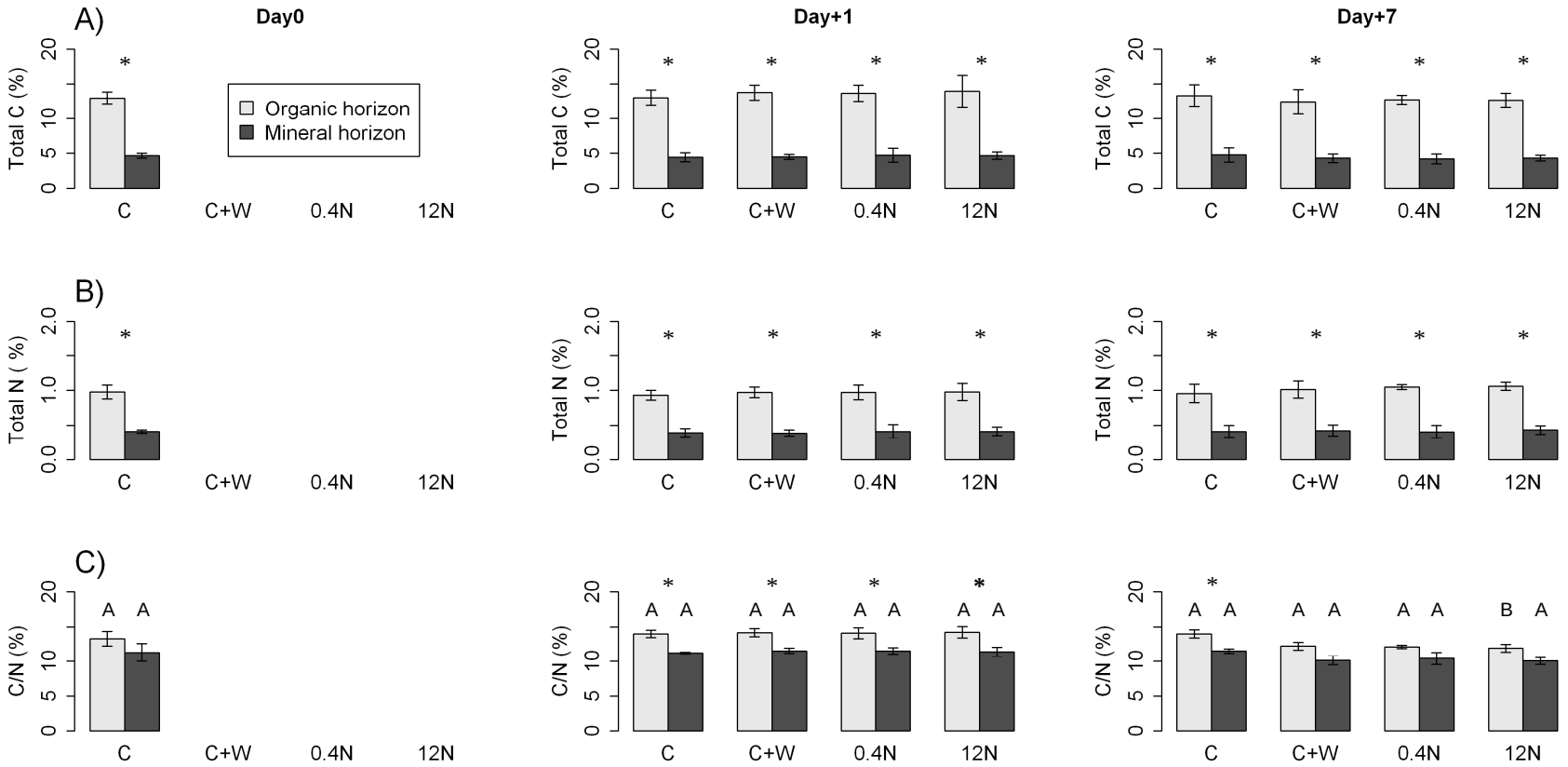

Figure 6.2: Variation in **A)** total C (%), **B)** total N (%) and **C)** C/N ratio between the organic and mineral soil horizons over time and in response to water and nitrogen addition. **Day0**: before any treatments; **Day+1**: one day after treatment; **Day+7**: seven days after treatment; **C**: Control microcosms, **C+W**: Control + water microcosms; **0.4N**: 0.4 kg N ha^{-1} yr^{-1} ~pH 4 microcosms; **12N**: 12 kg N ha^{-1} yr^{-1} ~pH 4 microcosms. Means values ± standard deviation (n = 3) are shown. * indicates significant ($P < 0.001$) difference between the organic and mineral horizons. Different capital letters indicate significant ($P < 0.05$) differences in C/N ratio over time for a specific treatment and soil horizon.

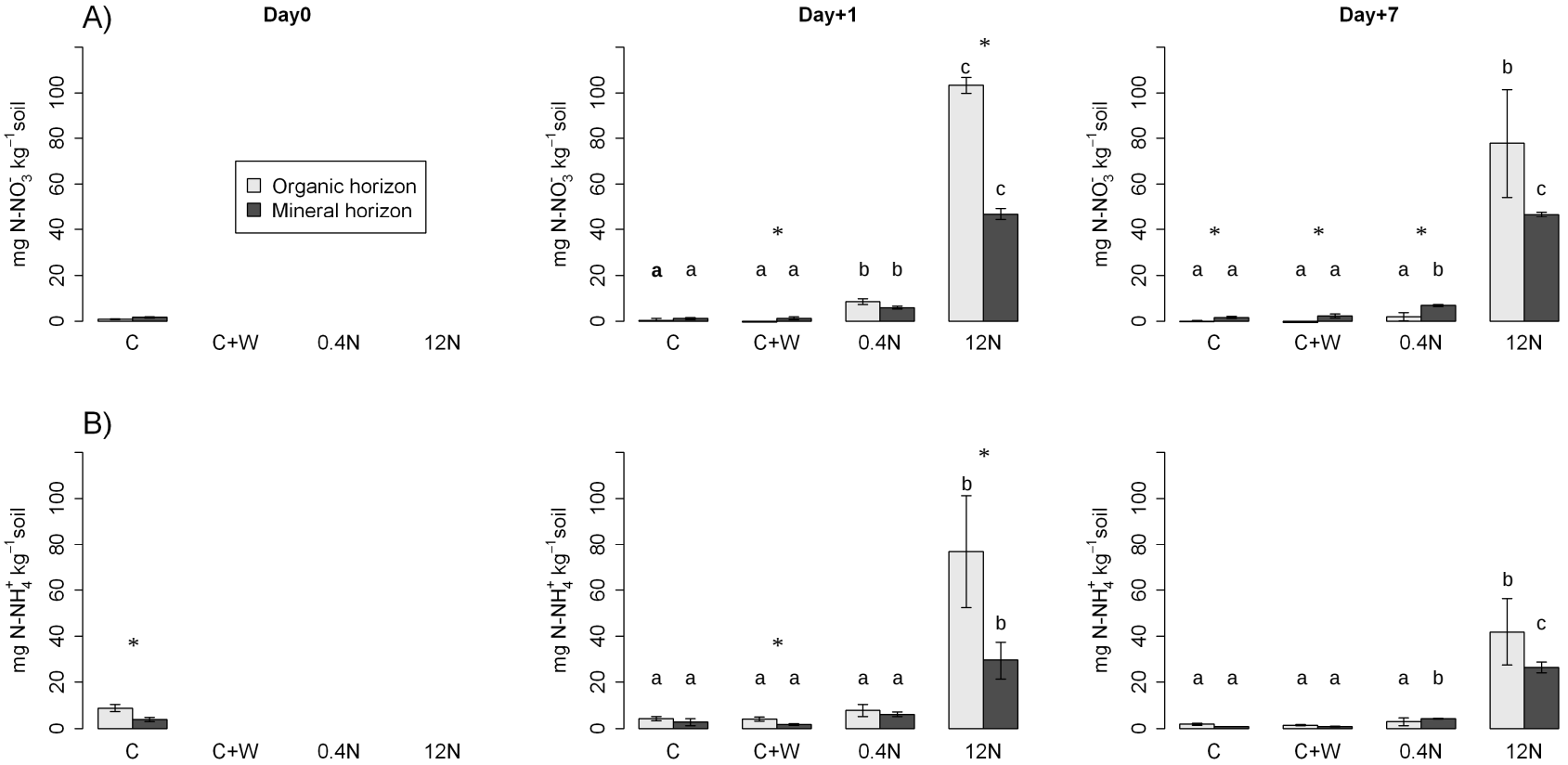

Figure 6.3: Variation in **A)** NO_3^- and **B)** NH_4^+ concentration (mg kg^{-1} soil) between organic and mineral horizon soil horizons over time and in response to water and nitrogen addition. **Day0**: before any treatments; **Day+1**: one day after treatment; **Day+7**: seven days after treatment; **C**: Control microcosms, **C+W**: Control + water microcosms; **0.4N**: 0.4 kg N ha^{-1} yr^{-1} ~pH 4 microcosms; **12N**: 12 kg N ha^{-1} yr^{-1} ~pH 4 microcosms. Means values ± standard deviation (n = 3) are shown. * indicates significant ($P < 0.05$) difference between the organic and mineral horizons. Different minuscule letters indicate significant ($P < 0.05$) difference between treatments for a specific soil horizon and date of sampling.

ha^{-1} yr^{-1} microcosms significantly ($P < 0.05$, Tukey HSD) decreased between Day+1 and Day+7 to 2.0 ± 1.8 N-NO_3 mg kg^{-1} soil, while the NO_3^- concentration in the mineral horizon did not change over time.

The 12 kg N ha^{-1} yr^{-1} microcosms showed a significantly ($P < 0.05$, Tukey HSD) higher NO_3^- concentration than 0.4 kg N ha^{-1} yr^{-1} microcosms within both soil horizons or over time. The 12 kg N ha^{-1} yr^{-1} microcosms NO_3^- concentration was significantly ($P < 0.05$, Tukey HSD) higher at Day+1 in the organic horizon (103.4 ± 3.4 N-NO_3^- mg kg^{-1} soil) than in the mineral horizon (46.9 ± 2.6 N-NO_3^- mg kg^{-1} soil) but not at Day+7 (Figure 6.3 A). The organic horizon of 12 kg N ha^{-1} yr^{-1} microcosms showed a decrease in NO_3^- concentration between Day+1 and Day+7 (77.9 ± 23.6 N- NO_3^- mg kg^{-1} soil at Day+7) but this decrease was not significant ($\chi^2 = 0.6$, df = 1, $P = 0.4$).

The NH_4^+ soil concentration was significantly higher in the organic (8.8 ± 1.5 N-NH_4^+ mg kg^{-1} soil) than in the mineral horizon (4.0 ± 0.9 N-NH_4^+ mg kg^{-1} soil) at Day0 (Figure 6.3 B). The NH_4^+ concentration in the control microcosms significantly ($P < 0.05$, Tukey HSD) decreased at Day+1 within the organic (4.3 ± 0.9 N-NH_4^+ mg kg^{-1} soil) but not in the mineral horizon (2.8 ± 1.5 N-NH_4^+ mg kg^{-1} soil), and significantly ($P < 0.05$, Tukey HSD) decreased at Day+7, in comparison to Day0, within both organic and mineral horizons (1.9 ± 0.4 and 0.9 ± 0.06 N-NH_4^+ mg kg^{-1} soil, respectively). The control + water microcosms showed similar NH_4^+ values and trends to those of the control microcosms, but only the organic horizon showed a significant decrease in NH_4^+ concentration at Day+7 (1.5 ± 0.2 N-NH_4^+ mg kg^{-1} soil).

The NH_4^+ concentrations in the 0.4 kg N ha^{-1} yr^{-1} microcosms were not significantly ($P > 0.05$, Tukey HSD) different to the ones found for the control and control + water microcosms within both soil horizons and over time, except ay Day+7 within the mineral horizon (Figure 6.3 B). The NH_4^+ concentration significantly ($P < 0.01$, Tukey HSD) decreased at Day+7 in the organic horizon (3.0 ± 1.6 N-NH_4^+ mg kg^{-1} soil) (Figure 6.3 B).

The 12 kg N ha^{-1} yr^{-1} microcosms had a significantly ($P < 0.05$, Tukey HSD) higher NH_4^+ concentrations than in all the other treatments within both soil horizons and over time. The NH_4^+ concentration was significantly ($P < 0.05$) higher at Day+1 in the organic horizon (76.9 ± 24.4 N-NH_4^+ mg kg^{-1} soil) than in the mineral horizon (29.3 ±

8.1 N-NH_4^+ mg kg^{-1} soil). The NH_4 concentration in the organic horizon decreased at Day+1 (41.8 ± 14.5 N-NH_4^+ mg kg^{-1} soil) but not significantly ($P > 0.05$, Tukey HSD), while in the mineral horizon, the NH_4^+ content did not change (26.2 ± 2.3 N-NH_4^+ mg kg^{-1} soil).

6.2.2 Variation in bacterial and archaeal community structure

DNA was extracted from the microcosm experiment soil samples of the organic and mineral horizons from of all the treatments (i.e. control, control + water, 4 kg N ha^{-1} h^{-1} and 12 kg N ha^{-1} yr^{-1}), taken one (Day+1) and seven (Day+7) days after N application. For the control microcosms, DNA was extracted from six soil samples (three from the organic and three from the mineral horizon) prior to incubation (Day0). DNA was extracted from a total of 54 soil samples from the microcosm experiment.

The T-RFLP profiles obtained for bacteria and archaea were complex, with a total of 111 and 106 T-RFs respectively. The bacterial community had on average more T-RFs per profile than the archaeal community, 40 ± 5 and 28 ± 5 T-RFs respectively (Figure 6.4). nMDS analysis showed that the bacterial and archaeal community structures from the organic and mineral horizons grouped separately (Figure 6.5 A). ANOSIM analysis showed that the structure of both bacterial and archaeal communities differed significantly ($P = 0.00005$) between the organic and mineral horizons (R = 0.79 and 0.68, respectively; Table 6.1). This result was consistent with the richness estimates and Shannon diversity indices at Day0, where both bacterial and archaeal communities showed significantly ($P < 0.05$, Tukey HSD) higher T-RF richness and Shannon diversity index in the organic compared to mineral horizons (Figure 6.4). However, this difference was not always present at Day+1 and Day+7, such that at Day+1 for the bacterial community in the 12 kg N ha^{-1} yr^{-1} treatment where T-RF richness and Shannon diversity index were significantly ($P < 0.05$, Tukey HSD) higher in the mineral than in the organic horizons. Nevertheless the bacterial and archaeal community structure always showed significant differences between the organic and mineral horizons even when the difference in T-RF richness and Shannon diversity index were absent.

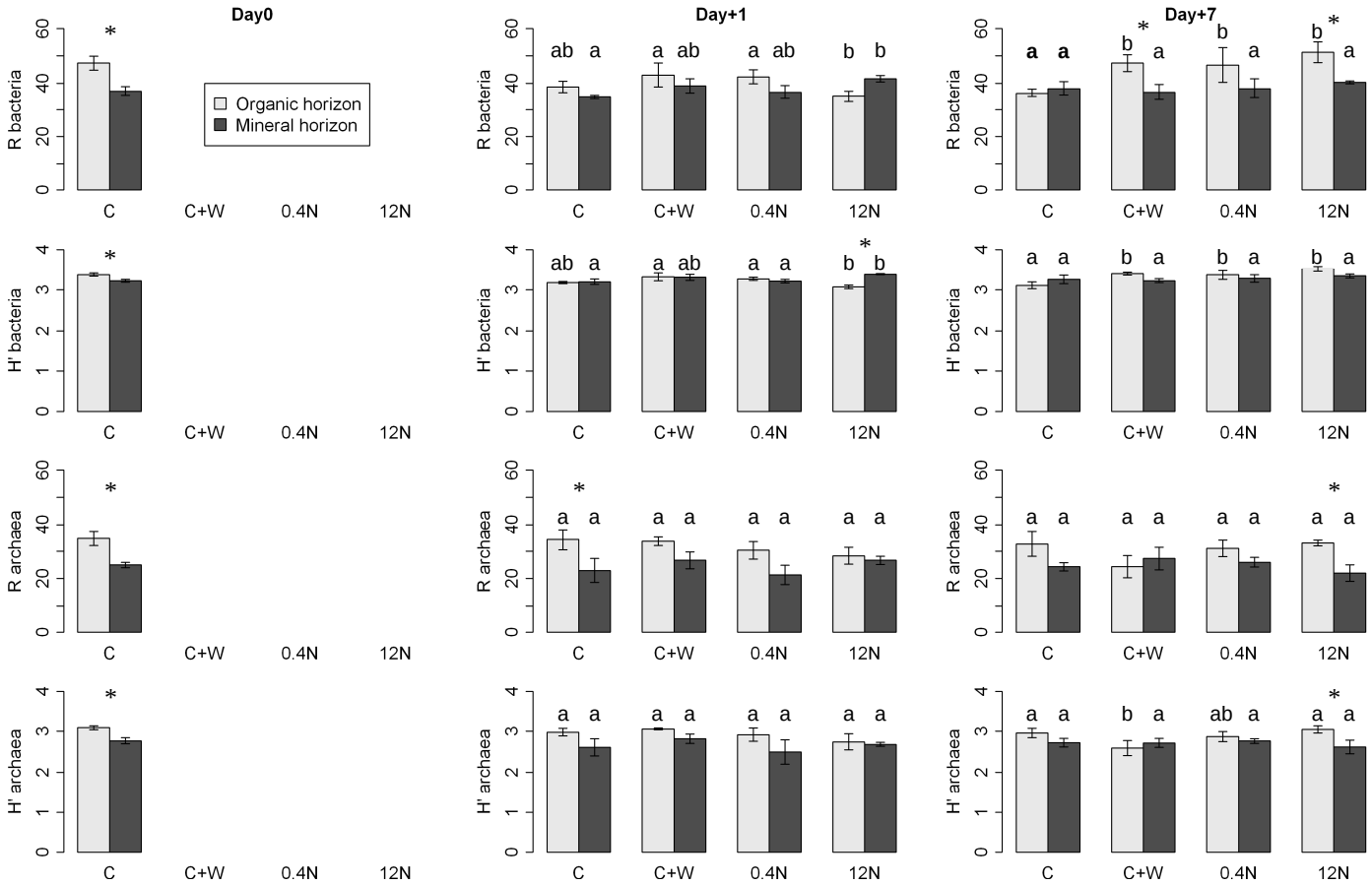

Figure 6.4: Variation in richness (**R**) and Shannon diversity index (**H'**) in the bacterial and archaeal communities between the organic and mineral soil horizons, over time and in response to water and nitrogen addition. **Day0**: before any treatments; **Day+1**: one day after treatment; **Day+7**: seven days after treatment; **C**: Control microcosms, **C+W**: Control + water microcosms; **0.4N**: 0.4 kg N ha^{-1} yr^{-1} ~pH 4 microcosms; **12N**: 12 kg N ha^{-1} yr^{-1} ~pH 4 microcosms. Means values ± standard deviation (n = 3) are shown. * indicates significant ($P < 0.05$) differences between the organic and mineral horizons. Different minuscule letters indicate significant ($P < 0.05$) differences between treatments for a specific soil horizon and date of sampling.

6.2.2.1 Variation in bacterial community structure in response to water and N addition over time

Bacterial community structure within the organic horizon of the control microcosms changed over time and was significantly (P = 0.01) different from that in other treatments (Figure 6.5; Table 6.1). ANOSIM indicated a strong separation between the control *vs.* control + water and 0.4 kg N h^{-1} yr^{-1} microcosms, while the R value was lower between the control and 12 kg N ha^{-1} yr^{-1} microcosms (Table 6.1) because at Day+1 the bacterial community structure of the 12 kg N ha^{-1} yr^{-1} microcosms was more similar to the control than the other treatments (Figure 6.5). This similarity at Day+1 between control and 12 kg N ha^{-1} yr^{-1} microcosms was reflected by similar T-RF richness and Shannon diversity indices, while the other treatments showed significantly (P < 0.05, Tukey HSD) higher T-RF richness and Shannon diversity indices values (~ 1.2 times) than in the 12 kg N ha^{-1} yr^{-1} microcosms in the organic horizon (Figure 6.4). Similarly, differences in bacterial community structure between control and other treatments were confirmed by the T-RF richness and Shannon diversity index at Day+7, where the control microcosms showed significantly (P < 0.05, Tukey HSD) lower values (1.3 and 1.1 times, respectively; Figure 6.4). Bacterial community structure within the organic horizon from the control + water and 0.4 kg N ha^{-1} yr^{-1} were not significantly (P = 0.45) different from each other, while bacterial community structure within the organic horizon in the 12 kg N ha^{-1} yr^{-1} microcosms was significantly ($P \leq 0.03$) different from in the control + water and 0.4 kg N ha^{-1} yr^{-1} microcosms (Table 6.1). Bacterial community structure within the mineral horizon of the control microcosms also changed over time and was significantly ($P \leq 0.03$) different from that in the other treatments (Figure 6.5; Table 6.1). ANOSIM indicated a high separation between the control and the treatments with N additions, while the R value between control and control + water microcosms was lower (R = 0.63) due to the bacterial community structure at Day+7 in the control + water microcosms being more similar to that in the control microcosms when compared at Day+1 (data not shown).

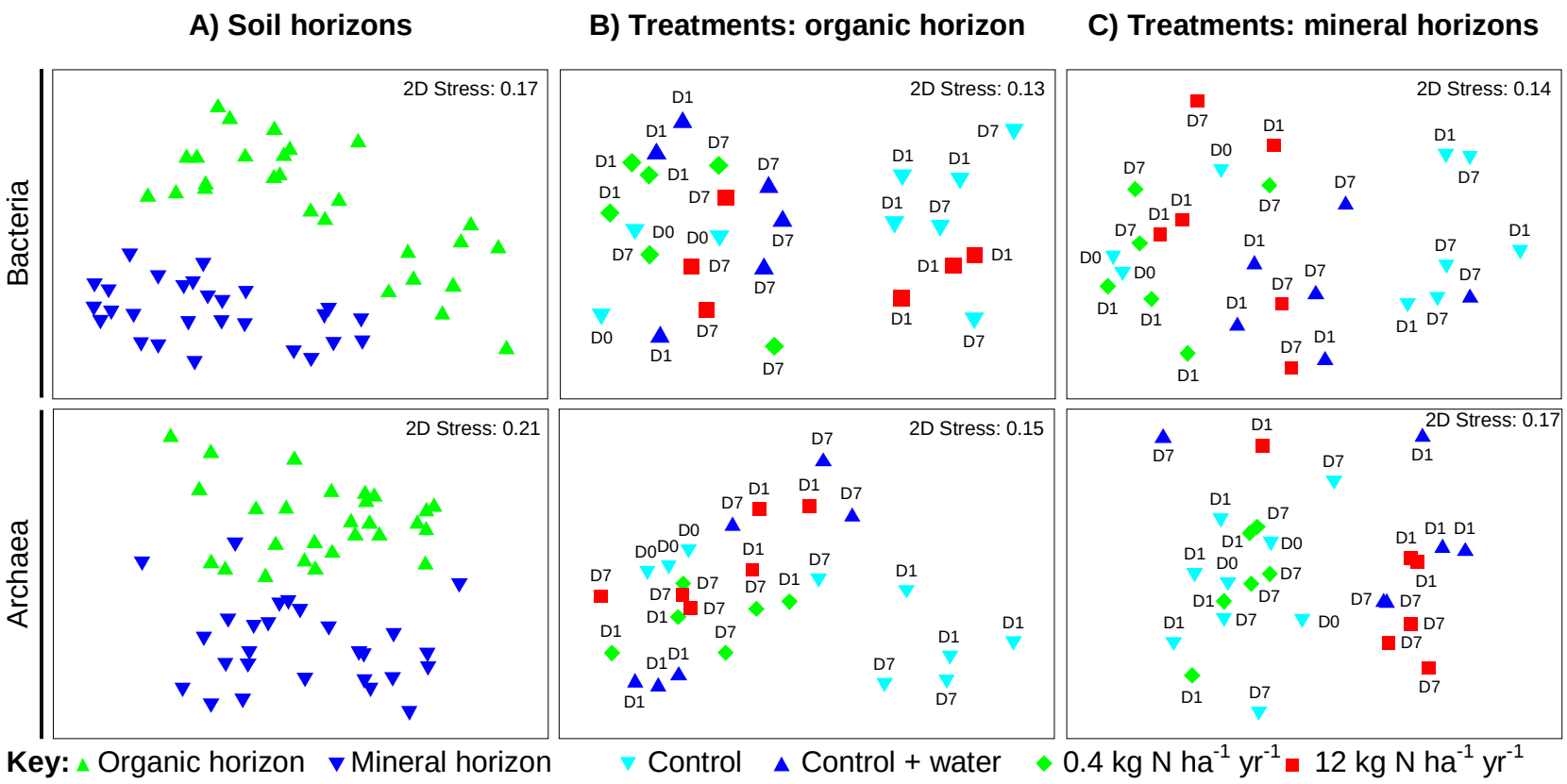

Figure 6.5: nMDS plots showing variation in bacterial and archaeal community structure in the microcosm experiment between the organic and mineral soil horizons over time and in response to water addition (control (without water and N) and control + water microcosms) and nitrogen addition (0.4 kg N ha^{-1} yr^{-1} ~pH 4 and 12 kg N ha^{-1} yr^{-1} ~pH 4 microcosms). **D0**: before any treatments; **D1**: one day after treatment; **D7**: seven days after treatment. **A**: plots showing the influence of soil horizons on microbial community structure; **B**: plots showing the influence of treatments on microbial community structure in the organic horizon; **C**: plots showing the influence of treatments on microbial community structure in the mineral horizon.

Table 6.1: Two-way ANOSIM showing variation in the structure of bacterial and archaeal communities between: organic and mineral horizons; between the different treatments for the organic and mineral horizons separately. **C**: control without water microcosms; **C+W**: control + water microcosms; **0.4N**: 0.4 kg N ha^{-1} yr^{-1} ~pH 4 microcosms; **12N**: 12 kg N ha^{-1} yr^{-1} ~pH 4 microcosms. The R values and the significance level (in brackets) are given. Significant values at $P < 0.05$ are shown in bold text.

Soil horizons	Factors compared	Bacteria	Archaea
	Organic *vs.* Mineral	**0.79 (0.00005)**	**0.68 (0.00005)**
Organic	C *vs.* C+W	**0.89 (0.01)**	**0.96 (0.01)**
	C *vs.* 0.4N	**0.87 (0.01)**	**0.93 (0.01)**
	C *vs.* 12N	**0.74 (0.01)**	**0.83 (0.01)**
	C+W *vs.* 0.4N	0.02 (0.45)	**0.61 (0.01)**
	C+W *vs.* 12N	**0.80 (0.02)**	**0.83 (0.01)**
	0.4N *vs.* 12N	**0.54 (0.03)**	0.04 (0.43)
Mineral	C *vs.* C+W	**0.63 (0.03)**	**0.63 (0.02)**
	C *vs.* 0.4N	**1 (0.01)**	0.24 (0.14)
	C *vs.* 12N	**0.85 (0.01)**	**0.82 (0.01)**
	C+W *vs.* 0.4N	**0.39 (0.04)**	**0.63 (0.02)**
	C+W *vs.* 12N	0.32 (0.07)	**0.30 (0.01)**
	0.4N *vs.* 12N	0.15 (0.27)	**0.94 (0.01)**

In contrast to the organic horizon, bacterial community structure within the mineral horizon was significantly (P = 0.03) different between the control + water and the 0.4 kg N ha^{-1} yr^{-1} microcosms, while the 12 kg N ha^{-1} yr^{-1} bacterial community did not show a significantly (P > 0.05) different structure from that in the control + water and 0.4 kg N ha^{-1} yr^{-1} microcosms (Table 6.1). However, bacterial community structure in the 12 kg N ha^{-1} yr^{-1} was nearly significantly different at P < 0.05 to that of the control + water microcosms (Figure 6.5; Table 6.1) primarily because at Day+1 both communities were strongly different.

6.2.2.2 Variation in archaeal community structure in response to water and N addition over time

Archaeal community structure within the organic horizon of the control microcosms was significantly (P = 0.01) and strongly (R > 0.8) different from that in the other treatments (Figure 6.5; Table 6.1). In the organic horizon, archaeal community structure in the control microcosms changed over time between Day0 and the other dates of sampling (Figure 6.5). No significant (P = 0.43) difference was found between the archaeal community structure in the 0.4 and 12 kg N ha^{-1} yr^{-1} microcosms. In contrast, archaeal community structure in the control + water microcosms was significantly (P = 0.01) different from that of the 0.4 and 12 kg N ha^{-1} yr^{-1} microcosms. Moreover, the archaeal community structure in the control + water microcosms showed variation between Day+1 and Day+7 (Figure 6.5).

In the mineral horizon, archaeal community structure of the control microcosms was significantly ($P \leq 0.02$) different from that in the control + water and 12 kg N ha^{-1} yr^{-1} microcosms, but was not significantly (P = 0.14) different from that in the 0.4 kg N ha^{-1} yr^{-1} microcosms (Figure 6.5; Table 6.1). Similarly, mineral horizon archaeal community structure in the 0.4 kg N ha^{-1} yr^{-1} microcosms was significantly ($P \leq 0.02$) different from that in the control + water and 12 kg N ha^{-1} yr^{-1} microcosms. The archaeal community in the control + water and 12 kg N ha^{-1} yr^{-1} microcosms were significantly (P = 0.01) different from each other but the low R value (R = 0.30) indicated a weak separation of the two communities (Figure 6.5; Table 6.1).

The archaeal and bacterial community structures within the mineral horizon was additionally influenced by the location from which soil was sampled for the microcosms experiment (hereafter referred to as soil sample replicates; Appendix 6.1). The soil replicate 1 had significantly ($P < 0.001$) different archaeal and bacterial community structure to that in the other two soil replicates. This difference of communities might to some extent influence the results within the mineral horizon, especially for the archaeal community (Appendix 6.1).

6.2.3 Variation in bacterial and archaeal abundance

Variation in bacterial and archaeal 16S rRNA genes abundance was investigated by Q-PCR between all of the treatments of the microcosm experiment at Day0, Day+1 and Day+7 (Figure 6.6). 16S rRNA gene abundance data was obtained from all of the soil samples, except from one sample from the mineral horizon of the control microcosms at Day0 from which bacterial 16S rRNA genes were not amplified.

6.2.3.1 Bacterial abundance

Bacterial 16S rRNA gene abundance did not differ significantly ($P > 0.05$, Kruskal-Wallis) between soil horizons, over time or between treatments despite changes in abundance between treatments over time. The control microcosms had ~1.8 and ~2.2 times higher number of bacterial 16S rRNA genes in the mineral than organic horizons at Day+1 and Day+7, respectively; and bacterial 16S rRNA gene numbers decreased between Day+1 and Day+7 by ~53% and 47% within the organic and mineral horizons, respectively. In contrast, bacterial 16S rRNA gene numbers in the control + water microcosms were ~2.9 and ~1.8 times higher in the organic horizon than in the mineral horizon at Day+1 and Day+7, respectively, and bacterial 16S rRNA gene numbers decreased by 27% in the organic horizon between Day+1 and Day+7. The 0.4 kg N ha^{-1} yr^{-1} microcosms also showed higher bacterial 16S rRNA gene numbers within the organic than in the mineral horizon at Day+1 (~1.4 times higher). However, at Day+7 the bacterial 16S rRNA gene number was ~4.4 higher in the mineral horizon because the

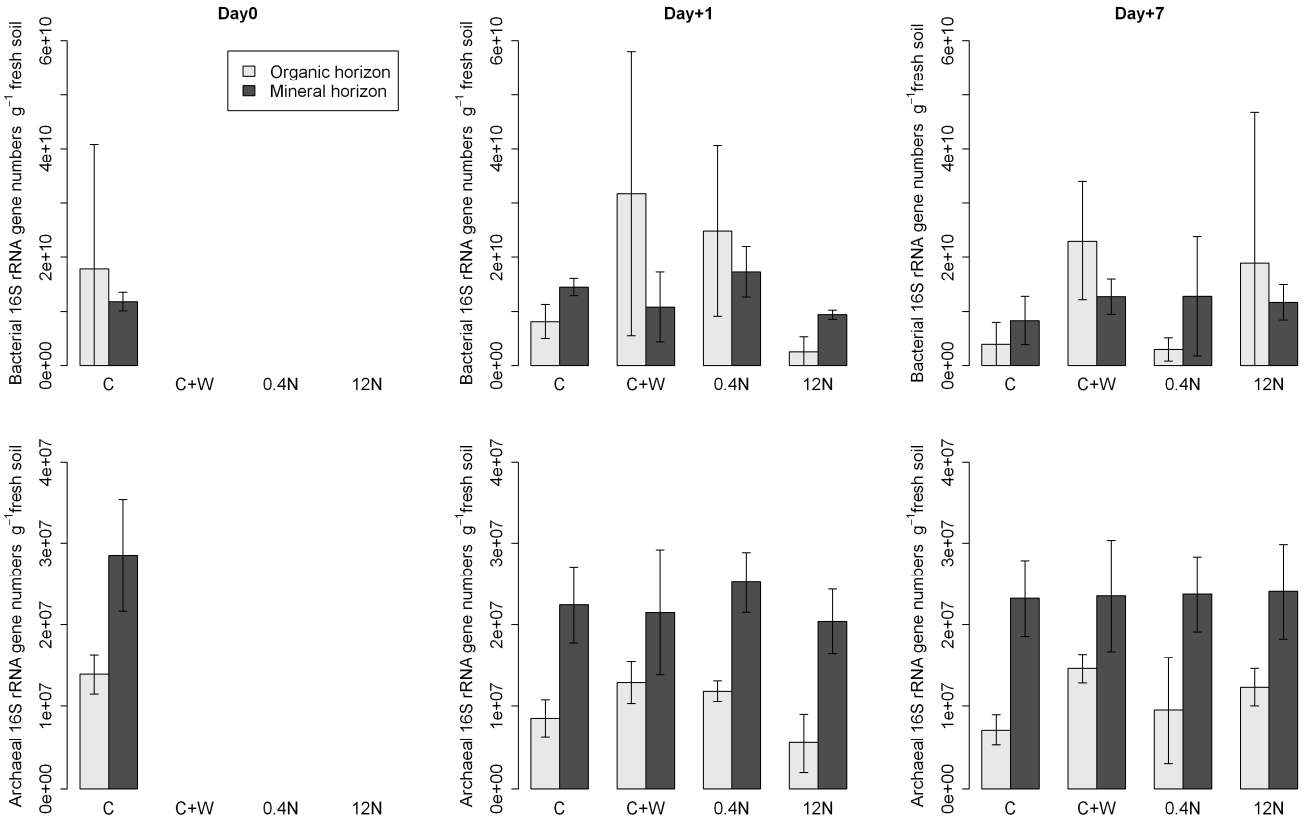

Figure 6.6: Variation in bacterial and archaeal gene abundance (16S rRNA gene numbers g^{-1} fresh soil) between the organic and mineral soil horizons over time and in response to water and nitrogen addition. **Day0**: before any treatments; **Day+1**: one day after treatment; **Day+7**: seven days after treatment; **C**: Control microcosms, **C+W**: Control + water microcosms; **0.4N**: 0.4 kg N ha^{-1} yr^{-1} ~pH 4 microcosms; **12N**: 12 kg N ha^{-1} yr^{-1} ~pH 4 microcosms. Means values ± standard deviation (n = 3, except when mentioned in the text) are shown. Gene numbers were calculated from the standard curve: bacteria: r^2 = 0.984, y intercept = 37.32, *E* (amplification efficiency) = 98.4 %, NTC Ct = 29.9; archaea: r^2 = 0.992, y intercept = 38.19, *E* (amplification efficiency) = 85.8 %, NTC Ct = 33.2. Archaea were significantly ($P < 0.001$) more abundant in the mineral than organic horizons.

bacterial abundance decreased by ~87% within the organic horizon between Day+1 and Day+7 (Figure 6.6). Conversely, the 12 kg N ha^{-1} yr^{-1} microcosms had ~3.8 times more bacterial 16S rRNA genes within the mineral than in the organic horizon at Day+1, but abundance was ~1.6 times higher within the organic horizon at Dayt+7 due to an ~87% increase in bacterial 16S rRNA genes number within the organic horizon between Day+1 and Day+7.

6.2.3.2 Archaeal abundance

Archaeal 16S rRNA gene abundance was significantly ($F = 111.7$, $df = 1$, $P = 1.4x10^{-12}$) higher (~2.2 times) in the mineral than the organic horizon for all of the treatments and over time (Figure 6.6). However, no significant ($P > 0.05$, Tukey HSD) differences were found over time or between treatments within either soil horizons, despite fluctuation of 16S rRNA gene numbers within the organic horizon (Figure 6.6).

6.2.4 Relationship between the structure and abundance of bacterial and archaeal communities and environmental variables

6.2.4.1 Bacterial community

Bacterial community structure was significantly ($P \leq 0.016$) correlated to the water content within both the organic and mineral horizons ($\rho = 0.28$ and 0.17, respectively) and to NH_4^+ concentration ($\rho = 0.23$) within the mineral horizon (Table 6.2). It is interesting to note that soil pH was significantly ($P < 0.05$) correlated to the bacterial community structure within the organic ($\rho = 0.41$) and mineral ($\rho = 0.38$) horizons at Day+1 and Day+7, respectively. In contrast to structure, no significant correlations ($P > 0.05$) were found between bacterial abundance and environmental variables investigated in either the organic or mineral horizons separately (Table 6.3). It is interesting to note that bacterial abundance was significantly ($P < 0.05$) correlated to

the soil pH within the organic horizon at Day+1 and Day+7 (ρ = 0.27 and 0.47, respectively).

6.1.4.2 Archaeal community

Archaeal community structure within the organic horizon was significantly ($P < 0.05$) and strongly correlated to the water content (ρ = 0.35), and to a lesser extent to the total C and ^{15}N (ρ = 0.26 and 0.20, respectively) (Table 6.2; Appendix 6.2). Archaeal community structure in the mineral horizon was only significantly ($P \leq 0.04$) correlated to NO_3^- and NH_4^+ concentration (ρ = 0.14 and 0.23, respectively). Archaeal community structures within either organic or mineral soil horizons, were significantly correlated ($P \leq 0.017$) to archaeal 16S rRNA gene abundance with ρ ~0.2 (Table 6.2). Archaeal abundance within the organic or mineral horizons was not significantly ($P > 0.05$) correlated to any of the environmental variables except for the C/N ratio, which was significantly (P = 0.043, ρ = 0.14) correlated to archaeal abundance within the organic horizon (Table 6.3).

Table 6.2: Correlations between microbial (i.e. bacterial and archaeal) structure and environmental variables or microbial (i.e. bacterial and archaeal) abundance within the organic or mineral horizons, obtained using the RELATE test from PRIMER software. The ρ values and the significance level (in brackets) are given. Significant values at $P < 0.05$ are shown in bold text.

Microbial community	Water	pH	Total C	Total N	^{15}N	C/N ratio	NO_3	NH_4	Abundance
Bacteria organic	**0.28 (0.003)**	0.10 (0.10)	0.05 (0.18)	0.07 (0.13)	0.20 (0.08)	0.04 (0.23)	-0.02 (0.62)	0.02 (0.37)	0.05 (0.20)
Bacteria mineral	**0.17 (0.016)**	0.05 (0.17)	0.11 (0.06)	0.04 (0.20)	0.03 (0.26)	-0.05 (0.79)	0.07 (0.11)	**0.23 (0.04)**	-0.02 (0.59)
Archaea organic	**0.35 (0.001)**	-0.02 (0.5)	**0.26 (0.034)**	0.05 (0.2)	**0.20 (0.016)**	0.04 (0.25)	-0.01 (0.49)	-0.02 (0.58)	**0.22 (0.017)**
Archaea mineral	0.05 (0.25)	0.08 (0.13)	0.03 (0.33)	-0.05 (0.75)	-0.09 (0.88)	-0.04 (0.70)	**0.14 (0.04)**	**0.23 (0.002)**	**0.17 (0.012)**

Table 6.3: Correlations of the microbial (i.e. bacterial and archaeal) abundance and environmental variables within the organic or mineral horizons, obtained using the RELATE test from PRIMER software. The ρ values and the significance level (in brackets) are given. Significant values at $P < 0.05$ are shown in bold text.

Microbial community	Water	pH	Total C	Total N	^{15}N	C/N ratio	NO_3	NH_4
Bacteria organic	-0.04 (0.71)	-0.05 (0.71)	-0.09 (0.91)	-0.03 (0.65)	-0.07 (0.86)	-0.025 (0.64)	-0.017 (0.52)	-0.01 (0.48)
Bacteria mineral	-0.08 (0.78)	-0.02 (0.56)	0.17 (0.63)	0.08 (0.16)	-0.10 (0.87)	-0.1 (0.87)	-0.02 (0.53)	-0.05 (0.67)
Archaea organic	0.12 (0.07)	0.14 (0.08)	0.06 (0.21)	-0.05 (0.75)	0.04 (0.29)	**0.14 (0.043)**	0.05 (0.20)	0.05 (0.23)
Archaea mineral	0.0 (0.45)	-0.002 (0.4)	-0.03 (0.59)	-0.01 (0.50)	-0.02 (0.580	0.04 (0.026)	-0.06 (0.84)	-0.04 (0.67)

6.2.5 N-cycling community

The presence of microorganisms involved in nitrogen-fixation, nitrification and denitrification were investigated by targeting the functional genes encoding for each different function via PCR within soil samples taken from the microcosm experiment at different dates of sampling (Table 6.4).

Table 6.4: Amplification of functional genes from DNA isolated from soil samples of the microcosm experiment from both soil horizons and over time. **Red**: no gene amplification; **Orange**: amplification of multiple amplicons of different sizes (bp), with one of the amplicons being similar by size to that of the gene of interest; **Green**: amplification of a single amplicon of a similar size to that of the gene of interest. **C**: clone library generated to determine if the sequence amplified was of the target gene of interest.

Functional genes		PCR amplification of target gene at different time (days of sampling)		
Target genes	Primer pairs	Day0	Day+1	Day+7
nifH	nifH3 / nifH4			
nifH	nifH(for A) / nifH(rev)			
amoA bacteria	amoA-1F / amoA-2R			
amoA archaea	amo111F / amo643R			**C**
nxrA	F1norA / R1norA			
Nitrobacter spp. 16S rRNA gene	Nitro-1198F / Nitro-1423R			
napA	napAv66 / napAv67			
narG	narG1960F / narG2659R			
nirS	NirS1F / NirS6R			
nirS	nirSHeme832F / nirSHeme1606R			
nirK	nirKCopper583F / nirKCopper909R			
nosZ	nosZ661b / nosZ1773			

6.2.5.1 N fixation

The *nifH* gene (encoding nitrogenase enzyme) could not be amplified from any of the microcosms despite the use of two different primer pairs, different PCR solution mix and annealing temperature (data not shown).

6.2.5.2 Nitrification

The two steps within nitrification were investigated: i) ammonia oxidation (encoded by *amoA* gene), and ii) nitrite oxidation (encoded by *nxrA* gene and *Nitrobacter spp.* 16S rRNA gene).

6.2.5.2.1 amoA gene analysis

PCR amplification of the bacterial *amoA* gene yielded a specific amplicon of a similar size to that of the gene of interest (i.e. ~491 bp; Figure 6.7). Agarose gel electrophoresis of PCR-amplified bacterial *amoA* genes showed that the intensity of the PCR products from the mineral horizon were stronger than those from the organic horizon and that some variability between treatments was present (Figure 6.7). In order to confirm that PCR products amplified were related to bacterial *amoA* genes, a small clone library was generated from PCR products amplified from the soil samples of three mineral horizon replicates from the control + water microcosms, sampled seven days post treatment (Figure 6.7). 11 sequences were generated and compared to the GenBank database using BLASTn. All 11 sequences were related to bacterial *amoA* genes, and to the same phylum (i.e. Proteobacteria), class (i.e. Betaproteobacteria) and order (i.e. Nitrosomonadales) (Table 6.5). Sequences similarity to closest related sequences varied between 74 to 85%. Bacterial *amoA* sequences were related to those from forest and cultivated soils but also from meadow soils from cold environments in Tibet (Table 6.5).

The clone library showed that PCR products obtained were related to the bacterial *amoA* gene. Therefore, variation in bacterial *amoA* gene numbers could be investigated by Q-PCR with confidence of targeting the gene of interest. Bacterial *amoA*

genes number were significantly (F = 82.8, df = 1, P = 7.2x10^{-11}) higher (~2.4 times) in the mineral than in the organic horizon over time (Figure 6.8). However, no significant (P > 0.05, Tukey HSD) differences were found over time or between treatments within each soil horizons.

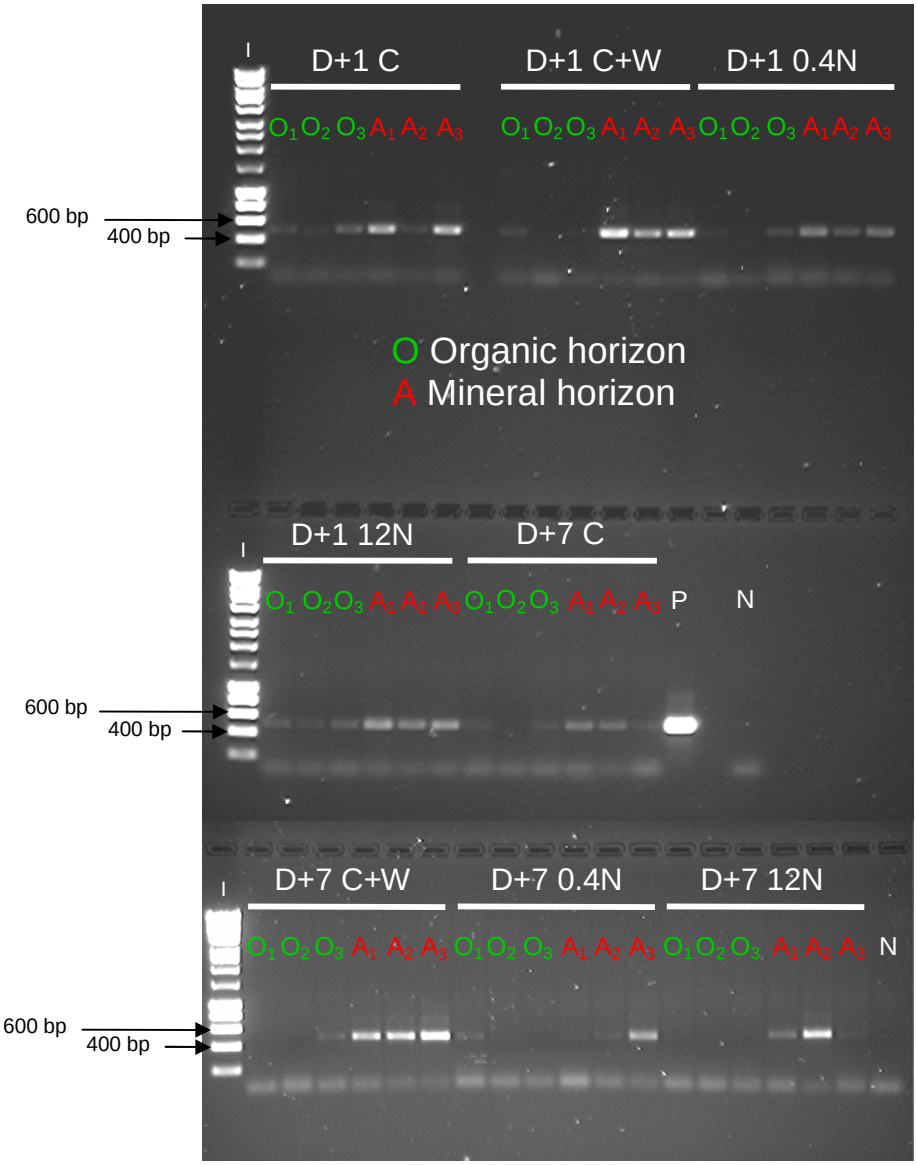

Figure 6.7: Agarose gel electrophoresis (1% agarose) of PCR amplifications targeting the bacterial *amoA* gene from the microcosm experiment soil samples of the organic (**O**) and mineral (**A**) horizons. **C**: control without water microcosms; **C+W**: control + water microcosms; **0.4N**: 0.4 kg N ha^{-1} yr^{-1} ~pH 4 microcosms; **12N**: 12 kg N ha^{-1} yr^{-1} ~pH 4 microcosms; **D+1**: one day after treatment; **D+7**: seven days after treatment; **N**: PCR negative control. **P**: PCR positive control. The numbers beside O and A indicate the microcosm replicate numbers. The Hyperladder™ I (Bioline, London, UK; **l**) was used as a size standard.

Table 6.5: Identification of bacterial *amoA* sequences from the microcosm experiment soil samples. Sequences were identified by BLASTn comparison to the GenBank database. Bacterial *amoA* sequences were amplified from the soil samples of the three mineral horizon replicate from control + water microcosms, sampled seven days post treatment (see Figure 6.7).

Closest related sequence	Accession number	Origin (ecosystem)	Phylum	Class	Order	% identity	% coverage
Uncultured ammonia-oxidizing bacterium clone H12 *amoA* gene	HQ638950.1	Farm land	Proteobacteria	Betaproteobacteria	Nitrosomonadales	84	80
Uncultured ammonia-oxidizing bacterium clone H12 *amoA* gene	HQ638950.1	Farm land	Proteobacteria	Betaproteobacteria	Nitrosomonadales	80	97
Uncultured ammonia-oxidizing bacterium clone H12 *amoA* gene	HQ638950.1	Farm land	Proteobacteria	Betaproteobacteria	Nitrosomonadales	83	98
Uncultured ammonia-oxidizing bacterium clone AOB-D06 *amoA* gene,	HM113502.1	Forest, pasture, cropland	Proteobacteria	Betaproteobacteria	Nitrosomonadales	79	75
Uncultured ammonia-oxidizing bacterium clone ZEVZn6band2 *amoA* gene	HQ687667.1	Grassland	Proteobacteria	Betaproteobacteria	Nitrosomonadales	76	74
Uncultured bacterium isolate DGGE gel band J-GBO2654H *amoA* gene	HM461382.1	Lava Tubes, Azores	Proteobacteria	Betaproteobacteria	Nitrosomonadales	81	75
Uncultured ammonia-oxidizing bacterium GMSc41 *amoA* gene	AY249688.1	Meadow soils	Proteobacteria	Betaproteobacteria	Nitrosomonadales	79	74
Uncultured ammonia-oxidizing bacterium clone AOBu-A1B12 *amoA* gene	GQ143466.1	Meadow soil Tibetan Plateau	Proteobacteria	Betaproteobacteria	Nitrosomonadales	79	89
Uncultured ammonia-oxidizing bacterium clone AOBu-A6A1 *amoA* gene	GQ143496.1	Meadow soil Tibetan Plateau	Proteobacteria	Betaproteobacteria	Nitrosomonadales	85	80
Uncultured ammonia-oxidizing bacterium clone AOBu-B6D5 *amoA* gene	GQ143640.1	Meadow soil Tibetan Plateau	Proteobacteria	Betaproteobacteria	Nitrosomonadales	85	92
Uncultured bacterium clone RT-250_07 *amoA* gene	DQ480797.1	-	Proteobacteria	Betaproteobacteria	Nitrosomonadales	74	93

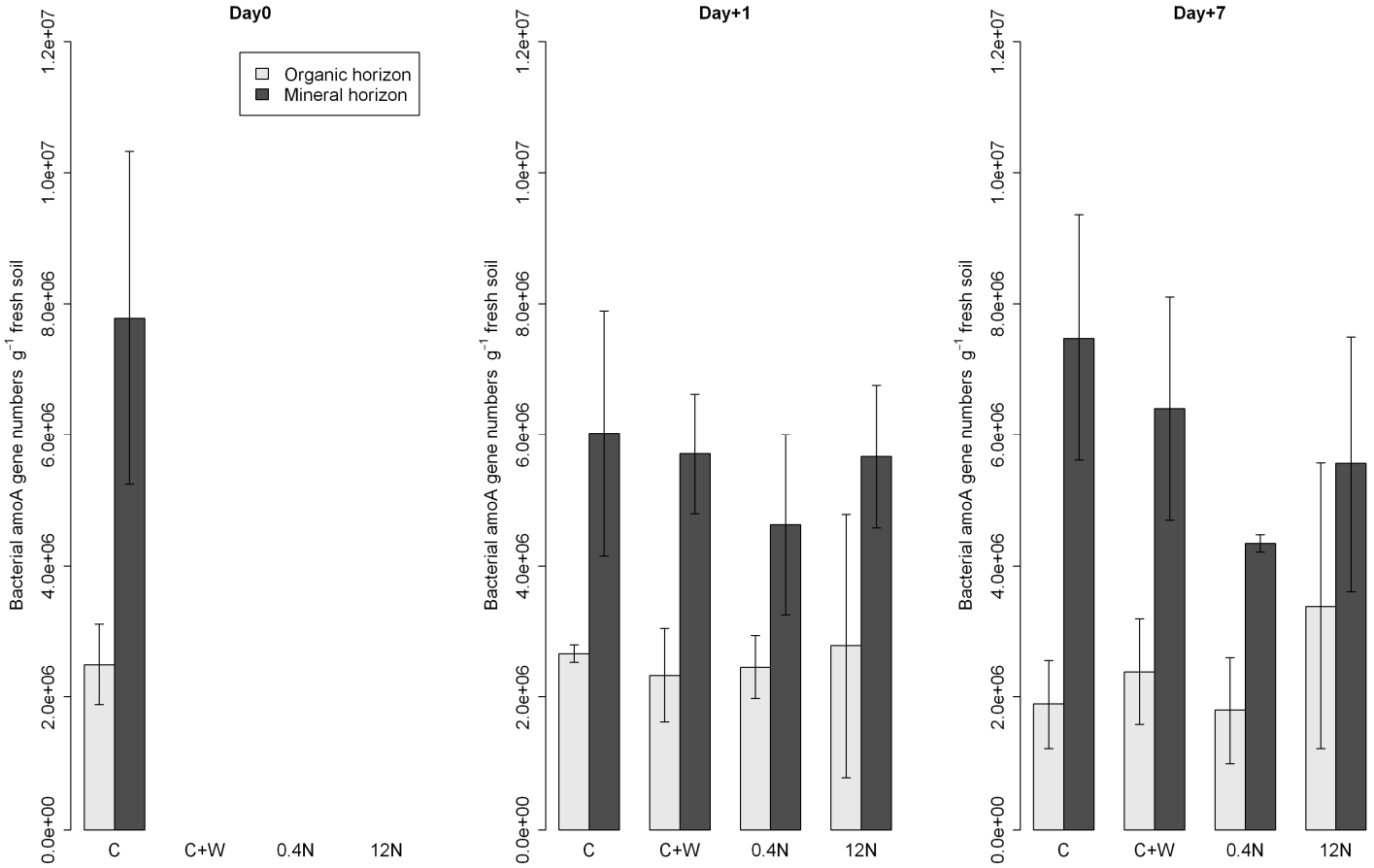

Figure 6.8: Variation in bacterial *amoA* gene numbers (*amoA* gene numbers g^{-1} fresh soil) between the organic and mineral soil horizons over time and in response to water and nitrogen addition. **Day0**: before any treatments; **Day+1**: one day after treatment; **Day+7**: seven days after treatment; **C**: Control microcosms, **C+W**: Control + water microcosms; **0.4N**: 0.4 kg N ha^{-1} yr^{-1} ~pH 4 microcosms; **12N**: 12 kg N ha^{-1} yr^{-1} ~pH 4 microcosms. Means values ± standard deviation (n = 3) are shown. Gene numbers were calculated from the standard curve: bacterial *amoA*: $r^2 = 0.955$, y intercept = 41.29, *E* (amplification efficiency) = 98.4 %, NTC Ct = 32.0. Bacterial *amoA* genes were significantly ($P < 0.001$) more abundant in the mineral than in the organic horizons.

In contrast to the bacterial *amoA* gene, amplification of archaeal *amoA* gene showed either one or multiple amplicons being amplified but one of the amplicons was of a similar size to that of the gene of interest (i.e. ~557 bp; Figure 6.9). Despite, several attempts to improve the PCR by using different PCR solution mixtures and different annealing temperatures; PCR yields were not sufficient to generate a clone library to confirm the amplification of archaeal *amoA* genes.

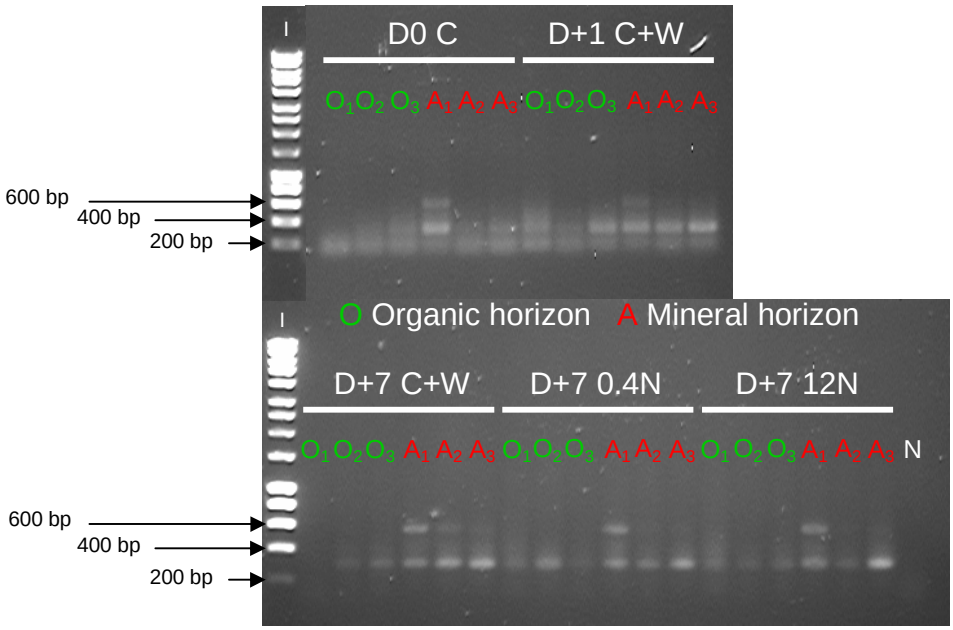

Figure 6.9: Agarose gel electrophoresis (1% agarose) of representative PCR amplifications targeting the archaeal *amoA* genes from the microcosm experiment soil samples of the organic (**O**) and mineral (**A**) horizons at Day+7. **C**: control without water microcosms; **C+W**: control + water microcosms; **0.4N**: 0.4 kg N ha^{-1} yr^{-1} ~pH 4 microcosms; **12N**: 12 kg N ha^{-1} yr^{-1} ~pH 4 microcosms; **D0**: before any treatments; **D+1**: one day after treatment; **D+7**: seven days after treatment; **N**: PCR negative control. The numbers beside O and A indicate the microcosm replicate numbers. The Hyperladder™ I (Bioline, London, UK; **l**) was used as a size standard.

6.2.5.2.2 nxrA and Nitrobacter spp. 16S rRNA gene analysis

The second step of the nitrification process was investigated via the targeting of the *nxrA* gene and the *Nitrobacter spp*. 16S rRNA gene. PCR amplification of the *nxrA* gene yielded multiple different sized amplicons with one of these amplicons being of a

similar size to that of the gene of interest (data not shown). However, no further PCR improvements or sequencing were performed in order to determine whether the amplicons were related to the gene of interest. In contrast, amplification of *Nitrobacter spp*. 16S rRNA gene yielded specific and strong PCR products of a similar size to that of expected (i.e. 225 bp; Figure 6.10). The intensity of PCR products did not differ between soil horizons or treatments at Day+7. However, no clone library was generated to confirm that the PCR products were related to *Nitrobacter spp*. 16S rRNA gene.

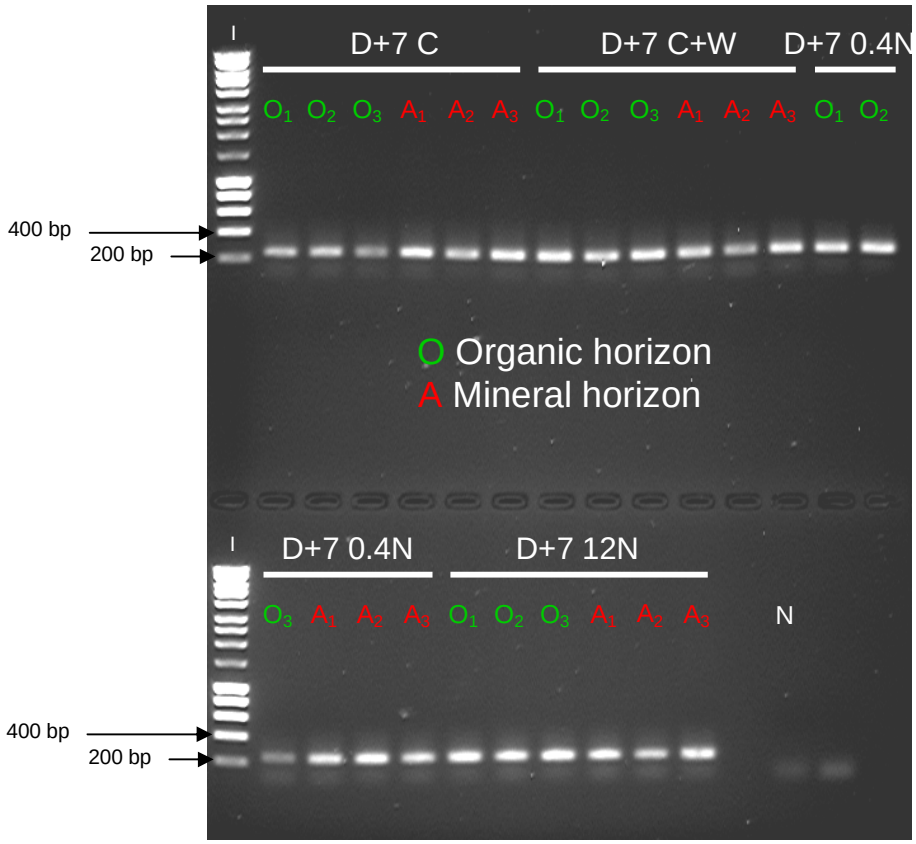

Figure 6.10: Agarose gel electrophoresis (1% agarose) of representative PCR amplifications targeting *Nitrobacter spp.* 16S rRNA genes in the microcosm experiment soil samples of the organic (**O**) and mineral (**A**) horizons at Day+7. **C**: control without water microcosms; **C+W**: control + water microcosms; **0.4N**: 0.4 kg N ha^{-1} yr^{-1} ~pH 4 microcosms; **12N**: 12 kg N ha^{-1} yr^{-1} ~pH 4 microcosms; **D+7**: seven days after treatment; **N**: PCR negative control. The numbers beside O and A indicate the microcosm replicate numbers. The Hyperladder™ I (Bioline, London, UK; **I**) was used as a size standard.

6.2.5.3 Denitrification

narG and *napA* genes (encoding for nitrate reduction) and *nirS* gene (encoding for nitrite reductase) could not be amplified by PCR from any of the microcosms despite the used of different PCR solution mixes, different annealing temperatures and the use of different primer pairs for the *nirS* gene (Table 6.4). PCR amplification of *nosZ* gene (encoding for the nitrous oxide respiration) yielded amplicons of different sizes and one of these amplicons was of a similar size to that of the gene of interest but the intensity of PCR products was extremely low (data not shown). No further PCR improvements or clone library were attempted. In contrast, *nirK* genes (encoding for nitrite reductase) were amplified with a product similar in size to that expected (i.e. 326 bp; Figure 6.11). However, no clone library was generated from these PCR products to confirm that the amplicon amplified were related to *nirK* genes. No difference in the intensity of *nirK* PCR products were found between soil horizons, over time or between treatments (Figure 6.11).

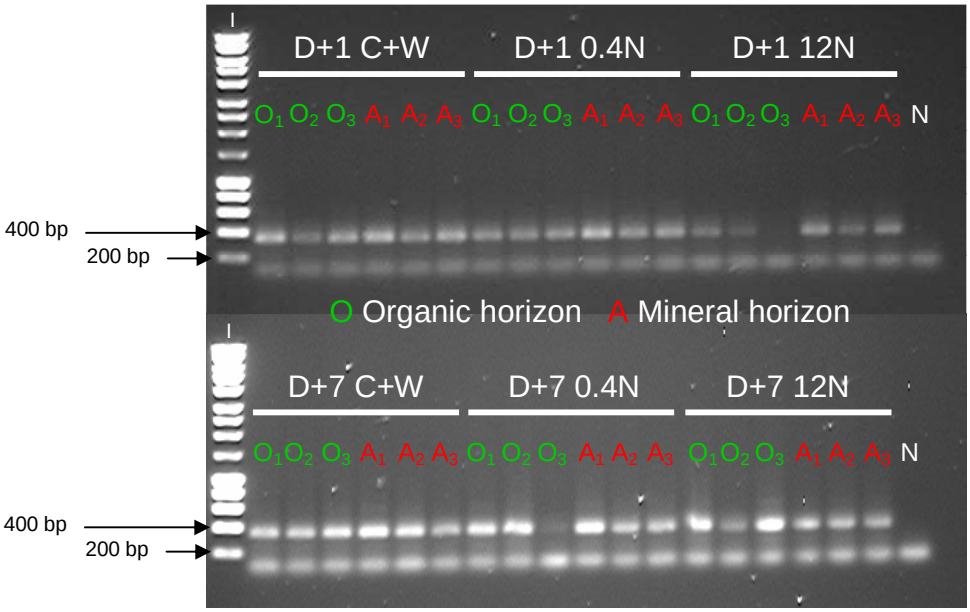

Figure 6.11: Agarose gel electrophoresis (0.8% agarose) of representative PCR amplifications targeting *nirK* genes from the microcosm experiment soil samples of the organic (**O**) and mineral (**A**) horizons at Day+7. **C+W**: control + water microcosms; **0.4N**: 0.4 kg N ha^{-1} yr^{-1} ~pH 4 microcosms; **12N**: 12 kg N ha^{-1} yr^{-1} ~pH 4 microcosms; **D+1**: one day after treatment; **D+7**: seven days after treatment; **N**: PCR negative control. The numbers beside O and A indicate the microcosm replicate numbers. The Hyperladder™ I (Bioline, London, UK; **l**) was used as a size standard.

6.3 Discussion

The structure of both bacterial and archaeal communities were very different between organic and mineral horizons (Figure 6.5; Table 6.1). Microbial abundance also showed differences between soil horizons, with ~2.2 times more archaea in the mineral than in the organic horizons. Bacterial *amoA* gene abundance was also ~2.4 times higher in the mineral than organic horizon showing also that for some N-cycling functional guilds different soil horizons may represent a different environment, which confirmed this trend found within soil samples of the plot experiment (see Chapter 5). Bacterial *amoA* gene abundance was previously found to decrease with soil depth within different pasture soils but at deeper soil depth than investigated in this current microcosm experiment (Di *et al.*, 2010). Therefore, these considerable differences in the microbial communities between soil horizons showed that investigating the different microbial communities within both horizons is relevant and of importance to understand their responses to different environmental changes.

6.3.2 Soil water content is a dominant driver of microbial communities

This study showed that soil water content had a strong effect on both bacterial and archaeal communities in High Arctic tundra soil. Water-addition increased the soil water content in comparison to the control microcosms by 18% and 23% within the organic and mineral horizons, respectively (Figure 6.1). Bacterial community structure differed greatly between microcosms without and with water-addition within both soil horizons (Figure 6.1; Table 6.1). Archaeal community structure was also strongly affected by water-addition in the organic horizon; while in the mineral horizon, a clear difference due to water-addition was only found between control and control + water microcosms (Figure 6.1; Table 6.1). The influence of water was confirmed by the significant correlations between bacterial community structure and soil water content within each soil horizon, while for the archaeal community structure, correlations were significant only within the organic horizon (Table 6.2).

The absence of a significant correlation between archaeal community structure and soil water content within the mineral horizon indicated that water was not the main driver of the changes in archaeal community structure within this horizon. Rinnan *et al.*, (2007) found that warming and shading had significant effects on the bacterial community structure as determined by PLFA analysis not only within the organic horizon of subarctic heath. However, both warming and shading increased only the soil temperature of 1.2 – 2.0 ºC, but significantly decreased the soil water content by 37% and 21% in the warming and shading treatments, respectively. Thus, the impact of warming and shading on the bacterial community structure could in fact be a side effect of the decrease in soil water content and so water would remain the dominant controlling factor.

Effects of water-addition on the structure of microbial communities differed between communities and soil horizons. The addition of water significantly increased terminal restriction fragments (T-RF) richness and the Shannon diversity index for the bacterial community within the organic horizon of all the microcosms which received water (with or without N addition) at Day+7 (Figure 6.4). In contrast, for the archaeal community structure, T-RF richness decreased and the Shannon diversity index significantly decreased within the organic horizon of the control + water microcosms in comparison to the control microcosms at Day+7. Thus, the effect of water-addition on microbial community structures can be positive, such as for the bacterial, or negative for the archaeal community structure. Increases in soil water content might represent more favourable environmental conditions for the bacterial community structure enabling higher diversity of dominant bacterial groups, whilst diversity within the archaeal community seems to be inhibited by water-addition, decreasing the diversity of dominant archaeal group. For example, Høj *et al.* (2006) found a new euryarchaeotal cluster within relatively well-drained solifluction samples which was not present within poorly drained soil and lake sediments samples taken in Svalbard.

Bacterial and archaeal abundance showed less noticeable effects due to water-addition than was found for changes in the structure of these communities. Bacterial abundance increased, but not significantly and only within the organic horizon of the control + water microcosms when compared to the control microcosms (Figure 6.6).

Archaeal abundance slightly increased, but not significantly, within the organic horizon of the control + water microcosms. However, no changes in the abundance of either domains were found within the mineral horizon. Rinnan *et al.* (2007) found a decrease of C microbial biomass (measured by chloroform fumigation) within the organic and mineral horizons by 10-17% in warming and shading treatments, which lead to a strong decrease in soil water content (see above). They also investigated the total bacterial PLFA content within both soil horizons and did not find any significant effect of warming or shading treatments. Microbial biomass (measured by chloroform fumigation) within the top soil (0-5 cm) in High Arctic semi-desert was found to increase by 24% after weekly water-addition over ~10 weeks, corresponding to 8 mm precipitation per plot (Illeris *et al.*, 2003). Thus, increases in soil water content may increase the microbial community abundance in arctic soils and inversely, longer periods of drought might decrease the microbial biomass.

Addition of water had a stronger effect on the bacterial and archaeal communities within the organic than in the mineral horizons. ANOSIM of the bacterial and archaeal community structure within the organic horizon showed higher R value (R = 0.89 and 0.96, respectively) between control and control + water microcosms than within the mineral horizon (R = 0.63 for both communities) indicating that bacterial and archaeal communities structure from the control and control + water microcosms were more different within the organic than the mineral horizon. Changes of bacterial and archaeal T-RF richness, Shannon diversity index and abundance were found only within the organic horizon, where stronger correlation (i.e. higher ρ values) between bacterial or archaeal communities structure and soil water content were found. Moreover, the bacterial and archaeal community structure within the organic horizon showed greater changes in the control + water microcosms over time, which were not found in the mineral horizon. Thus, the bacterial and archaeal communities within the organic horizon showed higher sensitivity to changes in soil water content than in the mineral horizon. The higher sensitivity of bacterial and archaeal community within the organic than in the mineral horizon might be due to the lower water availability in the organic horizon, as the volumetric water content was 23% and 28% lower in the organic than in the mineral horizon for the control and control + water microcosms, respectively.

Changes in soil water content due to snowmelt, increase in precipitation, or permafrost melting, are likely to affect the bacterial and archaeal community structure within both soil horizons.

6.3.3 Responses of microbial communities to N addition

Bacterial and archaeal communities showed strong responses to the addition of nitrogen. However, responses of microbial communities to N addition differed between microbial communities, soil horizons and rates of N addition.

6.3.3.1 Response of bacterial community to N addition

Bacterial community structure within the organic horizon did not change with N addition of 0.4 kg N ha^{-1} yr^{-1} but was affected by rate of 12 kg N ha^{-1} yr^{-1} (Figure 6.5; Table 6.1). However, at Day+1 the bacterial community structure in the 12 kg N ha^{-1} yr^{-1} microcosms showed greater variation to those in the control + water and 0.4 kg N ha^{-1} yr^{-1} microcosms to those in the control microcosms. This particular difference of bacterial community structure within the organic horizon of the 12 kg N ha^{-1} yr^{-1} microcosms at Day+1 was possibly due to the soil pH. Decreases in soil pH after addition of NH_4NO_3 has been previously reported in alpine tundra (Fisk & Schmidt, 1996; Schmidt *et al.*, 2004). The decrease of soil pH is unlikely due to the addition of water with ~pH 4, as the soil pH was significantly lower in the 12 kg N ha^{-1} yr^{-1} than 0.4 kg N ha^{-1} yr^{-1} microcosms despite addition of water ~pH 4 for both treatments. Bacterial community structure within the organic horizon was significant and strongly (P = 0.07; ρ = 0.41) correlated to the soil pH. T-RF richness and Shannon diversity index significantly decreased, and bacterial abundance decreased in the organic horizon (Figure 6.6), indicating that the decrease of soil pH (of ~1 pH unit) is likely to negatively affect the bacterial community structure and abundance of the 12 kg N ha^{-1} yr^{-1} microcosms at Day+1. However, the bacterial community structure within the organic horizon of the 12 kg N ha^{-1} yr^{-1} microcosms at Day+7 was more similar to the control + water and 0.4 kg N ha^{-1} yr^{-1} microcosms than to the control microcosms, with

similar T-RF richness and Shannon diversity index (Figure 6.4), and the correlation between bacterial community structure and soil pH was no longer significant at Day+7. Moreover, bacterial abundance increased at Day+7 (Figure 6.6). Thus, the effect of low soil pH was not continuous and both the structure and abundance of bacterial communities, showed some resilience to changes in soil pH. Nevertheless, bacterial community structure within the organic horizon of the 12 kg N ha^{-1} yr^{-1} microcosms remained significantly different from those in the control + water and 0.4 kg N ha^{-1} yr^{-1} microcosms at Day+7. Therefore, bacterial community structure within the organic horizon seemed to be only affected by a high rate of N addition. Rinnan *et al.* (2007) found significant changes in bacterial community structure within the organic horizon in subarctic tundra determined by PLFA analysis, after 15 years of N addition at rate of 10 kg N ha^{-1} yr^{-1} (a rate similar to, but much longer in duration to the 12 kg ha^{-1} treatment used in this thesis). Schmidt *et al.* (2000) also found changes in bacterial community structure in the organic horizon assessed by PLFA after N fertilisation of a very considerable 400 kg N ha^{-1} over 4 years.

In contrast to the organic horizon, bacterial community structure within the mineral horizon was significantly affected by N addition of 0.4 kg N ha^{-1} yr^{-1} in comparison to the control + water microcosms, showing that bacterial community was sensitive to low N addition and might be N-limited within the mineral horizon. However, N addition of 12 kg N ha^{-1} yr^{-1} did not increase the effect further on the bacterial community structure, although differences were nearly significant to the control + water microcosms at $P < 0.05$ (Table 6.1). The absence of a significant difference between the bacterial community structure of the 12 kg N ha^{-1} yr^{-1} and the control + water microcosms might be due to different bacterial community structures that were found between soil replicates used (Appendix 6.1). Nevertheless, bacterial community structure of the 0.4 kg N ha^{-1} yr^{-1} and 12 kg N ha^{-1} yr^{-1} microcosms were not significantly different, showing that there is no linear correlation between N addition rates and effects on bacterial community structure. The absence of a greater effect on bacterial community structure with a higher N addition might indicate that other nutrients may also limit or influence the bacterial community. Little is known about changes of bacterial community to N addition within mineral or deeper soil horizons.

Only Rinnan *et al.* (2007) showed significant changes in bacterial community structure after N fertilisation within the mineral horizon in subarctic heath.

Bacterial abundance showed lower variation in response to N addition than was found for bacterial community structure within both soil horizons. Microcosms which received N, did not show clear trends toward an increase or decrease in bacterial abundance. Rinnan *et al.* (2007) found no changes in total bacterial PLFA content within the organic horizon in subarctic tundra after N addition. In contrast, increases in bacterial biomass (obtained by microscopy) were found 44 days after addition of 5 kg N-NH_4^+ ha^{-1} yr^{-1} within the organic horizon at an experimental site near Ny-Ålesund (Stapleton *et al.*, 2005). Decrease in bacterial abundance was found only at Day+1 in 12 kg N ha^{-1} yr^{-1} microcosms which could be related to a decrease in soil pH, while at Day+7 bacterial abundance decreased in 0.4 kg N ha^{-1} yr^{-1} microcosms which could not be related to a decrease in soil pH. Thus, low rates of N addition might decrease bacterial abundance within the organic horizon. No changes in bacterial abundance were found within the mineral horizon. Thus, N addition clearly did not affect bacterial abundance within the mineral horizon. Conversely, Rinnan *et al.* (2007) found that total bacterial PLFA content increased by 22% within the mineral horizon, after 15 years of N addition in subarctic heath. Therefore, higher N additions, over longer periods of time might be needed to change bacterial abundance in the mineral horizon.

6.3.3.2 Response of archaeal community to N addition

N addition had a strong effect on archaeal community structure within the organic horizon. Both communities from the 0.4 kg N ha^{-1} yr^{-1} and 12 kg N ha^{-1} yr^{-1} microcosms were significantly different from those in the control + water microcosms (Figure 6.5; Table 6.1). Increases in N addition rates from 0.4 to 12 kg N ha^{-1} yr^{-1} seemed to increase the effect on archaeal community structure (i.e. an increase of R value from 0.61 to 0.83; Table 6.1), although no significant difference was found between the archaeal community structure of the 0.4 and 12 kg N ha^{-1} yr^{-1} microcosms. The effect of N addition on the archaeal community structure could not be related to any positive or negative effect on the T-RF richness or Shannon diversity index. Archaeal

abundance was not affected by N addition within the organic horizon, which is in contrasts with a study in the alpine tundra that showed a decrease in archaeal abundance in the top soil after N addition (under the form of urea) of 115 kg N ha^{-1} over 10 years (Nemergut *et al.*, 2008).

Responses of archaeal community structure within the mineral horizon to N addition were much more complex than within the organic horizon. The different rates of N addition resulted in opposite effects on archaeal community structure which was highlighted by the significant (P = 0.001) archaeal community structure differences between the 0.4 and 12 kg N ha^{-1} yr^{-1} microcosms (R = 0.94). Archaeal community structure in the 0.4 kg N ha^{-1} yr^{-1} microcosms grouped with the community from the control microcosms, whilst the archaeal community structure from the 12 kg N ha^{-1} yr^{-1} microcosms was more similar to those of the control + water microcosms but remained significantly different from these (Figure 6.5; Table 6.1). The absence of differences in structure of archaeal community between control and 0.4 kg N ha^{-1} yr^{-1} microcosms indicated that a low rate of N addition may have counter-balanced the effect of water-addition and that N might be a more important driver of the archaeal community structure within the mineral horizon than water. This is confirmed by the significant correlations between archaeal community structure in the mineral horizon and the NO_3^- and NH_4^+ concentration and the absence of significant correlation to soil water content (Table 6.2). The difference in the structure of archaeal communities between control + water and 12 kg N ha^{-1} yr^{-1} microcosms was low (R = 0.30) showing that a high rate of N addition did not strongly affect the archaeal community structure. Thus, in comparison to the control + water microcosms, N addition of 0.4 kg N ha^{-1} yr^{-1} had a stronger effect on the archaeal community structure than the addition of 12 kg N ha^{-1} yr^{-1}. However, N addition by itself cannot explain why the archaeal community structure of 12 kg N ha^{-1} yr^{-1} microcosms was more similar to that in the control + water microcosms than in the 0.4 kg N ha^{-1} yr^{-1} microcosms. Other factors differentially influenced the archaeal community structure within the N treatments. The decrease of soil pH in the mineral horizon related to N addition, which differed between N addition rates may explained these differences. Changes in the structure of Crenarchaeal 16S rRNA genes and *amoA* genes or Group 1.1c Crenarchaeota have been found with changes in soil pH (Nicol *et*

al., 2008; Lehtovirta *et al.*, 2009). However, decreases in soil pH were also found to increase the abundance of archaeal *amoA* gene and Group 1.1c Crenarchaeota (Nicol *et al.*, 2008; Lehtovirta *et al.*, 2009) over a similar decrease in soil pH to that found after N addition (i.e. ~1.5 pH unit) in this current study; while no changes in archaeal abundance were found in the 0.4 or 12 kg N ha^{-1} yr^{-1} microcosms (Figure 6.6). Thus, the potential effects of soil pH on the archaeal community structure remain unclear.

6.3.3.3 Response of N-functional guilds to N addition

The different N-functional guilds were not affected by N addition. PCR amplification of genes representative of the N-cycling functional guilds involved in N fixation, nitrification and denitrification were not higher in presence/absence and/or band intensity in the N treatments than in the control or control + water microcosms (Figure 6.9 – 11). Bacterial *amoA* gene abundance did not show any clear trend in response to N addition. Lamb *et al.* (2011) similarly did not find any changes in bacterial *amoA* abundance within the organic horizon after 15 years of N fertilisation in High Arctic tundra. Verhamme *et al.* (2011) found that bacterial *amoA* abundance significantly increased in response to NH_4^+ addition only at a rate of 2 g N-NH_4^+ kg^{-1} soil after 14 days of incubation in microcosms, but not at a rate of 0.2 g N-NH_4^+ kg^{-1} soil. Both of these rates are higher than the rate of N-NH_4^+ added in the microcosms in both soil horizons in this current study. Thus, a higher N addition rate might be needed to change the bacterial *amoA* abundance. The decrease in soil pH did not have any effect on the bacterial *amoA* abundance, confirming the results of Nicol *et al.* (2008) showing no influence of soil pH on bacterial *amoA* gene abundance. It is surprising that no increases in amplification/abundance of some the N-functional guilds involved in nitrification and denitrification were found as both NO_3^- and NH_4^+ concentration decreased over time within the organic horizon, indicating that nitrification and denitrification may occur. Moreover, amounts of NH_4NO_3 added to both soil horizons were similar at the beginning of the microcosm experiment, showing that within the mineral horizon a rapid decrease in both NO_3^- and NH_4^+ concentration may have occurred. Thus, the absence of clear changes in N-functional guilds despite changes in

NO_3^- and NH_4^+ concentration, may indicate that only the activity of these communities is affected and not the abundance. Other microbial communities might also be involved in these processes, such as fungi which were shown to potentially play an important role in denitrification in arctic soil (Ma *et al.*, 2008; Siciliano *et al.*, 2009). However, methodological issues to amplify the different N-functional genes cannot be excluded when explaining the differences in functional gene amplification in relation to NO_3^- and NH_4^+ concentration changes over time. Therefore, the knowledge of the communities involved in N-cycling and their response to N addition remains limited.

6.4 Conclusions

An increase in soil water content by ~20% strongly affected both bacterial and archaeal communities within the organic and mineral soil horizons in High Arctic tundra. However, responses of microbial communities to water-addition differed between communities and soil horizons. The bacterial community was positively affected by water-addition with increases in both bacterial abundance and in the diversity of dominant groups, whilst water-addition negatively affected archaeal abundance and the diversity of dominant groups. Both bacterial and archaeal communities showed greater sensitivity to water-addition within the organic than in the mineral horizons. Therefore, soil water content was found to be a dominant driver of the bacterial and archaeal communities in different soil horizons. Consequently, potential increases in soil water content due to increases in precipitation or melting of the permafrost as a result of global changes, is likely to affect the bacterial and archaeal communities in the different soil horizons of High Arctic tundra soil.

N deposition was found to significantly affect bacterial and archaeal communities within the organic and mineral soil horizons. Responses of microbial communities to N deposition were dependant firstly upon the microbial community investigated, secondly on the soil horizons examined and finally upon the rates of N deposition. Indeed, bacterial community structure was only affected by an N addition rate of 12 kg N ha^{-1} yr^{-1} within the organic horizon, while within the mineral horizon N addition rates of 0.4 and 12 kg N ha^{-1} yr^{-1} resulted in similar effects upon the structure of

the bacterial communities. In contrast, the effect of N deposition on archaeal community structure in the organic horizon increased with increasing N addition rates, while in the mineral horizon the N addition rate of 0.4 kg N ha^{-1} yr^{-1} had a stronger effect upon community structure than was found with the higher N addition rate. Hence overall, responses of bacterial and archaeal communities to N deposition, within different soil horizons in High Arctic tundra were complex, but highlighted the fact that N is an important driver of these communities and that increases in N deposition in the High Arctic may affect the structure of both bacterial and archaeal communities. Decreases in soil pH due to N addition was also likely to affect microbial communities to some extent, as was seen for bacterial community structure within the organic horizon which was possibly negatively affected by decrease in soil pH. Thus, this study showed that changes in soil pH following N deposition may offer a possible additional explanation for changes in microbial communities.

In summary, bacterial and archaeal communities are highly sensitive to changes in soil water content mainly, but also to nitrogen content within different soil horizons. Thus, increases in precipitation, and N deposition are likely to affect High Arctic soil microbial communities. This study also demonstrate that responses of bacterial and archaeal communities to environmental changes differ between soil horizons and stress the importance of investigating responses of microbial communities to global changes within the different soil horizons. Most studies investigating responses of microbial communities to global changes in arctic ecosystems have focused only on the top soil layer (e.g. Schmidt *et al.*, 2000; Stapleton *et al.*, 2005; Lamb *et al.*, 2011) leading possibly to an underestimation of the full impact of global change on microbial communities in arctic soils.

Chapter 7: Conclusions and perspectives

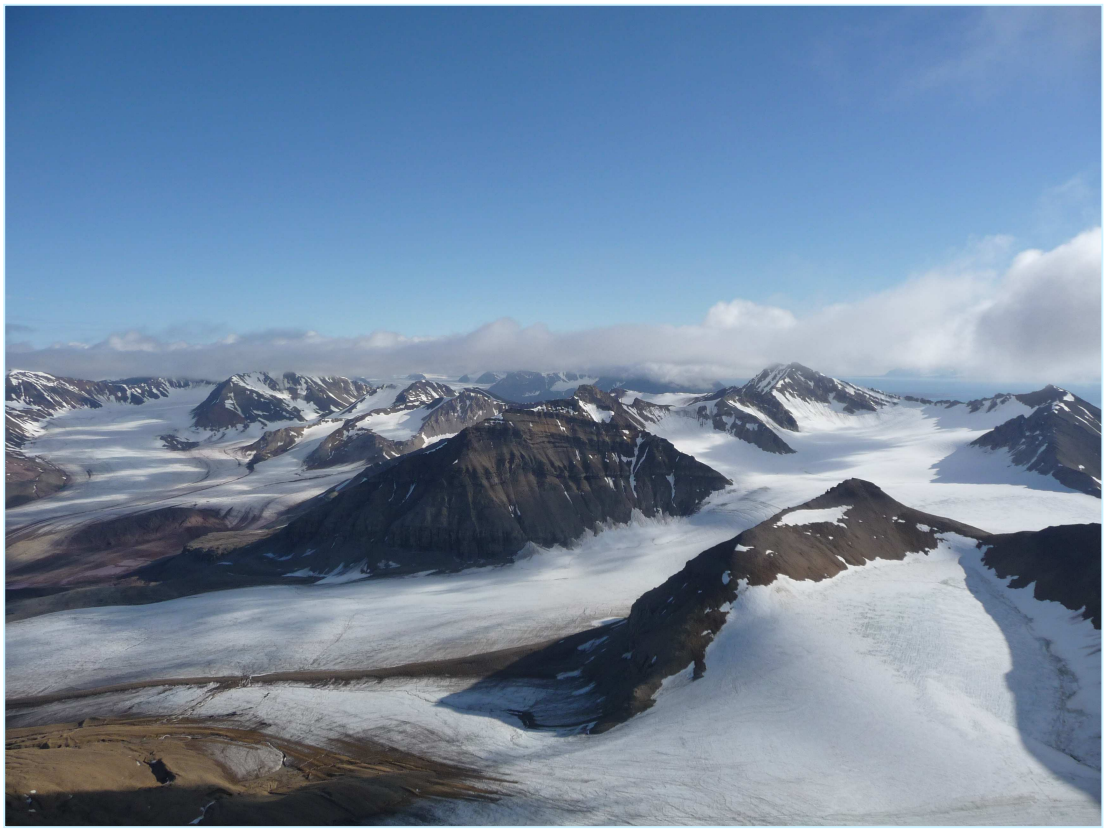

View of glaciers Vestre Brøggerbreen (on the right) and Austre Brøggerbreen (on the left) from Schetelig mountain (694 m alt.) the 1st of August 2010.

7.1 Summary of the main findings

7.1.1 Soil horizons harbour distinct microbial communities

This study showed that bacterial and archaeal community structures differed significantly between the organic and mineral horizon in High Arctic tundra soil near Ny-Ålesund (Svalbard). Although some differences were found in the fungal community structure from both soil horizons, fungi showed high variability between the organic and mineral horizon, maybe due to the presence of mycelium overlapping both soil horizons (Landeweert *et al.*, 2003; Hartmann *et al.*, 2009). These results for the bacterial, archaeal and fungal community structure were found for the plot experiment in 2009 (Chapter 3), 2010 (Chapter 4) and the microcosm experiment (Chapter 6). Moreover, when the nMDS and ANOSIM analysis were performed on a similarity matrix for each microbial community structure including the samples from fieldwork 2009 and 2010, similar results were found (Figure 7.1 A; Table 7.1), highlighting the consistency of differences in microbial community structure between the organic and mineral horizons between years.

Table 7.1: Two-way ANOSIM of the archaeal, bacterial and fungal communities structure between soil horizons (i.e. organic *vs.* mineral) and years of soil sampling (i.e. 2009 *vs.* 2010) against the others factors (i.e. soil horizons, year of soil sampling, days of soil sampling and N treatments). The R values and the significance level (in brackets) are given.

Factors compared	Bacteria	Archaea	Fungi
Organic *vs.* Mineral	0.62 (0.00005)	0.64 (0.00005)	0.18 (0.005)
2009 *vs.* 2010	0.63 (0.00005)	0.70 (0.0001)	0.25 (0.002)

The abundance of bacterial, archaeal and fungal communities varied with soil horizons. Hence bacterial and fungal communities showed in 2009 for the plot experiment higher abundance in the mineral horizon, whilst in 2010 similar abundances between both soil horizons were found. The archaeal community consistently showed a

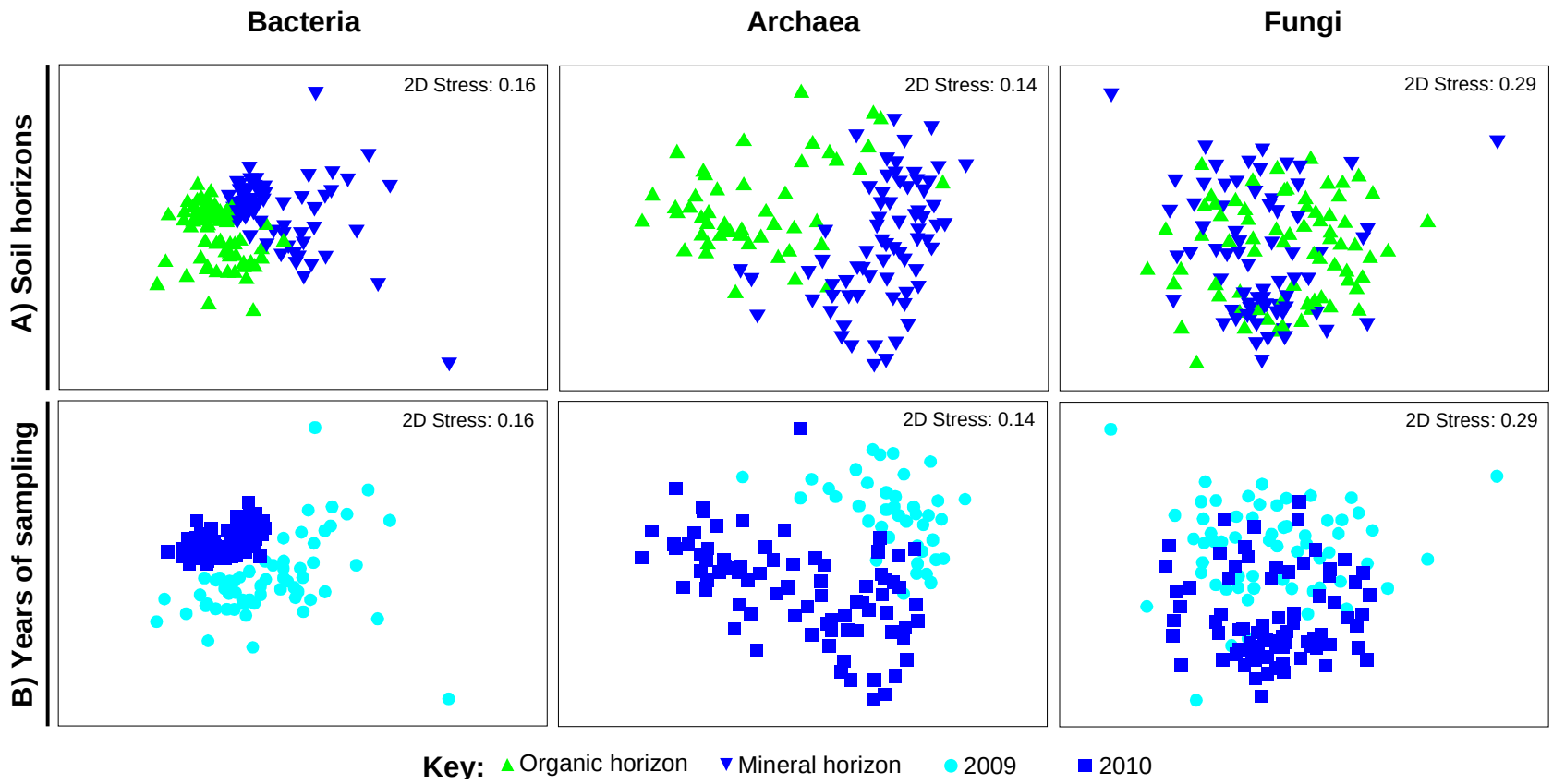

Figure 7.1: nMDS plots of the bacterial, archaeal and fungal community structure between the organic and mineral soil horizons, and between 2009 and 2010 soil sampling, from soil samples taken from the organic and mineral horizons in the control + water plots, 4 kg N ha^{-1} yr^{-1} ~pH 4 plots in 2009 and 12 kg N ha^{-1} yr^{-1} ~pH 4 plots in 2010 and for the different date of sampling for each year (see Figures 3.13 and 4.9) **A**: plots showing the influence of soil horizons on microbial community structure; **B**: plots showing the influence of year of sampling on microbial community structure. Soil horizons and years of soil sampling are as indicated in the key. The 2D stress is given for each nMDS plot.

higher abundance in the mineral horizon than in the organic horizon for the plot experiment (2009 and 2010 sampling) and for the microcosm experiment. Thus, the mineral horizon seems to represent an important habitat for the archaeal community, which should be taken into consideration when archaeal communities are studied.

Surprisingly, microbial community abundance did not decrease with soil depth despite the sharp decrease in soil total C, total N and water content. This contrasted with most results from the literature that show decreases in microbial abundance with soil depth/horizon (e.g. Fritze *et al.*, 2000; Taylor *et al.*, 2002; Fierer *et al.*, 2003; Brockett *et al.*, 2012). Thus, the mineral horizon may have more microhabitats for microbial communities to grow, protecting them against predation, and/or the higher water availability might explain this contrasting result with the prior literature.

The soil water content, total C and total N were found to be important drivers of the bacterial and archaeal community structure, and to a lesser extent to their abundance. Despite common drivers between bacteria and archaea, the hierarchy of drivers and the strength of their influence varied between communities. Nevertheless, the microcosm experiment clearly showed that soil water content was a dominant driver, greatly influencing the structure of bacterial and archaeal communities, and bacterial abundance. The influence of soil water content in bacterial and archaeal communities seemed to be stronger within the organic than the mineral horizon. The fungal community structure and abundance was only weakly correlated to environmental variables, likely due to the high variability of the fungal community, making it difficult to determine the main environmental drivers of the community.

7.1.2 Microbial communities are dynamic in High Arctic tundra soil

Variations in the structure and abundance of bacterial, archaeal and fungal communities were found over time for the plot experiment, and differed between microbial communities and soil horizons. The changes in microbial community structure and abundance over time occurred mainly within the mineral horizon. Thus, dynamic changes in microbial communities in the High Arctic tundra soil studied differed between the organic and mineral horizons. The archaeal community structure showed

greater changes in structure over time in comparison to the bacterial and fungal communities, and the bacterial community showed only small changes in structure over time. When the nMDS and ANOSIM analysis were performed on a similarity matrix for each microbial community structure including the samples from fieldwork 2009 and 2010, significant difference in the bacterial and archaeal communities structure between 2009 and 2010 were found (Figure 7.1 B; Table 7.1), indicating that changes in microbial communities over time occurred over both short (i.e. few days/weeks) and long (i.e. over years) period of time. Although, the difference in microbial communities structure between 2009 and 2010 could be due to either difference between year or between time of the summer period, as the 2009 sampling represented late summer sampling and in 2010 samples were taken in mid-summer. The abundance of bacterial and fungal community increased over time within the mineral horizon (and also within the organic horizon for the fungi) in the plot experiment in 2009, while no general trend was found in 2010. Thus, changes in microbial abundance are not consistent over the summer period. The changes in structure and abundance of microbial communities occurred over both a short period of time in 2009 (i.e. 9 days) and a longer period of time in 2010 (i.e. 27 days), showing that microbial communities in High Arctic soil are able to change rapidly in structure and/or abundance.

7.1.3 Microbial communities are sensitive to N deposition

Microbial community structure was affected by N deposition in the High Arctic tundra soil studied, and the changes differed between microbial communities, soil horizons, and rates of N deposition. In contrast, microbial community abundance was not affected by N deposition. Bacterial and fungal community structure changed one and seven days post N application, respectively, only within the mineral horizon of the plot experiment in 2010. Thus, the response of the bacterial and fungal community structure to N deposition was specific to the mineral horizon, was rapid, and not continuous over time.

Bacterial community structure within the mineral horizon was affected by low rate of N deposition (i.e. 4 kg N ha^{-1} yr^{-1}), but a higher rate of N deposition (i.e. 12 kg N

ha^{-1} yr^{-1}) did not increase the effect on bacteria. Similar results were found during the microcosm experiment, showing no increase in the response of the bacterial community structure with increase in N addition rate within the mineral horizon. Thus the bacterial community in the mineral horizon was sensitive to low rate of N deposition, but other nutrients might also drive the bacterial community as the response of this community is limited in time and did not increase with higher rates of N addition.

The absence of an effect of N deposition on microbial community structures within the organic horizon for the plot experiment is likely to be explained by the need of higher N input rate to affect the microbial community from the organic horizon. The microcosm experiment confirmed that the bacterial community structure within the organic horizon is only affected by a higher rate of N input. Thus, N was perhaps readily available within the organic horizon in the form of organic compounds, and only a high rate of mineral N can overcome the ready availability of organic N.

The archaeal community structure was not affected within either horizons of the plot experiment but was affected within both soil horizons of the microcosm experiment. Thus, the specific conditions of the microcosm experiment, such as the absence of competition with the plant community for nutrient uptake, the high amount of water used for the N application, are likely to explain the specific response of the archaeal community structure within the microcosms experiment. Thus, other environmental drivers than N, are likely to drive archaeal community in arctic soil

The response of microbial communities to N deposition was extremely rapid, only one day post N application was needed to affect the bacterial community structure in the plot and microcosms experiment, seven days post N application for the fungal community structure in the plot experiment, and only one day for the archaeal community structure of the microcosm experiment. This is in contrast with some studies suggesting that the response of microbial communities structure to environmental changes such as warming, N addition, shading can take more than one decade in arctic ecosystems due to the slow turnover of microbial communities (Rinnan *et al.*, 2007; Walker *et al.*, 2008; Lamb *et al.*, 2011). In conclusion, this study showed that N deposition event in High Arctic may impact upon the microbial community in soil.

7.2 Limitations and future directions of the study

7.2.1 What are the differences in microbial communities between soil horizons?

This study clearly showed that microbial community structure and abundance greatly differed between the organic and mineral soil horizons. However, several questions in relation to the extent of the difference remain unresolved. Does the diversity of bacteria, archaea and fungi differed greatly between soil horizons or does the microbial diversity within one horizon represent a subset of the diversity of the other one? Do both soil horizons harbour the same diversity of microbial functions, or some functions are occurring predominantly or specifically within one soil horizon? Answering these questions is important to understand the importance of studying microbial communities in both soil horizons and their response to environmental changes, and to assess the real diversity in arctic soil, which have been mainly studied within the organic horizon until now (e.g. Chu *et al.*, 2010).

T-RFLP analysis already gave some information about the extent of the differences between the microbial communities from the organic and mineral horizon, although it focuses only on the dominant microbial taxa. Hence, T-RF richness and Shannon diversity index of the bacterial community showed either no difference between soil horizons or higher richness and diversity within the mineral horizon, for the plot experiment. In contrast, the richness and diversity of the archaeal community was always higher and often significantly higher within the organic horizon for the plot and microcosm experiments, despite the lower overall relative abundance of the archaeal community within this horizon. The fungal community did not show any trends or significant differences. However, these microbial indices do not represent the real microbial diversity in soil (Blackwood *et al.*, 2007). High-throughput sequencing (e.g. 454 pyrosequencing) enabling the investigation of an important part of the metagenome of an ecosystem, has previously been used to target bacterial, archaeal (Roesch *et al.*, 2007) and fungal communities (Buée *et al.*, 2009) in soil. Thus, the use of high-

throughput sequencing would clearly indicate the differences in diversity, and relative abundance of microbial taxa in the different soil horizons.

The investigation of N-functional genes involved in the different processes of the N-cycle, already gave some indications about the potential difference in microbial functions between soil horizons. Thus, bacterial *amoA* genes were found to be more abundant in the mineral horizon of the microcosm experiment. Similarly, *nxrA* gene, encoding for the nitrite oxidoreductase, was also potentially found in higher abundance within the mineral horizon (i.e. PCR products yielded higher intensity within the mineral horizon). These results may indicate that nitrification occurs preferentially within the mineral horizon. Thus, investigating a microbial function within only one soil horizon may underestimate the extent of the function within arctic soil. Shotgun metagenomic was used to identify metabolic pathways and functional genes in soil (Tyson *et al.*, 2004; Allen & Banfield 2005), and its use on the different soil horizons would characterise the diversity of microbial functions within each horizon, and their potential specificity to a soil horizon, avoiding the technical problem to set up PCRs for each gene studied.

7.2.2 What is the nature of N deposition effects on microbial communities?

N deposition was found in this study to affect microbial communities in the High Arctic. However, the understanding of the effect of N deposition on microbial communities is limited. Only a change in microbial community structure was found, which could not be related to an increase or decrease in richness or diversity in the community profiles obtained or changes in gene abundance. Thus, the first objectives would be to investigate if N deposition positively or negatively affects microbial communities and which microbial groups are affected. The use of high-throughput sequencing (e.g. 454 pyrosequencing) on the soil samples where responses of bacterial and fungal community structures to N deposition were found, would enable greatly improved understanding of the effect of N deposition. Firstly, the use of high-throughput sequencing on this samples (including samples from control and 12 kg N ha^{-1} yr^{-1} plots) would enable confirmation (or not) of the results obtained by T-RFLP, indicating if both

techniques can be used in parallel, with T-RFLP as a first step technique to reduce the number of samples of interest to target with high-throughput sequencing. Secondly, effects of N deposition on the diversity and on the relative abundance of the bacterial and fungal communities would be obtained using high-throughput sequencing.

This study did not manage to properly assess changes in function related to the N-cycle after N deposition, and did not investigate the response to other microbial function (e.g. related to C-cycle). Shotgun metagenomics would enable relevant genes to be identified (Tyson *et al.*, 2004; Allen & Banfield 2005), such as the genes related to the N-cycle but also related to other biogeochemical cycles, and identify any changes in the relative abundance and diversity in response to N deposition.

For the plot experiment in 2010, ^{15}N-dual labelled NH_4NO_3 was used to simulate N deposition, enabling the fate of N within the soil to be followed. However, the fate of ^{15}N can also be followed within the microorganisms that assimilated ^{15}N. Stable isotope probing (SIP) has been used in microbial ecology to characterize the microbial activity, by targeting the active microbial community that uptake isotope-labelled substrate (Neufeld *et al.*, 2007). Thus, DNA-SIP could be used to target the bacteria, archaea and fungi that assimilated the added ^{15}N, then by performing pyrosequencing the diversity and relative abundance of these communities could be determined. DNA-SIP followed by pyrosequencing had already been used in the arctic using ^{15}N-labelled mono-ammonium phosphate (Bell *et al.*, 2011). Hence, the use of DNA-SIP for the plot experiment would enable determination of which microbial community (i.e. bacterial, archaeal and fungal) uptake ^{15}N, within each community which taxa uptake ^{15}N, and the proportion of the community that assimilate N in comparison to the total community (i.e. unlabelled and labelled). Thus, DNA-SIP could determine if all the communities assimilate N from N deposition or a specific part of the community, and if N represent an important nutrient for the entire microbial community.

Several improvements in the plot experiment could be made in order to increase the understanding of the impact of N deposition on microbial communities in the arctic. The plot experiment took place at the end of the summer period in 2009 and from mid-July to mid-August in 2010. However, none of these fieldworks started at the time of snowmelt, although the snowmelt period might represent an important period with an

important release of nutrients from the snowpack, including N from N deposition that mainly occur in solid form over winter (Kühnel *et al.*, 2011). Moreover, snowmelt represents the major input of water to High Arctic ecosystems which might have a major effect on microbial community, as water was shown to be a dominant factor in the soil studied. Thus, N deposition simulation could take place during or just after the snowmelt period with soil sampling following the N application. The soil sampling of this study focused on the vegetated area. However, polar desert and semi-desert ecosystems cover ~93% of the High Arctic (Bliss & Matveyeva, 1992) with plant cover that is not continuous to extremely sporadic or non-existent. Thus, the impact of N deposition might be different on bare soil, as soil organic matter is likely to be extremely low, making bare soil potentially more sensitive to input of N.

7.3 Perspectives

Studying microbial communities within different soil horizons in High Arctic soil was found in this study to be extremely important to estimate the real microbial diversity in arctic soil, but also to accurately estimate the response of microbial communities to environmental changes such as warming, potential increase in precipitation and N deposition. Thus, future studies in arctic soil investigating microbial communities should take into consideration the vertical distribution of microorganisms within the soil. Moreover, in this study the mineral horizon appeared to be the microbial habitat where microbial community was often more abundant, and where changes over time and in response to N deposition occurred. However, most of the prior studies in arctic soils have investigated the response of microbial communities to N addition only within the organic horizon (e.g. Schmidt *et al.*, 2000; Stapleton *et al.*, 2005; Lamb *et al.*, 2011). Moreover, Chu *et al.* (2010) investigated the bacterial diversity across the arctic region, focusing only on organic soil. Thus, if the mineral horizon in arctic tundra soil is indeed an important habitat for microbial activity, understanding of microbial communities in the Arctic could be extremely limited in that work. The importance of studying microbial communities and their response to environmental changes in different soils is unlikely to be limited in High Arctic tundra however, as many soils

have different soil horizons, and many studies found different microbial communities within different soil horizons (e.g. Berg *et al.*, 1997; Taylor *et al.*, 2002; Fierer *et al.*, 2003; Robinson *et al.*, 2009; Hartmann *et al.*, 2009)

The extreme environmental conditions in arctic regions and especially the low temperature are often considered to reduce the turnover of microbial communities (e.g. Rinnan *et al.*, 2007; Walker *et al.*, 2008; Lamb *et al.*, 2011). However, rapid responses of microbial communities to N deposition that changed only one or seven days post N application indicate that microbial communities can present a high turnover. Most studies that investigated the response of microbial communities in the Arctic to environmental changes did not take any soil samples in the following days post N application (e.g. Schmidt *et al.*, 2000; Stapleton *et al.*, 2005). Moreover, many studies had one sampling date over the entire summer period (e.g. Schmidt *et al.*, 2000; Rinnan *et al.*, 2007; Lamb *et al.*, 2011). Thus, having only one sampling date and a long time following N application is likely to miss a potential response of the microbial community. Studies that took only one sampling date imply that the response of microbial communities to environmental change is continuous in time but the microbial community is likely to be resilient to some extent. The studies that suggested that changes in microbial communities to environmental changes may take more than a decade, may in fact determine how many years is needed for the microbial community to be affected by the treatment in continuous or for a longer period of time over the summer (Rinnan *et al.*, 2007; Walker *et al.*, 2008; Lamb *et al.*, 2011). Thus, this thesis stresses the importance of taking early soil samples (i.e. during the week post treatment) and not only on one date of sampling, in order to accurately determine the response of microbial communities to environmental changes.

References

Aber JD, Nadelhoffer KJ, Steudler P & Melillo JM (1989) Nitrogen Saturation in Northern Forest Ecosystems. *BioScience* 39: 378–386.

ACIA (2005) Arctic climate impact assessment. *Cambridge University Press*, pp. 1042. Cambridge, UK.

Agnelli A, Ascher J, Corti G, Ceccherini MT, Nannipieri P & Pietramellara G (2004) Distribution of microbial communities in a forest soil profile investigated by microbial biomass, soil respiration and DGGE of total and extracellular DNA. *Soil Biol Biochem* 36: 859–868.

Ågren GI & Bosatta E (1988) Nitrogen saturation of terrestrial ecosystems. *Environ Pollut* 54: 185–197.

Allen EE & Banfield JF (2005) Community genomics in microbial ecology and evolution. *Nat Rev Microbiol* 3: 489–498.

Altschul SF (1991) Amino acid substitution matrices from an information theoretic perspective. *J Mol Biol* 219: 555–565.

AMAP (1998) Assessment report: Arctic pollution issues. *Arctic monitoring and assessment programme*, pp.859. Oslo, Norway.

Anisimov O & Fitzharris B (2001) Polar regions (Arctic and Antarctic). *Climate Change 2001: Impacts, Adaptation, and Vulnerability, Intergovernmental Panel on Climate Change (McCarthy JJ, Canziani OF, Leary NA, Dokken DJ and White KS, Eds.), pp. 801–841*. American Society for Microbiology, Washington, DC.

Becker S, Boger P, Oehlmann R & Ernst A (2000) PCR Bias in Ecological Analysis: a Case Study for Quantitative Taq Nuclease Assays in Analyses of Microbial Communities. *Appl Environ Microbiol* 66: 4945–4953.

Bell TH, Yergeau E, Arrowsmith C, Juck D, Whyte LG & Greer CW (2011) Identification of nitrogen-incorporating bacteria in petroleum-contaminated Arctic soils using ^{15}N DNA-SIP and pyrosequencing. *Appl Environ Microbiol* 77: 4163-4171.

Bent E, Kiekel P, Brenton R & Taylor DL (2011) Root-associated ectomycorrhizal fungi Shared by various boreal forest seedlings naturally regenerating after a fire in interior Alaska and correlation of different fungi with host growth responses. *Appl Environ Microbiol* 77: 3351–3359.

Berg MP, Kniese JP & Verhoef HA (1998) Dynamics and stratification of bacteria and fungi in the organic layers of a scots pine forest soil. *Biol Fert Soils* 26: 313–322.

Berthelet M, Whyte LG & Greer CW (1996) Rapid, direct extraction of DNA from soils for PCR analysis using polyvinylpolypyrrolidone spin columns. *FEMS Microbiol Lett* 138: 17–22.

Bjorbækmo M, Carlsen T, Brysting A, Vrålstad T, Høiland K, Ugland K, Geml J, Schumacher T & Kauserud H (2010) High diversity of root associated fungi in both alpine and arctic *Dryas octopetala*. *BMC Plant Biol* 10: 244.

Blackwood CB, Hudleston D, Zak DR & Buyer JS (2007) Interpreting ecological diversity indices applied to terminal restriction fragment length polymorphism data: insights from simulated microbial communities. *Appl Environ Microbiol* 73: 5276–5283.

Bleeker A, Hicks WK, Dentener F, Galloway J & Erisman JW (2011) N deposition as a threat to the World's protected areas under the Convention on Biological Diversity. *Environ Pollut* 159: 2280–2288.

Bliss LC, Svoboda J & Bliss DI (1984) Polar deserts, their plant cover and plant production in the Canadian High Arctic. *Holarctic Ecol* 7: 305–324.

Bliss LC & Matveyeva NV (1992) Circumpolar arctic vegetation. *Arctic Ecosystems in a Changing Climate: An Ecophysiological Perspective (Chapin FS III, Jeffries RL, Reynolds JF, Shaver GR & Svoboda J,* Eds.*)*, pp 59–89. Academic Press, San Diego.

Bobbink R, Hornung M & Roelofs JGM (1998) The effects of air-borne nitrogen pollutants on species diversity in natural and semi-natural European vegetation. *J Ecol* 86: 717–738.

Bowden RD, Davidson E, Savage K, Arabia C & Steudler P (2004) Chronic nitrogen additions reduce total soil respiration and microbial respiration in temperate forest soils at the Harvard Forest. *Forest Ecol Manag* 196: 43–56.

Boyle SA, Yarwood RR, Bottomley PJ & Myrold DD (2008) Bacterial and fungal contributions to soil nitrogen cycling under Douglas fir and red alder at two sites in Oregon. *Soil Biol Biochem* 40: 443–451.

Braker G, Fesefeldt A & Witzel K-P (1998) Development of PCR primer systems for amplification of nitrite reductase genes (*nirK* and *nirS*) to detect denitrifying bacteria in environmental samples. *Appl Environ Microbiol* 64: 3769–3775.

Braker G & Tiedje JM (2003) Nitric oxide reductase (*norB*) genes from pure cultures and environmental samples. *Appl Environ Microbiol* 69: 3476–3483.

Brockett BFT, Prescott CE & Grayston SJ (2012) Soil moisture is the major factor influencing microbial community structure and enzyme activities across seven biogeoclimatic zones in western Canada. *Soil Biol Biochem* 44: 9–20.

Buée M, Reich M, Murat C, Morin E, Nilsson RH, Uroz S & Martin F (2009) 454 Pyrosequencing analyses of forest soils reveal an unexpectedly high fungal diversity. *New Phytol* 184: 449–456.

Burgmann H, Widmer F, Von Sigler W & Zeyer J (2004) New molecular screening tools for analysis of free-living diazotrophs in soil. *Appl Environ Microbiol* 70: 240–247.

Butterbach-Bahl & Gundersen, 2011 (2011) Nitrogen processes in terrestrial ecosystems. *The European Nitrogen Assessment (Sutton MA, Howard CM, Erisman JW, Bleeker A, Greenfelt P, Grinsven HV & Grizzeti B, Eds.)*, pp. 99-125. Cambridge, UK.

Cabello P, Roldan MD & Moreno-Vivian C (2004) Nitrate reduction and the nitrogen cycle in archaea. *Microbiology* 150: 3527–3546.

Cadillo-Quiroz H, Brauer S, Yashiro E, Sun C, Yavitt J & Zinder S (2006) Vertical profiles of methanogenesis and methanogens in two contrasting acidic peatlands in central New York State, USA. *Environ Microbiol* 8: 1428–1440.

Cairney JWG & Ashford AE (2002) Biology of mycorrhizal associations of epacrids (Ericaceae). *New Phytol* 154: 305–326.

Carreiro MM, Sinsabaugh RL, Repert DA & Parkhurst DF (2000) Microbial enzyme shifts explain litter decay responses to simulated nitrogen deposition. *Ecology* 81: 2359–2365.

Chapin FS, Shaver GR, Giblin AE, Nadelhoffer KJ & Laundre JA (1995) Responses of Arctic tundra to experimental and observed changes in climate. *Ecology* 76: 694.

Chu H, Fierer N, Lauber CL, Caporaso JG, Knight R & Grogan P (2010) Soil bacterial diversity in the Arctic is not fundamentally different from that found in other biomes. *Environ Microbiol* 12: 2998–3006.

Chu H, Neufeld JD, Walker VK & Grogan P (2011) The Influence of vegetation type on the dominant soil bacteria, archaea, and fungi in a Low Arctic tundra Landscape. *Soil Sci Soc Am J* 75: 1756.

Clarke KR (1993) Non-parametric multivariate analyses of changes in community structure. *Austral Ecol* 18: 117–143.

Clarke KR & Ainsworth M (1993) A method of linking multivariate community structure to environmental variables. *Mar Ecol-Prog Ser* 92: 205–205.

Clarke KR & Green RH (1988) Statistical design and analysis for a“ biological effects” study. *Mar Ecol-Prog Ser* 46: 213–226.

Clarke KR, Somerfield PJ & Chapman MG (2006) On resemblance measures for ecological studies, including taxonomic dissimilarities and a zero-adjusted Bray-Curtis coefficient for denuded assemblages. *J Exp Mar Biol Ecol* 330: 55–80.

Clemmensen KE, Michelsen A, Jonasson S & Shaver GR (2006) Increased ectomycorrhizal fungal abundance after long-term fertilization and warming of two arctic tundra ecosystems. *New Phytol* 171: 391–404.

Cole JR, Wang Q, Cardenas E, Fish J, Chai B, Farris RJ Kulam-Syed-Mohideen AS, McGarrell DM, Marsh T, Garrity GM & Tiedje JM (2009) The Ribosomal Database Project: improved alignments and new tools for rRNA analysis. *Nucleic Acids Res* 37: D141–D145.

Compton JE, Watrud LS, Porteous AL & DeGrood S (2004) Response of soil microbial biomass and community composition to chronic nitrogen additions at Harvard forest. *Forest Ecol Manag* 196: 143–158.

DeForest JL, Zak DR, Pregitzer KS & Burton AJ (2005) Atmospheric nitrate deposition and enhanced dissolved organic carbon leaching: test of a potential mechanism. *Soil Sci Soc Am J* 69: 1233–1237.

DeLong EF (1992) Archaea in coastal marine environments. *P Natl Acad Sci USA* 89: 5685–5689.

Deslippe JR, Egger KN & Henry GHR (2005) Impacts of warming and fertilization on nitrogen-fixing microbial communities in the Canadian High Arctic. *FEMS Microbiol Ecol* 53: 41–50.

Deslippe JR & Egger KN (2006) Molecular diversity of *nifH* genes from bacteria associated with High Arctic dwarf shrubs. *Microb Ecol* 51: 516–525.

Deslippe JR, Hartmann M, Mohn WW & Simard SW (2011) Long-term experimental manipulation of climate alters the ectomycorrhizal community of *Betula nana* in Arctic tundra. *Glob Change Biol* 17: 1625–1636.

Di HJ, Cameron KC, Shen J-P, Winefield CS, O'Callaghan M, Bowatte S & He J-Z (2010) Ammonia-oxidizing bacteria and archaea grow under contrasting soil nitrogen conditions. *FEMS Microbiol Ecol* 72: 386–394.

Duprè C, Stevens CJ, Ranke T, Bleeker, A, Peppler-Lisbach C, Gowing DJG, Dise NB, Dorland E, Bobbink R & Diekmann M (2010) Changes in species richness and composition in European acidic grasslands over the past 70 years: the contribution of cumulative atmospheric nitrogen deposition. *Glob Change Biol* 16: 344–357.

Egerton-Warburton L & Allen EB (2000) Shifts in arbuscular mycorrhizal communities along an anthropogenic nitrogen deposition gradient. *Ecol Appl* 10: 484–496.

Ekelund F, Rønn R & Christensen S (2001) Distribution with depth of protozoa, bacteria and fungi in soil profiles from three Danish forest sites. *Soil Biol Biochem* 33: 475–481.

Enwall K, Philippot L & Hallin S (2005) Activity and composition of the denitrifying bacterial community respond differently to long-term fertilization. *Appl Environ Microbiol* 71: 8335–8343.

Fenn ME, Poth MA, Aber JD, Baron JS, Bormann BT, Johnson DW, Lemly AD. McNulty SG, Ryan DF & Stottlemyer R (1998) Nitrogen excess in North American ecosystems: predisposing factors, ecosystem responses, and management strategies. *Ecol Appl* 8: 706–733.

Fields S (2004) Global Nitrogen: Cycling out of Control. *Environ Health Perspect* 112: 556–563.

Fierer N, Schimel JP & Holden PA (2003) Variations in microbial community composition through two soil depth profiles. *Soil Biol Biochem* 35: 167–176.

Fierer N, Jackson JA, Vilgalys R & Jackson RB (2005) Assessment of soil microbial community structure by use of taxon-specific quantitative PCR assays. *Appl Environ Microbiol* 71: 4117–4120.

Fierer N & Jackson RB (2006) The diversity and biogeography of soil bacterial communities. *P Natl Acad Sci USA* 103: 626 –631.

Fierer N, Bradford MA & Jackson RB (2007) Toward an ecological classification of soil bacteria. *Ecology* 88: 1354–1364.

Fierer N, McCain CM, Meir P, Zimmermann M, Rapp JM, Silman MR & Knight R (2011) Microbes do not follow the elevational diversity patterns of plants and animals. *Ecology* 92: 797–804.

Fischer H, Wagenbach D & Kipfstuhl J (1998) Sulfate and nitrate firn concentrations on the Greenland ice sheet 1. Large-scale geographical deposition changes. *J Geophys Res* 103: 21935–21942.

Fisk MC & Schmidt SK (1996) Microbial responses to nitrogen additions in alpine tundra soil. *Soil Biol Biochem* 28: 751–755.

Flanagan DA, Gregory LG, Carter JP, Karakas-Sen A, Richardson DJ & Spiro S (1999) Detection of genes for periplasmic nitrate reductase in nitrate respiring bacteria and in community DNA. *FEMS Microbiol Lett* 177: 263–270.

Francis CA, Roberts KJ, Beman JM, Santoro AE & Oakley BB (2005) Ubiquity and diversity of ammonia-oxidizing archaea in water columns and sediments of the ocean. *P Natl Acad Sci USA* 102: 14683–14688.

Francis CA, Beman JM & Kuypers MMM (2007) New processes and players in the nitrogen cycle: the microbial ecology of anaerobic and archaeal ammonia oxidation. *ISME J* 1: 19–27.

Frey SD, Knorr M, Parrent JL & Simpson RT (2004) Chronic nitrogen enrichment affects the structure and function of the soil microbial community in temperate hardwood and pine forests. *Forest Ecol Manag* 196: 159–171.

Fritze H, Pietikäinen J & Pennanen T (2000) Distribution of microbial biomass and phospholipid fatty acids in Podzol profiles under coniferous forest. *Eur J Soil Sci* 51: 565–573.

Fujimura KE, Egger KN & Henry GHR (2007) The effect of experimental warming on the root-associated fungal community of *Salix arctica*. *ISME J* 2: 105–114.

Fujiyoshi M, Yoshitake S, Watanabe K, Murota K, Tsuchiya Y, Uchida M & Nakatsubo T (2011) Successional changes in ectomycorrhizal fungi associated with the polar willow *Salix polaris* in a deglaciated area in the High Arctic, Svalbard. *Polar Biol* 34: 667–673.

Gallo M, Amonette R, Lauber C, Sinsabaugh RL & Zak DR (2004) Microbial community structure and oxidative enzyme activity in nitrogen-amended north temperate forest soils. *Microb Ecol* 48: 218–229.

Galloway JN, Levy H & Kasibhatla PS (1994) Year 2020: Consequences of population growth and development on deposition of oxidized nitrogen. *Ambio* 23: 120–123.

Galloway JN, Aber JD, Erisman JW, Seitzinger SP, Howarth RW, Cowling EB & Cosby BJ (2003) The nitrogen cascade. *BioScience* 53: 341.

Galloway JN, Dentener FJ, Capone DG, Boyer EW, Howarth RW, Seitzinger SP, Asner GP, Cleveland CC, Green PA & Holland EA (2004) Nitrogen cycles: past, present, and future. *Biogeochemistry* 70: 153–226.

Ganzert L, Jurgens G, Münster U & Wagner D (2007) Methanogenic communities in permafrost-affected soils of the Laptev Sea coast, Siberian Arctic, characterized by 16S rRNA gene fingerprints. *FEMS Microbiol Ecol* 59: 476–488.

Gardes M & Bruns TD (1993) ITS primers with enhanced specificity for basidiomycetes-application to the identification of mycorrhizae and rusts. *Mol Ecol* 2: 113–118.

Gattinger A, Höfle MG, Schloter M, Embacher A, Böhme F, Munch JC & Labrenz M (2007) Traditional cattle manure application determines abundance, diversity and activity of methanogenic archaea in arable European soil. *Environ Microbiol* 9: 612–624.

Geml J, Laursen GA, Timling I, McFarland JM, Booth MG, Lennon N, Nusbaum C & Taylor DL (2009) Molecular phylogenetic biodiversity assessment of arctic and boreal ectomycorrhizal *Lactarius Pers.* (Russulales; Basidiomycota) in Alaska, based on soil and sporocarp DNA. *Mol Ecol* 18: 2213–2227.

Geml J, Timling I, Robinson CH, Lennon N, Nusbaum HC, Brochmann C, Noordeloos M & Taylor DL (2012) An arctic community of symbiotic fungi assembled by long-distance dispersers: phylogenetic diversity of ectomycorrhizal basidiomycetes in Svalbard based on soil and sporocarp DNA. *J Biogeogr* 39: 74–88.

Gordon C, Wynn JM & Woodin SJ (2001) Impacts of increased nitrogen supply on High Arctic heath: the importance of bryophytes and phosphorus availability. *New Phytol* 149: 461–471.

Graham DW, Knapp CW, Van Vleck ES, Bloor K, Lane TB & Graham CE (2007) Experimental demonstration of chaotic instability in biological nitrification. *ISME J* 1: 385–393.

Gregory LG, Karakas-Sen A, Richardson DJ & Spiro S (2000) Detection of genes for membrane-bound nitrate reductase in nitrate-respiring bacteria and in community DNA. *FEMS Microbiol Lett* 183: 275–279.

Griffiths RI, Whiteley AS, O'Donnell AG & Bailey MJ (2000) Rapid method for coextraction of DNA and RNA from natural environments for analysis of ribosomal DNA- and rRNA-based microbial community composition. *Appl Environ Microbiol* 66: 5488–5491.

Gubry-Rangin C, Nicol GW & Prosser JI (2010) Archaea rather than bacteria control nitrification in two agricultural acidic soils. *FEMS Microbiol Ecol* 74: 566–574.

Hansel CM, Fendorf S, Jardine PM & Francis CA (2008) Changes in bacterial and archaeal community structure and functional diversity along a geochemically variable soil profile. *Appl Environ Microbiol* 74: 1620–1633.

Hartmann M, Lee S, Hallam SJ & Mohn WW (2009) Bacterial, archaeal and eukaryal community structures throughout soil horizons of harvested and naturally disturbed forest stands. *Environ Microbiol* 11: 3045–3062.

He J-P, Shen J-P, Zhang L-M, Zhu Y-M, Zheng Y-M, Xu M-G & Di H (2007) Quantitative analyses of the abundance and composition of ammonia-oxidizing bacteria and ammonia-oxidizing archaea of a Chinese upland red soil under long-term fertilization practices. *Environ Microbiol* 9: 2364–2374.

Heal OW (1999) Looking North: Current issues in Arctic soil ecology. *Appl Soil Ecol* 11: 107–109.

Henry GHR & Svoboda J (1986) Dinitrogen fixation (Acetylene Reduction) in High Arctic sedge meadow communities. *Arctic Alpine Res* 18: 181–187.

Hobbie SE (1996) Temperature and plant species control over litter decomposition in Alaskan tundra. *Ecol Monogr* 66: 503–522.

Hodkinson ID & Wookey PA (1999) Functional ecology of soil organisms in tundra ecosystems: towards the future. *Appl Soil Ecol* 11: 111–126.

Hodson AJ, Mumford PN, Kohler J & Wynn PM (2005) The High Arctic glacial ecosystem: new insights from nutrient budgets. *Biogeochemistry* 72: 233–256.

Hodson A, Roberts TJ, Engvall A-C, Holmén K & Mumford P (2010) Glacier ecosystem response to episodic nitrogen enrichment in Svalbard, European High Arctic. *Biogeochemistry* 98: 171–184.

Högberg M, Högberg P & Myrold D (2007) Is microbial community composition in boreal forest soils determined by pH, C-to-N ratio, the trees, or all three? *Oecologia* 150: 590–601.

Høj L, Olsen RA & Torsvik VL (2005) Archaeal communities in High Arctic wetlands at Spitsbergen, Norway (78°N) as characterized by 16S rRNA gene fingerprinting. *FEMS Microbiol Ecol* 53: 89–101.

Høj L, Rusten M, Haugen LE, Olsen RA & Torsvik VL (2006) Effects of water regime on archaeal community composition in Arctic soils. *Environ Microbiol* 8: 984–996.

Høj L, Olsen RA & Torsvik VL (2008) Effects of temperature on the diversity and community structure of known methanogenic groups and other archaea in High Arctic peat. *ISME J* 2: 37–48.

Holland EA, Dentener FJ, Braswell BH & Sulzman JM (1999) Contemporary and pre-industrial global reactive nitrogen budgets. *Biogeochemistry* 46: 7–43.

Howard JB & Rees DC (1996) Structural Basis of Biological Nitrogen Fixation. *Chem Rev* 96: 2965–2982.

Illeris L, Michelsen A & Jonasson S (2003) Soil plus root respiration and microbial biomass following water, nitrogen, and phosphorus application at a High Arctic semi desert. *Biogeochemistry* 65: 15–29.

IPCC (2007) Contribution of working groups I, II and III to the fourth assessment report of the intergovernmental panel on climate change *(Pachauri RK & Reisinger A, Eds.)*, pp 104. Geneva, Switzerland.

Izquierdo J & Nüsslein K (2006) Distribution of Extensive *nifH* Gene Diversity Across Physical Soil Microenvironments. *Microb Ecol* 51: 441–452.

Jefferies RL & Maron JL (1997) The embarrassment of riches: atmospheric deposition of nitrogen and community and ecosystem processes. *Trends Ecol Evol* 12: 74–78.

Jentten MSM, van Niftrik L, Strous M, Kartal B, Keltjens JT & Op den Camp HJM (2009) Biochemistry and molecular biology of anammox bacteria. *Crit Rev Biochem Mol* 44: 65–84.

Jetten MSM (2008) The microbial nitrogen cycle. *Environ Microbiol* 10: 2903–2909.

Jonasson S, Michelsen A, Schmidt IK & Nielsen EV (1999) Responses in microbes and plants to changed temperature, nutrient, and light regimes in the Arctic. *Ecology* 80: 1828–1843.

Jones AV, Stolbovoy C, Tarnocai G, Broll O, Spaargaren & Montanarella L. (Eds.) (2009) Soil atlas of the Northern circumpolar region. *European Commission, Office for Official Publications of the European Communities*, pp.142 Luxembourg, Luxembourg.

Kamphake LJ, Hannah SA & Cohen JM (1967) Automated analysis for nitrate by hydrazine reduction. *Water Res* 1: 205–216.

Kemnitz D, Kolb S & Conrad R (2007) High abundance of Crenarchaeota in a temperate acidic forest soil. *FEMS Microbiol Ecol* 60: 442–448.

Kowalchuk GA, Stephen JR, De Boer W, Prosser JI, Embley TM & Woldendorp JW (1997) Analysis of ammonia-oxidizing bacteria of the beta subdivision of the class Proteobacteria in coastal sand dunes by denaturing gradient gel electrophoresis and sequencing of PCR-amplified 16S ribosomal DNA fragments. *Appl Environ Microbiol* 63: 1489–1497.

Kreader CA (1996) Relief of amplification inhibition in PCR with bovine serum albumin or T4 gene 32 protein. *Appl Environ Microbiol* 62: 1102–1106.

Krom MD (1980) Spectrophotometric determination of ammonia: a study of a modified Berthelot reaction using salicylate and dichloroisocyanurate. *Analyst* 105: 305–316.

Kruskal WH & Wallis WA (1952) Use of ranks in one-criterion variance analysis. *J Am Stat Assoc* 47: 583.

Kühnel R, Roberts TJ, Björkman MP, Isaksson E, Aas W, Holmén K & Ström J (2011) 20-Year climatology of NO_3^- and NH_4^+ wet deposition at Ny-Ålesund, Svalbard. *Adv Meteorol* 2011: 1–10.

Laj P, Palais JM & Sigurdsson H (1992) Changing sources of impurities to the Greenland ice sheet over the last 250 years. *Atmos Environ* 26: 2627–2640.

Lamb EG, Han S, Lanoil BD, Henry GR, Brumell ME, Banerjee S & Siciliano SD (2011) A High Arctic soil ecosystem resists long-term environmental manipulations. *Glob Change Biol* 17: 3187–3194.

LaMontagne MG, Schimel JP & Holden PA (2003) Comparison of subsurface and surface soil bacterial communities in California grassland as assessed by terminal restriction fragment length polymorphisms of PCR-amplified 16S rRNA genes. *Microb Ecol* 46: 216–227.

Landeweert R, Leeflang P, Kuyper TW, Hoffland E, Rosling A, Wernars K & Smit E (2003) Molecular identification of ectomycorrhizal mycelium in soil horizons. *Appl Environ Microbiol* 69: 327 –333.

Lane DJ (1991) 16S/23S rRNA sequencing. *Nucleic acid techniques in bacterial systematics (Stackebrandt E & Goodfellow M, Eds.)*, pp. 115-175. West Sussex, UK.

Lauber CL, Hamady M, Knight R & Fierer N (2009) Pyrosequencing-based assessment of soil pH as a predictor of soil bacterial community structure at the continental scale. *Appl Environ Microbiol* 75: 5111 –5120.

Lehtovirta LE, Prosser JI & Nicol GW (2009) Soil pH regulates the abundance and diversity of Group 1.1c Crenarchaeota. *FEMS Microbiol Ecol* 70: 35–44.

Leininger S, Urich T, Schloter M, Schwark L, Qi J, Nicol GW, Prosser JI, Schuster SC & Schleper C (2006) Archaea predominate among ammonia-oxidizing prokaryotes in soils. *Nature* 442: 806–809.

Lensi R, Clays-Josser A & Jocteur Monrozier L (1995) Denitrifiers and denitrifying activity in size fractions of a mollisol under permanent pasture and continuous cultivation. *Soil Biol Biochem* 27: 61–69.

Lilleskov EA, Fahey TJ & Lovett GM (2001) Ectomycorrhizal fungal aboveground community change over an atmospheric nitrogen deposition gradient. *Ecol Appl* 11: 397–410.

Lilleskov EA, Hobbie EA & Fahey TJ (2002) Ectomycorrhizal fungal taxa differing in response to nitrogen deposition also differ in pure culture organic nitrogen use and natural abundance of nitrogen isotopes. *New Phytol* 154: 219–231.

Liu WT, Marsh TL, Cheng H & Forney LJ (1997) Characterization of microbial diversity by determining terminal restriction fragment length polymorphisms of genes encoding 16S rRNA. *Appl Environ Microbiol* 63: 4516–4522.

Ma WK, Farrell RE & Siciliano SD (2008) Soil formate regulates the fungal nitrous oxide emission pathway. *Appl Environ Microbiol* 74: 6690 –6696.

Ma WK, Schautz A, Fishback L-AE, Bedard-Haughn A, Farrell RE & Siciliano SD (2007) Assessing the potential of ammonia oxidizing bacteria to produce nitrous oxide in soils of a high arctic lowland ecosystem on Devon Island, Canada. *Soil Biol Biochem* 39: 2001–2013.

Madan NJ, Deacon LJ & Robinson CH (2007) Greater nitrogen and/or phosphorus availability increase plant species' cover and diversity at a High Arctic polar semidesert. *Polar Biol* 30: 559–570.

Männistö MK, Tiirola M & Häggblom MM (2007) Bacterial communities in Arctic fjelds of Finnish Lapland are stable but highly pH-dependent. *FEMS Microbiol Ecol* 59: 452–465.

Manter DK & Vivanco JM (2007) Use of the ITS primers, ITS1F and ITS4, to characterize fungal abundance and diversity in mixed-template samples by qPCR and length heterogeneity analysis. *J Microbiol Meth* 71: 7–14.

Marchesi JR, Sato T, Weightman AJ, Martin TA, Fry JC, Hiom SJ & Wade WG (1998) Design and evaluation of useful bacterium-specific PCR primers that amplify genes coding for bacterial 16S rRNA. *Appl Environ Microbiol* 64: 795–799.

Maskell LC, Smart SM, Bullock JM, Thompson K & Stevens CJ (2010) Nitrogen deposition causes widespread loss of species richness in British habitats. *Glob Change Biol* 16: 671–679.

Matson PA, McDowell WH, Townsend AR & Vitousek PM (1999) The globalization of N deposition: ecosystem consequences in tropical environments. *Biogeochemistry* 46: 67–83.

Matson P, Lohse KA & Hall SJ (2002) The globalization of nitrogen deposition: consequences for terrestrial ecosystems. *Ambio* 31: 113–119.

McMahon SK, Wallenstein MD & Schimel JP (2011) A cross-seasonal comparison of active and total bacterial community composition in Arctic tundra soil using bromodeoxyuridine labeling. *Soil Biol Biochem* 43: 287–295.

McMahon SK, Wallenstein MD & Schimel JP (2009) Microbial growth in Arctic tundra soil at -2°C. *Environ Microbiol Reports* 1: 162–166.

Messing J (1983) New M13 vectors for cloning. *Methods in enzymology (Colowick SP, Fuir TW & Abelson JN Eds)*, pp 20–78.

Metje M & Frenzel P (2007) Methanogenesis and methanogenic pathways in a peat from subarctic permafrost. *Environ Microbiol* 9: 954–964.

Meyer F, Paarmann D, D'Souza M, Olson R, Glass E, Kubal M, Paczian T, Rodriguez A, Stevens R, Wike A, Wilkening J & Edwards R (2008) The metagenomics

RAST server – a public resource for the automatic phylogenetic and functional analysis of metagenomes. *BMC Bioinformatics* 9: 386.

Milne JM, Ennos RA & Hollingsworth PM (2006) Vegetation influence on ectomycorrhizal inoculum Available to sub-arctic willow (*Salix lapponum* L.) planted in an upland Site. *Botan J Scotland* 58: 19–34.

Mohan SB, Schmid M, Jetten M & Cole J (2004) Detection and widespread distribution of the *nrfA* gene encoding nitrite reduction to ammonia, a short circuit in the biological nitrogen cycle that competes with denitrification. *FEMS Microbiol Ecol* 49: 433–443.

Morin S, Savarino J, Frey MM, Yan N, Bekki S, Bottenheim JW & Martins JMF (2008) Tracing the origin and fate of NO_x in the Arctic atmosphere using Stable isotopes in nitrate. *Science* 322: 730–732.

Muyzer G, de Waal EC & Uitterlinden AG (1993) Profiling of complex microbial populations by denaturing gradient gel electrophoresis analysis of polymerase chain reaction-amplified genes coding for 16S rRNA. *Appl Environ Microbiol* 59: 695–700.

Nadelhofer K & Geiser LH (2010) Tundra. *Assessment of nitrogen deposition effects and empirical critical loads of nitrogen for ecoregions of the United States (Pardo LH, Robin-Abbott MJ & Driscoll CT, Eds.),* pp. 37-47. Philadelphia, USA.

Nemergut DR, Costello EK, Meyer AF, Pescador MY, Weintraub MN & Schmidt SK (2005) Structure and function of alpine and arctic soil microbial communities. *Research in Microbiology* 156: 775–784.

Nemergut DR, Townsend AR, Sattin SR, Freeman KR, Fierer N, Neff JC, Bowman WD, Schadt CW, Weintraub MN & Schmidt SK (2008) The effects of chronic nitrogen fertilization on alpine tundra soil microbial communities: implications for carbon and nitrogen cycling. *Environ Microbiol* 10: 3093–3105.

Neufeld JD, Yu Z, Lam W & Mohn WW (2004) Serial analysis of ribosomal sequence tags (SARST): a high-throughput method for profiling complex microbial communities. *Environ Microbiol* 6: 131–144.

Neufeld JD & Mohn WW (2005) Unexpectedly high bacterial diversity in Arctic tundra relative to boreal forest soils, revealed by serial analysis of ribosomal sequence tags. *Appl Environ Microbiol* 71: 5710–5718.

Neufeld JD, Wagner M & Murrell JC (2007) Who eats what, where and when? Isotope-labelling experiments are coming of age. *ISME J* 1: 103–110.

Newell K (1984) Interaction between two decomposer basidiomycetes and a collembolan under Sitka spruce: Distribution, abundance and selective grazing. *Soil Biol Biochem* 16: 227–233.

Nicol GW & Schleper C (2006) Ammonia-oxidising Crenarchaeota: important players in the nitrogen cycle? *Trends Microbiol* 14: 207–212.

Nicol GW, Leininger S, Schleper C & Prosser JI (2008) The influence of soil pH on the diversity, abundance and transcriptional activity of ammonia oxidizing archaea and bacteria. *Environ Microbiol* 10: 2966–2978.

Nilsson L, Bååth E, Falkengren-Grerup U & Wallander H (2007) Growth of ectomycorrhizal mycelia and composition of soil microbial communities in oak forest soils along a nitrogen deposition gradient. *Oecologia* 153: 375–384.

Nogales B, Timmis KN, Nedwell D. & Osborn AM (2002) Detection and Diversity of Expressed Denitrification Genes in Estuarine Sediments after Reverse Transcription-PCR Amplification from mRNA. *Appl Environ Microbiol* 68: 5017–5025.

Nordin A, Schmidt IK & Shaver GR (2004) Nitrogen uptake by Arctic soil microbes and plants in relation to soil nitrogen supply. *Ecology* 85: 955–962.

Osborn AM, Moore ERB & Timmis KN (2000) An evaluation of terminal-restriction fragment length polymorphism (T-RFLP) analysis for the study of microbial community structure and dynamics. *Environ Microbiol* 2: 39–50.

Øvreas L, Forney L, Daae FL & Torsvik V (1997) Distribution of bacterioplankton in meromictic Lake Saelenvannet, as determined by denaturing gradient gel electrophoresis of PCR-amplified gene fragments coding for 16S rRNA. *Appl Environ Microbiol* 63: 3367–3373.

Palmer K, Biasi C & Horn MA (2011) Contrasting denitrifier communities relate to contrasting N_2O emission patterns from acidic peat soils in arctic tundra. *ISME J*. 6: 1058-1077.

Penton CR, Devol AH & Tiedje JM (2006) Molecular evidence for the broad distribution of anaerobic ammonium-oxidizing bacteria in freshwater and marine sediments. *Appl Environ Microbiol* 72: 6829–6832.

Pesaro M & Widmer F (2002) Identification of novel Crenarchaeota and Euryarchaeota clusters associated with different depth layers of a forest soil. *FEMS Microbiol Ecol* 42: 89–98.

Peters GP, Nilssen TB, Lindholt L, Eide MS, Glomsrød S, Eide LI & Fuglestvedt JS (2011) Future emissions from shipping and petroleum activities in the Arctic. *Atmos Chem Phys* 11: 5305–5320.

Philippot L (2002) Denitrifying genes in bacterial and Archaeal genomes. *Biochimi Biophys Acta* 1577: 365–376.

Philippot L, Piutti S, Martin-Laurent F, Hallet S & Germon JC (2002) Molecular analysis of the nitrate-reducing community from unplanted and maize-planted soils. *Appl Environ Microbiol* 68: 6121–6128.

Philippot L (2005) Tracking nitrate reducers and denitrifiers in the environment. *Biochem Soct* 33: 200–204.

Phoenix GK, Hicks WK, Cinderby S, Kuylenstierna JCI, Stock WD, Dentener FJ, Giller, KE, Austin AT, Lefroy RDB, Gimeno BS, Ashmore MR & Ineson P (2006) Atmospheric nitrogen deposition in world biodiversity hotspots: the need for a greater global perspective in assessing N deposition impacts. *Glob Change Biol* 12: 470–476.

Phoenix GK, Emmett BA, Caporn SJM, Dise NB, Helliwell R, Jones L, Leake JR, Leith ID & Sheppard LJ (2012) Impacts of atmospheric nitrogen deposition: responses of multiple plant and soil parameters across contrasting ecosystems in long-term field experiments. *Glob Change Biol* 18: 1197–1215.

Poly F, Wertz S, Brothier E & Degrange V (2008) First exploration of *Nitrobacter* diversity in soils by a PCR cloning-sequencing approach targeting functional gene *nxrA*. *FEMS Microbiol Ecol* 63: 132–140.

R Development Core Team (2010) R: A language and environment for statistical computing.

Ralser M, Querfurth R, Warnatz H-J, Lehrach H, Yaspo M-L & Krobitsch S (2006) An efficient and economic enhancer mix for PCR. *Biochem Bioph Res Co* 347: 747–751.

Ranjard L, Poly F, Lata J-C, Mougel C, Thioulouse J & Nazaret S (2001) Characterization of bacterial and fungal soil communities by automated ribosomal intergenic spacer analysis fingerprints: biological and methodological variability. *Appl Environ Microbiol* 67: 4479–4487.

Ranjard L & Richaume A (2001) Quantitative and qualitative microscale distribution of bacteria in soil. *Res Microbiol* 152: 707–716.

Rennenberg H, Dannenmann M, Gessler A, Kreuzwieser J, Simon J & Papen H (2009) Nitrogen balance in forest soils: nutritional limitation of plants under climate change stresses. *Plant Biol* 11: 4–23.

Reysenbach A-L & Pace NR (1995) Reliable amplification of hyperthermophilic Archaeal 16S rRNA genes by the polymerase chain reaction. *Archaea: A Laboratory Manual (Rob FT, Place AR, Sowers KR, Schreier AR, DasSarna S & Fleischman EM Eds.)*, pp. 101–105. New York, USA.

Rich JJ, Heichen RS, Bottomley PJ, Cromack K & Myrold DD (2003) Community composition and functioning of denitrifying bacteria from adjacent meadow and forest soils. *Appl Environ Microbiol* 69: 5974–5982.

Rinnan R, Michelsen A, Bååth E & Jonasson S (2007) Fifteen years of climate change manipulations alter soil microbial communities in a subarctic heath ecosystem. *Glob Change Biol* 13: 28–39.

Ririe KM, Rasmussen RP & Wittwer CT (1997) Product differentiation by analysis of DNA melting curves during the polymerase chain reaction. *Anal Biochem* 245: 154–160.

Robinson CH, Wookey PA, Parsons AN, Potter JA, Callaghan TV, Lee JA, Press MC & Welker JM (1995) Responses of plant litter decomposition and nitrogen mineralisation to simulated environmental change in a high arctic polar semi-desert and a subarctic dwarf shrub heath. *Oikos* 74: 503–512.

Robinson CH, Fisher PJ & Sutton BC (1998) Fungal biodiversity in dead leaves of fertilized plants of Dryas octopetala from a high Arctic site. *Mycol Res* 102: 573–576.

Robinson CH (2001) Cold adaptation in Arctic and Antarctic fungi. *New Phytol* 151: 341–353.

Robinson CH, Saunders PW, Madan NJ, Pryce-Miller EJ & Pentecost A (2004) Does nitrogen deposition affect soil microfungal diversity and soil N and P dynamics in a high Arctic ecosystem? *Glob Change Biol* 10: 1065–1079.

Robinson CH, Szaro TM, Izzo AD, Anderson IC, Parkin PI & Bruns TD (2009) Spatial distribution of fungal communities in a coastal grassland soil. *Soil Biol Biochem* 41: 414–416.

Roesch LFW *et al.*, (2007) Pyrosequencing enumerates and contrasts soil microbial diversity. *ISME J* 1: 283–290.

Rooney-Varga JN, Giewat MW, Duddleston KN, Chanton JP & Hines ME (2007) Links between archaeal community structure, vegetation type and methanogenic pathway in Alaskan peatlands. *FEMS Microbiol Ecol* 60: 240–251.

Rotthauwe JH, Witzel KP & Liesack W (1997) The ammonia monooxygenase structural gene amoA as a functional marker: molecular fine-scale analysis of natural ammonia-oxidizing populations. *Appl Environ Microbiol* 63: 4704–4712.

Rousk J, Baath E, Brookes PC, Lauber CL, Lozupone C, Caporaso JG, Knight R & Fierer N (2010) Soil bacterial and fungal communities across a pH gradient in an arable soil. *ISME J* 4: 1340–1351.

Le Roux X *et al.*, (2008) Effects of aboveground grazing on coupling among nitrifier activity, abundance and community structure. *ISME J* 2: 221–232.

Ruess L, Michelsen A, Schmidt I & Jonasson S (1999) Simulated climate change affecting microorganisms, nematode density and biodiversity in subarctic soils. *Plant Soil* 212: 63–73.

Sander G, Holst & Shears J (2006) Environmental impact of the research activities in Ny-Ålesund 2006. *Norwegian Polar Institute*, pp. 56. Tromsø, Norway.

Saiya-Cork KR, Sinsabaugh RL & Zak DR (2002) The effects of long term nitrogen deposition on extracellular enzyme activity in an *Acer saccharum* forest soil. *Soil Biol Biochem* 34: 1309–1315.

Scala DJ & Kerkhof LJ (1998) Nitrous oxide reductase (*nosZ*) gene-specific PCR primers for detection of denitrifiers and three *nosZ* genes from marine sediments. *FEMS Microbiol Lett* 162: 61–68.

Scala DJ & Kerkhof LJ (1999) Diversity of nitrous oxide reductase (*nosZ*) genes in continental shelf sediments. *Appl Environ Microbiol* 65: 1681–1687.

Schmidt IK, Ruess L, Bååth E, Michelsen A, Ekelund F & Jonasson S (2000) Long-term manipulation of the microbes and microfauna of two subarctic heaths by addition of fungicide, bactericide, carbon and fertilizer. *Soil Biol Biochem* 32: 707–720.

Schmidt SK, Lipson DA, Ley RE, Fisk MC & West AE (2004) Impacts of chronic nitrogen additions vary seasonally and by microbial functional group in tundra soils. *Biogeochemistry* 69: 1–17.

Schuur EAG *et al.*, (2008) Vulnerability of permafrost carbon to climate change: implications for the global carbon cycle. *BioScience* 58: 701–714.

Serreze MC, Holland MM & Stroeve J (2007) Perspectives on the Arctic's shrinking sea-ice cover. *Science* 315: 1533 –1536.

Shannon CE (1948) A mathematical theory of communication. *Bell Syst Tech J* 27: 379–423.

Shaver GR & Chapin FS (1980) Response to fertilization by various plant growth Forms in an Alaskan tundra: nutrient accumulation and growth. *Ecology* 61: 662.

Shaver GR, Billings WD, Chapin FS, Giblin AE, Nadelhoffer KJ, Oechel WC & Rastetter EB (1992) Global change and the carbon balance of Arctic ecosystems. *BioScience* 42: 433–441.

Shaver GR, Bret-Harte MS, Jones MH, Johnstone J, Gough L, Laundre J & Chapin FS (2001) Species composition interacts with fertilizer to control long-term change in tundra productivity. *Ecology* 82: 3163–3181.

Siciliano SD, Ma WK, Ferguson S & Farrell RE (2009) Nitrifier dominance of Arctic soil nitrous oxide emissions arises due to fungal competition with denitrifiers for nitrate. *Soil Biol Biochem* 41: 1104–1110.

Sinsabaugh RL, Gallo ME, Lauber C, Waldrop MP & Zak DR (2005) Extracellular enzyme activities and soil organic matter dynamics for Northern Hardwood Forests receiving simulated nitrogen deposition. *Biogeochemistry* 75: 201–215.

Smalla K, Cresswell N, Mendonca-Hagler L., Wolters A & van Elsas JD (1993) Rapid DNA extraction protocol from soil for polymerase chain reaction-mediated amplification. *J Appl Microbiol* 74: 78–85.

Smith CJ, Danilowicz BS, Clear AK, Costello FJ, Wilson B & Meijer WG (2005) T-Align, a web-based tool for comparison of multiple terminal restriction fragment length polymorphism profiles. *FEMS Microbiol Ecol* 54: 375–380.

Smith CJ, Nedwell DB, Dong LF & Osborn AM (2006) Evaluation of quantitative polymerase chain reaction-based approaches for determining gene copy and gene transcript numbers in environmental samples. *Environ Microbiol* 8: 804–815.

Smith CJ & Osborn AM (2009) Advantages and limitations of quantitative PCR (Q-PCR)-based approaches in microbial ecology. *FEMS Microbiol Ecol* 67: 6–20.

Stapleton LM, Crout NMJ, Säwström C, Marshall WA, Poulton PR, Tye AM & Laybourn-Parry J (2005) Microbial carbon dynamics in nitrogen amended Arctic tundra soil: Measurement and model testing. *Soil Biol Biochem* 37: 2088–2098.

Stevens CJ, Dise NB, Mountford JO & Gowing DJ (2004) Impact of nitrogen deposition on the species richness of grasslands. *Science* 303: 1876–1879.

Stoumann Jensen L & Schjoerring JK (2011) Benefits of nitrogen for food, fibre and industrial production. *The European Nitrogen Assessment (Sutton MA, Howard CM, Erisman JW, Bleeker A, Greenfelt P, Grinsven HV & Grizzeti B, Eds.)*, pp. 31-61. Cambridge, UK.

Suding KN, Collins SL, Gough L, Clark C, Cleland EE, Gross KL, Milchunas DG & Pennings S (2005) Functional- and abundance-based mechanisms explain diversity loss due to N fertilization. *P Natl Acad Sci USA* 102: 4387 –4392.

Sutton MA, Howard CM, Erisman JW, Bleeker A, Greenfelt P, Grinsven HV & Grizzeti B (2011) The European nitrogen assessment. *Cambridge University Press*, pp. 612 Cambridge, UK.

Suzuki MT, Taylor LT & DeLong EF (2000) Quantitative analysis of small-subunit rRNA genes in mixed microbial populations via 5'-Nuclease Assays. *Appl Environ Microbiol* 66: 4605–4614.

Takai K & Horikoshi K (2000) Rapid detection and quantification of members of the archaeal community by quantitative PCR using fluorogenic probes. *Appl Environ Microbiol* 66: 5066–5072.

Taylor JP, Abbas B, Mills MS & Burns RG (2002) Comparison of microbial numbers and enzymatic activities in surface soils and subsoils using various techniques. *Soil Biol Biochem* 34: 387–401.

Taylor DL, Herriott IC, Long J & O'Neill K (2007) TOPO TA is A-OK: a test of phylogenetic bias in fungal environmental clone library construction. *Environ Microbiol* 9: 1329–1334.

Taylor DL, Booth MG, McFarland JW, Herriott IC, Lennon NJ, Nusbaum C & Marr TG (2008) Increasing ecological inference from high throughput sequencing of fungi in the environment through a tagging approach. *Mol Ecol Resour* 8: 742–752.

Tebbe CC & Vahjen W (1993) Interference of humic acids and DNA extracted directly from soil in detection and transformation of recombinant DNA from bacteria and a yeast. *Appl Environ Microbiol* 59: 2657–2665.

Throbäck IN, Enwall K, Jarvis Å & Hallin S (2004) Reassessing PCR primers targeting *nirS*, *nirK* and *nosZ* genes for community surveys of denitrifying bacteria with DGGE. *FEMS Microbiol Ecol* 49: 401–417.

Tourna M, Freitag TE, Nicol GW & Prosser JI (2008) Growth, activity and temperature responses of ammonia-oxidizing archaea and bacteria in soil microcosms. *Environ Microbiol* 10: 1357–1364.

Treseder KK (2004) A meta-analysis of mycorrhizal responses to nitrogen, phosphorus, and atmospheric CO_2 in field studies. *New Phytol* 164: 347–355.

Treseder KK (2008) Nitrogen additions and microbial biomass: a meta-analysis of ecosystem studies. *Ecol Lett* 11: 1111–1120.

Treusch AH, Leininger S, Kletzin A, Schuster SC, Klenk H-P & Schleper C (2005) Novel genes for nitrite reductase and *Amo*-related proteins indicate a role of uncultivated mesophilic crenarchaeota in nitrogen cycling. *Environ Microbiol* 7: 1985–1995.

Tukey JW (1953) The collected works of John W. Tukey, vol VIII. *Multiple Comparisons: 1948-1983, . 300*. Chapman and Hall, New York, NY.

Tye AM, Young SD, Crout NMJ, West HM, Stapleton LM, Poulton PR & Laybourn-Parry J (2005) The fate of ^{15}N added to high Arctic tundra to mimic increased inputs of atmospheric nitrogen released from a melting snowpack. *Glob Change Biol* 11: 1640–1654.

Tyson GW, Chapman J, Hugenholtz P, Allen EE, Ram RJ, Richardson PM, Solovyev VV, Rubin EM, Rokshar DS & Banfield JF (2004) Community structure and metabolism through reconstruction of microbial genomes from the environment. *Nature* 428: 37–43.

Urcelay C, Bret-Harte MS, Díaz S & Chapin FS (2003) Mycorrhizal colonization mediated by species interactions in arctic tundra. *Oecologia* 137: 399–404.

Verhamme DT, Prosser JI & Nicol GW (2011) Ammonia concentration determines differential growth of ammonia-oxidising archaea and bacteria in soil microcosms. *ISME J* 5: 1067–1071.

Vilgalys R & Hester M (1990) Rapid genetic identification and mapping of enzymatically amplified ribosomal DNA from several *Cryptococcus species. J Bacteriol* 172: 4238–4246.

Vitousek PM & Howarth RW (1991) Nitrogen limitation on land and in the sea: How can it occur? *Biogeochemistry* 13: 87-115.

Vitousek P., Aber JD, Howarth RW, Likens GE, Matson P., Schindler DW, Schlesinger WH & Tilman DG (1997) Human alteration of the global nitrogen cycle: sources and consequences. *Ecol Appl* 7: 737–750.

Vitousek PM, Cassman K, Cleveland C, Crews T, Field CB, Grimm NB, Howarth RW, Mariano R, Martinelli L, Rastetter EB & Sprent JI (2002) Towards an ecological understanding of biological nitrogen fixation. *Biogeochemistry* 57-58: 1–45.

Vrålstad T (2004) Are ericoid and ectomycorrhizal fungi part of a common guild? *New Phytol* 164: 7–10.

Waldrop MP, Zak DR & Sinsabaugh RL (2004) Microbial community response to nitrogen deposition in northern forest ecosystems. *Soil Biol Biochem* 36: 1443–1451.

Walker JF, Aldrich‐Wolfe L, Riffel A, Barbare H, Simpson NB, Trowbridge J & Jumpponen A (2011) Diverse Helotiales associated with the roots of three species of Arctic Ericaceae provide no evidence for host specificity. *New Phytol* 191: 515–527.

Walker JKM, Egger KN & Henry GHR (2008) Long-term experimental warming alters nitrogen-cycling communities but site factors remain the primary drivers of community structure in high arctic tundra soils. *ISME J* 2: 982–995.

Wallenstein MD, McNulty S, Fernandez IJ, Boggs J & Schlesinger WH (2006) Nitrogen fertilization decreases forest soil fungal and bacterial biomass in three long-term experiments. *Forest Ecol Manag* 222: 459–468.

Wallenstein MW, McMahon S & Schimel J (2007) Bacterial and fungal community structure in Arctic tundra tussock and shrub soils. *FEMS Microbiol Ecol* 59: 428–435.

Wang Z, Binder M, Schoch CL, Johnston PR, Spatafora JW & Hibbett DS (2006) Evolution of helotialean fungi (Leotiomycetes, Pezizomycotina): A nuclear rDNA phylogeny. *Molecular Phylogenetics and Evolution* 41: 295–312.

Wartiainen I, Hestnes AG & Svenning MM (2003) Methanotrophic diversity in high arctic wetlands on the islands of Svalbard (Norway) - denaturing gradient gel electrophoresis analysis of soil DNA and enrichment cultures. *Can J Microbiol* 49: 602–612.

Wartiainen I, Hestnes AG, McDonald IR & Svenning MM (2006) *Methylocystis Rosea Sp.* Nov., a novel methanotrophic bacterium from Arctic wetland soil, Svalbard, Norway (78° N). *Int J Syst Evol Microbiol* 56: 541–547.

Weathers KC & Lyinch JA (2010) Deposition. *Assessment of nitrogen deposition effects and empirical critical loads of nitrogen for ecoregions of the United States (Pardo LH, Robin-Abbott MJ & Driscoll CT, Eds.)*, pp 15-24. Philadelphia, USA.

White TJ, Bruns TD, Lee S & Taylor J (1990) Amplification and direct sequencing of fungal ribosomal RNA genes for phylogenetics. *PCR protocols: a guide to methods and application*, pp. pp 315–322. Academic Press, New York.

Widmer F, Shaffer BT, Porteous LA & Seidler RJ (1999) Analysis of *nifH* Gene Pool Complexity in Soil and Litter at a Douglas Fir Forest Site in the Oregon Cascade Mountain Range. *Appl Environ Microbiol* 65: 374–380.

Van Wijk MT, Clemmensen KE, Shaver GR, Williams M, Callaghan TV, Chapin III FS, Cornelissen JHC, Gough L, Hobbie SE & Jonasson S (2004) Long-term ecosystem level experiments at Toolik Lake, Alaska, and at Abisko, Northern Sweden: generalizations and differences in ecosystem and plant type responses to global change. *Glob Change Biol* 10: 105–123.

Wilhelm RC, Niederberger TD, Greer C & Whyte LG (2011) Microbial diversity of active layer and permafrost in an acidic wetland from the Canadian High Arctic. *Can J Microbiol* 57: 303–315.

Wittwer CT, Herrmann MG, Moss AA & Rasmussen RP (1997) Continuous fluorescence monitoring of rapid cycle DNA amplification. *BioTechniques* 22: 130–131, 134–138.

Woodin (1997) Ecology of Arctic Environments *(Woodin SJ & Marquiss M, Eds.)*, pp. 219–239. Blackwell Science, Oxford.

Wrage N, Velthof G., van Beusichem M. & Oenema O (2001) Role of nitrifier denitrification in the production of nitrous oxide. *Soil Biol Biochem* 33: 1723–1732.

Yan T, Fields MW, Wu L, Zu Y, Tiedje JM & Zhou J (2003) Molecular diversity and characterization of nitrite reductase gene fragments (*nirK* and *nirS*) from nitrate- and uranium-contaminated groundwater. *Environ Microbiol* 5: 13–24.

Yao H, Gao Y, Nicol GW, Campbell CD, Prosser JI, Zhang L, Han W & Singh BK (2011) Links between ammonia oxidizer community structure, abundance, and nitrification potential in acidic soils. *Appl Environ Microbiol* 77: 4618–4625.

Yergeau E, Arbour M, Brousseau R, Juck D, Lawrence JR, Masson L, Whyte LG & Greer CW (2009) Microarray and real-time PCR analyses of the responses of High-Arctic soil bacteria to hydrocarbon pollution and bioremediation treatments. *Appl Environ Microbiol* 75: 6258 –6267.

Yergeau E, Hogues H, Whyte LG & Greer CW (2010) The functional potential of high Arctic permafrost revealed by metagenomic sequencing, qPCR and microarray analyses. *ISME J* 4: 1206–1214.

Zang MY (1990) A new taxon in the genus Cordyceps from China. *Mycotaxon* 295–299.

Zehr JP & McReynolds LA (1989) Use of degenerate oligonucleotides for amplification of the nifH gene from the marine cyanobacterium *Trichodesmium thiebautii*. *Appl Environ Microbiol* 55: 2522–2526.

Zehr JP, Jenkins BD, Short SM & Steward GF (2003) Nitrogenase gene diversity and microbial community structure: a cross-system comparison. *Environ Microbiol* 5: 539–554.

Zhang L-M, Offre PR, He J-Z, Verhamme DT, Nicol GW & Prosser JI (2010) Autotrophic ammonia oxidation by soil Thaumarchaea. *P Natl A Sci* 107: 17240 –17245.

Zhou J, Xia B, Treves DS, Wu L-Y, Marsh TL, O'Neill RV, Palumbo AV & Tiedje JM (2002) Spatial and resource factors influencing high microbial diversity in soil. *Appl Environ Microbiol* 68: 326 –334.

Zumft WG (1997) Cell biology and molecular basis of denitrification. *Microbiol Mol Biol Re.* 61: 533–616.

Appendices

View of the last peak of Schetelig mountain (694 m alt.)
from walking down the second peak (718 m alt.) the 1st of August 2010.

Appendix 1.1: Scientific productions from and outside the thesis over the period of the thesis.

1.1 Scientific production from the thesis

1.1.1 Articles submitted

Blaud A, Phoenix GK, Osborn AM
Variation in bacterial, archaeal and fungal community structure and abundance between organic and mineral soil horizons in High Arctic tundra.
Submitted to FEMS Microbiology Ecology.

1.1.2 Articles in preparation

Blaud A, Choudhary S, Phoenix GK, Osborn AM
Microbial communities changes in response to short term atmospheric nitrogen deposition in High Arctic tundra are rapid and soil horizons specific.
In preparation for Global Change Biolgy.

Blaud A, Phoenix GK, Osborn AM
A microcosm experiment to evaluate the impact of precipitation and nitrogen deposition on the structure and abundance of microbial communities in different soil horizons of High Arctic tundra.

1.1.3 Oral presentations at scientific conferences

Blaud A, Phoenix GK, Osborn AM
Short-term responses of soil microbial community structure to atmospheric nitrogen deposition in Arctic tundra soils.
Molecular Microbial Ecology Group Meeting (MMEG), Warwick (England), 14th – 15th December 2010.

Choudhary S, **Blaud A**, Oulehle F, Evans C, Osborn AM, Phoenix GK (shared talk with Choudhary S)
Fate and impact of acute atmospheric nitrogen deposition on plants and microbial communities in the High Arctic tundra.
Nitrogen and Global Change Key findings – future challenges, Edinburgh (Scotland), 11th – 14th April 2011.

Blaud A, Choudhary S, Phoenix GK, Osborn AM
Impact of acute nitrogen deposition on microbial communities structure and abundance in the High Arctic tundra soil
Polar and Alpine Microbiology 2011, Ljubljana (Slovenia), 4th – 8th September 2011
The **FEMS Young Scientist Meeting Grant** was obtained to attend this conference.

1.1.4 Oral presentations at NSINK network meeting

Blaud A, Phoenix GK, Osborn AM
Impact of acute nitrogen deposition on microbial community structure and function of microbial communities in Arctic tundra soil.
Tromsø (Norway), 26th – 27th May 2009.

Blaud A, Phoenix GK, Osborn AM
Impact of acute nitrogen deposition on structure and function of microbial communities in Arctic tundra soil.
Uppsala (Sweden), 11th – 12th January 2010.

Blaud A, Phoenix GK, Osborn AM
Impact of acute nitrogen deposition on structure of microbial communities in Arctic tundra soil.
Mid-term review meetings, Sheffield (England), 22nd – 23rd November 2010.

Blaud A, Choudhary S, Phoenix GK, Osborn AM
Microbial communities response to atmospheric nitrogen deposition in High Arctic tundra soil.
Obergurgl (Austria), 17th – 20th October 2011.

1.1.5 Poster presentations at scientific conferences

Blaud A, Osborn AM, Choudhary S, Phoenix GK, Oulehle F, Evans C
Fate and impacts of acute atmospheric nitrogen deposition in High Arctic terrestrial ecosystems: a multidisciplinary approach.
35th Annual meeting of Committee on Air Pollution Effects Research (CAPER), University of York (England), 29th – 31st March 2010.

Blaud A, Choudhary S, Phoenix GK, Osborn AM
Impact of acute nitrogen deposition on microbial community structure in the Arctic tundra soil.
Ecology of Soil Microorganisms, Prague (Czech Republic), 27th April – 1st May 2011.

Blaud A, Choudhary S, Phoenix GK, Osborn AM
Impact of acute nitrogen deposition on microbial communities structure and abundance in the High Arctic tundra soil.
British Ecological Society, Sheffield (England), 12th – 14th September 2011.

1.2 Scientific production outside the thesis during period of the PhD

1.2.1 Articles published

Blaud A, Lerch TZ, Chevallier T, Nunan N, Chenu C, Brauman A (2012). Dynamics of bacterial communities in relation to soil aggregates formation during the decomposition of ^{13}C-labelled rice straw. Applied Soil Ecology, 53, 1-9.

1.2.2 Poster presentation at scientific conference

Blaud A, Lerch TZ, Chevallier T, Nunan N, Chenu C, Chotte JL, Brauman A
Dynamics of the bacterial community within different soil fractions during the decomposition of ^{13}C-labelled rice straw.
SOM 2010: Organic matter stabilization and ecosystem functions, Presqu'île de Giens (France), 19th – 23rd September 2010.

Appendix 2.1: Description of the plot experiment established in 2009 in the high Arctic tundra (Svalbard).

Table A2.1: Location and elevation (m) of each field plots. → indicate plot treatments which changed from 2009 to 2010.

Plot	Treatment	N			E			Elevation
n º		º	'	''	º	'	''	m
1	HNO_3 pH = 4 → NH_4Cl *vs.* $NaNO_3$	78	55	231	11	49	819	28
2	Control + water	78	55	231	11	49	800	24
3	4 kg N ha^{-1} pH = 4	78	55	231	11	49	795	26
4	0.4 kg N ha^{-1} pH = 6 → 12 kg N ha^{-1} pH = 4	78	55	226	11	49	806	25
5	Control + water	78	55	225	11	49	810	25
6	0.4 kg N ha^{-1} pH = 6 → 12 kg N ha^{-1} pH = 4	78	55	229	11	49	785	26
7	HNO_3 pH = 4 → NH_4Cl *vs.* $NaNO_3$	78	55	228	11	49	780	28
8	0.4 kg N ha^{-1} pH = 4	78	55	228	11	49	768	27
9	Control + water	78	55	228	11	49	749	27
10	0.4 kg N ha^{-1} pH = 6 → 12 kg N ha^{-1} pH = 4	78	55	223	11	49	744	30
11	HNO_3 pH = 4 → NH_4Cl *vs.* $NaNO_3$	78	55	224	11	49	751	29
12	4 kg N ha^{-1} pH=4	78	55	223	11	49	758	28
13	0.4 kg N ha^{-1} pH = 4	78	55	229	11	49	745	27
14	4 kg N ha^{-1} pH = 4	78	55	232	11	49	734	28
15	0.4 kg N ha^{-1} pH = 6 → 12 kg N ha^{-1} pH = 4	78	55	237	11	49	722	28
16	HNO_3 pH = 4 → NH_4Cl *vs.* $NaNO_3$	78	55	234	11	49	707	27
17	0.4 kg N ha^{-1} pH = 4	78	55	235	11	49	698	27
18	HNO_3 pH = 4 → NH_4Cl *vs.* $NaNO_3$	78	55	229	11	49	707	26
19	Control + water	78	55	228	11	49	675	27
20	4 kg N ha^{-1} pH = 4	78	55	230	11	49	651	28
21	Control + water	78	55	240	11	49	732	29
22	0.4 kg N ha^{-1} pH = 4	78	55	243	11	49	744	27
23	0.4 kg N ha^{-1} pH = 6 → 12 kg N ha^{-1} pH = 4	78	55	247	11	49	729	27
24	0.4 kg N ha^{-1} pH = 4	78	55	253	11	49	720	28
25	4 kg N ha^{-1} pH = 4	78	55	251	11	49	747	27

Appendix 2.2: Variation in plants coverage within the plot experiment during the summer of 2010.

Day -6 (13-07-10) Day + 7 (25-07-10) Day + 21 (08-08-10) Day + 35 (23-08-10)

Plot 2: Control + water

Plot 4: 12 kg N ha^{-1}

Figure A2.2: Photos of a control + water plot (plot 2) and 12 kg N ha^{-1} pH = 4 plot (plot 4) through the 2010 summer. Sampling date as indicated. Scale bar as shown (all plots).

Appendix 2.3: Profiles of the internal size standard ROX-labelled GS500 and GS2500 (Applied Biosystems, Warrington, UK) highlighting the peaks used.

The ROX-labelled internal standard GS500 was composed of DNA sequences of different sizes (nucleotides) of single strain DNA. Thus, after the step of DNA denaturation at 94 ºC for 3 min, followed by the electrophoresis on an ABI 3730 PRISM® capillary genetic analyser using POP7 polymer (Applied Biosystems, Warrington, UK), the electropherogram obtained for the ROX-labelled internal standard GS500 presented single peak for each sequence of the standard (Figure A2.3.1), which were automatically assigned to a specific size by GeneMapper® v3.7 software (Applied Biosystems, Warrington, UK). However, the ROX-labelled internal standard GS2500 was composed of DNA sequences of different sizes (base pairs) of double strain DNA. Thus, after the step of DNA denaturation at 94 ºC for 3 min, the double strain DNA was separated into two single strains of DNA for each sequence, leading to a double peak for each sequence after electrophoresis on the genetic analyser (Figure A2.3.2). The assignment of the size for the corresponding peak was done manually to ensure that the size of the different sequences was always assigned to the same peak of the double peak.

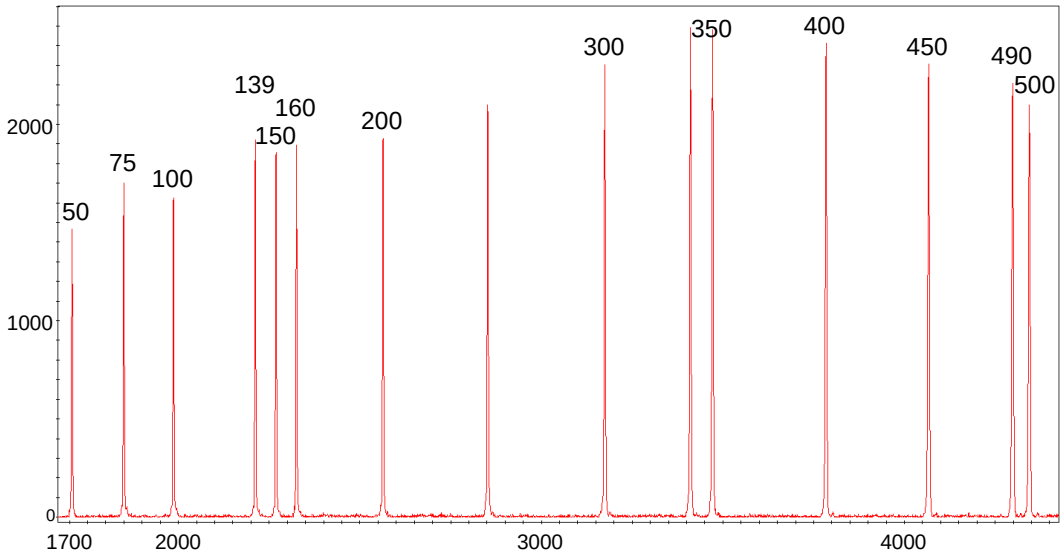

Figure A2.3.1: Electropherogram of the ROX-labelled internal size standard GS500 ROX (Applied Biosystems, Warrington, UK) used for T-RFLP analysis showing the size (nucleotides) of the different fragments. The *x* axis corresponds to the data points and the *y* axis corresponds to the relative fluorescence (arbitrary units) of each T-RFs.

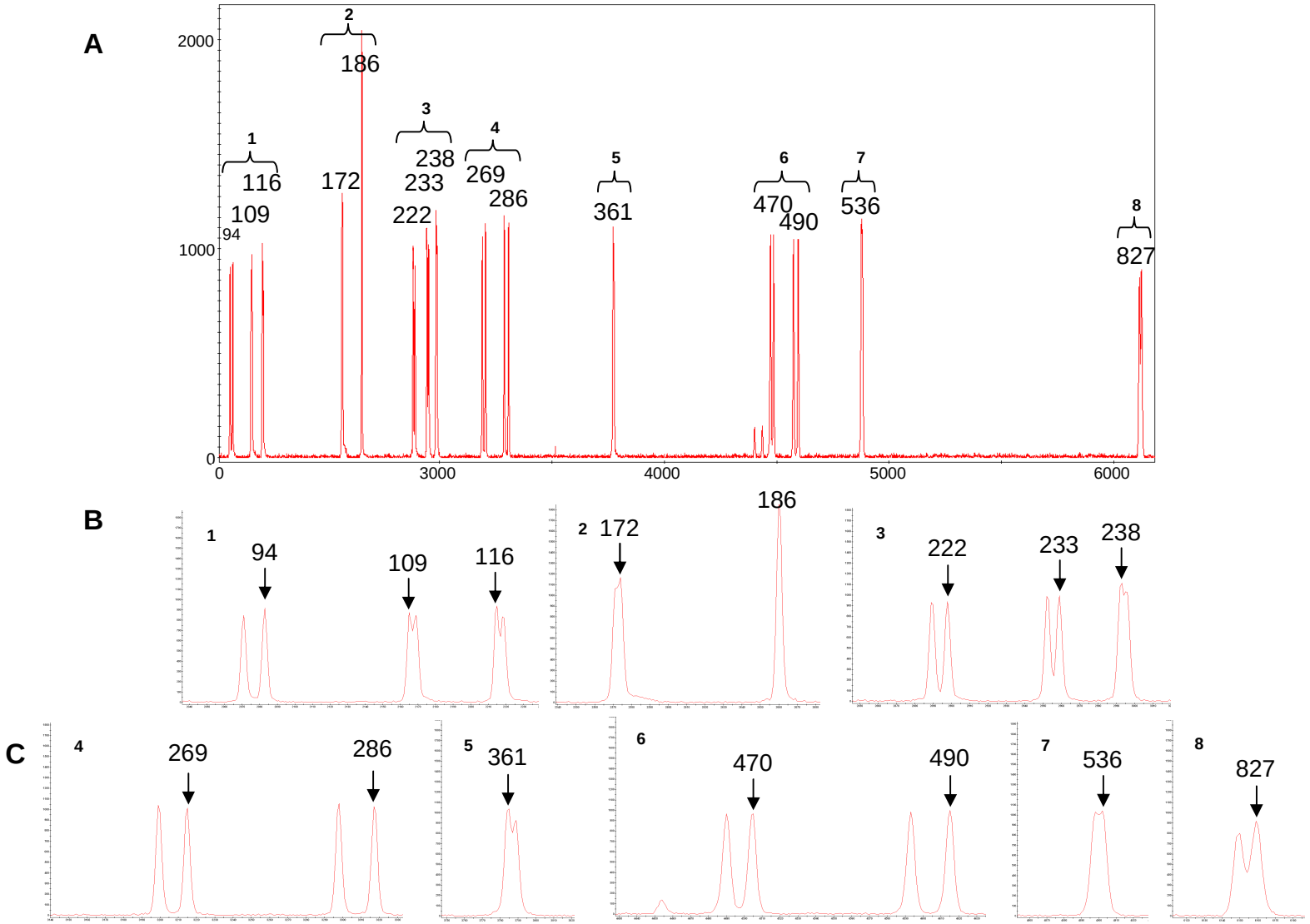

Figure A2.3.2: Electropherogram of the ROX-labelled internal size standard GS2500 ROX (Applied Biosystems, Warrington, UK) used for ARISA showing the size (nucleotides) of the different fragments. The *x* axis corresponds to the data points and the *y* axis corresponds to the relative fluorescence (arbitrary units) of each T-RFs. **A**: image showing the entire electropherogram; **B**: image showing a zoom of the electropherogram between 0 – 240 nucleotides; **C**: imagne showing a zoom of the electropherogram between 240 – 830 nucleotides.

Appendix 3.1: Variation in soil ^{15}N enrichment during the plot experiment in 2009.

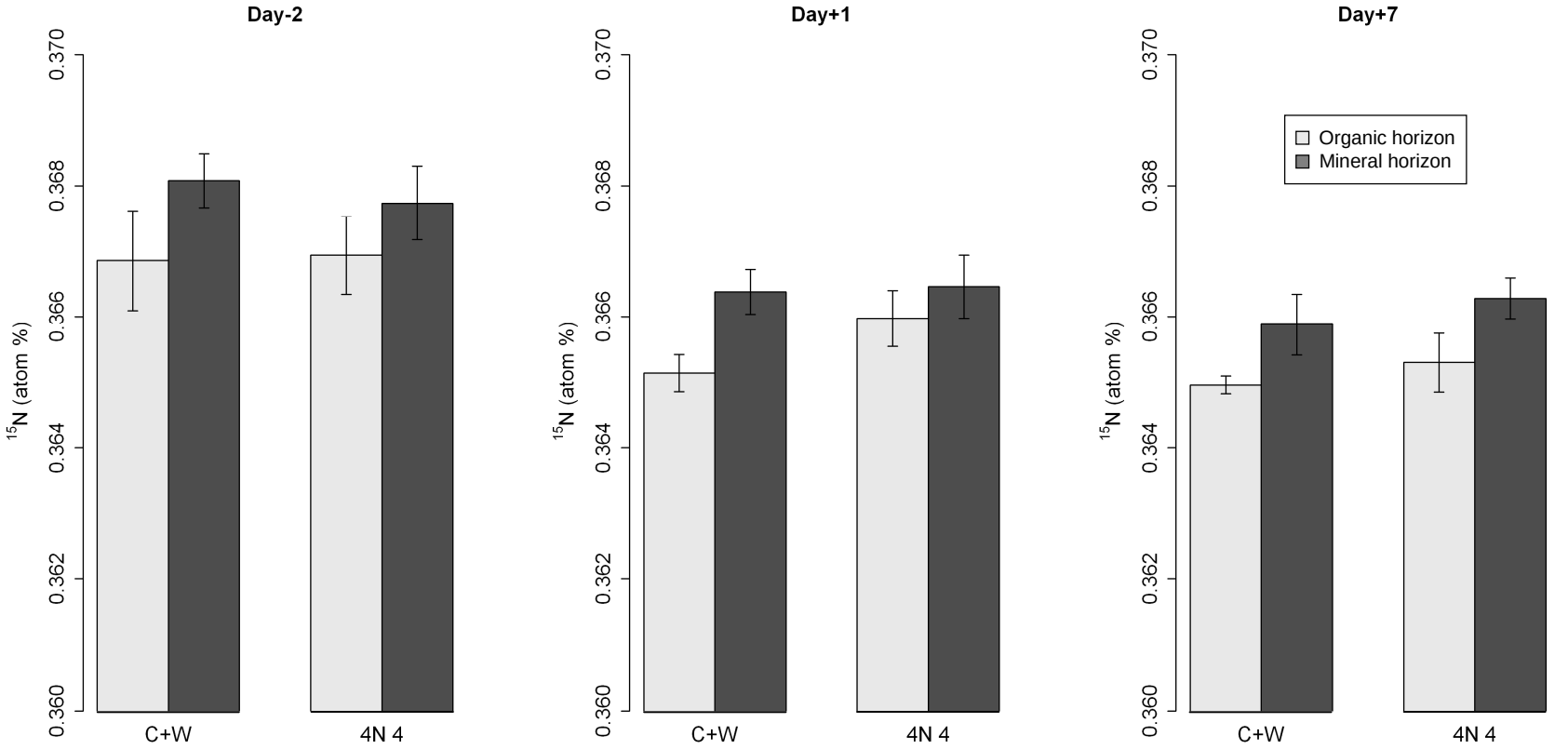

Figure A3.1: Variation in soil ^{15}N enrichment (atom %) between the organic and mineral soil horizons, over time and in response to simulated episodic nitrogen deposition events. Plots were established and sampled in summer 2009. **Day-2**: before N application; **Day+1**: one day after N application; **Day+7**: seven days after N application; **C+W**: control + water plots; **4N 4**: 4 kg N ha^{-1} yr^{-1} ~pH 4 plots. Means values ± standard deviation (n = 5) are shown.

Appendix 3.2: Variation in precipitation and temperature during the 2009 N application and sampling period.

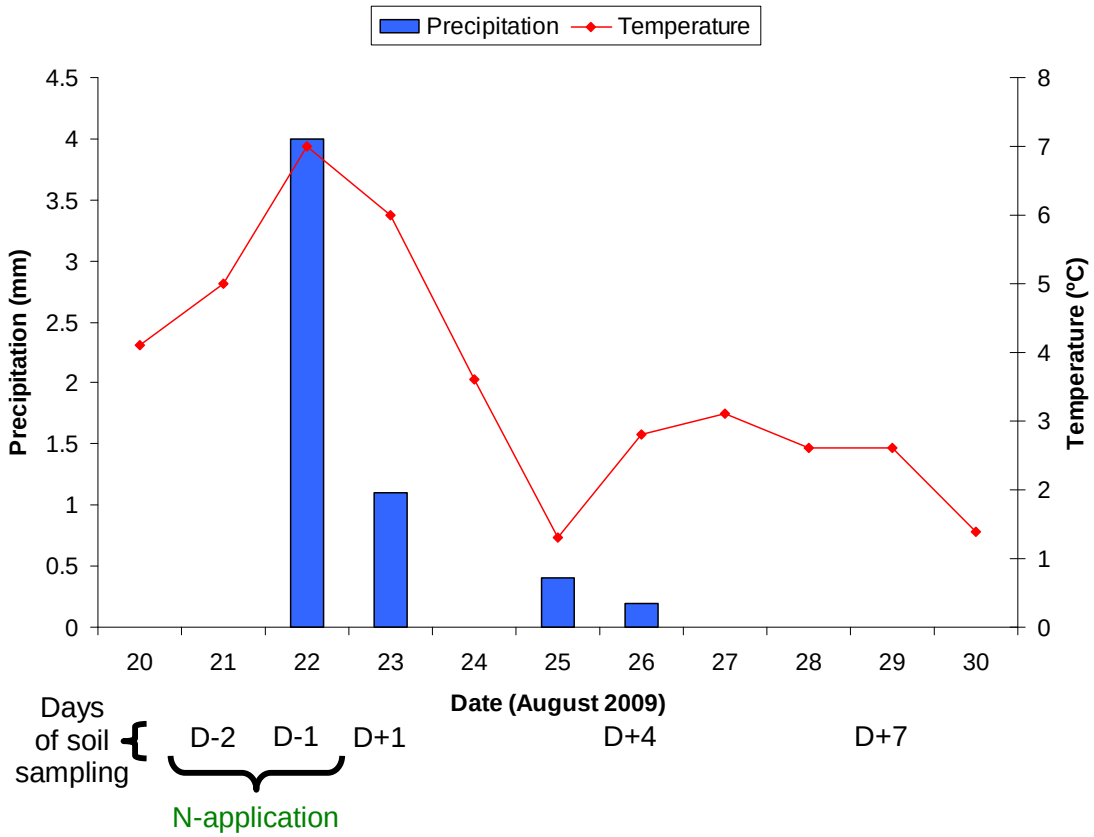

Figure A3.2: Daily average precipitation (mm) and temperature (ºC) during the N application and soil sampling period: **D-2**: before N application; **D-1**: before the second day of N application; **D+1**: one day after N application; **D+4**: four days after N application; **D+7**: seven days after N application. The precipitation and temperature data were obtained from: http://www.yr.no/place/Norway/Svalbard/Ny-%C3%85lesund/detailed_statistics.html.

Appendix 3.3: Specificity of the Q-PCR for the bacterial, archaeal and fungal communities obtained from soil samples taken in 2009 from the plot experiment.

The SYBR Green detection method used for Q-PCR is not specific to the gene of interested (in contrast to the TaqMan method) but binds to all the double stranded DNA present in the Q-PCR. Thus, if non-specific product or primer dimer are synthesised during the Q-PCR, this will lead to an overestimation of the abundance of the gene of interest. Thus, to assess the specificity of any Q-PCR amplification, using SYBR Green method, a melting curve analysis has to be performed to determine the specificity of the amplification (Ririe *et al.*, 1997). The melting curve consists of measuring the fluorescence during the denaturation of the Q-PCR products with a constant increase of temperature. The increase of temperature denatures the amplified product, leading to a decrease in the fluorescence at a constant rate. When the melting temperature (T_m) of the product is reached, the fluorescence decreases rapidly until denaturation is complete. Thus, primer dimers which are shorter sequences than the gene targeted will be denatured first. As the T_m depends on the GC/AT ratio, length and sequence, if non-specific products were amplified, the decrease in fluorescence should be different than for the targeted gene. The results of the melting curve are presented by plotting the relative fluorescence (RFU) of all the samples against the increase in temperature (T) (Figure A3.3). The results can also be presented as a melting peak, corresponding to a plot of the negative first regression of fluorescence versus temperature (-d(RFU)/dT) against the increase of temperature (Figure A3.3). The later plot shows the dramatic decrease of fluorescence by a peak, indicating the T_m of the double-strand DNA of the targeted gene or different Q-PCR products.

The bacterial and archaeal community showed a melting curve/peak for the samples which reveal specificity for the amplified targeted gene (Figure A3.3). However, the no template control (NTC) showed different patterns between the melting curves of the bacterial and archaeal community. For the melting curves of the bacterial community, the NTC showed curves similar to the samples while the archaeal NTC showed curves with a different slope than for the samples. The NTC do not contain any template, only the SYBR Green mix and the primers. Thus, only primers dimers can be

syntheses within the NTC, which should show different melting curves than found for the samples (i.e. drop in fluorescence at lower temperature). However, similar NTC curves than the samples might indicate potential Q-PCR contamination. The archaeal melting curve of the NTC showed the expected pattern for NTC, with a rapid decrease of fluorescence, as reported in the literature (see Ririe *et al.*, 1997). The peak for the archaeal NTC indicated substantial primer dimer formation. However, this peak related to the primer dimers was not found for the samples, indicating that large numbers of the primer dimer were not formed for the samples, which did not lead to an overestimation of the archaeal abundance. This was confirmed by the fact that only 17 genes in average were found for the NTC. The bacterial melting curve/peak of the NTC indicated a potential contamination which was confirmed by the gene number of the NTC (average of 160 gene numbers 25 μl^{-1}). However, the NTC gene numbers were extremely low in comparison to the lowest gene numbers of 2×10^5 25 μl^{-1} found for some samples. Thus, the presence of an amplification signal within the reaction did not significantly affect the total gene numbers of the bacteria.

The fungal melting curve/peak showed that more than one product was amplified during the Q-PCR. This is not surprising as the ITS show high variability in length, as found with the ARISA of the fungal community targeting the whole ITS region. Fierer *et al.* (2005) used the same primers pairs to assess the fungal abundance within different soil using Q-PCR, indicated a significant variation in the length of the targeted sequence but did not discuss more about the potential issues that it could represent for Q-PCR. Thus, the multiple sequences amplified are likely to be amplified from different members of the fungal community. The fungal NTC showed a different pattern from the samples and the ITS region numbers detected was below one for the NTC. Thus, fungal Q-PCR results provide a good indicator of the relative abundance changes between samples, but the ITS region numbers should be interpreted with extreme caution. Only a few studies have investigated fungal abundance by Q-PCR (e.g. Fierer *et al.*, 2005; Manter & Vivanco, 2007; Boyle *et al.*, 2008; Rousk *et al.*, 2010) but no rigorous evaluation of the accuracy of the fungal Q-PCR has been done. Thus, more studies are needed to investigate the use of Q-PCR to determine the abundance of fungal communities.

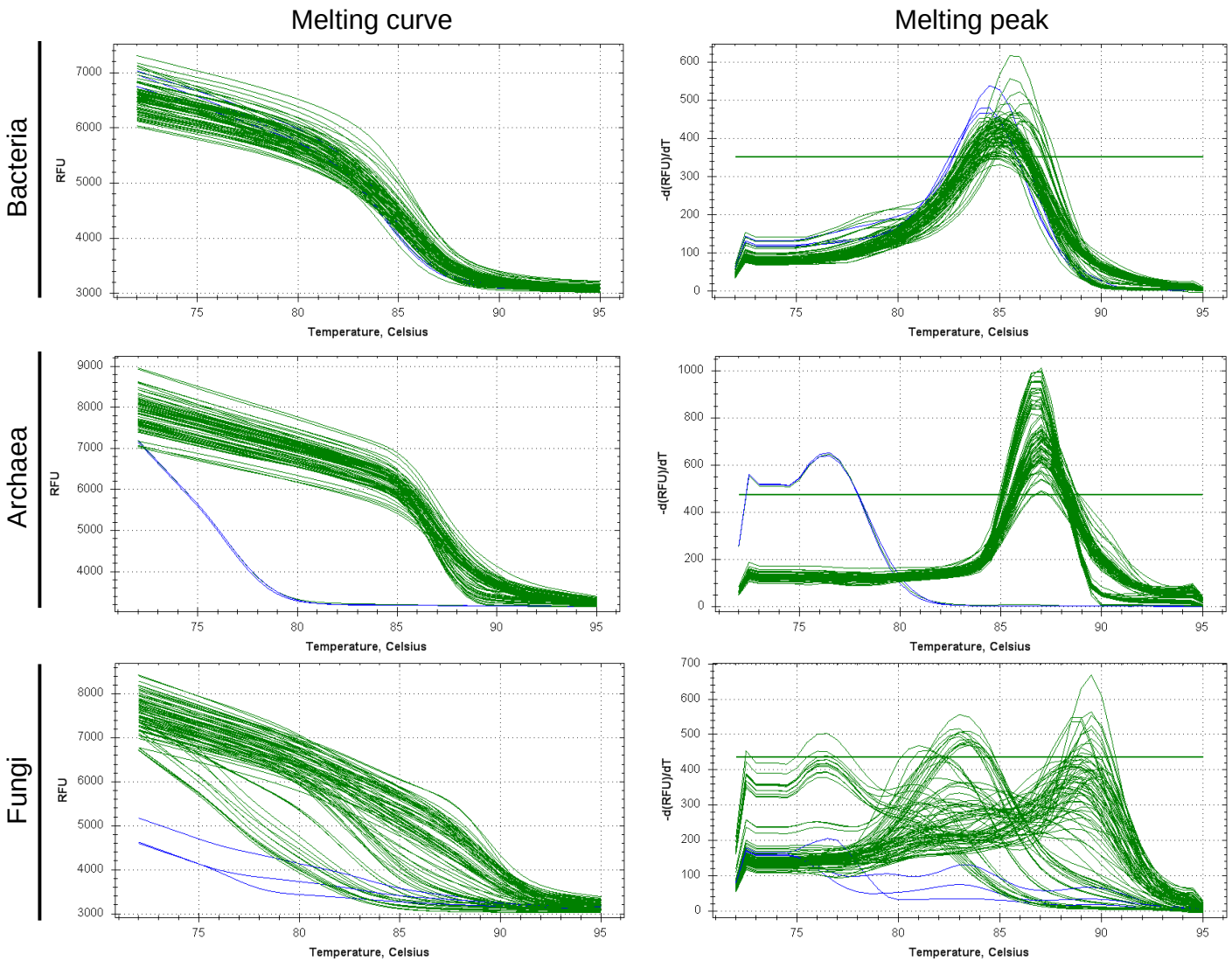

Figure A3.3: Melting curve and melting peak of the bacterial, archaeal and fungal community obtained by Q-PCR with the Bio-Rad CFX Manager software. The melting curve/peak included all the soil samples (green curves) used for the Q-PCR from the plot experiment in summer 2009 (see text for detail) and the Q-PCR NTC (blue curves). The horizontal line on the melting peak plots is an arbitrary line set up by the Bio-Rad software to indicate the threshold that the software uses to consider a peak as valid.

Appendix 4.1: Variation in precipitation and temperature during the 2010 N application and sampling period.

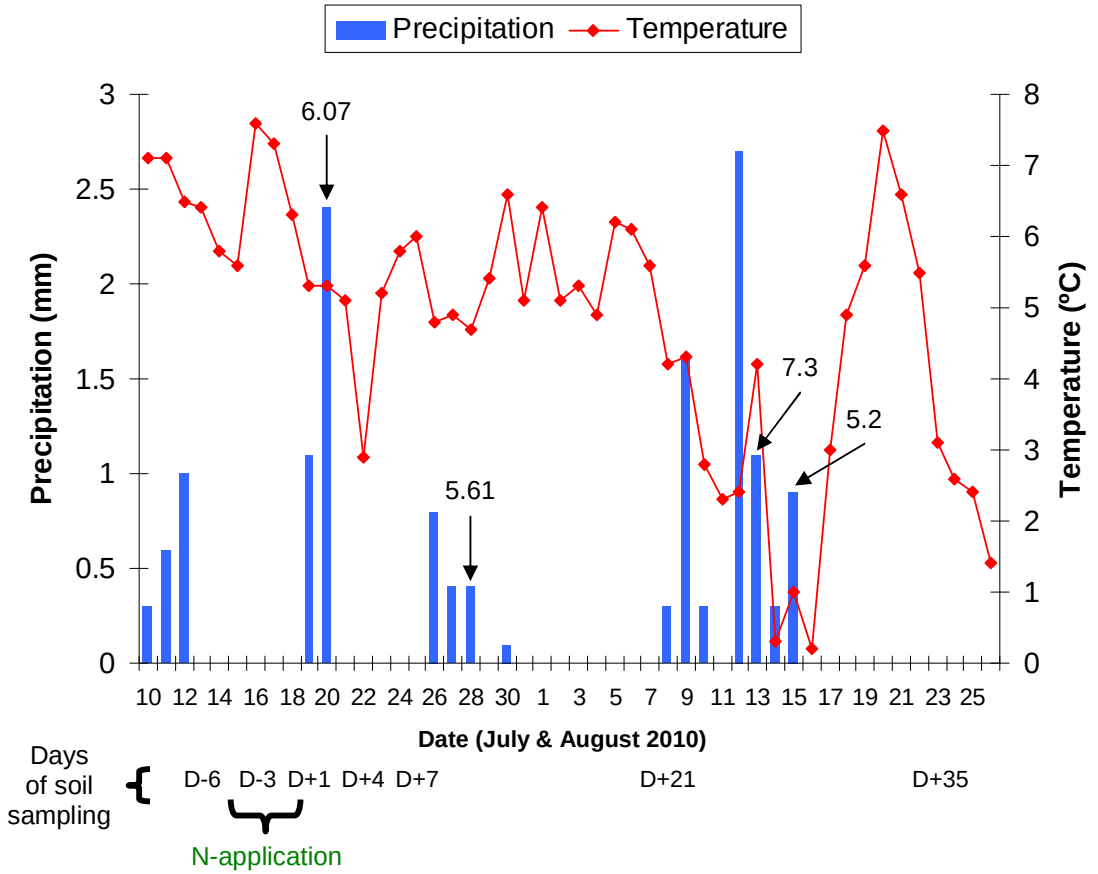

Figure A4.2: Daily average precipitation (mm) and temperature (ºC) during the N application and soil sampling period: **D-6**: two days before N application; **D-3**: after the second N application; **D+1**: one day after N application; **D+4**: four days after N application; **D+7**: seven days after N application; **D+21**: twenty-one days after N application; **D+35**: thirty five days after N application. The values above the precipitation bars give the pH values of the rain, taken from precipitation sampler located on the plots area. The precipitation and temperature data were obtained from: http://www.yr.no/place/Norway/Svalbard/Ny-%C3%85lesund/detailed_statistics.html.

Appendix 6.1: Influence of soil sampling location on variation in structure and abundance of the bacterial and archaeal communities.

Variation in the structure and abundance of the bacterial and archaeal communities was compared between each soil replicate within each soil horizon to evaluate the potential effect of the different soil replicates. One-way ANOSIM between the different soil replicates of the bacterial or archaeal community structure from the organic horizon showed no significant ($P > 0.05$) differences between the three different soil replicates over time, although the soil samples 1 and 2 were nearly significantly different at $P < 0.05$ for bacterial community structure (Table A6.1). However, the structure of both the bacterial and archaeal communities within the mineral horizon differed significantly between soil replicate 1 and soil replicates 2 and 3 (Figure A6.1; Table A6.1). However, neither the structures of the bacterial nor archaeal communities within the mineral horizon from samples 2 and 3 were significantly ($P \geq 0.15$) different. Bacterial 16S rRNA gene numbers were not significantly ($P \geq 0.13$) different between soil replicates within both soil horizons. Similarly, archaeal abundance was not significantly ($P \geq 0.12$) different between soil replicates within the organic horizon (Table A6.1). However, archaeal abundance was significantly different ($P = 0.0001$) between the soil samples replicate 1 *vs.* 2 (R = 0.56) and 1 *vs.* 3 (R = 0.80).

Table A6.1: One-way ANOSIM to investigate the influence of microcosm soil sample replicates on the structure and abundance of the bacterial and archaeal communities in the organic and mineral horizons for all treatments and days of sampling. The R values and the significance level (in brackets) are given. Significant values at $P < 0.05$ are shown in bold text.

Soil horizons	Soil replicate compared	Bacterial structure	Archaeal structure	Bacterial abundance	Archaeal abundance
Organic	1 *vs.* 2	0.17 (0.052)	0.05 (0.21)	-0.00 (0.39)	0.02 (0.28)
	1 *vs.* 3	0.02 (0.29)	0.03 (0.28)	-0.03 (0.55)	0.01 (0.27)
	2 *vs.* 3	0.005 (0.37)	-0.003 (0.42)	0.09 (0.13)	0.08 (0.12)
Mineral	1 *vs.* 2	**0.31 (0.009)**	**0.27 (0.009)**	-0.05 (0.70)	**0.56 (0.0001)**
	1 *vs.* 3	**0.32 (0.006)**	**0.26 (0.007)**	-0.01 (0.43)	**0.80 (0.0001)**
	2 *vs.* 3	0.08 (0.15)	-0.03 (0.54)	-0.05 (0.66)	0.04 (0.22)

Soil replicate 1 exhibited differences in bacterial and archaeal community structure and in archaeal abundance within the mineral horizon in comparison to the other soil replicates used in the microcosm experiment. These differences between soil replicates were not related to differences in the environmental variables measured. These differences in bacterial and archaeal communities in soil replicate 1 from those in other soil replicates need to be considered during interpretation of data.

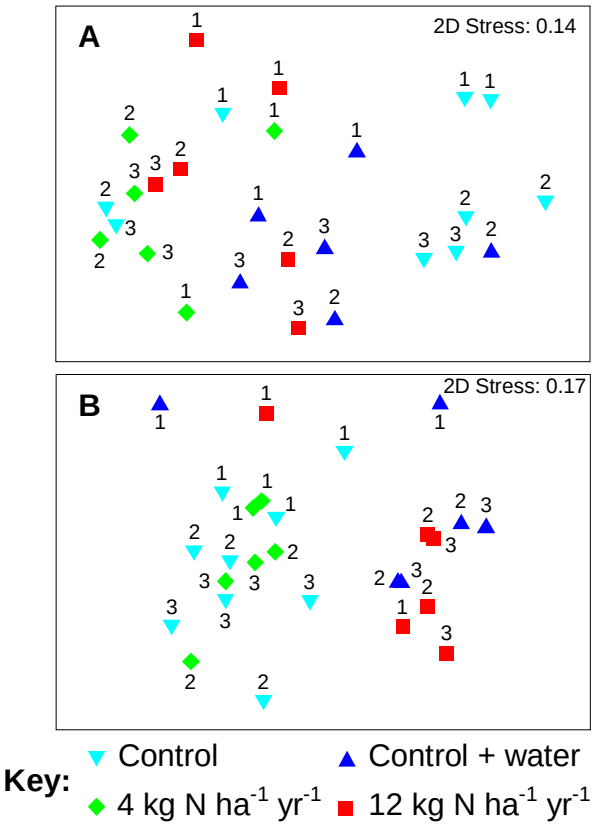

Figure A6.1: nMDS plots showing variation in bacterial (**A**) and archaeal (**B**) community structure in the microcosm experiment for the mineral horizon in response to water addition (control (without water and N) and control + water microcosms) and nitrogen addition (4 kg N ha^{-1} yr^{-1} ~pH 4 and 12 kg N ha^{-1} yr^{-1} ~pH 4 microcosms). Numbers above symbols refer to the soil sample replicates.

R values between samples from soil replicate 1 and the other soil replicates (Table A6.1) were much lower than those obtained when investigating the influence of the different treatments on microbial communities structure (Table A6.1), indicating that despite having different microbial communities, that treatment effects are stronger than the soil replicate effects. Archaeal abundance was more strongly influenced by the

different soil replicates ($R \geq 0.56$; Table A6.1). However, archaeal abundance within the mineral horizon of soil replicate 1 was only on average 1.4 times higher than in soil replicates 2 and 3. Despite, these differences between soil replicates in the experiment, the microbial communities nevertheless seem to follow similar trends in response to the different experimental treatments. Consequently, the results are likely overall to represent the responses of bacterial and archaeal communities to water and N additions.

Appendix 6.2: Variation in soil ^{15}N enrichment during the microcosm experiment.

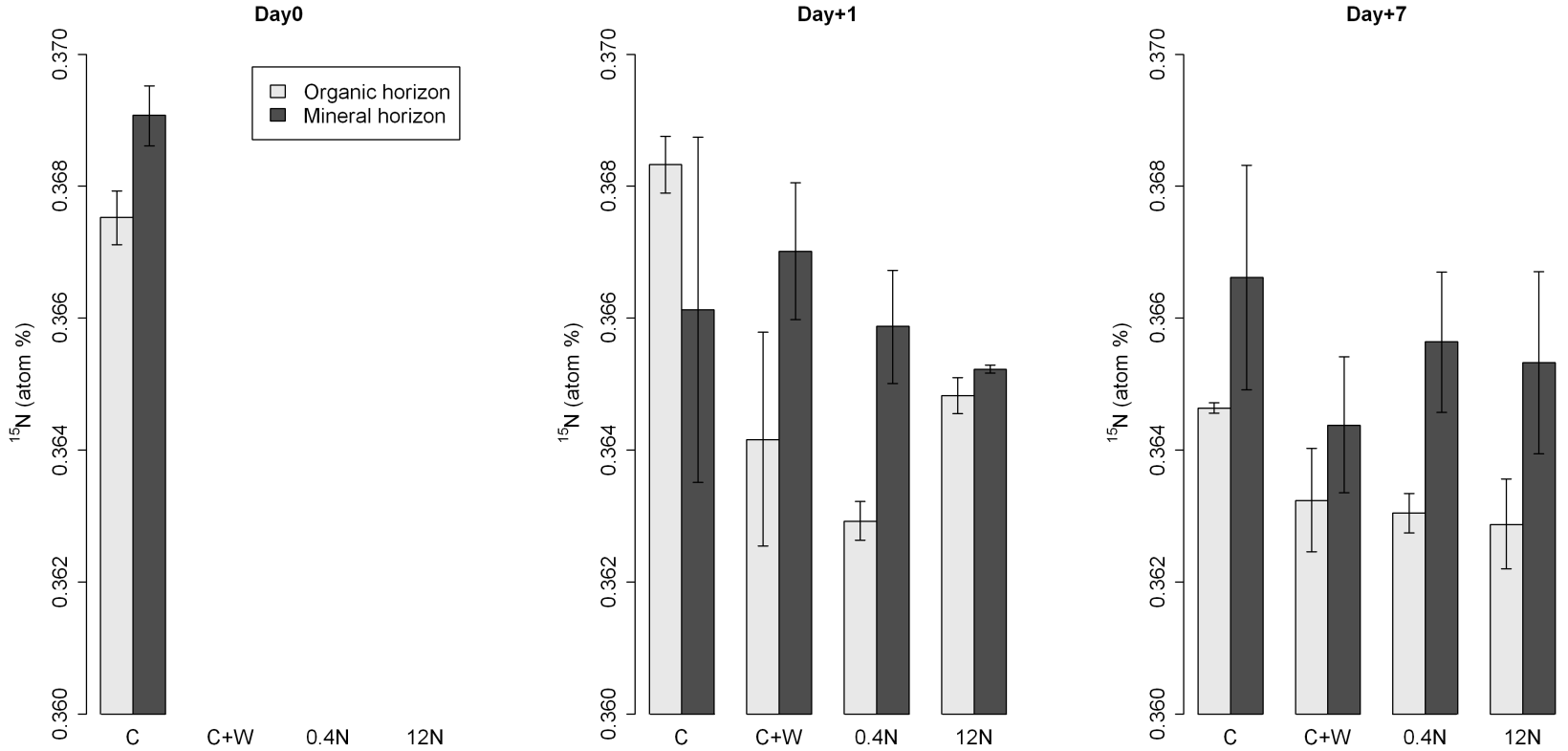

Figure A6.2: Variation in ^{15}N enrichment (atom %) between the organic and mineral soil horizons over time and in response to water and nitrogen addition. **Day0**: before any treatments; **Day+1**: one day after treatment; **Day+7**: seven days after treatment; **C**: Control microcosms, **C+W**: Control + water microcosms; **0.4N**: 0.4 kg N ha^{-1} yr^{-1} ~pH 4 microcosms; **12N**: 12 kg N ha^{-1} yr^{-1} ~pH 4 microcosms. Means values ± standard deviation (n = 5) are shown.